GEOLOGICAL SURVEY BRANCH
DEPARTMENT OF MINES AND ENERGY
GOVERNMENT OF NEWFOUNDLAND AND LABRADOR

GEOLOGY OF THE NORTH BAY GRANITE SUITE AND METASEDIMENTARY ROCKS IN SOUTHERN NEWFOUNDLAND (NTS 11P/15E, 11P/16 AND 12A/2E)

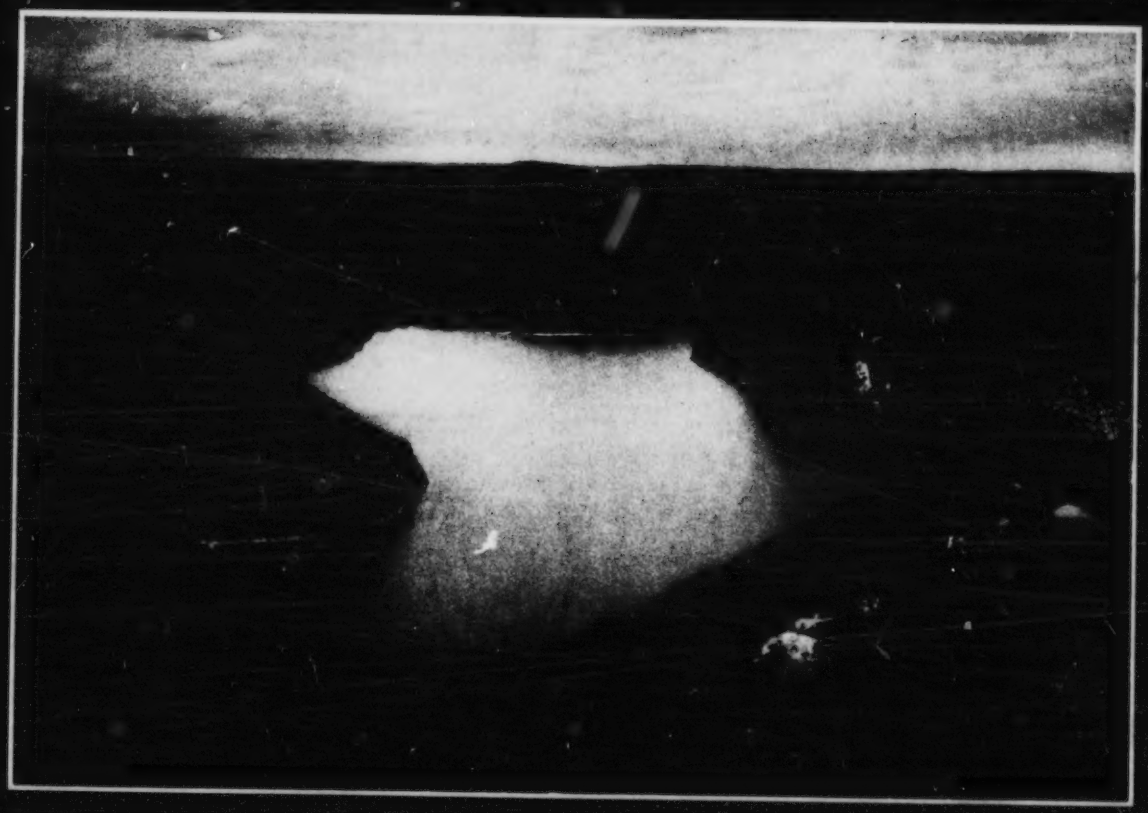

W. Lawson Dickson

Report 90-3

St. John's, Newfoundland
1990

Cover

View looking north across East Bay of the barren terrain typical of the North Bay Granite Suite. The plateau is underlain by the East Bay Granite.

91-05096/

GEOLOGICAL SURVEY BRANCH
DEPARTMENT OF MINES AND ENERGY
GOVERNMENT OF NEWFOUNDLAND AND LABRADOR

GEOLOGY OF THE NORTH BAY GRANITE SUITE AND METASEDIMENTARY ROCKS IN SOUTHERN NEWFOUNDLAND (NTS 11P/15E, 11P/16 AND 12A/2E)

W. Lawson Dickson

Report 90–3

St. John's, Newfoundland
1990

EDITING, LAYOUT AND DRAFTING

Senior Geologist R.F. BLACKWOOD

Editor C.P. G. PEREIRA

Copy Editor D.G. WALSH

Typesetting B. STRICKLAND

Word Processing D. DOWNEY
J. MATTHEWS
M. VEY

Supervisor, Cartographic and Photomechanical Services K. BYRNE

Cartography D. LEONARD (Photomechanical)
G. DENIEF
T. PALTANAVAGE
T. SEARS

Publications of the Geological Survey Branch are available through the Publications and Information Section, Geological Survey Branch, Department of Mines & Energy, P.O. Box 8700, St. John's, Newfoundland, A1B 4J6.
Telephone: (709) 576-3159
Telex: 016-4721
Fax: (709) 576-3493

This project is a contribution to the Canada–Newfoundland mineral development agreements for the period 1976–1989. Project carried out by Newfoundland Department of Mines and Energy.

ISBN 0-920769-52-7

Author's Address *W. Lawson Dickson*
Newfoundland Mapping Section
Geological Survey Branch
Department of Mines and Energy
P.O. Box 8700
St. John's, Newfoundland
Canada
A1B 4J6

CONTENTS

	Page
ABSTRACT	xvi
INTRODUCTION	1
LOCATION AND ACCESS	1
PHYSIOGRAPHY	1
DEFINITION OF THE NORTH BAY GRANITE SUITE AND ITS MEMBERS	2
HISTORY OF NOMENCLATURE	2
NAME TO ABANDON	4
BOUNDARY REVISION AND RANK ELEVATION TO NORTH BAY GRANITE SUITE	4
NEW NAMES	4
PREVIOUS WORK	5
SEDIMENTARY AND VOLCANIC ROCKS	7
INTRODUCTION	7
SPRUCE BROOK FORMATION (UNIT 2)	9
BAIE D'ESPOIR GROUP (UNIT 3)	11
Salmon River Dam Formation (Subunits 3a, 3b)	11
Riches Island Formation (Subunits 3c, 3d)	12
North Steady Pond Formation (Subunits 3e to 3h)	13
BAY DU NORD GROUP (UNIT 4)	14
SILURIAN? CLASTIC SEDIMENTARY ROCKS–UNIT 5	15
SEDIMENTOLOGY OF THE ORDOVICIAN UNITS	16
DEFORMATION AND METAMORPHISM OF THE SPRUCE BROOK FORMATION (UNIT 2)	17
DEFORMATION OF THE BAIE D'ESPOIR GROUP (UNIT 3)	18
METAMORPHISM OF THE BAIE D'ESPOIR GROUP (UNIT 3)	20
DEFORMATION AND METAMORPHISM OF THE BAY DU NORD GROUP (UNIT 4)	22
DEFORMATION AND METAMORPHISM OF UNIT 5–SILURIAN? CLASTIC SEDIMENTS	23
INTRUSIVE ROCKS	23
INTRODUCTION	23
UNIT 1–MAGNESITE	24
BURGEO GRANITE (UNITS 6 AND 7)	25
NORTH BAY GRANITE SUITE (UNITS 8 TO 21)	25
Introduction	25
Radiometric Dating	26
Previous Rb–Sr Age Determinations	26
New Rb–Sr Age Determinations	27
East Bay Granite	28
Upper Salmon Road Granite	29
New U–Pb Age Determinations	30
Gneissic granodiorite–part of Subunit 3d	30
Dolland Brook Granite	30
Summary of New Age Determinations	31
Description of the North Bay Granite Suite	31
Unit 8 and the D'Espoir Brook Granite (Unit 9)	31
Distribution	31
Contact Relations	31
Petrography	32
Wolf Lake North Granodiorite (Unit 10)	33
Distribution	33
Contact Relations	33
Petrography	35
East Bay and Bottom Brook Granites (Units 11 and 12)	35
Distribution	35
Contact Relations	35

Page

Petrography 35
Unit 13 37
Meelpaeg Lake Granite (Unit 14) 37
Distribution 37
Contact Relations 37
Petrography 37
Unit 15 38
Distribution 38
Contact Relations 39
Petrography of the Altered Granite 39
Wolf Lake Granite (Unit 16) 39
Distribution 39
Contact Relations 40
Petrography 41
Dolland Brook and Facheux Bay East Granites (Subunits 17a, 17b) 41
Distribution 41
Contact Relations 41
Petrography 42
Wolf Mountain Granite (Unit 18) 43
Distribution 43
Contact Relations 43
Petrography 43
Dolland Pond, Morgan Brook, Hughes Brook and D'Espoir Lake Granites (Subunits 19a to 19d) 43
Distribution 43
Contact Relations 44
Petrography 45
Upper Salmon Road Granite (Unit 20) 46
Distribution 46
Contact Relations 46
Petrography 47
Unit 21 48
Distribution 48
Contact Relations 48
Petrography 49

OTHER INTRUSIVE ROCKS 49
INTRODUCTION 49
MICROGRANITE DYKES (UNIT 22) 49
Distribution and Contact Relations 49
Petrography 50
QUARTZ–FELDSPAR PORPHYRY DYKES (UNIT 23) 50
Distribution and Contact Relations 50
Petrography 50
QUARTZ VEINS (UNIT 24) 50
Distribution and Contact Relations 50
Petrography and Economic Potential 51
DIABASE DYKES (UNIT 25) 51
Distribution and Contact Relations 51
Petrography 51
SUMMARY OF THE GEOLOGY OF THE NORTH BAY GRANITE SUITE 51

GEOCHEMISTRY OF THE NORTH BAY GRANITE SUITE AND ASSOCIATED IGNEOUS ROCKS 52
INTRODUCTION 52
SAMPLING AND FIELD METHODS 52
GEOCHEMISTRY OF THE MAGNESITE (UNIT 1) 53
GEOCHEMISTRY OF THE BURGEO GRANITE (UNIT 6) 53
GEOCHEMISTRY OF THE NORTH BAY GRANITE SUITE 53

Page

GEOCHEMISTRY OF THE UNITS OF COMPONENT 1 OF THE NORTH BAY GRANITE SUITE..... 55
Unit 8 and D'Espoir Brook Granite (Unit 9)..... 55
East Bay and Bottom Brook Granites (Units 11 and 12)..... 57
Dolland Brook and Facheux Bay East Granites (Subunits 17a, 17b), Wolf Mountain Granite (Unit 18), the Dolland Pond, Morgan Brook, Hughes Brook and D'Espoir Lake Granites (Subunits 19a to 19d) and Unit 21..... 58
GEOCHEMISTRY OF COMPONENT 2 OF THE NORTH BAY GRANITE SUITE..... 62
PETROGENESIS OF THE NORTH BAY GRANITE SUITE..... 67
SUMMARY OF PETROGENETIC PROCESSES..... 75
GEOCHEMISTRY OF THE OTHER IGNEOUS UNITS..... 78

ECONOMIC POTENTIAL OF THE NORTH BAY GRANITE SUITE..... 78

SUMMARY..... 80

ACKNOWLEDGMENTS..... 81

REFERENCES..... 81

APPENDIX 1..... 89
Explanatory Notes..... 89
Explanation of Abbreviations..... 89
Field Data—Part 1..... 89
Field Data—Part 2..... 89
Major-Element-Oxide Data..... 90
Trace-Element Data..... 90
Normative-Mineral Data..... 90
a—Field Data—Part 1..... microfiche
b—Field Data—Part 2..... microfiche
c—Major-Element-Oxide Data..... microfiche
d—Trace-Element Data..... microfiche
e—Normative-Mineral Data..... microfiche

APPENDIX 2 PRECISION OF MAJOR- AND TRACE-ELEMENT DETERMINATIONS..... 91
a—Precision of major-element determinations based on 40 analytical splits..... 91
b—Precision of trace-element determinations based on analytical splits..... 91

APPENDIX 3 ACCURACY..... 92
a—Accuracy of major-element determinations at the Newfoundland Department of Mines and Energy, Geological Survey Branch Laboratory. Usable values from Abbey (1980)..... 92
b—Accuracy of trace elements, determined by the Newfoundland Department of Mines and Energy, Geological Survey Branch Laboratory. Usable values from Abbey (1980)..... 98
c—Accuracy of trace elements determined by XRF at the Department of Earth Sciences, Memorial University of Newfoundland. Usable values from Abbey (1980)..... 99

APPENDIX 4..... 100
a—Detailed sample location and description card used to format data..... 100
b—Explanation of Coding Scheme for Granite Sample Card..... 101

FIGURES

Page

Figure 1: Regional setting of the North Bay Granite Suite. C=Cochrane Pond Granite..... 1

Figure 2: Map of the North Bay Granite Suite indicating the distribution of the main units..... 2

Figure 3: Schematic diagram of the contact relations of the various components of the North Bay Granite Suite and adjacent units..... 8

Figure 4: Tectonostratigraphic subdivisions of the Newfoundland Appalachians (from Williams *et al.*, 1988).. 9

Figure 5: Equal area stereographic projection of poles to bedding (S_0), S_1, S_2, with plunge and direction of plunge of small folds, from various areas of the Spruce Brook Formation (Unit 2)..... 17

Figure 6: Equal area stereographic projection of poles to bedding (S_0), S_1, S_2, with plunge and direction of plunge of small folds, from the Salmon River Dam Formation (subunit 3a), in the Dolland Pond–D'Espoir Lake and D'Espoir Lake east areas..... 19

Figure 7: Equal area stereographic projection of poles to bedding (S_0), S_1, S_2, with plunge and direction of plunge of small folds for the Riches Island Formation (subunit 3c), in the East Bay–Lampidoes Passage area 19

Figure 8: Equal area stereographic projection of poles to bedding (S_0), S_1, with plunge and direction of plunge of small folds, from the North Steady Pond Formation (subunits 3e to 3h), in the Meelpaeg Lake area 20

Figure 9: Equal area stereographic projection of poles to bedding (S_0) and cleavage (S_1) with plunge and direction of plunge of F_1 and F_2 folds in Unit 5 at Dolland Pond..... 23

Figure 10: Modal proportions of Q:K:P for Unit 6 of the Burgeo granite; Q = quartz, K = alkali feldspar (including perthite), P = plagioclase. Classification of granitoid rocks used in this report from Streckeisen (1976) 24

Figure 11: Map of the Dragon Bay Fault mylonite zone in the Dolland Brook (east half) map area..... 26

Figure 12: Location map of samples A1 to A4 used by Fryer (1983) for Rb–Sr isotopic dating of the Upper Salmon Road Granite..... 27

Figure 13: Location map of samples B1 to B5 used by Fryer (1983) for Rb–Sr isotopic dating of the East Bay Granite 27

Figure 14: $^{87}Sr/^{86}Sr$ vs. $^{87}Rb/^{86}Sr$ isochron for samples B1 to B5 of the East Bay Granite..... 28

Figure 15: $^{87}Sr/^{86}Sr$ vs. $^{87}Rb/^{86}Sr$ isochron for the East Bay Granite with sample B5 omitted..... 28

Figure 16: $^{87}Sr/^{86}Sr$ vs. $^{87}Rb/^{86}Sr$ isochron for the East Bay Granite with samples B4 and B5 omitted..... 28

Figure 17: Plot of (1/Sr x 1000) vs. ($\Delta^{87}Sr/^{86}Sr \times 10^6$) for samples B1 to B5 from the East Bay Granite..... 29

Figure 18: $^{87}Sr/^{86}Sr$ vs. $^{87}Rb/^{86}Sr$ isochrons for the Upper Salmon Road Granite. Elias (1981) isochron (A) with data points shown by squares; Fryer (1983) isochron (B) from samples A1 to A4 (see Figure 19)... 29

Figure 19: $^{87}Sr/^{86}Sr$ vs. $^{87}Rb/^{86}Sr$ isochrons for the Upper Salmon Road Granite. Fryer (1983) isochron (B) from samples A1 to A4 indicated by crosses; Elias (1981) isochron (A) from Figure 18..... 29

Figure 20: (a) Location map of sample 12-1 used by T.E. Krogh (written communication, 1985) for U–Pb isotopic dating of zircons from subunit 3d migmatitic granodiorite screens within the East Bay Granite; (b) location map of sample 12-2 used by T.E. Krogh (written communication, 1985) for U–Pb isotopic dating of zircons from subunit 3d migmatitic granodiorite screens within the East Bay Granite..... 30

Page

Figure 21: Location map of sample LD33-1-83 used by T.E. Krogh (written communication, 1985) for U--Pb isotopic dating of zircons from the Dolland Brook Granite..... 31

Figure 22: $^{206}Pb/^{238}U$ vs. $^{207}Pb/^{235}U$ concordia for data obtained by T.E. Krogh (written communication, 1985) on samples 12-1, 12-2, and LD33-1-83. See text for details of plots..... 32

Figure 23: Modal proportions of Q:K:P for Unit 8 and the D'Espoir Brook Granite (Unit 9); classification and abbreviations as in Figure 10..... 35

Figure 24: Equal area stereographic projection of poles to main foliation, with plunge and direction of plunge of small folds, from Unit 8 granite and the D'Espoir Brook Granite..... 37

Figure 25: Modal proportions of Q:K:P for the Wolf Lake North Granodiorite, Meelpaeg Lake and Wolf Lake granites; classification and abbreviations as in Figure 10..... 38

Figure 26: Modal proportions of Q:K:P for the East Bay (Unit 11) and Bottom Brook (Unit 12) granites; classification and abbreviations as in Figure 10..... 39

Figure 27: Modal proportions of Q:K:P for Unit 17 and the Wolf Mountain Granite (Unit 18); classification and abbreviations as in Figure 10..... 45

Figure 28: Modal proportions of Q:K:P for Unit 19 of the North Bay Granite Suite; classification and abbreviations as in Figure 10..... 47

Figure 29: Modal proportions of Q:K:P for the Upper Salmon Road Granite (Unit 20) and Unit 21; classification and abbreviations as in Figure 10..... 49

Figure 30: Data sheet used in field during sample collection by helicopter..... 54

Figure 31: Variation diagrams for means of selected oxides and elements for the units in each component of the North Bay Granite Suite; solid symbols for Component 1 and open symbols (circles and crosses) for Component 2..... 58

Figure 32: Variation diagrams of Al_2O_3 and CaO vs. SiO_2 (all weight percent) for Unit 8 and the D'Espoir Brook Granite (Unit 9)..... 58

Figure 33: Variation diagrams of FeO, Na_2O and K_2O vs. SiO_2 (all weight percent) for Unit 8 and the D'Espoir Brook Granite (Unit 9)..... 59

Figure 34: Variation diagrams of $\log_{10}$ Rb, $\log_{10}$ Sr (in g/t) and $\log_{10}$ Rb/Sr vs. SiO_2 (in weight percent) for Unit 8 and the D'Espoir Brook Granite (Unit 9)..... 59

Figure 35: Variation diagrams of $\log_{10}$ Zr, $\log_{10}$ Li and $\log_{10}$ U (in g/t) vs. SiO_2 (all weight percent) for Unit 8 and the D'Espoir Brook Granite (Unit 9)..... 60

Figure 36: Variation diagrams of $\log_{10}$ K (in weight percent) vs. $\log_{10}$ Rb (in g/t) for Unit 8 and the D'Espoir Brook Granite (Unit 9)..... 60

Figure 37: Plot of $K_2O + Na_2O$ (Alk_{tot}):Total iron as FeO (FeO_{tot}):MgO (all weight percent) for Unit 8 and the D'Espoir Brook Granite (Unit 9). Curved line separates tholeiitic compositions (above) from calc-alkaline (below); from Irvine and Barager (1971). Dashed line indicates field of calc-alkaline granitoid rocks from part of the Coastal Batholith of Peru; from Atherton *et al.* (1979)..... 60

Figure 38: Variation diagrams of Al_2O_3 and CaO vs. SiO_2 (all weight percent) for the East Bay Granite (Unit 11) and the Bottom Brook Granite (Unit 12)..... 61

Page

Figure 39: Variation diagram of total iron as FeO (FeO_{tot}) vs. SiO_2 (all weight percent) the East Bay Granite (Unit 11) and the Bottom Brook Granite (Unit 12)..... 61

Figure 40: Variation diagrams of K_2O and Na_2O vs. SiO_2 (all weight percent) for the East Bay Granite (Unit 11) and the Bottom Brook Granite (Unit 12)..... 61

Figure 41: Variation diagrams of $\log_{10}$ Rb and $\log_{10}$ Sr (in g/t) vs. SiO_2 (in weight percent) for the East Bay Granite (Unit 11) and the Bottom Brook Granite (Unit 12)..... 61

Figure 42: Variation diagrams of $\log_{10}$ Rb/Sr ratios and $\log_{10}$ Li (in g/t) vs. SiO_2 (in weight percent) for the East Bay Granite (Unit 11) and the Bottom Brook Granite (Unit 12)..... 62

Figure 43: Variation diagrams of $\log_{10}$ Zr and $\log_{10}$ U (in g/t) vs. SiO_2 (in weight percent) for the East Bay Granite (Unit 11) and Bottom Brook Granite (Unit 12)..... 62

Figure 44: Variation diagrams of $\log_{10}$ K (in weight percent) vs. $\log_{10}$ Rb (in g/t) for the East Bay Granite (Unit 11) and Bottom Brook Granite (Unit 12)..... 62

Figure 45: Plot of K_2O + Na_2O (Alk_{tot}):Total iron as FeO (FeO_{tot}):MgO (all weight percent) for the East Bay Granite (Unit 11) and Bottom Brook Granite (Unit 12). Curved line separates tholeiitic compositions (above) from calc-alkaline (below); from Irvine and Barager (1971). Dashed line indicates field of calc-alkaline granitoid rocks from part of the Coastal Batholith of Peru; from Atherton *et al.* (1979)..... 63

Figure 46: Variation diagrams of Al_2O_3 vs. SiO_2 (both weight percent) for Unit 17, the Wolf Mountain Granite (Unit 18), and Units 19 and 21 of the North Bay Granite Suite..... 63

Figure 47: Variation diagrams of total iron as FeO (FeO_{tot}) vs. SiO_2 (both weight percent) for Unit 17, the Wolf Mountain Granite (Unit 18), and Units 19 and 21 of the North Bay Granite Suite..... 63

Figure 48: Variation diagrams of CaO vs. SiO_2 (both weight percent) for Unit 17, the Wolf Mountain Granite (Unit 18), and Units 19 and 21 of the North Bay Granite Suite..... 64

Figure 49: Variation diagrams of Na_2O vs. SiO_2 (both weight percent) for Unit 17, the Wolf Mountain Granite (Unit 18), and Units 19 and 21 of the North Bay Granite Suite..... 64

Figure 50: Variation diagrams of K_2O vs. SiO_2 (both weight percent) for Unit 17, the Wolf Mountain Granite (Unit 18), and Units 19 and 21 of the North Bay Granite Suite..... 64

Figure 51: Variation diagrams of $\log_{10}$ Rb (in g/t) vs. SiO_2 (in weight percent) for Unit 17, the Wolf Mountain Granite (Unit 18), and Units 19 and 21 of the North Bay Granite Suite..... 64

Figure 52: Variation diagrams of $\log_{10}$ Sr (in g/t) vs. SiO_2 (in weight percent) for Unit 17, the Wolf Mountain Granite (Unit 18), and Units 19 and 21 of the North Bay Granite Suite..... 65

Figure 53: Variation diagrams of $\log_{10}$ Rb/Sr (in g/t) vs. SiO_2 (in weight percent) for Unit 17, the Wolf Mountain Granite (Unit 18), and Units 19 and 21 of the North Bay Granite Suite..... 65

Figure 54: Variation diagrams of $\log_{10}$ Li (in g/t) vs. SiO_2 (in weight percent) for Unit 17, the Wolf Mountain Granite (Unit 18), and Units 19 and 21 of the North Bay Granite Suite..... 65

Figure 55: Variation diagrams of $\log_{10}$ U (in g/t) vs. SiO_2 (in weight percent) for Unit 17, the Wolf Mountain Granite (Unit 18), and Units 19 and 21 of the North Bay Granite Suite..... 65

Figure 56: Variation diagrams of $\log_{10}$ Zr (in g/t) vs. SiO_2 (in weight percent) for Unit 17, the Wolf Mountain Granite (Unit 18), and Units 19 and 21 of the North Bay Granite Suite..... 66

Figure 57: Variation diagrams of $\log_{10}$ K (in weight percent) vs. $\log_{10}$ Rb (in g/t) for Unit 17, the Wolf Mountain Granite (Unit 18), and Units 19 and 21 of the North Bay Granite Suite..... 66

Figure 58: Plot of K_2O + Na_2O (Alk_{tot}) : Total iron as FeO (FeO_{tot}) : MgO (all weight percent) for Unit 17, and the Wolf Mountain Granite (Unit 18), and Units 19 and 21 of the North Bay Granite Suite. Curved line separates tholeiitic compositions (above) from calc-alkaline (below); from Irvine and Barager (1971). Dashed line indicates field of calc-alkaline granitoids from part of the Coastal Batholith of Peru; from Atherton *et al.* (1979)..... 67

Figure 59: Variation diagrams of Al_2O_3 vs. SiO_2 (both weight percent) for the Wolf Lake North Granodiorite (Unit 10), the Meelpaeg Lake Granite (Unit 14), Unit 15, the Wolf Lake Granite (Unit 16) and the Upper Salmon Road Granite (Unit 20) of the North Bay Granite Suite..... 67

Figure 60: Variation diagrams of total iron as FeO (FeO_{tot}) vs. SiO_2 (both weight percent) for the Wolf Lake North Granodiorite (Unit 10), the Meelpaeg Lake Granite (Unit 14), Unit 15, the Wolf Lake Granite (Unit 16) and the Upper Salmon Road Granite (Unit 20) of the North Bay Granite Suite..... 68

Figure 61: Variation diagrams of CaO vs. SiO_2 (both weight percent) for the Wolf Lake North Granodiorite (Unit 10), the Meelpaeg Lake Granite (Unit 14), Unit 15, the Wolf Lake Granite (Unit 16) and the Upper Salmon Road Granite (Unit 20) of the North Bay Granite Suite..... 68

Figure 62: Variation diagrams of Na_2O vs. SiO_2 (both weight percent) for the Wolf Lake North Granodiorite (Unit 10), the Meelpaeg Lake Granite (Unit 14), Unit 15, the Wolf Lake Granite (Unit 16) and the Upper Salmon Road Granite (Unit 20) of the North Bay Granite Suite..... 69

Figure 63: Variation diagrams of K_2O vs. SiO_2 (both weight percent) for the Wolf Lake North Granodiorite (Unit 10), the Meelpaeg Lake Granite (Unit 14), Unit 15, the Wolf Lake Granite (Unit 16) and the Upper Salmon Road Granite (Unit 20) of the North Bay Granite Suite..... 69

Figure 64: Variation diagrams of $\log_{10}$ Rb (in g/t) vs. SiO_2 (in weight percent) for the Wolf Lake North Granodiorite (Unit 10), the Meelpaeg Lake Granite (Unit 14), Unit 15, the Wolf Lake Granite (Unit 16), and the Upper Salmon Road Granite (Unit 20) of the North Bay Granite Suite..... 70

Figure 65: Variation diagrams of $\log_{10}$ Sr (in g/t) vs. SiO_2 (in weight percent) for the Wolf Lake North Granodiorite (Unit 10), the Meelpaeg Lake Granite (Unit 14), Unit 15, the Wolf Lake Granite (Unit 16), and the Upper Salmon Road Granite (Unit 20) of the North Bay Granite Suite..... 70

Figure 66: Variation diagrams of $\log_{10}$ Rb/Sr (in g/t) vs. SiO_2 (in weight percent) for the Wolf Lake North Granodiorite (Unit 10), the Meelpaeg Lake Granite (Unit 14), Unit 15, the Wolf Lake Granite (Unit 16), and the Upper Salmon Road Granite (Unit 20) of the North Bay Granite Suite..... 71

Figure 67: Variation diagrams of $\log_{10}$ Zr (in g/t) vs. SiO_2 (in weight percent) for the Wolf Lake North Granodiorite (Unit 10), the Meelpaeg Lake Granite (Unit 14), Unit 15, the Wolf Lake Granite (Unit 16), and the Upper Salmon Road Granite (Unit 20) of the North Bay Granite Suite..... 71

Figure 68: Variation diagrams of $\log_{10}$ Li (in g/t) vs. SiO_2 (in weight percent) for the Wolf Lake North Granodiorite (Unit 10), the Meelpaeg Lake Granite (Unit 14), Unit 15, the Wolf Lake Granite (Unit 16), and the Upper Salmon Road Granite (Unit 20) of the North Bay Granite Suite..... 72

Figure 69: Variation diagrams of $\log_{10}$ U (in g/t) vs. SiO_2 (in weight percent) for the Wolf Lake North Granodiorite (Unit 10), the Meelpaeg Lake Granite (Unit 14), Unit 15, the Wolf Lake Granite (Unit 16), and the Upper Salmon Road Granite (Unit 20) of the North Bay Granite Suite..... 72

Figure 70: Variation diagrams of $\log_{10}$ K (in weight percent) vs. $\log_{10}$ Rb (in g/t) for the Wolf Lake North Granodiorite (Unit 10), the Meelpaeg Lake Granite (Unit 14), Unit 15, the Wolf Lake Granite (Unit 16), and the Upper Salmon Road Granite (Unit 20) of the North Bay Granite Suite..... 73

Figure 71: Plot of K_2O + Na_2O (Alk_{tot}) : Total iron as FeO (FeO_{tot}) : MgO (all weight percent) for the Wolf Lake North Granodiorite (Unit 10), the Meelpaeg Lake Granite (Unit 14), Unit 15, the Wolf Lake Granite (Unit 16), and the Upper Salmon Road Granite (Unit 20) of the North Bay Granite Suite. Curved line separates tholeiitic compositions (above) from calc-alkaline (below); from Irvine and Barager (1971). Dashed line indicates field of calc-alkaline granitoids from part of the Coastal Batholith of Peru; from Atherton *et al.* (1979)..... 73

Figure 72: (a) Histogram in frequency percent of $Al_2O_3/(CaO + Na_2O + K_2O)$ (all molecular weight percent) for Component 1 of the North Bay Granite Suite; (b) histogram in frequency percent of $Al_2O_3/(CaO + Na_2O + K_2O)$ (all molecular weight percent) for Component 2 of the North Bay Granite Suite. 74

Figure 73: Variation diagrams of Na_2O vs. K_2O (both weight percent) for each unit of the North Bay Granite Suite. Fields of I-, S- and A-type granites based on data graphically represented in White and Chappell (1983) 75

Figure 74: Plot of normative quartz (Q) : albite (Ab) : orthoclase (Or) for Units 9, 15 and 16 of the North Bay Granite Suite. After Currie and Pajari (1981); cotectics from Tuttle and Bowen (1958)..... 75

Figure 75: Logarithmic plot of Rb (g/t) vs. Y + Nb (g/t) for each unit (except Unit 21) of the North Bay Granite Suite. Boundaries shown (solid lines) are from Pearce *et al.* (1984). Dashed line is lower limit of D'Espoir Brook Granite analyses. Abbreviations: VAG = volcanic-arc granites; ORG = ocean-ridge granites; syn-COLG = syn-collisional granites; WPG = within-plate granite..... 76

PLATES

		Page
Plate 1:	Thin-bedded, laminated psammite and semipelite of the Spruce Brook Formation (subunit 2a); 3 km southeast of Wolf Lake; lens cap is 5 cm in diameter	9
Plate 2:	Zoned andalusite porphyroblast in fine-grained pelitic biotite–muscovite schist (subunit 2b) of the Spruce Brook Formation; cross-polarized light; scale: 25 mm = 1 mm; sample P14-1-83; 0.75 km east of Wolf Lake	10
Plate 3:	Orthoquartzite-pebble conglomerate (subunit 2c); pebbles aligned parallel to cleavage; 2 km southeast of Wolf Lake	10
Plate 4:	Migmatitic Spruce Brook Formation (subunit 2d); island in northeastern part of Meelpaeg Lake; lens cap is 5 cm in diameter	11
Plate 5:	Gently north-dipping, medium-bedded sandstones of the Salmon River Dam Formation (subunit 3a); 2 km west of D'Espoir Lake	12
Plate 6:	Northeast view of southeast-verging, overturned folds of Riches Island Formation semipelites (subunit 3c); 2.5 km northwest of Pomley Cove; lens cap is 5 cm in diameter	12
Plate 7:	(a) Xenoliths of migmatite (subunit 3d) in East Bay Granite; 7 km west of Garland Cove, North Bay; (b) gneissic granodiorite xenolith (subunit 3d) in the D'Espoir Brook Granite; 16 km west of D'Espoir Lake; lens caps in both photographs are 5 cm in diameter	13
Plate 8:	Embayed phenocryst in schistose tuff of the North Steady Pond Formation (subunit 3e); cross-polarized light; scale: 25 mm = 1 mm; sample L30-11-83; 1 km south of southeast corner of Meelpaeg Lake.	14
Plate 9:	Cordierite porphyroblasts (retrogressed to sericite and chlorite) in pelite (subunit 3h) of the North Steady Pond Formation; east side of 3-km-long pond, 7.5 km east of Wolf Lake; lens cap is 5 cm in diameter	15
Plate 10:	Isoclinally folded, biotite–muscovite psammites of the Bay du Nord Group (Unit 4); 1.5 km southeast of the southern end of Moon Pond; lens cap is 5 cm in diameter	15
Plate 11:	Laminated, medium-bedded sandstone having interbedded pebble breccia (Unit 5); northwest corner of Dolland Pond; lens cap is 5 cm in diameter	15
Plate 12:	(a) Feldspar-phyric basalt fragment in Silurian(?) granule conglomerate (Unit 5); (b) quartz and fine-grained cherty fragments in granule conglomerate having anastomosing cleavage; cross-polarized light; scale: 25 mm = 1 mm for both plates; sample L2-1A-83; on west side of Dolland Pond	16
Plate 13:	Riches Island Formation semipelite (subunit 3c) showing a staurolite porphyroblast having aligned quartz inclusions; matrix consists of recrystallized quartz and crenulated muscovite–biotite foliae; cross-polarized light; scale: 25 mm = 1 mm; sample L36-7-82; 2 km northwest of Pomley Cove	20
Plate 14:	Schistose crystal tuff of the North Steady Pond Formation (subunit 3e); cross-polarized light; scale: 25 mm = 1 mm; sample L30-11-83; 1 km south of east end of Meelpaeg Lake	22
Plate 15:	Strongly schistose, cataclastically deformed migmatite of the Bay du Nord Group (Unit 4); cross-polarized light; sample P27-9-83; scale: 25 mm = 1 mm; 2.5 km west of Moon Pond	22
Plate 16:	(a) Sheared magnesite (Unit 1) having exposed fresh (white) surface; 0.75 km southwest of D'Espoir Lake; lens cap is 5 cm in diameter; (b) fine-grained magnesite (Unit 1) having chromite (black) specks; 0.75 km southwest of D'Espoir Lake; plane-polarized light; sample L26-13-82; scale: 25 mm = 1 mm	24
Plate 17:	Strongly foliated granite and pegmatite of the D'Espoir Brook Granite (Unit 9) having north-dipping foliation; on D'Espoir Brook, 1.5 km southeast of D'Espoir Lake; lens cap is 5 cm in diameter	33

Page

Plate 18: Ridge of vein quartz (Unit 24) injected along the Meelpaeg Lake Fault Zone; 1 km south of D'Espoir Lake 33

Plate 19: Angular, biotite psammite xenoliths of the Spruce Brook Formation migmatite (subunit 2d) in the moderately foliated Wolf Lake North Granodiorite (Unit 10); northwest side of 7-km-long pond, northeast of Wolf Lake 37

Plate 20: Dyke of equigranular biotite granite cuts the East Bay Granite (Unit 11); 1.75 km northwest of Garland Cove, North Bay; hammer is 30 cm long..... 38

Plate 21: Aligned feldspar phenocrysts in the Bottom Brook Granite (Unit 12); northeastern end of East Bay; lens cap is 5 cm in diameter..... 39

Plate 22: Gently dipping, biotite-rich layers in the East Bay Granite (Unit 11); east side, northern end of Facheux Bay; layers are approximately 30 cm wide..... 39

Plate 23: (a) Meelpaeg Lake Granite (Unit 14) showing zoned plagioclase, biotite (grey, mottled) and plagioclase lath (white), set in poikiolitic microcline; cross-polarized light; sample L12-2-83; (b) oscillatory-zoned plagioclase set in poikiolitic microcline; Meelpaeg Lake Granite (Unit 14); sample L12-2-83; (as Plate 23a); scale for both plates: 25 mm = 1 mm; east side of Meelpaeg Lake..... 41

Plate 24: Equigranular, massive, biotite–muscovite granite of the Wolf Lake Granite (Unit 16); southern end of Wolf Lake; lens cap is 5 cm in diameter..... 42

Plate 25: (a) Massive, K-feldspar-porphyritic, biotite granite of the Dolland Brook Granite (subunit 17a); site of geochronology sample LD33-1-83; on Dolland Brook, 13.5 km north of southern end of map area 11P/15E (see Figure 18); lens cap is 5 cm in diameter; (b) south-trending ridges of vein quartz (Unit 24) on the west side of Dolland Brook, 5 km northeast of Moon Pond..... 43

Plate 26: Massive, K-feldspar-porphyritic, muscovite–biotite granite of the Wolf Mountain Granite (Unit 18); 12 km southwest of Dolland Pond (map area 11P/15); lens cap is 5 cm in diameter..... 44

Plate 27: (a) Massive, equigranular, muscovite–biotite granite of the Morgan Brook Granite (subunit 19b); 1.5 km west of the southern end of Dolland Brook (map area 11P/15); coin is 18 mm in diameter; (b) ridge of vein quartz (Unit 24) injected along a fault into the Morgan Brook Granite (subunit 19b); 2 km north-northeast of the southern end of Dolland Brook..... 46

Plate 28: (a) Massive, garnet–biotite–muscovite granite of the Hughes Brook Granite (subunit 19c) having prominent garnet phenocrysts (up to 1.5 cm in diameter); 7.5 km northeast of Thomey Cove, North Bay; (b) euhedral, fractured garnets (high relief) having quartz inclusions; fractures contain chlorite; Hughes Brook Granite (subunit 19c); plane-polarized light, sample L23-4-82; scale: 25 mm = 1 mm; location as Plate 28a 48

Plate 29: Euhedral microcline phenocrysts in the Upper Salmon Road Granite (Unit 20); north end of Salmon River (map area 11P/16); lens cap is 5 cm in diameter..... 48

Plate 30: Euhedral quartz (white) and sanidine (grey) phenocrysts in quartz–feldspar porphyry dykes (Unit 23); cross-polarized light; sample L24-8-83; scale: 25 mm = 1 m; 2.5 km southeast of Moon Pond..... 51

Plate 31: Tourmaline rosettes (black, top left of photograph) and pyrite cubes (black, centre) in the East Bay Granite (Unit 11); 3 km northwest of Brent Cove, Facheux Bay (map area 11P/9); lens cap is 5 cm in diameter 79

TABLES

Page

Table 1: Modal analysis of the Burgeo granite (Unit 6)..... 25

Table 2: Rb–Sr isotopic analyses from the East Bay Granite (R.F. Cormier, written communication to S.P. Colman-Sadd (1976))..... 26

Table 3: Rb–Sr isotopic data for the North Bay Granite Suite (from Elias, 1981)..... 27

Table 4: Rb–Sr data for the North Bay Granite Suite, D'Espoir Brook map area. Samples A-1 to A-4 are from the Upper Salmon Road Granite (Unit 20); samples B-1 to B-5 are from the East Bay Granite (Unit 11). The error quoted for the $^{87}Rb/^{86}Sr$ ratio is one standard deviation of the mean based on within-run statistics 28

Table 5: Main features of the granitoid rocks in the North Bay Granite Suite..... 34

Table 6: Modal analyses of Unit 8 and the D'Espoir Brook Granite..... 36

Table 7: Modal analyses of the Wolf Lake North Granodiorite (Unit 10)..... 38

Table 8: Modal analyses of the East Bay and Bottom Brook granites..... 40

Table 9: Modal analyses of the Meelpaeg Lake Granite (Unit 14) and the Wolf Lake Granite (Unit 16)..... 42

Table 10: Modal analyses of Unit 17 of the North Bay Granite Suite..... 44

Table 11: Modal analyses of the Wolf Mountain Granite (Unit 18)..... 45

Table 12: Modal analyses of Unit 19 of the North Bay Granite Suite..... 47

Table 13: Modal analyses of the Upper Salmon Road Granite (Unit 20)..... 49

Table 14: Modal analyses of Unit 21 of the North Bay Granite Suite..... 49

Table 15: Sampling statistics for the North Bay Granite Suite in map areas 1M/13, 11P/9, 11P/15, 11P/16, 12A/1, 12A/2 and 12A/3 east half..... 53

Table 16: Analysis of magnesite (Unit 1); sample 2241372..... 55

Table 17: Chemical composition of the Burgeo granite in the Dolland Brook (east half) map area; sample 2241500 55

Table 18: (a) Mean composition of each unit of Component 1 of the North Bay Granite Suite..... 56
(b) Mean composition of each unit of Component 2 of the North Bay Granite Suite..... 57

Table 19: Mean of A/CNK [molecular weight percent $Al_2O_3/(CaO+Na_2O+K_2O)$] and COR (normative corundum in weight percent) for each unit in Components 1 and 2 of the North Bay Granite Suite..... 73

Table 20: (a) Chemistry of the quartz–sanidine-porphyry dykes (Unit 23); major elements in weight percent; trace elements in g/t; (b) chemistry of the diabase dyke (Unit 25); major elements in weight percent; trace elements in g/t..... 78

MAPS

		Page
Map 1:	Geology of the Twillick Brook map area and geochemical sample locations	6
Map 89-98:	Geology of the Wolf Mountain (west half), and Burnt Pond (east half) map areas with geochemical sample sites in the North Bay Granite Suite	back pocket
Map 89-99:	Geology of the D'Espoir Brook map area with geochemical sample sites	back pocket
Map 89-100:	Geology of the Cold Spring Pond map area with geochemical sample sites in the North Bay Granite Suite	back pocket
Map 89-101:	Geology of the Dolland Brook (east half) map area with geochemical sample sites	back pocket
Map 89-102:	Geology of the Facheux Bay map area with geochemical sample sites in the North Bay Granite Suite	back pocket
Map 89-103:	Geology of the Wolf Mountain (east half) map area with geochemical sample sites	back pocket
Map 89-104:	Geology of the Dolland Brook (west half) map area with geochemical sample sites in the North Bay Granite Suite	back pocket
Map 89-105:	Geology of the St. Alban's map area with geochemical sample sites	back pocket

ABSTRACT

The North Bay Granite Suite, in southeastern Newfoundland, consists of syn- to post-Acadian granodiorites and granites that intruded the metasedimentary rocks of the Ordovician Baie d'Espoir and Bay du Nord groups, and the Spruce Brook Formation. The suite is composed of syntectonic, medium-grained biotite granodiorite and medium-grained muscovite–biotite granodiorite and granite, syn- and posttectonic garnet–biotite–muscovite granite, and posttectonic, coarse-grained, K-feldspar porphyritic muscovite–biotite granite. This latter granite has been dated at 396 Ma (U–Pb zircon). The Meelpaeg Lake Fault Zone, extending from the Meelpaeg Lake area to Salmon River, separates the suite into two, generally distinctive, components. The granites are extensively mylonitized along the fault zone, which contains inclusions of magnesite and metasedimentary rocks.

The Spruce Brook Formation consists of a lower sequence of psammites and semipelites overlain by pelites, quartz-rich psammites and quartzite-cobble conglomerates. The Baie d'Espoir Group and the stratigraphically equivalent Bay du Nord Group are dominated by semipelitic schist and psammite. The North Steady Pond Formation, of the Baie d'Espoir Group, contains a large proportion of felsic tuff and volcaniclastic sandstones. A tectonostratigraphic subdivision of central Newfoundland shows that the Spruce Brook Formation, in the Meelpaeg Lake area, forms part of the Meelpaeg Subzone of the Gander Zone, and the Baie d'Espoir and Bay du Nord groups form part of the Exploits Subzone of the Dunnage Zone. The contacts between the subzones are everywhere faulted.

The Ordovician units have been polydeformed and have recumbent folds and later open folding, and have been metamorphosed mainly in the greenschist to lower amphibolite facies. However, the Spruce Brook Formation, the Riches Island Formation of the Baie d'Espoir Group, and the Bay du Nord Group also have been metamorphosed in the upper amphibolite facies and contain extensive areas of migmatite.

The granites were sampled using a 2- by 2-km grid and have been analyzed for major elements and 21 trace elements. The chemistry indicates that the syntectonic biotite granodiorite is calc-alkaline and was probably derived by partial melting of lower crust or mantle. The medium-grained muscovite–biotite granodiorite and granite may have formed by nearly in situ melting of the Riches Island Formation. The garnet–biotite–muscovite granites are near-minimum melts that probably formed by partial melting of the Ordovician sediments. These granites are comparable to granites in northeastern Newfoundland. The posttectonic, coarse-grained, K-feldspar–porphyritic, muscovite–biotite granites have limited chemical variation and were probably derived by partial melting in the mid-crust, under relatively dry conditions.

The main mineral occurrence is tungsten mineralization in a posttectonic granite at Dolland Brook. There is some potential for gold mineralization in the volcanic units and the pyritic metasedimentary rocks of the Riches Island Formation. Barren quartz veins, up to 600 m long, occur along the major faults. The largest vein has been assessed to contain 1.2-m tonnes of 96 percent SiO_2. Samples from the various veins were assayed for gold but none was detected.

INTRODUCTION

The North Bay Granite Suite (North Bay Granite of Jewell, 1939) is a 4000-km² composite granitoid batholith, situated in southern and central Newfoundland (Figure 1) in the southeastern corner of the Hermitage Flexure (Williams *et al.*, 1970; see Figure 4), which is a sinuous belt of Lower Paleozoic metasedimentary and metavolcanic rocks. These rocks, which include the Middle Ordovician Baie D'Espoir Group (Anderson, 1967; Series of Jewell, 1939), the Ordovician Bay du Nord Group (Cooper, 1954; revised by Chorlton, 1978) and the Spruce Brook Formation (Colman-Sadd and Swinden, 1984) have been intruded by numerous granitoid plutons. The Burgeo granite is an extensive composite batholith that lies to the south of the Bay du Nord Group. To the north, the equally extensive North Bay Granite Suite has intruded all the Lower Paleozoic strata. Parts of the suite have been deformed with the adjacent metasedimentary rocks indicating that the batholith is a syn- to posttectonic intrusion.

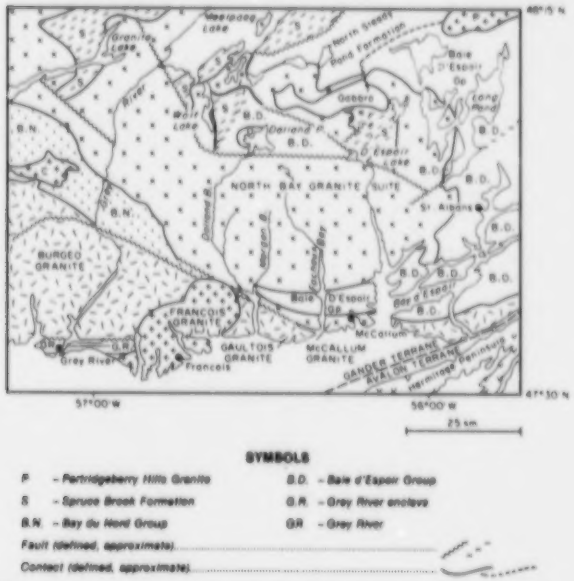

Figure 1. *Regional setting of the North Bay Granite Suite. C=Cochrane Pond Granite.*

The areas mapped cover most of the central and eastern parts of the North Bay Granite Suite; namely Dolland Brook (11P/15E), D'Espoir Brook (11P/16) and Wolf Mountain (12A/2E; Figure 2). The North Bay Granite Suite was sampled for geochemical analysis in these map areas and also to the south, in the Facheux Bay map area (11P/9). Map area 11P/15W, (the North Bay Granite Suite) was sampled by Blackwood (1984). The geology of map areas 11P/15 and 16 is summarized in O'Brien and Dickson (1986). Neighbouring parts of the North Bay Granite Suite were sampled in 1M/13, 2D/4, 12A/2W and 12A/3; this augmented work by Dickson (1982) and Colman-Sadd *et al.* (1981).

LOCATION AND ACCESS

The map areas are located in southern and central Newfoundland. The closest communities are St. Alban's, at Bay d'Espoir, which is located 8 km east of map area 11P/16, and McCallum, located on the coast, 5 km south of the North Bay Granite Suite, in map area 11P/9. Access to parts of map area 11P/16 is gained from St. Alban's by the Newfoundland Hydro road to the Upper Salmon hydro-generating station and to map area 12A/2 by the 70-km-long Newfoundland Hydro and Abitibi-Price (Nfld.) Limited road from Millertown to Meelpaeg Lake. The southern parts of map areas 11P/9 and 11P/16 can be reached by boat along the fiords known as East Bay, North Bay and Facheux Bay but access to the interior from these bays is hindered by high cliffs and steep river valleys. Access is best gained by helicopter from St. Alban's or Milltown, to the east of the project area. Float planes often land on Dolland Pond and the central part of Wolf Lake. The other ponds and lakes are generally too shallow for float planes.

PHYSIOGRAPHY

The map areas form part of the Atlantic Uplands of Twenhofel and MacClintock (1940). The Uplands have been dissected into two topographic levels or peneplains. The highest peneplain is represented by the southerly trending ridge to the southwest of Meelpaeg Lake having a high point of 434 m (1424 ft) and several hill tops over 400 m (1300 ft). This corresponds to the High Valley Peneplain of Twenhofel and MacClintock (1940). The majority of the map area is included in the Lawrence Peneplain with an average height of about 300 m and numerous rolling hills (average height 330 m). The southern part of this plateau has been deeply dissected by fiords and glacial valleys. The fiords attain depths in excess of 600 m below sea level (Williams, 1971) with near-vertical walls up to 350 m.

The area is covered by extensive till deposits and bog. Only the upland areas toward the coast are well exposed. Till deposits are probably over 10 m thick over much of the undulating terrain. Drumlins and eskers are common. An esker over 10 km in length is preserved in the Wolf Lake area. Crag-and-tail, stoss-and-lee features, and striae indicate a southerly ice-flow direction. Some serpentinite erratics were located about 30 km south of the nearest known ultramafic bodies. However, most erratics are of local origin.

Drainage is generally poor with numerous small lakes and bogs. The main rivers drain to the south and, toward the coast, are contained within steep-sided valleys. The low-lying area around Meelpaeg Lake was flooded following construction of a dam at the head of Grey River. Thus, extensive areas of the lake are very shallow with numerous tree stumps and rocks at or near the surface in the flooded areas.

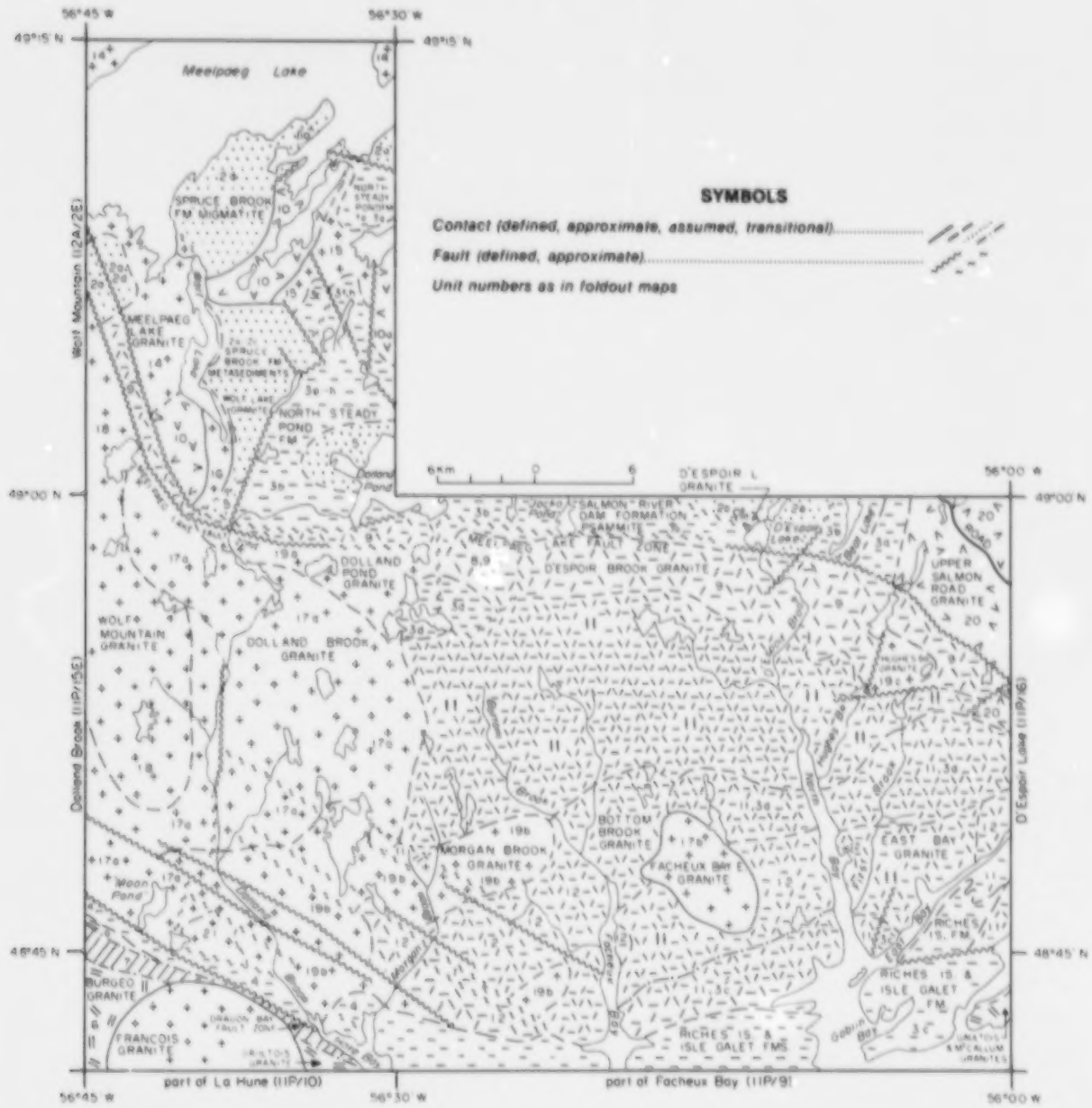

Figure 2. *Map of the North Bay Granite Suite indicating the distribution of the main units.*

DEFINITION OF THE NORTH BAY GRANITE SUITE AND ITS MEMBERS

The purpose of this section is to redefine the North Bay Granite of Jewell (1939), elevate the rank of the North Bay Granite and to formally name some of its members.

HISTORY OF NOMENCLATURE

The term North Bay Granite was introduced by Jewell (1939) following reconnaissance field work in the Bay (Baie) d'Espoir area. Jewell's field work concentrated on the extensive coastal exposures. The name was introduced for the granites in the Long Pond (west of St. Alban's)–North

LEGEND (for Figure 2)

SILURIAN–DEVONIAN

NORTH BAY GRANITE SUITE (Units 8 to 21)

21 — *Pink to buff, weakly foliated, medium grained, equigranular to feldspar porphyritic, muscovite–biotite granite*

20 — UPPER SALMON ROAD GRANITE: *Grey to pink, massive to weakly foliated, K-feldspar porphyritic, biotite granite*

19 — *Pink, massive to weakly foliated, medium grained, K-feldspar porphyritic, muscovite–biotite ± garnet granite*; **19a,** DOLLAND POND GRANITE; **19b,** MORGAN BROOK GRANITE; **19c,** HUGHES BROOK GRANITE; **19d,** D'ESPOIR LAKE GRANITE

18 — WOLF MOUNTAIN GRANITE: *Pink to buff, massive to weakly foliated, coarse grained, K-feldspar porphyritic, muscovite–biotite granite*

17 — *Pink to buff, massive to weakly foliated, coarse grained, K-feldspar porphyritic, biotite granite*: **17a,** DOLLAND BROOK GRANITE; **17b,** FACHEUX BAY EAST GRANITE

16 — WOLF LAKE GRANITE: *White to buff, massive, coarse grained, equigranular, garnet–biotite–muscovite granite*

15 — *Buff, massive, medium grained, equigranular, muscovite–biotite granite*

14 — MEELPAEG LAKE GRANITE: *Buff, weakly foliated to massive, medium grained, equigranular, biotite ± muscovite granite and granodiorite*

13 — *Pink to orange, foliated, medium grained, equigranular, muscovite–biotite granite*

12 — BOTTOM BROOK GRANITE: *Grey to orange, weakly foliated to massive, feldspar porphyritic, biotite ± muscovite granite and granodiorite*

11 — EAST BAY GRANITE: *Grey to buff, weakly foliated to massive, medium grained, equigranular, biotite ± muscovite granite and granodiorite; commonly contains screens of migmatite*

10 — WOLF LAKE NORTH GRANODIORITE: *Grey to buff, foliated, medium grained, equigranular to feldspar porphyritic, biotite granodiorite; commonly contains screens of migmatite*

9 — D'ESPOIR BROOK GRANITE: *Pink to white, strongly foliated to massive, medium- to coarse-grained, equigranular, garnet–biotite–muscovite granite; locally contains abundant granite pegmatite*

8 — *Pink to buff, strongly foliated, coarse grained, microcline porphyritic, biotite granite*

SILURIAN

BURGEO GRANITE (Units 6 and 7)

7 — *Pink, protomylonitic to mylonitic, K-feldspar porphyroclastic granite*

6 — *Pink, very strongly foliated to protomylonitic, medium grained, equigranular, muscovite–biotite granite*

SILURIAN?

5 — *Interbedded sandstone, siltstone and slate, and polymict pebble conglomerate; minor, thickly bedded, subangular, polymict cobble conglomerate*

LOWER TO MIDDLE ORDOVICIAN

BAY DU NORD GROUP

4 — *Highly deformed, migmatitic metasediment and psammite cut by numerous granite veins, dykes and plugs*

BAIE D'ESPOIR GROUP (Units 3a to 3h)

NORTH STEADY POND FORMATION (Units 3e to 3h)

3h — *Grey and green, thin bedded, slate and minor sandstone*

3g — *Very thickly bedded, brown weathering, grey, massive sandstone and minor interbeds of Unit 3f*

3f — *Thin bedded, black, highly folded and quartz veined, graphitic slate and siltstone*

3e — *Very thickly bedded, schistose, quartz–feldspar crystal tuff and coarse grained, epiclastic sandstone*

RICHES ISLAND FORMATION (Units 3c and 3d)

3d — *Migmatite locally with sillimanite porphyroblasts; probably derived from Unit 3c*

3c — *Highly deformed, highly metamorphosed, pelitic, semipelitic and psammitic schist; intruded by numerous dykes of East Bay Granite*

SALMON RIVER DAM FORMATION (Units 3a and 3b)

3b — *Thin bedded, strongly cleaved, commonly rust coloured, biotite pelite*

3a — *Thin- to medium-bedded, well-cleaved, grey to cream coloured, thin- to medium-bedded sandstone, calcareous sandstone and siltstone, and thick bedded limestone*

SPRUCE BROOK FORMATION (Units 2a to 2e)

2e — *Highly deformed, psammitic and semipelitic schist and minor phyllitic rhyolitic tuff; locally intruded by strongly foliated granitoid dykes*

2d — *Migmatite and biotite psammite intruded by numerous weakly foliated granitoid dykes; high-grade equivalent of Units 2a and 2b*

2c — *Clast-supported, orthoquartzite-cobble conglomerate and minor matrix-supported, slate- and quartzite-pebble breccia and coarse sandstone; minor lapilli tuff*

2b — *Thin bedded, grey to black pelite and minor psammite and semipelite*

2a — *Biotite psammite and orthoquartzite; minor semipelite*

and East Bay–Facheux Bay area. The rock was described as "... a light grey, though locally reddish or pinkish, binary granite." (Jewell, 1939, page 9). Subsequent workers in the area (Winek, 1954; Colman-Sadd, 1974, 1976, 1980a,b,c, 1983, 1984, 1986, 1987; Elias, 1981; Elias and Strong, 1982; Dickson, 1982; Dickson and Tomlin, 1983; Dickson and Delaney, 1984a,b,c; Blackwood, 1985; O'Brien and Tomlin, 1985a) have maintained the use of the term North Bay Granite and extended the area defined as part of the North Bay Granite to include the Granite Lake and Meelpaeg Lake areas. However, several important studies (Riley, 1957; Williams, 1970, 1971) left the granite unnamed.

O'Brien and Tomlin (1985a) indicated that the North Bay Granite continues from the Burnt Pond (12A/3, west half) map area into the King George IV (12A/4) map area, where Kean (1983) mapped the Buck Lake Granite.

Williams (1978) introduced the name Facheau (= Facheux) Bay Batholith for areas traditionally included in the North Bay Granite.

NAME TO ABANDON

North Bay Granite has precedence over Facheau Bay Batholith. There is no provision for the term 'batholith' in the recommended code for stratigraphic nomenclature (North American Commission on Stratigraphic Nomenclature, 1983). Thus, the term Facheau Bay Batholith should be abandoned.

BOUNDARY REVISION AND RANK ELEVATION TO NORTH BAY GRANITE SUITE

Granitoid rocks extend from Long Pond and Salmon River, in the east, to the King George IV and Meelpaeg Lakes areas in the northwest and north-northwest, respectively. Within this 4000-km² area, lithologically distinct or geographically separated units have been outlined. Rock types include granite and granodiorite and small areas of tonalite and gabbro. The rock described by Jewell (1939) is dominantly granite by Streckeisen's (1976) classification and it is estimated that 95 percent of the study area is granite *(sensu stricto)*. However, as numerous distinctive granite plutons comprise the North Bay Granite, the rank of the North Bay Granite is elevated to North Bay Granite Suite.

The North Bay Granite Suite includes the syntectonic granites and granodiorites exposed in the North Bay, the northern portion of the Grey River, Facheux Bay and Meelpaeg Lake areas. It also consists of cataclastically deformed leucogranites between Meelpaeg Lake and Salmon River and the essentially posttectonic granites exposed between Meelpaeg Lake and Morgan Brook, with smaller posttectonic intrusions to the east at D'Espoir Lake and northeast of North Bay (Figure 2).

NEW NAMES

Names for the members of the North Bay Granite Suite are formally introduced and defined here. Detailed descriptions are given in this report and boundaries are indicated on the accompanying maps and Figure 2.

The D'Espoir Brook Granite (Figure 2 and Map 89-99) is named after D'Espoir Brook along which the granite is well exposed. The granite extends from Wolf Mountain to Salmon River. The main rock type is strongly deformed, medium-grained, muscovite–biotite–garnet granite containing minor aplite and pegmatite.

The Wolf Lake North Granodiorite (Figure 2 and Map 89-103) is named after Wolf Lake where, in the northern part of the lake, the granodiorite is well exposed. The granodiorite is also well exposed in an unnamed pond to the northeast of Wolf Lake. The rock type is foliated, biotite granodiorite.

The East Bay Granite (Figure 2 and Maps 89-99, 89-102) is named after East Bay. This name replaces North Bay Granite, which has been raised to Suite level, and now refers to the granite exposed in both the North Bay and East Bay area. The granite is typically a medium-grained, equigranular, weakly foliated, muscovite–biotite granite with lesser granodiorite. This unit, which may eventually require further revision, includes similar granites exposed around Facheux Bay.

The Bottom Brook Granite (Figure 2 and Maps 89-99, 89-102) is named after Bottom Brook, north of Facheux Bay, where the granite is well exposed. This granite occurs in association with the East Bay Granite. The Bottom Brook Granite is a weakly foliated, medium-grained, feldspar-porphyritic, muscovite–biotite granite.

The Meelpaeg Lake Granite (Figure 2 and Map 89-103) is named after Meelpaeg Lake and the granite is well exposed at its western end. The granite is a weakly deformed, medium-grained, feldspar-porphyritic, muscovite–biotite granite containing minor granodiorite.

The Wolf Lake Granite (Figure 2 and Map 89-103) is named after Wolf Lake where the granite is well exposed at its southern end. The typical rock is a massive, coarse-grained, equigranular, garnet–biotite–muscovite granite.

The Dolland Brook Granite (Figure 2 and Map 89-101) is named after Dolland Brook along which the granite is well exposed. The unit extends from Morgan Brook, west, to the Grey River (Map 89-104). The rock is a massive, medium- to coarse-grained, K-feldspar porphyritic, biotite granite. This granite has been dated by the U–Pb method at 396 Ma (see New U–Pb Age Determinations section; Dunning *et al.*, 1988).

The term Facheux Bay East Granite (Figure 2 and Map 89-99) is introduced for the granite located 2 km east of the

head of Facheux Bay. The granite is a massive, medium- to coarse-grained, K-feldspar porphyritic, biotite granite. The granite has intruded the East Bay and Bottom Brook granites.

The Wolf Mountain Granite (Figure 2 and Map 89-103) is named after Wolf Mountain where the granite is well exposed. This granite extends from Granite Lake, southeast, to Dolland Brook. The main rock type is massive, buff-coloured, coarse-grained, K-feldspar porphyritic, muscovite–biotite granite. The northern part of the granite, to the east of Granite Lake, has been hydrothermally altered to a bright pink colour containing exsolved hematite and secondary white mica and contains important W–Mo–Bi mineralization.

The Morgan Brook Granite (Figure 2 and Map 89-99) is named after Morgan Brook where the granite is well exposed. The main rock type is massive, medium-grained, K-feldspar porphyritic, muscovite–biotite granite.

The Dolland Pond Granite (Figure 2 and Map 89-101) is named after Dolland Pond, to the south of which, the granite is locally well exposed. The main rock type is massive, medium-grained, K-feldspar porphyritic, muscovite–biotite ± garnet granite.

The Hughes Brook Granite (Figure 2 and Map 89-99) is named after Hughes Brook located in the northern part of North Bay. The granite is well exposed around the headwaters of Hughes Brook. The main rock type is massive, coarse-grained, biotite–garnet ± muscovite granite.

The D'Espoir Lake Granite (Figure 2 and Map 89-99) is named after D'Espoir Lake where the granite is well exposed. The main rock is massive to very weakly foliated, K-feldspar porphyritic, garnet–biotite–muscovite granite.

The Upper Salmon Road Granite (Figure 2 and Maps 89-99, 89-100, 89-105 and Map 1) is named after the access road from St. Alban's to the Upper Salmon hydro-electric generating station. The granite is well exposed along the road, to the west of Long Pond. The main rock is massive to weakly foliated, coarse-grained, K-feldspar porphyritic, muscovite–biotite granite and granodiorite. This unit is in fault contact with the D'Espoir Brook Granite and has a gradational contact with medium-grained, equigranular granites assigned to the East Bay Granite.

PREVIOUS WORK

The earliest work in the 11P/9 and 11P/16 map areas was carried out by Jewell (1939) who mapped part of the North Bay Granite Suite in the North Bay, East Bay and Pomley Cove areas. Jewell (1939) noted that the granite is a muscovite–biotite granite having inclusions of schist and that the granite was massive except in the vicinity of schist inclusions. Phendler (1950) mapped the area around Lake Ebbegunbaeg, which is now part of the Meelpaeg Lake reservoir, and described briefly the granites and metasedimentary rocks. He concluded that the area to the southwest of Lake Ebbegunbaeg, which is dominated by granites, had little economic potential.

The southwestern part of the Dolland Brook map area (11P/15) was examined by Scott and Conn (1950) for the Buchans Mining Company. They mapped the deformed granitoid rocks and migmatites, southwest of Dolland Brook, which are intruded, to the north, by the Dolland Brook Granite and to the south by the Burgeo granite. Extensive fine-grained, quartz–feldspar-porphyry dykes were mapped in the Dolland Brook Granite. Scott and Conn's work was incorporated in Smyth's (1979) compilation map of the 11P/15 map area. Widmer (1950) included the work of Jewell (1939) in a map of the Hermitage Bay area. An aerial photographic interpretation of parts of the Dolland Brook, D'Espoir Brook and Wolf Mountain map areas was included in a series of maps and report by Baird *et al.* (1951), who attempted to outline areas of granitoid and metasedimentary rocks with little description of the bedrock.

Winek (1954) mapped the eastern contact of the East Bay Granite to the east and south of Salmon River. Dykes of granite and pegmatite within the adjacent metasedimentary rocks, and inclusions of schistose metasedimentary rocks within the granite, were noted. Most of Winek's work focussed on the molybdenite prospects within pegmatites associated with the East Bay Granite, around North West Cove, in the adjacent St. Alban's map area (1M/13).

Reconnaissance mapping, at a 1:250,000 scale, by Williams (1970, 1971), outlined the North Bay Granite Suite and indicated the presence of strongly foliated granitoid rocks and the metasedimentary rocks and migmatites of the Baie d'Espoir Group along its northern and southern contacts. Williams (1971) noted an abundance of migmatite screens in the East Bay Granite around North Bay.

Colman-Sadd (1974) carried out reconnaissance mapping of the North Bay and East Bay areas and outlined an area of gneisses within the North Bay Granite Suite. These gneisses were considered to be possibly Precambrian in age.

Butler and Greene (1976) examined in detail a large quartz vein, situated 15 km west of D'Espoir Lake, to determine the economic potential of the vein as a source of silica.

Butler and Davenport (1978), and Davenport and Butler (1981, 1982) carried out a lake-sediment geochemical survey, which included most of the area underlain by the North Bay Granite Suite. Within the Wolf Mountain (east half), Dolland Brook and D'Espoir Brook map areas, anomalous values for Mo and U were located over the North Bay Granite Suite, with multisample W anomalies in the East Bay Granite, south of East Bay. In the Dolland Brook Granite, two W anomalies are located in the vicinity of Dolland Brook, and another in the Bottom Brook area. These have been examined by McConnell (1983, 1984a,b, 1985) who carried out stream sediment, soil-sampling and bedrock geochemical surveys.

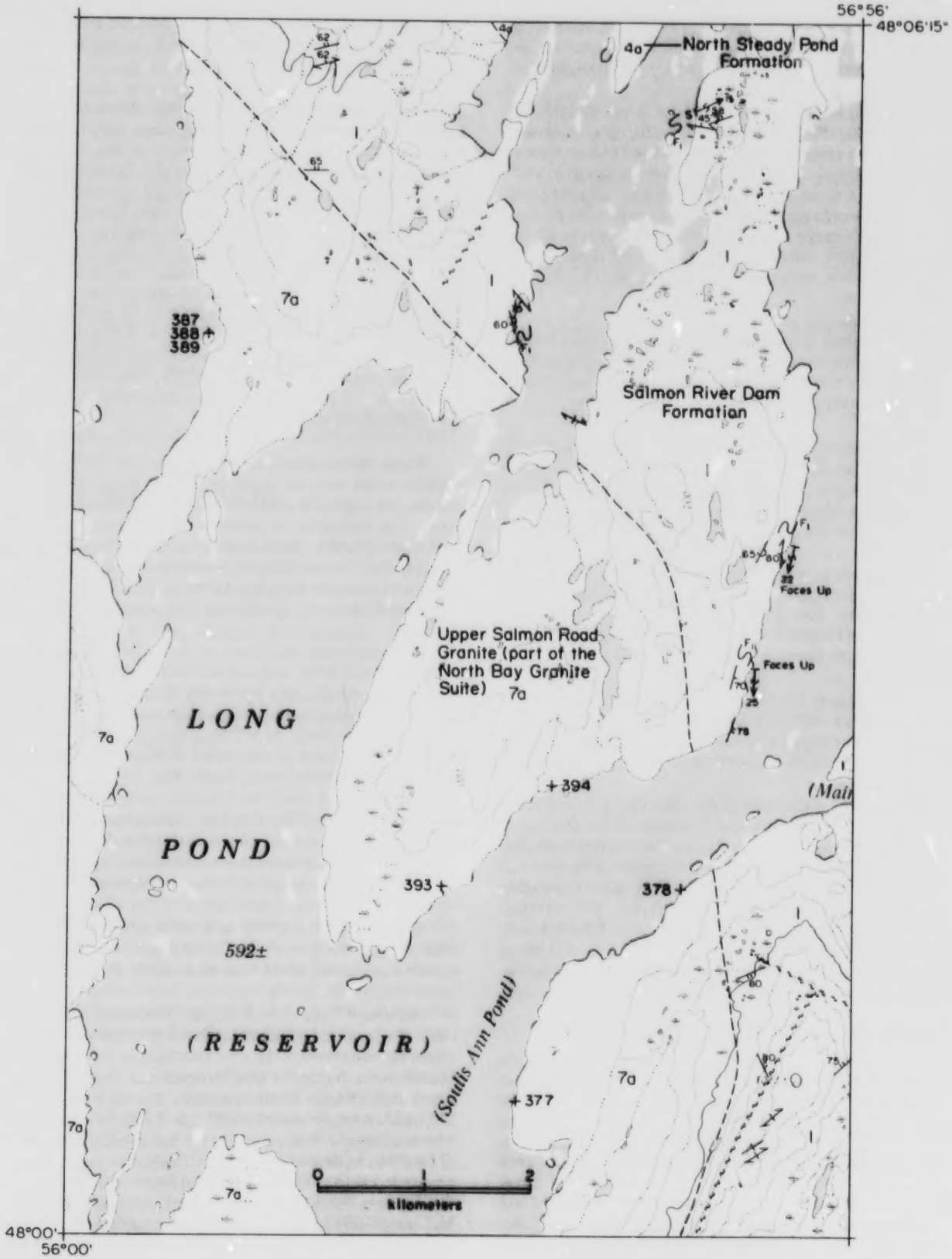

Map 1. *Geology of the Twillick Brook (2D/4) map area and geochemical sample locations.*

Dickson and Tomlin (1983, 1984) and Dickson and Delaney (1984a,b,c) produced the first 1:50,000-scale maps of the Wolf Mountain (east half), Dolland Brook (east half) and the D'Espoir Brook map areas.

An airborne gamma-ray spectrometric survey, which included the North Bay Granite Suite, was carried out by the Geological Survey of Canada (1983a,b,c).

Rio Algom Exploration Incorporated (Bucknell, 1984; Palster, 1984) examined several areas of the North Bay Granite Suite, which showed anomalous W in lake sediments (Davenport and Butler, 1982).

Adjacent parts of the North Bay Granite Suite were mapped and/or sampled for lithogeochemistry by Colman-Sadd (map area 1M/13, 1976; 2D/4, 1983, 1984); Blackwood (11P/9, 1985; 11P/15W, 1984) and O'Brien and Tomlin (12A/3W, 1985a).

SEDIMENTARY AND VOLCANIC ROCKS

INTRODUCTION

In the study area, the sedimentary and volcanic rocks are divided into two main zones separated by the Meelpaeg Lake Fault Zone, which forms the northern boundary of the eastern portion of the North Bay Granite Suite. The Spruce Brook Formation and the North Steady Pond and Salmon River Dam formations of the Baie D'Espoir Group, and unnamed clastic sediments (Unit 5) lie within and to the north of the fault zone; the Riches Island Formation of the Baie D'Espoir Group and Bay du Nord Group lie well to the south of the fault zone along the southern contact of the North Bay Granite Suite (Figures 2 and 3).

The Meelpaeg Lake Fault Zone is indicated, in the field, by brecciated granite, strongly foliated (see Plate 17) to mylonitic granite along the trace of the zone, abrupt changes in rock type across the trace, quartz veins (see Plate 18) and ultramafic and sedimentary slivers (see Plate 16a; also Colman-Sadd, 1976) along the trace, abrupt breaks in slope and gullies along the faulted contacts. The fault trace does not always follow contacts between units, e.g., metasedimentary rocks assigned to the Salmon River Dam Formation are, in places, in intrusive contact with the D'Espoir Brook Granite and the fault trace lies to the north of the contact within the Salmon River Dam Formation. Similarly, the Spruce Brook Formation, southwest of Meelpaeg Lake, is cut by a branch of the fault. To the west of Wolf Lake, the D'Espoir Lake Granite is fault-bounded along the eastern and western contacts.

The exact stratigraphic position of all the sedimentary and volcanic rocks within the map areas is uncertain. The Spruce Brook Formation (Unit 2; Colman-Sadd and Swinden, 1984) was considered to be Middle Ordovician (late Llanvirn to Llandeilo), based on fossils discovered in the Through Hill area (Colman-Sadd and Russell, 1982; Boyce, 1987) 60 km northeast of Meelpaeg Lake. The unit has been reinterpreted to unconformably overlie the Spruce Brook Formation indicating the unit is Arenig or older (Dec and Colman-Sadd, 1990). The Baie d'Espoir Group (Unit 3; Anderson, 1967) has been divided into several formations by Colman-Sadd (1976, 1980a,b). The lower part of the group is the Salmon River Dam Formation (subunits 3a, 3b). The Salmon River Dam Formation is overlain, from northwest to southeast, by the North Steady Pond Formation (subunits 3e to h) and St. Joseph's Cove Formation. The Riches Island Formation (subunits 3c, 3d) and the Isle Galet Formation may be lateral equivalents of the St. Joseph's Cove Formation and North Steady Pond Formation, respectively. The Isle Galet Formation is interpreted to be in tectonic contact with the more highly deformed and metamorphosed Little Passage gneisses (Colman-Sadd, 1980a); the tectonic contact replaces a possible angular unconformity.

Dunlop (1954), Anderson (1967) and Colman-Sadd (1976) obtained the few fossils known from the Baie d'Espoir Group. These fossils were obtained from the Riches Island, Isle Galet and St. Joseph's Cove formations and indicate that the age of these formations is "between the late Arenig and the early Caradoc, inclusive" (Colman-Sadd, 1976, page 6).

The Bay du Nord Group (Unit 4) is continuous with the Baie d'Espoir Group. The Bay du Nord Group is defined from southwestern Newfoundland (Cooper, 1954; revised by Chorlton, 1978). Fossils have not been found in the group but radiometric dates of 450 to 445 Ma on volcanic rocks within the group (Dallmeyer, 1980; Chorlton and Knight, 1983) indicate a Late Ordovician age (Ashgillian–Caradocian; Harland *et al.*, 1982) for the group. More recently, zircons from strongly schistose felsic volcanic rocks of the Bay du Nord Group in the Dolland Brook (west half) map area (Blackwood, 1984) have been dated by Dunning *et al.* (1990) and have a U–Pb age of 466 $\pm$ 3 Ma, indicating a mid-Ordovician (lower Llandeilan; Harland *et al.*, 1982) age for the Bay du Nord Group.

A sequence of interbedded pebble conglomerate, coarse sandstone, siltstone and subangular cobble conglomerate (Unit 5) is exposed around Dolland Pond (Colman-Sadd, 1984). The pebble- to coarse-sand-sized fragments are similar to the rock types in the North Steady Pond Formation. The age of Unit 5 is unknown, but on the basis of its low metamorphic grade and the polymict composition of the coarse clastic rocks, the unit is considered to be younger than the North Steady Pond Formation and, therefore, possibly Silurian. The unit is considered to be unrelated to the mainly oligomictic, orthoquartzite-boulder and cobble conglomerates (subunit 2c) of the Spruce Brook Formation in the Wolf Lake area (Williams, 1970).

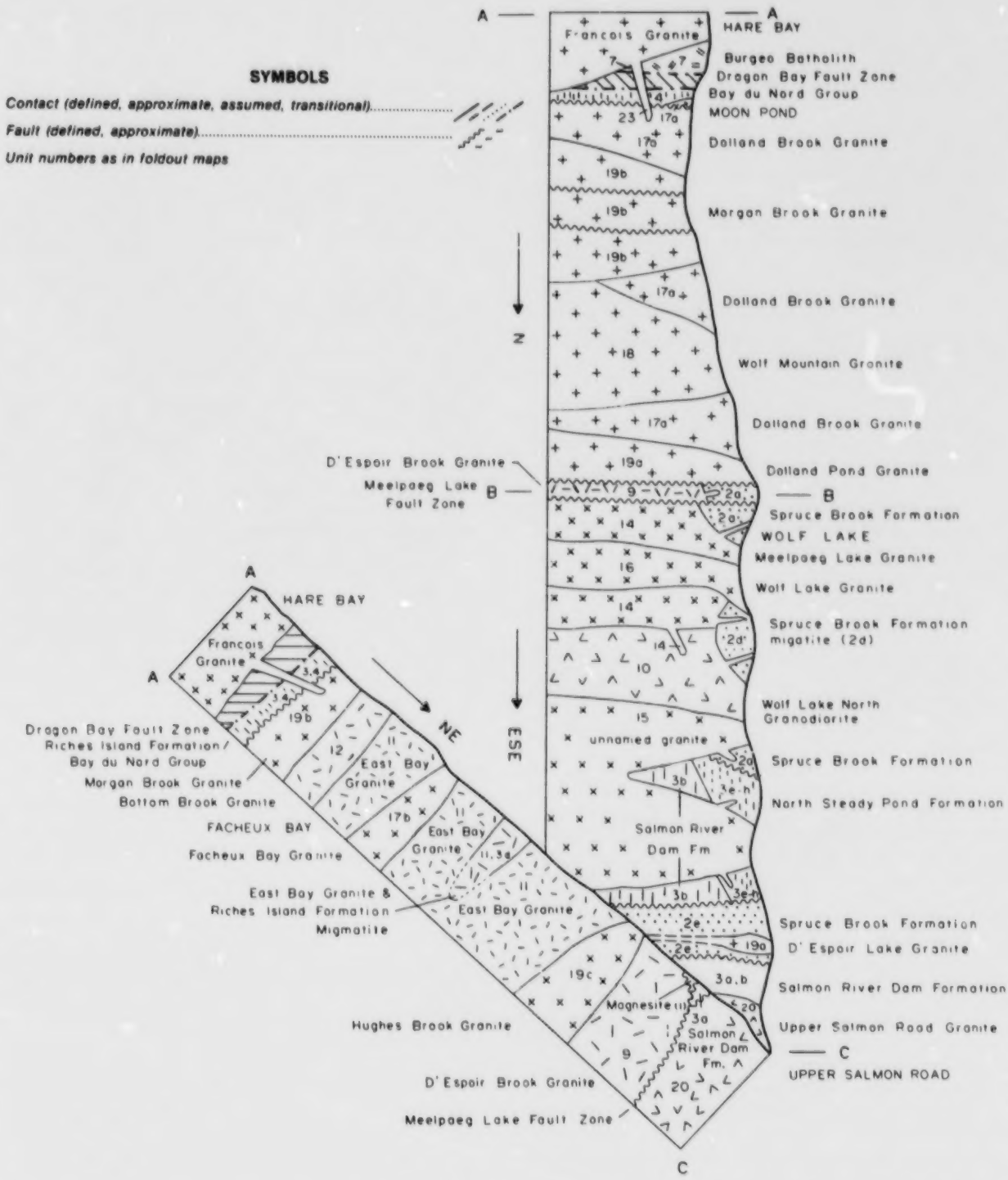

Figure 3. *Schematic diagram of the contact relations of the varios components of the North Bay Granite Suite and adjacent units.*

Williams *et al.* (1988) divided the central Newfoundland Lower Paleozoic rocks into the Dunnage and Gander zones (Figure 4). The Exploits Subzone of the Dunnage Zone includes the Baie d'Espoir and Bay du Nord groups. The Meelpaeg Subzone of the Gander Zone is represented by the Spruce Brook Formation. The contact between the Exploits

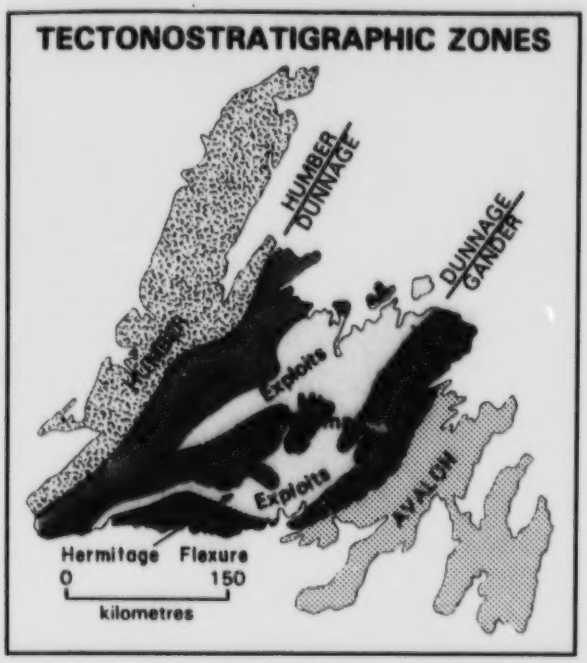

Figure 4. *Tectonostratigraphic subdivisions of the Newfoundland Appalachians (from Williams et al., 1988).*

and Meelpaeg subzones is everywhere faulted, supporting the model of Williams *et al.* (1988), which requires faulted contacts. The Spruce Brook Formation was interpreted by them to occur in structural windows in the overlying Exploits Subzone. Most exposed faults are steeply dipping but in the D'Espoir Lake area, gently dipping foliations in the D'Espoir Brook Granite may reflect southerly directed thrusts that contain slivers of ultramafic and sedimentary rocks. Certainly, the Meelpaeg Lake–D'Espoir Lake area contains a complicated juxtaposition of sedimentary and volcanic rocks of the Baie d'Espoir Group and Spruce Brook Formation. These relationships are shown schematically in Figure 3.

SPRUCE BROOK FORMATION (UNIT 2)

The Spruce Brook Formation (Colman-Sadd, 1985) is located mainly in the Wolf Mountain map area and continues, to the east and northeast, into the Cold Spring Pond (12A/1) and Great Burnt Lake (12A/8) map areas (Colman-Sadd, 1984, 1985); a small area to the north of D'Espoir Lake is underlain by the Spruce Brook Formation and here forms the southern termination of a more extensive belt, exposed to the north, in the Cold Spring Pond map area (12A/1; Colman-Sadd, 1983, 1984). Contacts between the Spruce Brook Formation and the Baie d'Espoir Group, in the study area, are faulted and the North Bay Granite Suite has intruded the formation. Two deformed diabase dykes (Unit 25) were located, which also have intruded the formation.

The Spruce Brook Formation has been divided into five subunits based on rock type (subunits 2a to 2c) and grade of metamorphism (subunits 2d, 2e). Subunit 2a is dominated by psammitic schist that forms an easterly trending belt to the east of Wolf Lake. Subunit 2b is dominated by pelitic schist. Subunit 2c is dominated by orthoquartzite-cobble conglomerate. Subunit 2d is composed of migmatite that is probably the high-grade equivalent of subunit 2a. Subunit 2e lies well to the east of the other units and is composed of semipelitic, psammitic and minor felsic volcanic schist.

The dominant rock type of subunit 2a is a medium-grained, massive to schistose, muscovite–biotite psammite having subordinate orthoquartzite, semipelite and rarely pelite (Plate 1). Bedding is locally preserved in the psammitic units and, in one place, a younging-direction was found. Beds range in thickness from 1 cm to over 1 m but are most commonly in the 4- to 20-cm range. Beds are generally parallel-sided having little local variation in grainsize or texture. Only in the most quartz-rich psammites are primary features such as parallel-laminations and cross laminations found. Metamorphism and strong deformation in subunit 2a has probably obliterated primary features in the less psammitic rocks. Similarly, in the less psammitic rocks the original mineralogy, apart from quartz and feldspar, has been converted to metamorphic minerals. The orthoquartzite contains less than 5 percent feldspar. Rock fragments have not been found. In the semipelites, plagioclase forms a higher proportion of the clasts. The pelites are completely converted to mica schist.

Plate 1. *Thin-bedded, laminated psammite and semipelite of the Spruce Brook Formation (subunit 2a); 3 km southeast of Wolf Lake; lens cap is 5 cm in diameter.*

Subunit 2b is located in the Wolf Lake area and is dominated by pelitic schist, as well as semipelite having minor psammite and rare pelite-clast intraformational breccia.

Bedding is apparent only in the psammitic units and is generally 10 cm thick. In the pelitic to semipelitic units, bedding planes are probably represented by narrow layers having a greater abundance of coarse metamorphic biotite. Andalusite porphyroblasts (Plate 2) are locally prominent in pelite near Wolf Lake.

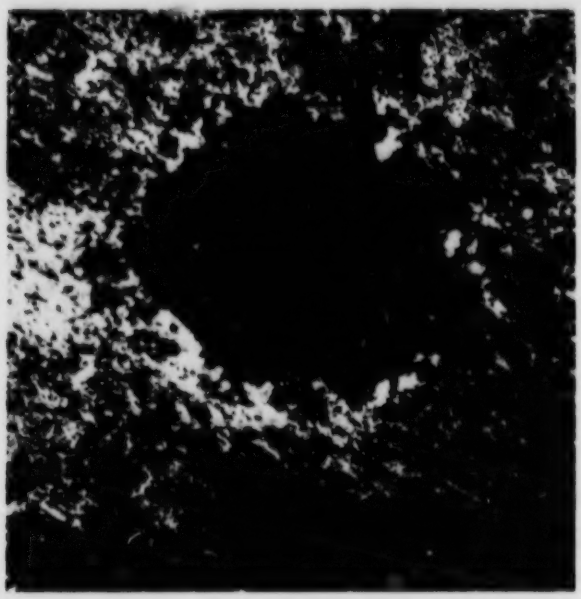

Plate 2. *Zoned andalusite porphyroblast in fine-grained pelitic biotite–muscovite schist (subunit 2b) of the Spruce Brook Formation; cross-polarized light; scale: 25 mm = 1 mm; sample P14-1-83; 0.75 km east of Wolf Lake.*

Subunit 2c is located mainly to the south of subunit 2b and also forms a narrow band 2.5 km south of Wolf Lake. The unit is characteristically a coarse rudite having pelitic-clast conglomerate, coarse orthoquartzite-cobble and pebble conglomerate (Plate 3), coarse sandstone and isolated lapilli tuff beds located near Wolf Lake. Graded and crossbedded units were rarely found and indicate that subunit 2c youngs to the south. The similarity of the pelitic clasts to the nearby pelites of subunit 2b also indicates that subunit 2c overlies subunit 2b and that the well-rounded cobble conglomerates overlie the pelitic breccia.

The pelite-clast conglomerate forms beds >15 m thick and is composed of subrounded clasts of black pelite cobbles ranging from 2 to 60 cm in diameter, having a mode of about 15 cm. Psammite cobbles also form part of this unit but are subordinate to the pelite. Locally, the pelite conglomerate contains interbedded semipelite units about 1 m thick, which are composed of sets of parallel-laminated beds, each about 5 cm thick.

The orthoquartzite-cobble conglomerate is composed of about 95 percent clasts of well-rounded white orthoquartzite that range in size from 2 to over 30 cm. The conglomerate

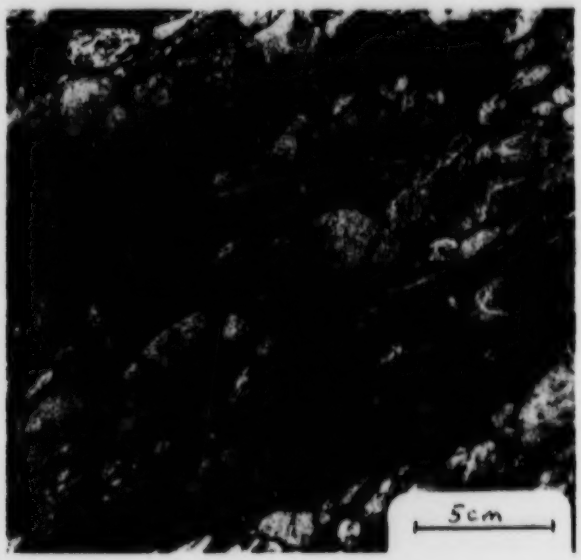

Plate 3. *Orthoquartzite-pebble conglomerate (subunit 2c); pebbles aligned parallel to cleavage; 2 km southeast of Wolf Lake.*

also contains a few 1 to 4 cm (possible) peridotite and semipelite clasts, which within each bed, are generally about 15 cm in diameter. The conglomerate beds are typically thicker than 10 m, and are about 5 m thick where they are interbedded with coarse sandstone. The conglomerate is clast supported with generally less than 10 percent interstitial coarse sandstone and granule conglomerate. Graded bedding was noted in one thick conglomerate unit. The southerly younging-direction indicated by this grading matches that given by crosslaminated sandstone lenses in the conglomerate.

A 1- to 2-km-thick sequence of thick-bedded, poorly sorted, coarse sandstone and granule to pebble conglomerate forms the southern portion of subunit 2c. These sandstones and conglomerates are dominated by orthoquartzite clasts but also contain a few clasts of quartz-porphyritic, flow-layered rhyolite and quartz–feldspar crystal tuff. Bedding in the sandstone and pebble conglomerate is 30 cm to 2 m thick. No evidence for younging-direction is apparent in the pebble conglomerates.

Thin lapilli tuff units are interbedded with the cobble conglomerates just to the east of the southern end of Wolf Lake. The lapilli tuffs are medium to coarse grained having phenoclasts of angular quartz and angular to equant plagioclase crystals. A thin crystal-tuff unit is interbedded with cobble conglomerate and coarse sandstone, 1.5 km north of the southern tip of Wolf Lake. This tuff consists of 1- to 3-mm euhedral plagioclase and 1- to 2-mm quartz crystals in a fine-grained recrystallized groundmass. The contacts with the overlying and underlying sediments are rarely exposed.

Subunit 2d is located between Wolf Lake and Meelpaeg Lake and is dominated by migmatite that is composed of 10- to 30-cm-thick layers of biotite granodiorite neosome and biotite–muscovite psammite paleosome (Plate 4). The granodioritic neosome veins commonly coalesce. The biotite–muscovite psammite paleosome generally displays a well-developed schistosity defined by biotite. Primary sedimentary features are rare but in a few places 3- to 5-cm-thick beds are preserved. Subunit 2a psammites southwest of Meelpaeg Lake are locally migmatitic being intimately associated with thin veins of granite neosome. The veins consist of medium-grained, equigranular to pegmatitic, muscovite–biotite granite, which contains a weak foliation defined by aligned mica.

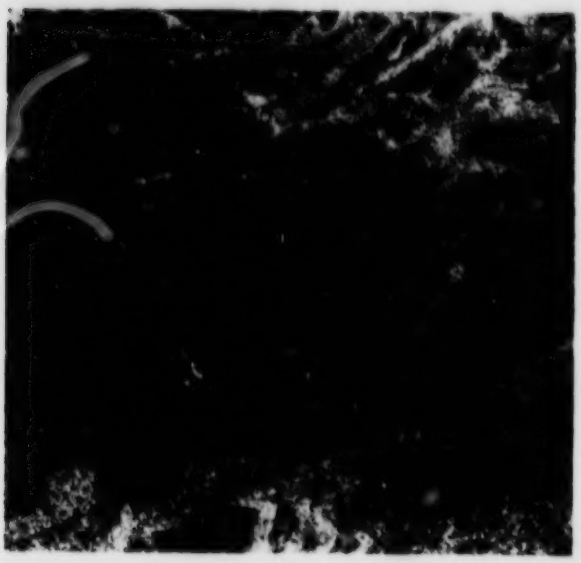

Plate 4. *Migmatitic Spruce Brook Formation (subunit 2d); island in northeastern part of Meelpaeg Lake; lens cap is 5 cm in diameter.*

Subunit 2e is located to the north of D'Espoir Lake and is composed mainly of strongly deformed and metamorphosed, grey to red metasandstone associated with rare phyllitic felsic volcanic rocks. Bedding is locally preserved and is indicated by alternating red and grey, 4- to 10-cm-thick, quartz-rich sandstones. Generally, the rocks are a monotonous sequence of grey, biotite–muscovite psammitic schist. The psammite locally contains coarser quartz clasts that form augen. Numerous granite veins have intruded and been deformed with the schists.

Isolated outcrops along the shore of the pond north of D'Espoir Lake, consist of strongly schistose, cream-coloured, muscovite–quartz phyllite, the protolith of which is interpreted to be a rhyolitic tuff.

BAIE D'ESPOIR GROUP (UNIT 3)

Three formations of the Baie d'Espoir Group are within the map areas. The Salmon River Dam Formation (subunits 3a, 3b), located mainly to the north of the North Bay Granite Suite, is composed of psammite and semipelite and has minor calcareous semipelite, limestone (subunit 3a) and pelite (subunit 3b). The Riches Island Formation (subunit 3c) is located to the south of the North Bay Granite Suite, and is composed mainly of highly metamorphosed psammite, semipelite and minor pelite. The migmatite (subunit 3d) which occurs within the North Bay Granite Suite is considered to be equivalent to the Riches Island Formation, as similar highly metamorphosed screens of Riches Island Formation are common close to the contact with the East Bay Granite in the North Bay and East Bay areas. The North Steady Pond Formation (subunits 3e to h) is located to the northwest of the Salmon River Dam Formation, between Dolland Pond and Meelpaeg Lake, and consists of interbedded tuff, pelite and psammite.

Salmon River Dam Formation (Subunits 3a, 3b)

The Salmon River Dam Formation (Colman-Sadd, 1976) has been divided into psammitic subunit 3a and pelitic subunit 3b. No contacts have been observed between the two units and their relative stratigraphic positions are unknown. However, the assumed contact is parallel to bedding and thus is possibly conformable.

Subunit 3a of the Salmon River Dam Formation is well exposed along the east-flowing brook, which flows into D'Espoir Lake and along D'Espoir Brook, which drains the lake. In this area, and in a few isolated exposures along the northern contact of the D'Espoir Brook Granite (Unit 9), and northeast of D'Espoir Lake, the dominant rock type is grey, generally featureless, north-dipping, 4- to 30-cm-thick bed of sandstone (Plate 5). Part of the sequence is highly calcareous about 2 km west of D'Espoir Lake. Toward Dolland Pond, the Salmon River Dam Formation is composed of thin-bedded psammite and semipelite. The intrusive contact with D'Espoir Brook Granite is locally well exposed and xenoliths of metasedimentary rocks occur within the granite. However, the contact is mainly faulted along the Meelpaeg Lake Fault Zone.

The sandstones, to the west of D'Espoir Lake, show graded bedding, parallel-laminations and rarely crosslaminations, which suggest that the sequence youngs to the north. South of D'Espoir Lake and close to the faulted contact with the D'Espoir Brook Granite, an isolated occurrence of weakly cleaved limestone apparently underlies the sandstones of the Salmon River Dam Formation. This limestone was examined for conodonts but none were found.

A thin, fault-bounded sliver of probable Salmon River Dam Formation occurs within the Meelpaeg Lake Fault Zone, 9 km east-southeast of D'Espoir Lake, between the D'Espoir Brook Granite and the Upper Salmon Road Granite. This highly deformed sliver consists of psammite and semipelite with a few 20- to 50-cm-thick limestone beds.

Plate 5. *Gently north-dipping, medium-bedded sandstones of the Salmon River Dam Formation (subunit 3a); 2 km west of D'Espoir Lake.*

Northeast of D'Espoir Lake and along Bear Lake (informal local name), the psammites of the Salmon River Dam Formation commonly exhibit parallel-laminations and very rare scours and crosslaminations. These indicate younging-directions to the west and east in the area northeast of D'Espoir Lake. Combined with the steep dips of the unit in this area, this alternation of younging-direction suggests that isoclinal folds are present.

Subunit 3b is a poorly exposed sequence of very thin-bedded (< 1 cm) and strongly cleaved, rusty brown and black pelite and semipelite having minor interbedded tuff. All sedimentary features, apart from the bedding, appear to have been obliterated by deformation and metamorphism; this has produced a very strong cleavage parallel to the bedding, and extensive recrystallization of the pelite and semipelite to aggregates of quartz, sericite, epidote, and chlorite having minor biotite and tremolite–actinolite.

Riches Island Formation (Subunits 3c, 3d)

To the south of East Bay (map area 11P/16), the dominant rock types are highly metamorphosed psammites, semipelites and pelites (subunit 3c). These form the continuation of the formation, which is well exposed, to the southwest, in the Facheux Bay (11P/9) map area (Blackwood, 1983, 1985), and to east, in the St. Alban's (1M/13) map area (Colman-Sadd, 1976) and the Gaultois map area (1M/12; Colman-Sadd *et al.*, 1979).

The Riches Island Formation is cut by numerous, very large dykes (50 m by 1 km) of the East Bay Granite, and also occurs as very large screens along the contact with the East Bay Granite on both sides of East Bay. The dominant rock type of the formation is psammite, which forms beds 10 to 100 cm thick. The psammites form sequences up to 100 m thick but commonly contain interbedded pelite and semipelite, which form beds 10 to 50 cm thick (Plate 6). The primary mineralogy and textures of the metasedimentary rocks have been removed by metamorphism and deformation. Only the quartz can be considered a primary mineral but it has been extensively deformed and recrystallized to sutured and polygonal, elongate aggregates.

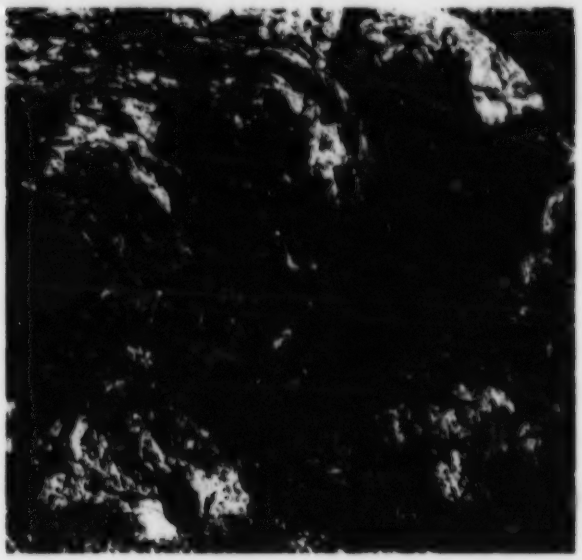

Plate 6. *Northeast view of southeast-verging, overturned folds of Riches Island Formation semipelites (subunit 3c); 2.5 km northwest of Pomley Cove; lens cap is 5 cm in diameter.*

To the south of the faulted intrusive contact with the East Bay Granite, at Pomley Cove, the Riches Island Formation is composed of thin-bedded, black, graphitic, pyritic pelite and minor psammite. This sequence appears to dip gently beneath a sequence of recumbently folded psammites exposed just to the south of Pomley Cove in map area 11P/9. However, no way-up criteria were found in either succession.

Within the Dolland Brook and D'Espoir Brook map areas, migmatite and gneissic granodiorite (subunit 3d) occur as xenoliths of variable size (10 cm to over 500 m) and of variable concentration, within the East Bay Granite (Plate 7 a and b). The main area of migmatite is around the central part of North Bay. Here, migmatite commonly covers over 50 percent of the outcrop area. The migmatite is commonly cut by dykes of East Bay Granite and pegmatite veins.

The neosome of the migmatitic metasedimentary rock is composed of quartz, plagioclase, microcline, biotite and muscovite and is equigranular having a variably developed foliation. It generally forms around 20 to 50 percent of the migmatite. The paleosome is dominantly quartz–plagioclase–biotite psammite having a well-developed

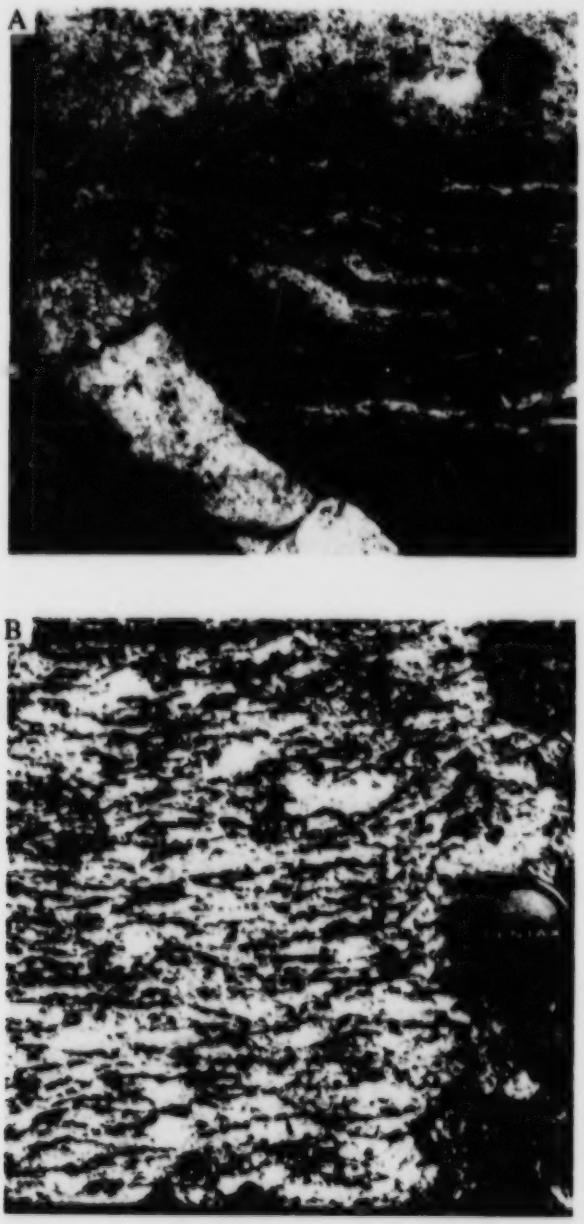

Plate 7. *(a) Xenoliths of migmatite (subunit 3d) in East Bay Granite; 7 km west of Garland Cove, North Bay; (b) gneissic granodiorite xenolith (subunit 3d) in the D'Espoir Brook Granite; 16 km west of D'Espoir Lake; lens cap in both photographs are 5 cm in diameter.*

foliation. In a few places, 1-cm-diameter knots of fibrolitic sillimanite were found. The paleosome is strongly schistose and locally the fabric is folded. Commonly, biotite–muscovite–sillimanite semipelitic schist forms isolated xenoliths.

The gneissic granodiorite contains a well-developed alignment of biotite-rich schlieren, which form layers 3 to 5 mm thick and 2 to 4 cm long. These patches are separated by medium-grained, muscovite–biotite granite that form anastomosing layers 1 to 2 cm thick. The biotite patches, which are gently folded, may represent a restite phase after advanced migmatization.

The metasedimentary migmatite is considered to be derived from the Riches Island and Salmon River Dam formations because of a pronounced increase in xenolith abundance in the East Bay Granite along the southern and northern contacts with the Ordovician metasedimentary rocks. Along the southern contact, in particular, there is a transitional contact between the granite and the metasedimentary rocks over 2 to 4 km. The location of the migmatitic metasedimentary rock belt in the central North Bay area may reflect either a roof-contact zone or a core zone of migmatite, which has been incorporated into the East Bay Granite.

There is little evidence that this zone of migmatite represents a remnant of Precambrian basement as indicated by Colman-Sadd (1980c), Colman-Sadd and Swinden (1982) and Dickson and Tomlin (1983). Virtually identical rocks occur with highly metamorphosed metasedimentary rocks of the Riches Island Formation (Blackwood, 1983, 1985). U–Pb monazite ages (see section on North Bay Granite Suite: New U–Pb Age Determinations) from the gneissic granodiorite indicate that the migmatite cooled below 600°C at around 416–410 Ma. Zircon ages indicate crystallization at around 450 Ma *(op cit.)*.

Migmatite is locally abundant in the areas south and southeast of Dolland Pond and is mainly associated with the D'Espoir Brook Granite. The source rock for these migmatites is less clear. The Salmon River Dam Formation and Silurian(?) rocks of Unit 5 are composed of generally lower greenschist-facies slates and semipelites in this area. The nearest exposed migmatite is the Spruce Brook Formation to the north of Wolf Lake. Xenoliths of non-migmatitic psammitic schist are similar to the psammites that form part of the Spruce Brook Formation in the area southwest of Meelpaeg Lake.

North Steady Pond Formation (Subunits 3e to 3h)

Various metasedimentary and metavolcanic rocks (subunits 3e to 3h), exposed along the eastern portion of the Wolf Mountain map area (12A/2) between the eastern part of Meelpaeg Lake and Dolland Pond, are interpreted to form the southwestern continuation of the North Steady Pond Formation (Colman-Sadd, 1980b, 1984) or of the Cold Spring Pond Formation (Swinden, 1988).

Contacts with the Spruce Brook Formation, which lie to the north and west of the North Steady Pond Formation, are interpreted to be faults because of a pronounced change in metamorphic grade and rock type across a northeast-trending lineament. The stratigraphic succession is not known

due to the absence of definitive younging criteria. Bedding is well preserved in the metasedimentary rocks but the only other sedimentary features present are parallel laminations.

Felsic tuff (subunit 3e) occurs along the western margin of the North Steady Pond Formation. At one locality, 1.5 km southeast of Meelpaeg Lake, a sharp planar contact occurs between an underlying thick sequence of crystal-lithic tuff (subunit 3e) and a very thin-bedded, black, siliceous pelite (subunit 3f). The lack of erosional features along the surface of the pelite, as would be expected during deposition of a massive tuff unit, is considered to indicate that the pelite overlies the tuff. Thus, the tuff (subunit 3e) is tentatively considered to be the older of the two.

Subunit 3e is a very thick-bedded sequence of weakly cleaved quartz–feldspar-crystal tuff and tuffaceous sandstone (Plate 8). The main tuff sequence is exposed along the ridge 2 km southeast of Meelpaeg Lake. About 7 km east of Wolf Lake, a sequence of tuffaceous sandstone having prominent quartz clasts in a finer grained matrix, is similar to the tuff unit. Feldspar crystals are, however, absent. The tuff strikes into the sandstone and they may represent facies variants. Bedding was noted in only a few places and is locally over 5 m thick. The tuff is grey to cream, and has prominent 2- to 5-mm diameter subangular clasts of quartz and anhedral plagioclase in a fine-grained matrix. Quartz commonly shows embayed margins. About 4 km southwest of the southern end of this part of subunit 3e, feldspar–quartz clast-rich sandstone or possibly tuff occurs in two isolated outcrops. This rock is very similar to subunit 3e to the north and is tentatively correlated with it. This southern area of subunit 3e may be part of the southern limb of a south-trending synform exposed between the areas of tuff and sandstone. Possibly overlying this sandstone, is a massive sequence of fine-grained tuff or tuffaceous sandstone, which contains abundant clasts of rounded quartz, plagioclase and possibly K-feldspar. Bedding was not observed in this widespread unit.

Subunit 3f is characterized by thin-bedded, fine-grained, grey to black, graphitic, siliceous slate and siltstone. Beds are mainly 2 to 20 cm thick and parallel but are locally up to 5 m thick having no apparent stratification. The thin-bedded sequences are tightly folded and highly fractured. Two generations of quartz veins are present. The early veins vary from 2 to 5 mm thick and are cut by thicker quartz veins. Subunit 3f occurs throughout the North Steady Pond Formation interbedded with subunits 3g and 3b, and thus, several sequences of subunit 3f are present, some of which may be repeated by folding.

Subunit 3g consists of a sequence of grey to brown, massive sandstone having a weakly developed cleavage. Thin layers of subunit 3f are interbedded with subunit 3g. Bedding was rarely observed in subunit 3g and thus, the thickness of beds is unknown. However, there are commonly massive exposures over 3 m of featureless sandstone. In thin section, quartz is set in a matrix of metamorphic mica and porphyroblasts of cordierite.

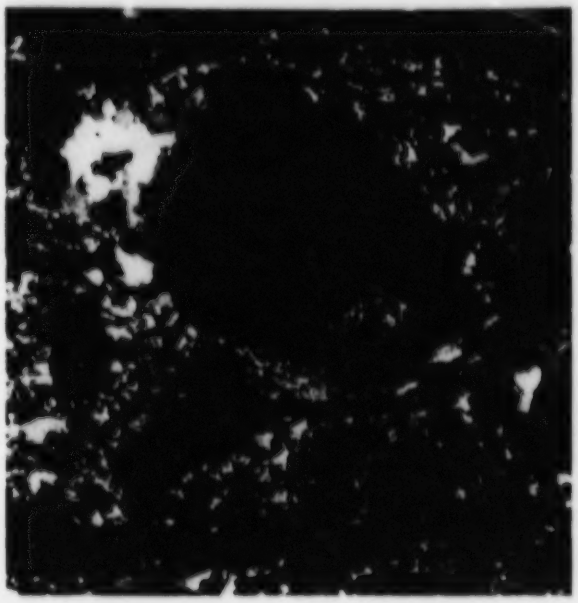

Plate 8. *Embayed phenocryst in schistose tuff of the North Steady Pond Formation (subunit 3e); cross-polarized light; scale: 25 mm = 1 mm; sample L30-11-83; 1 km south of southeast corner of Meelpaeg Lake.*

Subunit 3h is the most extensively developed unit of the North Steady Pond Formation and consists of a monotonous sequence of green and grey, generally thin- to medium-bedded shale, siltstone and fine-grained sandstone having a weakly developed cleavage. Locally, bedding is absent. Thin laminations are locally present but otherwise, sedimentary structures are absent. In thin section, quartz is set in a matrix of fine-grained aggregates of chlorite and sericite associated with locally abundant cordierite(?) pseudomorphs that have been replaced by chlorite and sericite (Plate 9).

BAY DU NORD GROUP (UNIT 4)

Rocks assigned to the Bay du Nord Group (Unit 4) form a 1.5-km-wide, northwest-trending belt in the southwestern corner of the Dolland Brook (east half) map area. This belt continues and widens to the northwest into the Dolland Brook (west half) map area (Blackwood, 1984) and to the southeast into the La Hune (11P/10) map area, where it remains a narrow but continuous southeast-trending zone (Dickson *et al.*, 1985a). The group extends into the Facheux Bay (11P/9) map area where the unit widens and forms part of the Baie d'Espoir Group (Blackwood, 1983, 1985).

The Bay du Nord Group consists of extensively migmatized metasedimentary rock that has been intruded by the Dolland Brook Granite to the north, and mylonitic Burgeo granite, to the south. The paleosome of the migmatites is biotite–muscovite psammite, which has a strong schistosity (Plate 10); bedding is locally preserved. The neosome is

Plate 9. *Cordierite porphyroblasts (retrogressed to sericite and chlorite) in pelite (subunit 3h) of the North Steady Pond Formation; east side of 3-km-long pond, 7.5 km east of Wolf Lake; lens cap is 5 cm in diameter.*

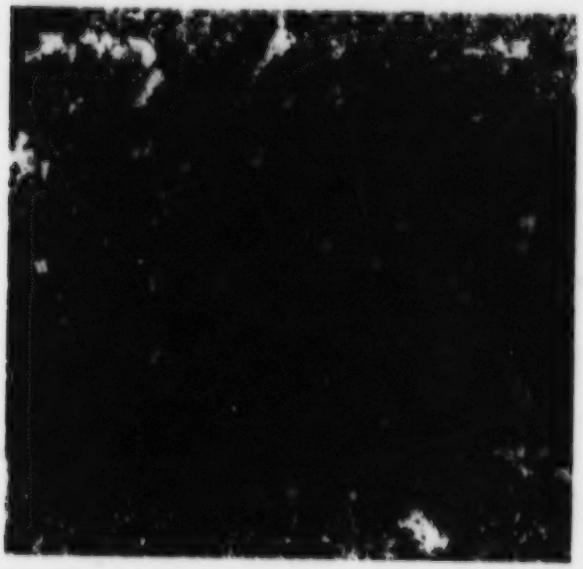

Plate 10. *Isoclinally folded, biotite–muscovite psammites of the Bay du Nord Group (Unit 4); 1.5 km southeast of the southern end of Moon Pond; lens cap is 5 cm in diameter.*

foliated anastomosing veins of muscovite–biotite granite and granodiorite having numerous pegmatites. Muscovite–garnet granite has also intruded the Bay du Nord Group.

Xenoliths of Bay du Nord Group migmatite are common within the Dolland Brook Granite and within 2 km of the fault intrusive contact, but are much less abundant in the Burgeo granite within the map area. One occurrence of hornblende–biotite schist, which may be a completely recrystallized mafic volcanic rock, was also noted.

In thin section, the biotite-psammite paleosome consists of quartz, plagioclase and zircon, all of which may be partly recrystallized detrital minerals, and a foliation defined by metamorphic biotite, muscovite and rarely sillimanite. The granitic neosome consists of quartz, plagioclase, rarely K-feldspar, biotite and muscovite having accessory zircon and magnetite.

SILURIAN(?) CLASTIC SEDIMENTARY ROCKS–UNIT 5

A poorly exposed sequence of thin- to medium-bedded, weakly to strongly cleaved shale, siltstone, sandstone, pebble conglomerate and coarse breccia (Plate 11) is exposed around the western half of Dolland Pond. Graded bedding in the coarse sandstone, and crosslaminations in the sandstone and siltstone, give clear younging-directions and indicate that the sequence forms an easterly plunging syncline having pebble conglomerate and finer grained clastic rocks in the core. These units apparently overlie strongly cleaved, thin-bedded slate and siltstone, exposed to the southwest of Dolland Pond, which in turn, overlie a poorly exposed pebble conglomerate and interbedded pebble conglomerate and coarse, poorly sorted breccia having clasts up to 30 cm long. These coarse sedimentary rocks apparently overlie another thick sequence of thin-bedded shale and siltstone, to the southwest of Dolland Pond, which is assigned to the Salmon River Dam Formation. This sequence continues to the south where it is in fault contact with the strongly foliated D'Espoir Brook Granite. Unit 5 is interpreted to be in fault contact with subunits 2b

Plate 11. *Laminated, medium-bedded sandstone having interbedded pebble breccia (Unit 5); northwest corner of Dolland Pond; lens cap is 5 cm in diameter.*

and 2c of the Spruce Brook Formation. The relationship of Unit 5 to the North Steady Pond Formation (Unit 3) is unknown, from the map area, because of lack of exposure. Colman-Sadd (1984) has indicated an assumed fault contact between Unit 5 and the Salmon River Dam Formation, in map area 12A/1, to the east of Dolland Pond.

Unit 5 is weakly metamorphosed. The slates are generally converted to chlorite and sericite, but small feldspar and quartz clasts were noted. The sandstones and pebble conglomerates contain similar clast assemblages. The pebbles are dominantly chert, orthoquartzite sandstone, shale, felsic and mafic volcanic rocks. Granules and coarse, sand-size lithic clasts are dominantly composed of chert and fine-grained plagioclase-rich basalt, having accessory sandstone, vein quartz, micrographic granitoid, shale, fine-grained orthoquartzite, and feldspar-phyric felsic volcanic rocks (Plates 12 a and b). Crystals are mainly quartz and plagioclase with rare K-feldspar. The matrix in the coarse clastic rocks is composed of various proportions of shale and carbonate and forms 10 to 20 percent of the rock.

Williams (1970) correlated the coarse clastic sequence at Dolland Pond (Unit 5) with the conglomerates and other coarse sandstones (subunit 2c) exposed to the southeast of Wolf Lake. That correlation is not supported in this study. The conglomerates of subunit 2c are oligomictic having well-rounded clasts of quartzite, generally well sorted, and few associated fine-grained sediments within the sequence (compare Plates 2 and 11). In contrast, Unit 5 has a much greater variety of clasts, in which sorting is poor, with little rounding and fine-grained clastic rocks form a major proportion of the sequence.

Unit 5 is similar to coarse clastic rocks interpreted to form part of the North Steady Pond Formation in the Cold Spring Pond map area (12A/1), to the northeast of Dolland Pond. Colman-Sadd (1984) and Colman-Sadd and Swinden (1982, 1984) have described polymict, poorly sorted conglomerates with interbedded sandstone and shale in this formation. The closest known source of mafic volcanic clasts would be the Cold Spring Pond Formation exposed 25 km to the northeast of Dolland Pond (Colman-Sadd and Swinden, 1984; Swinden, 1988).

SEDIMENTOLOGY OF THE ORDOVICIAN UNITS

The lack of sedimentary structures and extensive metamorphism and deformation of most of the Ordovician units has prevented the reconstruction of a comprehensive sedimentological history.

The Spruce Brook Formation (subunit 2a to 2e), in its less metamorphosed parts, is dominated by quartz-rich sandstone having minor interbedded semipelite and pelite. Parallel bedding and parallel laminations are the only commonly preserved sedimentary features. Colman-Sadd and Swinden (1984) have described other areas of the Spruce

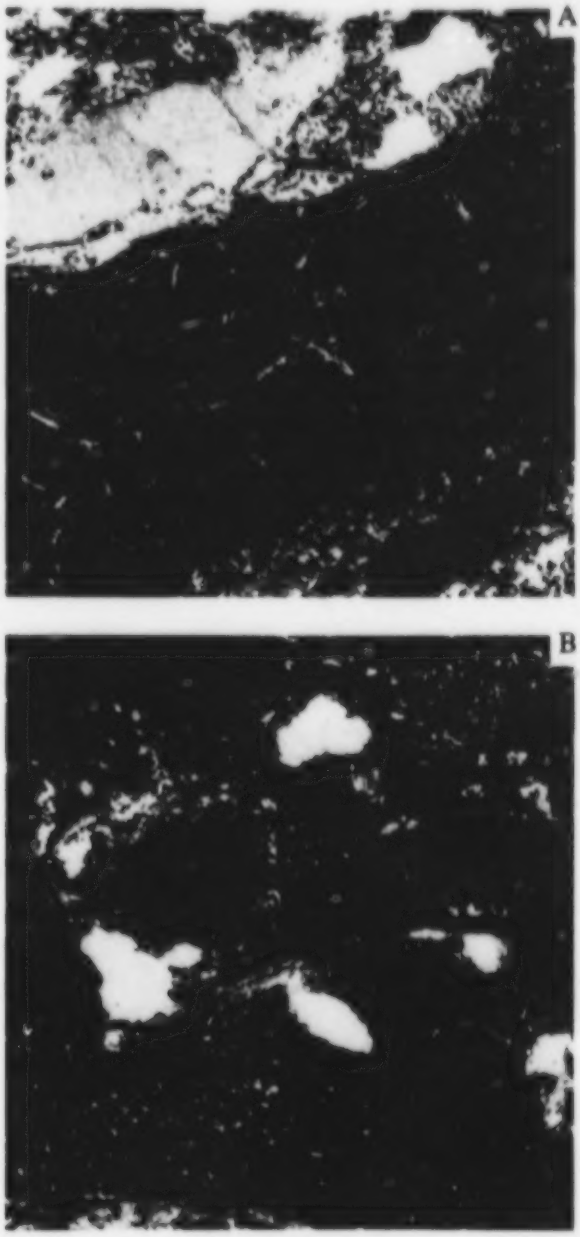

Plate 12. *(a) Feldspar-phyric basalt fragment in Silurian(?) granule conglomerate (Unit 5); (b) quartz and fine-grained cherty fragments in granule conglomerate having anastomosing cleavage; cross-polarized light; scale: 25 mm = 1 mm for both plates; sample L2-1A-83; on west side of Dolland Pond.*

Brook Formation as being turbidites. The Spruce Brook Formation, in the Wolf Mountain map area, could be turbidites but supporting evidence is sparse. Subunit 2c is dominated by coarse, well-rounded clasts and interbedded coarse sandstone that have an apparent source in the

underlying subunits 2a and 2b. The thick beds, lenses of sandstone, and well-rounded clasts indicate a high energy environment such as a beach or offshore bar. This conclusion would imply a period of uplift exposing the underlying lithified Spruce Brook Formation to active erosion in a shallow water environment.

Colman-Sadd (1976, 1980a, 1984) and Colman-Sadd and Swinden (1982, 1984) have described graded bedding and cross-, convolute- and parallel-laminations from the Salmon River Dam Formation of the Baie d'Espoir Group, which indicate turbidite deposition. The Salmon River Dam Formation (subunit 3a), west of D'Espoir Lake, shows the same features, which implies a similar origin, i.e., turbidite deposition in a submarine fan. The fine-grained, pelitic component of the Salmon River Dam Formation (subunit 3b) is possibly equivalent to lower fan or distal turbidites. The North Steady Pond Formation, with its thick-bedded tuffs and tuffaceous quartz feldspar-rich sandstones and minor interbedded black pelite and overlying siltstone, has probably been deposited in a proximal environment, close to a volcanic centre. Colman-Sadd (1980c) noted that the North Steady Pond Formation, in general, coarsens and is thicker-bedded toward the northwest. A similar situation in the Wolf Mountain area also indicates a possible source to the northwest.

The Riches Island Formation (subunit 3c) (and therefore the possibly equivalent Bay du Nord Group) has been described by Colman-Sadd (1980c) as having been deposited as shelf muds having storm sand-layers. In the East Bay area, the highly metamorphosed Riches Island Formation lacks sedimentary features other than bedding, but the sequence does contain rocks similar to those described by Colman-Sadd (1980c) and by analogy, is taken to have formed in a similar environment.

The rocks exposed around Dolland Pond (Unit 5) indicate a shallowing upward sequence where thin-bedded shales and siltstones form the lower part of the sequence, possibly representing distal turbidites. An upper sequence is dominated by well-bedded coarse clastic rocks and interbedded sandstone and shale indicative of shallower and more proximal environment. Such a regime exists in upper-fan environments with the coarse clastic units forming in channels as debris flows (e.g., Klein, 1985).

DEFORMATION AND METAMORPHISM OF THE SPRUCE BROOK FORMATION (UNIT 2)

The Spruce Brook Formation, in the Meelpaeg Lake area (subunits 2a, 2b), shows a dominant structural trend toward the northeast having generally steeply dipping planar structures. Cleavage is commonly parallel or sub-parallel to bedding (Plate 1), but locally crosscutting relationships were observed. An examination of thin sections indicates that the main fabric is the first fabric (S_1), and the later fabric (S_2) is associated with crenulations. Rare folds of bedding are commonly tight, contain an axial planar (S_1) fabric, and plunge steeply to the southwest. Generally, folds are uncommon in subunits 2a and 2b of the Spruce Brook Formation. East of Wolf Lake, bedding and cleavage are also northeasterly trending and steeply dipping. Folds were located in only one area where open gently plunging folds contain an axial planar, well-developed, vertical cleavage in pelite. Only one cleavage is apparent and crenulations of this cleavage are rare. A stereographic plot of the various structural features is given in Figure 5. Southeast of Meelpaeg Lake, subunit 2a of the Spruce Brook Formation has a strongly developed schistosity. This fabric is highly crenulated and wrapped around porphyroblasts of cordierite and andalusite but a crenulation cleavage is not associated with this deformation.

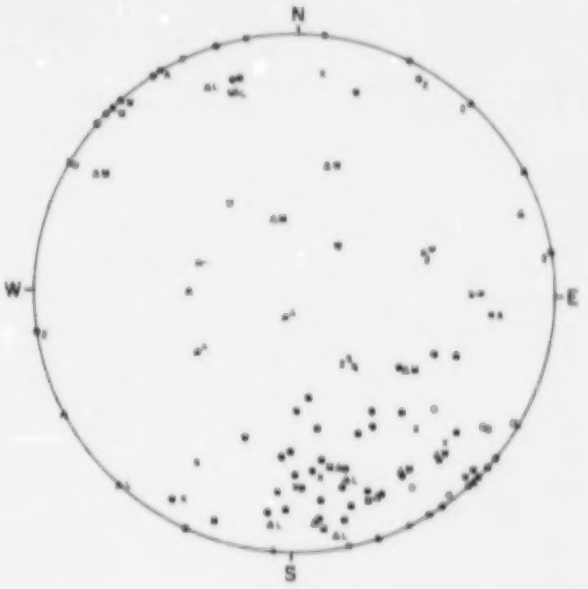
N
W
E
S
SYMBOLS
Wolf Lake area: S_0 = ΔL,S, = ●, S_1 = ●, crenulation lineation ←
Wolf Mountain area: S_0 = ΔW, S, = ○, F_1 fold plunge = ←, F_1 axial plane = ▪A
S.E. Meelpaeg Lake: S_0 = ΔM, S, = X, F_1 fold plunge = ←, F_2 fold plunge ←

Figure 5. *Equal area stereographic projection of poles to bedding (S_0), S_1, S_2, with plunge and direction of plunge of small folds, from various areas of the Spruce Brook Formation (Unit 2).*

The migmatite of the Spruce Brook Formation (subunit 2d) has not suffered any significant deformation subsequent to migmatization. The biotite schist paleosome commonly contains a strongly developed foliation, which is locally folded. However, the granitoid neosome contains at most, a very weak fabric (Plate 4), which indicates that migmatization succeeded the main deformation of the metasedimentary rocks.

Subunit 2e of the Spruce Brook Formation, northwest of D'Espoir Lake, consists of strongly deformed biotite–muscovite psammite having a strong, southeast-trending, generally steeply dipping cleavage, which is locally

gently dipping. The orientation of bedding is highly variable and in a few places isoclinal folds occur that plunge south at about 75° and have axial planes orientated at about 025°/65°E. Some psammitic schists have a very strong foliation and quartzite clasts have been flattened to form extremely elongate augen (10 by 3 mm). In several places, the main tectonic fabric has been folded and kinked by southwest-trending structures.

Regional metamorphism of the Spruce Brook Formation, in the Wolf Lake–Meelpaeg Lake area, varies from lower-greenschist-facies slate and phyllite, south and east of Wolf Lake, to partially melted amphibolite facies in the Meelpaeg Lake area.

Within the non-migmatitic units, the main regional fabric is defined by biotite and muscovite associated with extensive recrystallization of quartz. Garnet is only locally developed. Cordierite, andalusite and garnet occur in subunit 2b, southeast of Meelpaeg Lake. These porphyroblasts form augen, which were deformed during the second deformation and extensively retrogressed to chlorite and sericite. Chlorite has developed along fractures in the garnet.

Southwest of Meelpaeg Lake, the biotite–muscovite psammites locally contain andalusite. This is partly mantled by fibrous sillimanite (Dickson, 1982) and garnet contains chlorite-filled fractures. Mafic dykes within the Spruce Brook Formation have been completely metamorphosed to aggregates of blue-green hornblende–biotite–quartz–plagioclase. Within the migmatite terrane (subunit 2d), the paleosome consists of biotite–muscovite–plagioclase–quartz schist. Cordierite occurs in the northeastern part of subunit 2d on the islands in Meelpaeg Lake.

In the D'Espoir Lake area, the Spruce Brook Formation (subunit 2e), locally contains a very strong schistosity defined by biotite, muscovite and flattened, recrystallized quartz. Schistose felsic volcanic rocks, exposed northeast of D'Espoir Lake, have been metamorphosed to fine-grained aggregates of sericite, chlorite and quartz. The less schistose metasedimentary rocks contain a poorly developed fabric defined by biotite. Numerous andalusite-bearing, schistose glacial erratics, found to the northwest of D'Espoir Lake, have not been found in place within the map area. However, immediately to the north, in map area 12A/1, Colman-Sadd (1984) has indicated that the continuation of the Spruce Brook Formation contains either andalusite or sillimanite and this is the source of the andalusite-bearing erratics. Extensive contact metamorphism of the Spruce Brook Formation is not associated with the D'Espoir Lake Granite (subunit 19d) exposed to the south of the Spruce Brook Formation.

In the Wolf Lake area, contact metamorphism of the Spruce Brook Formation by the Meelpaeg Lake Granite has resulted in the extensive development of andalusite, garnet and cordierite porphyroblasts and even more extensive biotite porphyroblasts (Plate 2). The effects of this static recrystallization and metamorphism are most apparent in the pelites (subunit 2b) in which coarse garnet, andalusite and biotite occur up to 2 km from the nearest exposed granite. Overgrowths on inclusion-rich andalusites indicate that the contact metamorphism reached andalusite grade following regional metamorphism. Porphyroblastic biotite is common in the pelitic rocks close to the contact with the Wolf Lake Granite along the southern part of Wolf Lake, but andalusite, cordierite and garnet are conspicuously absent. The contact metamorphism may have been caused by the Meelpaeg Lake Granite rather than the Wolf Lake Granite, as the Meelpaeg Lake Granite appears to have a much more extensive metamorphic aureole. The Meelpaeg Lake Granite is probably present at a relatively shallow level beneath subunits 2b and 2c to account for the extensive metamorphic aureole. Southwest of Meelpaeg Lake, contact metamorphism is reflected by randomly orientated biotite and muscovite, and rarely garnet and andalusite, which overprinted the main fabric defined by biotite and muscovite. Quartz is extensively recrystallized to polygonal aggregates.

Retrogression of both regional and contact metamorphic minerals is common with cordierite retrogressed to sericite and chlorite, and garnet is partly retrogressed to chlorite along fractures and crystal edges. Biotite is locally retrogressed to chlorite in minor shear zones.

DEFORMATION OF THE BAIE D'ESPOIR GROUP (UNIT 3)

Deformation of the Baie d'Espoir Group is highly variable in intensity and apparent complexity. The common lack of younging criteria hinders interpretation of the structure. The Salmon River Dam Formation apparently has the simplest structure but several features such as recumbent folds and reversals in younging-direction indicate that it is also complex. To the west of D'Espoir Lake, younging-criteria such as graded beds and crosslaminations indicate that the gently dipping sequence youngs to the north. In several areas of this sequence, a strong cleavage is present that is parallel to the bedding. About 3.5 km west of D'Espoir Lake, a small, tight, northeast-plunging recumbent isoclinal fold was located, which closes to the northwest and has an axial-planar cleavage subparallel to the gently dipping bedding. Intersection lineations of bedding and cleavage also indicate folds plunging to the northeast. The sequence has been deformed into open folds that plunge to the northeast with a well-developed crenulation lineation along the bedding planes (Figure 6). This crenulation lineation is parallel to the plunge of the open folds and a poorly developed steeply dipping, fracture cleavage is parallel to the axial plane of these open folds.

As the Salmon River Dam Formation, in this area, is right-way-up, the sequence must form part of a recumbent fold that verges to the west. The cleavage parallel to bedding, and the isoclinal fold parallel to bedding are first structures, and the open folds, crenulation lineations and steeply dipping cleavage are second structures. The degree of deformation associated with the F_2 open folds (in subunit 3a) is unlikely to have produced the strong degrees of flattening and strong cleavage present in the other areas of subunits 3a (east of

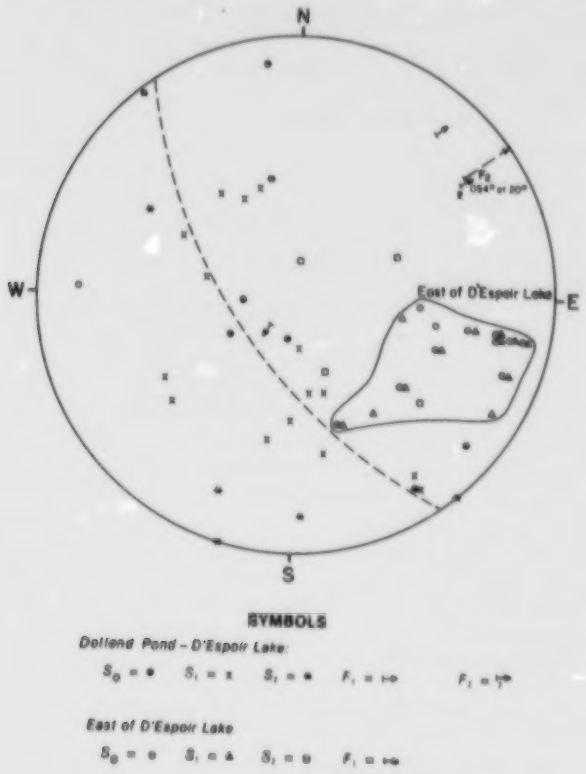

Figure 6. *Equal area stereographic projection of poles to bedding (S_0), S_1, S_2, with plunge and direction of plunge of small folds, from the Salmon River Dam Formation (subunit 3a), in the Dolland Pond–D'Espoir Lake and D'Espoir Lake east areas.*

D'Espoir Lake) and 3b. However, the strong degree of flattening associated with the F_1 folds, has probably produced the strong, bedding-parallel cleavage in the Salmon River Dam Formation. Thus, the main cleavage is related to F_1 deformation.

A feature of the Riches Island Formation is the folding of the prominent schistosity into generally northeast-trending folds. Folds of this schistosity are commonly overturned to the southeast having axial planes that dip to the northwest at 10 to 40° (Figure 7; Plate 6). Bedding is generally subparallel to this schistosity and is folded with this schistosity into similar orientations. Blackwood (1985) has suggested that this early schistosity is unrelated to folding and has been induced by an early recrystallization. There is no evidence of folding associated with the early fabric in the East Bay area. Folding of the gently dipping fabric by upright folds has resulted in a variably developed, moderate to steeply dipping second fabric defined by aligned mica and a fracture cleavage. Folding of the early fabric is shown in thin section by numerous, locally overturned, moderate to tight folds. Laminations are reflected by variations in mineral proportions and are generally parallel to the main cleavage and have been folded with the cleavage.

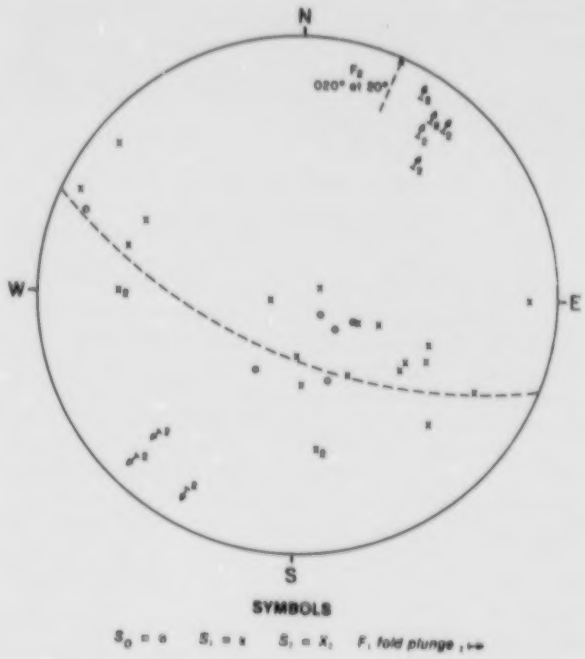

Figure 7. *Equal area stereographic projection of poles to bedding (S_0), S_1, S_2, with plunge and direction of plunge of small folds for the Riches Island Formation (subunit 3c), in the East Bay–Lampidoes Passage area.*

Blackwood (1983, 1985) has shown a similar sequence and style of deformation in the Riches Island Formation to the south of the East Bay–Pomley Cove area, where the formation is dominated by recumbent structures that are interpreted to be F_1 folds. The F_1 folds and associated gently dipping cleavage (S_1) have been folded by upright, gently plunging folds (F_2) with a steep axial-planar cleavage (S_2).

The Riches Island Formation has been intruded by numerous granite dykes and sills that have been deformed with the host rocks. The larger dykes (> 50 m thick) do not appear to have been folded but possess a weak, moderately dipping, northeast-trending fabric (subparallel to the S_1 schistosity in the sediments) and numerous xenoliths of schist. Smaller veins of granite and pegmatite are folded by upright F_2 folds and display a variably developed boudinage and a steep fracture cleavage axial planar to the F_2 folds. The granite dykes were, therefore, intruded during the later stages of the main deformation but prior to F_2 folding.

Migmatitic metasedimentary rock and gneissic granodiorite (subunit 3d) occur within the East Bay Granite and generally contain a strong east-trending schistosity or layering, which predates its incorporation into the granite. In a few places, these migmatitic rocks contain a strong L-S fabric and have a strong, steep-plunging lineation. The fabric in the migmatite is, locally, isoclinally folded, and rarely these folds are refolded along with granite veins that have intruded the migmatite.

Much of the migmatitic metasedimentary rock is similar in lithology and contains structures similar to those in the migmatite associated with the Isle Galet and Riches Island formations, exposed to the south of the North Bay Granite (see Blackwood, 1983, 1985).

The North Steady Pond Formation is dominated by northeast-trending bedding and cleavage (S_1) and southwest-plunging folds (F_1) (Figure 8). A major feature is a synformal structure (F_2); which trends to the southwest. This interpretation is based on the correlation of two areas of crystal tuff and quartz-clast-rich sandstone (subunit 3e) located on the northwestern and southeastern sides of the North Steady Pond Formation, in map area 12A/2, and an isoclinally folded sequence of sandstone, forms a westward-closing, overturned syncline that plunges to the south, 8 km north-northwest of Dolland Pond. The interpretation of this fold as a syncline is based on poorly developed graded bedding in the overturned limb of the fold.

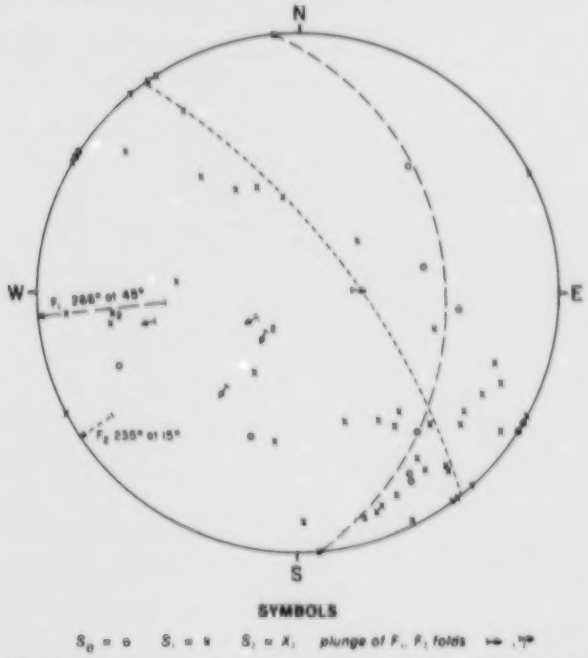

Figure 8. *Equal area stereographic projection of poles to bedding (S_0), S_1, with plunge and direction of plunge of small folds, from the North Steady Pond Formation (subunits 3e to 3h), in the Meelpaeg Lake area.*

Thin-bedded pelite and psammite (subunit 3f) are commonly highly folded with moderately tight, southwest-plunging folds and a variably developed, steep, axial-planar cleavage. In several places, the main fabric in the pelites is folded, indicating that the folds are at least second-phase folds. Southeast of Meelpaeg Lake, a weakly developed cleavage cuts the main fabric. This second cleavage trends toward the northwest and dips steeply to the southwest. This second phase of folding may have produced the outcrop pattern of the North Steady Pond Formation, which is concave toward the northwest, southeast of Meelpaeg Lake.

METAMORPHISM OF THE BAIE D'ESPOIR GROUP (UNIT 3)

The Salmon River Dam Formation contains abundant fine-grained biotite, sericite and rare actinolite, which define the main cleavage in the semipelites and psammites. Contact metamorphism, in the D'Espoir Lake area, has converted semipelites in the Salmon River Dam Formation (subunit 3b) into hard hornfelses having andalusite and cordierite porphyroblasts. To the southwest of D'Espoir Lake, there is small porphyroblast development where the sedimentary rocks are juxtaposed with the D'Espoir Brook Granite, along the Meelpaeg Lake Fault Zone. The schistose portion of the Salmon River Dam Formation (subunit 3a), 3 to 5 km east of D'Espoir Lake, is in intrusive contact with the Upper Salmon Road Granite but the only contact metamorphic effect appears to be a partial retrogression of biotite to chlorite in rocks with an assemblage of quartz, plagioclase, biotite and magnetite.

The Riches Island Formation is extensively metamorphosed to schistose assemblages commonly containing quartz–garnet–muscovite–biotite and locally also containing staurolite and sillimanite (Plate 13). At Pomley Cove, crenulated thin-bedded and strongly cleaved graphitic muscovite–chlorite–pyrite pelite, in fault contact with the East Bay Granite, show no evidence of contact metamorphism, even though pegmatite dykes have intruded the sequence of pelites.

Plate 13. *Riches Island Formation semipelite (subunit 3c) showing a staurolite porphyroblast having aligned quartz inclusions; matrix consists of recrystallized quartz and crenulated muscovite–biotite foliae; cross-polarized light; scale: 25 mm = 1 mm; sample L36-7-82; 2 km northwest of Pomley Cove.*

The gently dipping fabric (S_1) in most of the Riches Island Formation is defined by well-aligned biotite and muscovite, which occur as well-formed flakes. The main fabric is commonly crenulated (Plate 13) and cut by a variably developed cleavage (S_2) defined by biotite and muscovite.

Well-developed, euhedral, 1-cm-long staurolite and garnet porphyroblasts occur in the semipelitic biotite–muscovite–sillimanite schist. In thin section, fine-grained, aligned elongate inclusions are common in the staurolite porphyroblasts (Plate 13) and occur rarely in garnets. The inclusions are mainly very fine-grained, elongate, quartz blebs, which are not in optical continuity. The long axes of the quartz inclusions, within each porphyroblast, are commonly parallel to the axial planes of the crenulations and the alignment may reflect this deformation. The staurolite forms euhedral porphyroblasts enveloped by mica, and show little evidence of deformation. Thin, inclusion-free rims on the staurolite may reflect a later period of staurolite growth.

The metasedimentary rocks of the Riches Island Formation have been extensively recrystallized and annealed during a period of static metamorphism as indicated by strain-free, polygonal, quartz aggregates and a lack of deformation exhibited by micaceous foliae around fold hinges. At fold hinges, the mica flakes are straight and tangential to the fold axis, and display only minor undulose extinction.

The development of staurolite porphyroblasts is temporally related to the intrusion of the East Bay Granite. Veins of granite have intruded the Riches Island Formation commonly parallel to the gently dipping cleavage. However, the presence of strongly schistose metasedimentary xenoliths within the East Bay Granite indicate that the formation was extensively deformed prior to the intrusion of the granite. The garnet and staurolite porphyroblasts locally contain inclusion trails and, to the south of the map area (Blackwood, 1985) the inclusion trails have been deformed during a later deformation interpreted as D_2.

Porphyroblast development is thus pre-D_2 and is probably related to intrusion of the East Bay Granite and granite dykes. The annealing of the schists is possibly related to slow cooling of the metamorphic sequence.

The migmatites and associated biotite schists (subunit 3d) have been metamorphosed to amphibolite facies having locally developed coarse sillimanite porphyroblasts in the paleosome, which form 1-cm-diameter knots on exposed surfaces. The schists are composed mainly of biotite, muscovite and quartz. Sillimanite is not present in all the screens of migmatite. In most samples examined, the mineralogy of the paleosome is simply biotite–quartz–plagioclase with accessory zircon, apatite, opaque minerals (mainly magnetite and pyrite) and rarely sphene. The granitic neosome of the migmatites consists of generally hypidiomorphic-granular quartz–plagioclase–biotite.

An inclusion of layered psammite in the East Bay Granite, 5.75 km west-southwest of Bald Point, North Bay, contains subhedral diopside porphyroblasts in layers rich in sphene, polygonal quartz and finer grained diopside. The other layers contain aligned biotite, abundant polygonal quartz and only minor diopside. Plagioclase is completely lacking. The mineralogy indicates that this inclusion was originally a calcareous sandstone with the diopside possibly being formed by the reaction

$$\text{dolomite} + \text{quartz} + (H_2O) = \text{diopside} + CO_2 + (H_2O)$$

(from Winkler, 1976, p. 113). The lack of carbonate in the metasedimentary rocks is presumably the result of complete reaction of the carbonate to form diopside.

There are two probable sources for these calcareous metasedimentary rocks. The Salmon River Dam Formation locally contains carbonate-bearing sandstone and siltstone in the D'Espoir Lake area, which locally contains actinolite. Colman-Sadd (1983) noted that metamorphism of the calcareous pelites of the Salmon River Dam Formation has produced tremolite–actinolite-bearing, biotite psammites. Blackwood (1983, 1985) has also recorded carbonate in the Isle Galet Formation to the south of the North Bay Granite Suite. As well, amphibole-bearing schists also occur as screens within the East Bay Granite, southwest of North Bay. Higher grade metamorphism of these various amphibole-bearing units could produce a diopside-bearing rock.

The North Steady Pond Formation (subunits 3e to 3h) has been metamorphosed in the lower- to upper-greenschist facies with a superimposed contact metamorphism. The tectonic fabrics in the North Steady Pond Formation are defined by aligned biotite, chlorite and locally muscovite, in a variably recrystallized matrix of quartz and feldspar (Plate 14). The metamorphic grade is lowest in the area east of Wolf Lake with chlorite and biotite as the dominant metamorphic minerals. Southeast of Meelpaeg Lake, the metasedimentary and metavolcanic rocks contain coarse muscovite, and recrystallized quartz is common.

Contact metamorphism has produced locally abundant andalusite porphyroblasts in subunit 3f, close to the contacts with Unit 15 of the North Bay Granite Suite and the Wolf Lake North Granodiorite. Small porphyroblasts of retrogressed cordierite(?) occur in the semipelites of subunit 3h (Plate 9). These round spots are 2 to 3 mm in diameter and in thin section are seen to be composed of very fine-grained sericite and chlorite. These are commonly found up to 2.5 km from the nearest exposed granite. Garnet was found in one location in the pelitic rocks of subunit 3f and has overgrown the tectonic fabrics. Randomly oriented biotite and muscovite are common near the contact with the North Bay Granite Suite.

In subunit 3g, cordierite and locally staurolite porphyroblasts have overgrown the weak schistosity in the thick-bedded sandstones. Andalusite porphyroblasts were found in sandstones interbedded with the tuffs of subunit 3e. Porphyroblast development is concentrated around the southern portion of subunits 3e and 3g, to the southeast of

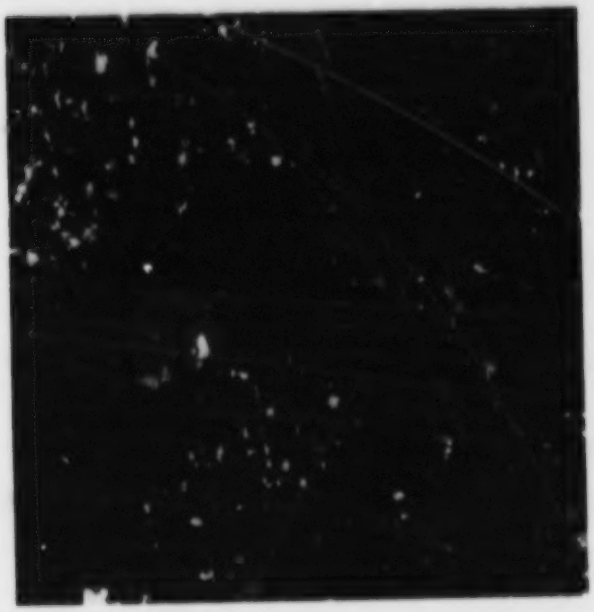

Plate 14. *Schistose crystal tuff of the North Steady Pond Formation (subunit 3e); cross-polarized light; scale: 25 mm = 1 mm; sample L30-11-83; 1 km south of east end of Meelpaeg Lake.*

Plate 15. *Strongly schistose, cataclastically deformed migmatite of the Bay du Nord Group (Unit 4); cross-polarized light; sample P27-9-83; scale: 25 mm = 1 mm; 2.5 km west of Moon Pond.*

Meelpaeg Lake and is, therefore, probably related to metamorphism during intrusion of the posttectonic Meelpaeg Lake Granite to the south.

DEFORMATION AND METAMORPHISM OF THE BAY DU NORD GROUP (UNIT 4)

Deformation of the Bay du Nord Group resulted in a steep-dipping northwest-trending orientation of structures such as bedding, schistosity, fold axial planes and migmatite veins. Bedding is locally folded into tight, similar folds, with a steep-dipping, axial-planar schistosity (S_1). These folds plunge to the west at 75° and are interpreted to be F_1 structures as no tectonic fabric is folded. In the semipelitic schists, a strong schistosity is defined by biotite and muscovite. This schistosity is parallel to that associated with the F_1 folds and is interpreted to be an S_1 schistosity. A poorly developed crenulation cleavage is locally present in the schists and, in a few places, kink bands cut the S_1 fabric. That part of the Bay du Nord Group within the Dolland Brook (east half) map area forms part of the hinge zone of F_1 structures described by Blackwood (1984) from the Dolland Brook (west half) map area.

The migmatites have been cataclastically deformed (Plate 15) along with the Burgeo granite along a 500-m to 1.5-km-wide zone, which forms part of the Dragon Bay fault zone of Blackwood (1985). The mylonitic fabric is steeply dipping and trends northwesterly. The granitic neosome shows a variably developed porphyroclastic texture having plagioclase and perthite augen in a recrystallized matrix of quartz, feldspar and mica. In thin section, quartz shows extensive new grain development with sutured grain boundaries. The mylonitic foliation is parallel to the regional foliation in the Bay du Nord Group. The cataclastic fabric increases in intensity toward the Burgeo granite, which contains zones of protomylonite and mylonite (Blackwood, 1984) in the Dolland Brook (west half) map area. Dickson *et al.* (1985a) have shown that the Bay du Nord Group and the mylonites continue to the southeast, through the La Hune (11P/10) map area, and join migmatites and mylonites described by Blackwood (1985; O'Brien and Dickson, 1986).

Metamorphism of the Bay du Nord Group reached upper-amphibolite facies along with the local development of sillimanite and extensive migmatization. The neosome of the migmatites consists of quartz–plagioclase–K-feldspar–muscovite–biotite granite and the paleosome of quartz–plagioclase–biotite–muscovite–sillimanite schist. Tourmaline was found in a small area of the migmatite. The non-migmatitic parts of the Bay du Nord Group consist of quartz–plagioclase–biotite assemblages. Subsequent metamorphism of the mylonitic migmatites resulted in the variable development of retrograde chlorite after biotite, recrystallization of quartz and sericitization of plagioclase.

DEFORMATION AND METAMORPHISM OF UNIT 5– SILURIAN? CLASTIC SEDIMENTS

The clastic sediments exposed at Dolland Pond (Unit 5) are generally steeply dipping and display the effects of two deformations. The first deformation has produced a strong cleavage in the slates. The coarser grained rocks have a less well-developed cleavage, which is generally parallel to bedding (Figure 9; Plate 12b). Bedding is locally slightly overturned, to the northwest of Dolland Pond, and this is indicated by graded bedding and small-scale crossbedding. To the west of Dolland Pond, bedding in breccias trends to the northeast and is interpreted to reflect closure of the main syncline defined by bedding to the east at Dolland Pond. However, cleavage is parallel to bedding and indicates that the syncline forms part of a recumbent (F_1) structure that closes to the west.

However, using the attitude of S_0 and S_1 on the limbs of the fold only, a stereographic plot suggests that the fold closes to the west. The F_1 fold has been tilted by the later deformation, which is indicated by crenulation of cleavage and thin beds. These crenulations plunge to the west at 25° and have gently west-dipping axial planes showing a poorly developed axial-planar cleavage. Metamorphism of this unit is in the lower-greenschist facies having sporadic development of sericite and chlorite that define the cleavage. No effects of contact metamorphism are apparent in this unit.

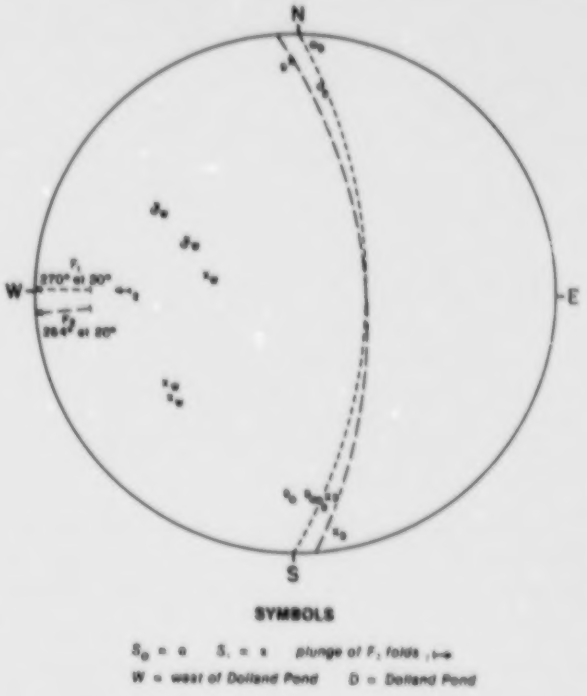

Figure 9. *Equal area stereographic projection of poles to bedding (S_0) and cleavage (S_1) with plunge and direction of plunge of F_1 and F_2 folds in Unit 5 at Dolland Pond.*

INTRUSIVE ROCKS

INTRODUCTION

Plutonic rocks within the map areas probably range in age from Lower Ordovician to Devonian. Probably the oldest unit within the map area is a small exposure of carbonatized and quartz-veined ultramafic rock (magnesite; Unit 1, Map 89-99) located 1 km to the south of D'Espoir Lake (Figure 2). Dunning and Krogh (1985) dated trondhjemite within ophiolitic complexes, 50 km north- northeast of D'Espoir Lake, at 494 to 489 Ma and the magnesite is assumed to have a similar age. The magnesite lies within the Meelpaeg Lake Fault Zone, which extends from 5 km northwest of Meelpaeg Lake dam (12A/2 map area; Williams, 1970; Dickson, 1982) to Salmon River (11P/16 map area). The Burgeo granite, in the southwest of the Dolland Brook Map area, and North Bay Granite Suite are dated as Silurian–Devonian (Dunning *et al.* 1988) and the quartz–feldspar porphyry dykes are probably related to the post-Acadian (Devonian) François Granite. The few microgranite and diabase dykes, which are massive, are considered to be mainly Devonian or younger.

Intrusive contacts within the North Bay Granite Suite were found only rarely, mainly because of poor exposure over extensive areas. Most internal contacts are based on changes in critical features such as texture, mineralogy and rarely the colour of the rock. Aeromagnetic patterns locally indicate the juxtaposition of different granites.

The nomenclature used to define the rock type is that of Streckeisen (1976) and indicated in Figure 10. The order of minor minerals used in the description of the rock is in order of increasing abundance; these are followed by significant but rarely present minerals that are preceded by "±". The term leucocratic is used here to describe a granitic rock having less than 1 percent biotite and generally containing muscovite and/or garnet. Grain size of igneous rocks is based on the average size of the matrix and is here defined as follows:

very fine grained	-	< 0.5 mm
fine grained	-	0.5 mm < 1.0 mm
medium grained	-	1.0 mm < 2.0 mm
medium-coarse grained	-	2.0 mm < 5.0 mm
coarse grained	-	5.0 mm < 10.0 mm
very coarse grained	-	> 10.0 mm

The proportions of minerals are based on modal analyses of thin sections with at least 500 points counted per thin section.

Figure 10. *Modal proportions of Q:K:P for Unit 6 of the Burgeo granite; Q = quartz, K = alkali feldspar (including perthite), P = plagioclase. Classification of granitoid rocks used in this report from Streckeisen (1976).*

UNIT 1–MAGNESITE

The oldest plutonic unit (Unit 1), located 1.3 km south-southwest of D'Espoir Lake, is considered to be a small magnesite occurrence. The magnesite is situated in the Meelpaeg Lake Fault Zone between the D'Espoir Brook Granite (Unit 9) to the south, and cleaved limestones of the Salmon River Dam Formation (subunit 3a) to the north. The magnesite underlies an exposed area about 50 m across and is highly fractured. The rock is brown on weathered surfaces and cream-coloured on fresh surfaces (Plate 16a). Numerous thin quartz veins cut the magnesite. On fresh surfaces, tiny specks (1 mm diameter) of black chromite are visible. The weathered surface of the rock is leached indicating the presence of abundant carbonate. However, the rock does not readily effervesce with cold 10 percent HCl acid. Powdered rock does readily dissolve in the acid. The brown colour may be due to weathering of minor amounts of iron carbonate disseminated throughout the rock. The identification of the rock as magnesite, having trace amounts of chromite, is based on the chemistry, which indicates that the rock contains a much greater proportion of magnesium, as compared to calcium and also upon the fact that there is over 1250 g/t nickel and 2200 g/t chromium in the sample analyzed (analysis 221372, Appendix 1; also Table 15, Geochemistry Section). The presence of iron-bearing carbonate is also indicated by the chemistry, which gives 4.10 percent FeO; only trace amounts of mafic minerals are observed in thin section.

In thin section, two distinct carbonate minerals are observed; however, no positive identification based on optical properties can be made. The presence of two carbonates is indicated by differences in interference colours and the presence of twinning in a few grains. Twinning is very rare and supports identification of the main carbonate as magnesite

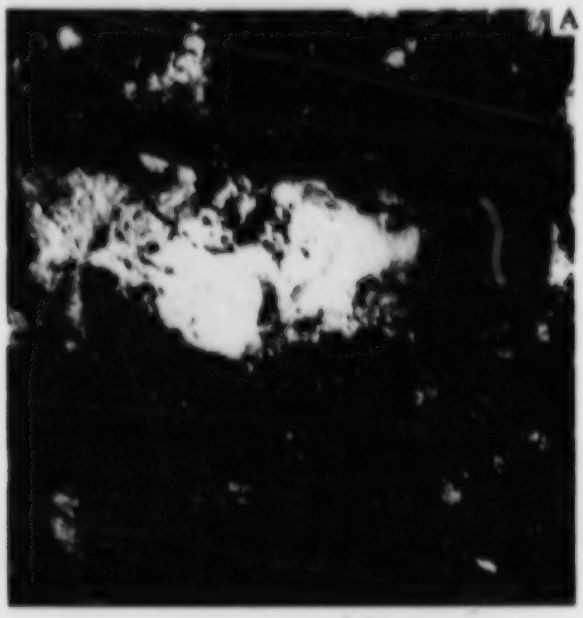

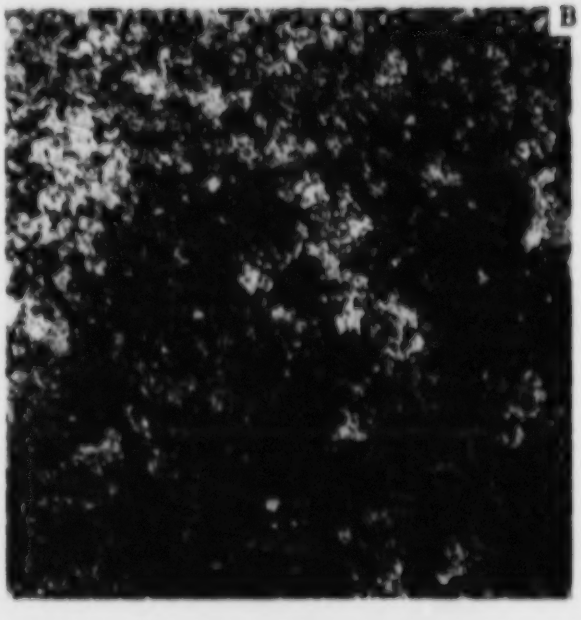

Plate 16. *(a) Sheared magnesite (Unit 1) having exposed fresh (white) surface; 0.75 km southwest of D'Espoir Lake; lens cap is 5 cm in diameter; (b) fine-grained magnesite (Unit 1) having chromite (black) specks; 0.75 km southwest of D'Espoir Lake; plane-polarized light; sample L26-13-82; scale: 25 mm = 1 mm.*

(Kerr, 1959, page 215). Chromite occurs as 1- to 0.1-mm anhedral grains having commonly ragged margins (Plate 16b). Chromite forms 1 percent of the mode. Quartz forms thin veinlets of polygonized crystals. Commonly, the quartz contains fine-grained inclusions of sericite. Other tentatively identified minerals are trace amounts of serpentine, picotite

Table 1. Modal analysis of the Burgeo granite (Unit 6)

Sample No.	Quartz	K-Feldspar	Plagioclase	Sericite	Chlorite	Opaques	Others
L25.4.83	47.2(%)	5.2	32.0	2.8	1.6	0.2	*

* Epidote 11 percent including trace apatite

and possibly perovskite. Fine-grained disseminations of limonite occur interstitially and probably account for the brown patches on fresh surfaces and brown crust on weathered surfaces.

The mineralogy and chemistry of this rock clearly indicates that it was originally an ultramafic rock. Magnesite is associated with the ultramafic rocks in the Miguels Lake and Cold Spring Pond areas (Colman-Sadd and Swinden, 1984) and these rocks are considered to be ophiolitic. The correlation with the ophiolitic rocks would also indicate a pre-Middle Ordovician age for the magnesite (Dunning and Krogh, 1985). The magnesite (Unit 1) is considered to be related to ophiolitic rocks and, thus, has been tectonically emplaced along the Meelpaeg Lake Fault Zone, which generally forms the northern margin of the North Bay Granite Suite. Colman-Sadd (1976) has noted the presence of peridotite in the adjacent St. Alban's (1M/13) map area, close to the contact with the East Bay Granite. These two occurrences may indicate that ultramafic rocks are more extensive but are hidden beneath the possibly overthrust Salmon River Dam Formation.

BURGEO GRANITE (UNITS 6 AND 7)

The southwestern corner of the Dolland Brook (east half) map area intersects part of the northeastern margin of the extensive (over 3,000 km²) Burgeo granite. The granite in this area is very strongly deformed by a part of the Dragon Bay fault zone (Blackwood, 1985; Figures 2 and 3). Ages obtained by T.E. Krogh (written communication, 1985), using zircons from the Burgeo granite in the White Bear River (11P/14) map area, indicate a probable age of crystallization of medium-grained, weakly foliated equigranular, muscovite–biotite granite at 415 ± 2 Ma (Dunning *et al.*, 1990). This granite has been interpreted by O'Brien and Tomlin (1984), Dickson *et al.* (1985b,c) and O'Brien *et al.* (1986) as the youngest major component of the Burgeo granite. The mylonitic granite is similar to that dated and therefore, is possibly the same age.

The Burgeo granite, to the southwest of the Dolland Brook map area, is dominated by medium- and coarse-grained, equigranular to porphyritic, muscovite–biotite granites. Toward the northern intrusive contact with the Ordovician Bay du Nord Group migmatites, the granite is mainly a medium-grained, equigranular, muscovite–biotite granite, and shows a pronounced increase in deformation to the northeast. Within the Dolland Brook (east half) map area, the Burgeo granite varies from strongly deformed to mylonitic. Intense mylonitic fabrics occur within the granite and decrease in intensity toward the contact with the Bay du Nord Group migmatites.

The contact between the Bay du Nord Group and the Burgeo granite is intrusive and numerous granite dykes have intruded the migmatite; screens of migmatite are common within the granite. The contact trends toward the northwest, generally parallel to the strike of the Bay du Nord Group.

The Burgeo granite, where least deformed in the map area (Unit 6), is a medium-grained, variably feldspar porphyritic, biotite granodiorite. Small phenocrysts of K-feldspar and plagioclase form augen up to 1 cm in length, in a medium-grained foliated groundmass (Table 1; Figure 10). Biotite and elongate feldspar augen define the fabric. Toward the southwest, deformation becomes more intense (Unit 7) and the rock is leucocratic having trace amounts of biotite and muscovite and isolated, 2- to 4-mm-long feldspar porphyroclasts. The groundmass is very fine grained, altered to sericite and epidote, and appears glassy on glacially polished surfaces. The foliation is defined by elongate quartz–feldspar aggregates and fine-grained mica.

The mylonitization intensity varies across the Dragon Bay fault zone and two bands of intense mylonitization (Unit 7) appear to coalesce in this area (Figure 11). Blackwood (1984) has shown that these two zones diverge in the Dolland Brook (west half) map area. The mylonitic fabric generally trends 110° and dips to the south at around 75° although steep northerly dips are also present. Displacement along the mylonite zone is considered to be minor as similar rock types occur on both sides of the zone in the Dolland Brook–Hare Bay area (Dickson *et al.*, 1985a) and in the Dolland Brook (west half) map area (Blackwood, 1984).

NORTH BAY GRANITE SUITE (UNITS 8 TO 21)

Introduction

The North Bay Granite Suite is a composite batholith composed of fourteen generally distinctive units. However, in several areas, the distinction is based on the presence of apparently minor features such as trace amounts of muscovite, changes in grain size of the matrix, or colour of the feldspars. The Meelpaeg Lake Fault Zone separates the larger portion of the batholith, here termed Component 1, from the smaller portion to the north, here termed Component 2. Component 1 consists of Unit 8, D'Espoir Brook Granite (Unit 9), East

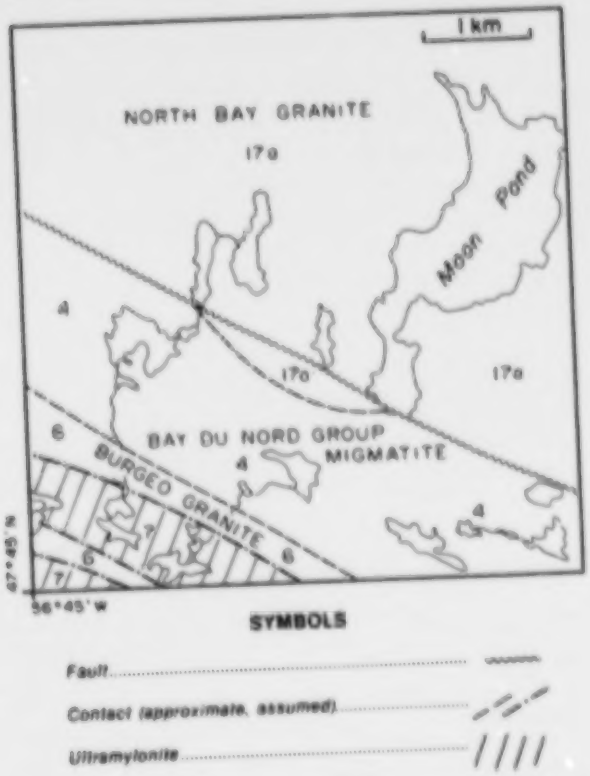

Figure 11. *Map of the Dragon Bay Fault mylonite zone in the Dolland Brook (east half) map area.*

Bay Granite (Unit 11), Bottom Brook Granite (Unit 12), Unit 13, Dolland Brook Granite (subunit 17a), Facheux Bay East Granite (subunit 17b), Wolf Mountain Granite (Unit 18), Dolland Brook Granite (subunit 19a), Morgan Brook Granite (subunit 19b), Hughes Brook Granite (subunit 19c), D'Espoir Lake Granite (subunit 19d), and Unit 21. Component 2 consists of the Wolf Lake North Granodiorite (Unit 10), Meelpaeg Lake Granite (Unit 14), Unit 15, Wolf Lake Granite (Unit 16) and the Upper Salmon Road Granite (Unit 20). The D'Espoir Lake Granite lies to the north of the fault zone, but is assigned to Component 1 on the basis of petrographic similarities to the other members of Unit 19. Contact relationships between the various units were rarely observed and gradational contacts are assumed to occur between several of the units, particularly between moderately deformed and weakly deformed granitoid rocks having similar rock types. Xenoliths of one granite in another were rarely found. However, in a few cases, granite dykes have intruded other distinct granites and the dykes are similar to other nearby units indicating possible age relationships. Thus, the exact age relationships between the units is poorly known and only locally is the sequence of intrusion understood. Intrusive relationships are summarized in Figure 3.

Radiometric Dating

Previous Rb–Sr Age Determinations

Cormier (written communication to S.P. Colman-Sadd, 1973, in Colman-Sadd, 1976) and Elias (1981) have reported dates for the southeastern (map area 1M/13) and northeastern (map areas 1M/13 and 2D/4) parts of the North Bay Granite Suite. Cormier (see Colman-Sadd, 1976) reported a Rb–Sr whole-rock age determination of 573 ± 40 Ma (2 standard deviations) having an initial Sr ratio of 0.706, from samples collected from the East Bay Granite, (mainly to the east of East Bay in map area 1M/13; Table 2). Colman-Sadd (1976) noted that this age conflicts with the field evidence as the granite has intruded the Middle Ordovician Riches Island Formation.

Table 2. Rb–Sr isotopic analyses from the East Bay Granite (R.F. Cormier, written communication to S.P. Colman-Sadd, 1976)

Sample	Rb g/t	Sr g/t	$^{87}Rb/^{86}Sr$	$^{87}Sr/^{86}Sr$
Leuco 1	172	92	5.4	0.7512
Leuco 2	128	529	0.7	0.7128
Leuco 3	205	134	4.4	0.7396
Leuco 4	184	358	1.5	0.7172
Leuco 5	105	582	0.5	0.7099

The samples collected were medium-grained, weakly foliated, muscovite–biotite granodiorite and granite. Metasedimentary xenoliths from the Baie d'Espoir Group are common in the East Bay Granite in this area. If the analyses are subdivided into two groups using Rb/Sr ratios, $^{87}Rb/^{86}Sr$ or $^{87}Sr/^{86}Sr$, Leuco 1 and 3 and Leuco 2, 4 and 5 apparently form two sets. Leuco 1 and 3 indicate an age of about 817 Ma having an initial Sr ratio of 0.689. Leuco 2, 4 and 5 give an age of 452 Ma and an initial ratio of 0.709. The results for Leuco 1 and 3 are clearly impossible. Leuco 2, 4 and 5 appear to give a reasonable age. This date is similar to that obtained from zircons in gneissic granodiorite (subunit 3d; see section on U–Pb determinations).

Elias (1981) carried out an isotopic analysis of samples from the North Bay Granite Suite to the northeast of the D'Espoir Brook map area. Using the Salmon River Dam fault (see Colman-Sadd, 1976) as a boundary, the analyses were divided into two groups, termed the southern and northern lobes (Elias and Strong, 1982). The data from Elias (1981) for each lobe are given in Table 3. These data gave Elias and Strong (1982) an age of 430 ± 4 Ma having an initial Sr ratio of 0.7066 ± 0.0001 for the northern lobe and an age of 427 ± 12 Ma with an initial Sr ratio of 0.7053 ± 0.0003 for the southern lobe.

Table 3. Rb–Sr isotopic data for the North Bay Granite Suite (from Elias, 1981)

Sample	Rb (g/t)	Sr (g/t)	$^{87}Rb/^{86}Sr$	$^{87}Sr/^{86}Sr$
Northern Lobe				
NB5	57.14	355.6	0.465	0.7095
NB6	146.1	218.1	1.94	0.7184
NB8	133.1	240.4	1.603	0.7163
NB9	129.6	230.8	1.626	0.7166
NB10	168.1	174.8	2.78	0.7239
NB11	108.5	198.3	1.585	0.7164
170374	75.5	223.2	0.966	0.7124
170385	132.8	237	1.624	0.7164
Southern Lobe = East Bay Granite				
NB1	132.1	198.2	1.930	0.7170
170072	175.1	463.7	1.093	0.7116
170080	136.4	456.9	0.864	0.7107
170198	128.5	536.0	0.694	0.7091

The northern lobe of the North Bay Granite Suite in map areas 2D/4 and 12A/1 (Colman-Sadd, 1980b, 1983) is composed of a marginal zone of medium-grained, equigranular biotite granite having a core of coarse-grained, porphyritic biotite granite. The northern lobe samples are from the marginal zone. The samples used by Elias (1981) are mainly medium-grained, equigranular to feldspar porphyritic, muscovite–biotite diorite to granite having a dominance of granodiorite. Samples NB5 and NB6 are from apparently separate intrusions outside the main mass of the North Bay Granite Suite and should not be included in the age determination. Their omission from the calculation does significantly effect the results (447 Ma and initial Sr ratio of 0.7062, approximately).

The southern lobe (= East Bay Granite) is composed of medium-grained, equigranular to feldspar porphyritic granite and granodiorite. Xenoliths of migmatite are common and form a zone dominated by migmatite, which bisects the lobe. Sample NB1 is from the southern contact of the southern zone and is spatially separated from the other three samples, which are from the northern half of the southern lobe. NB1 appears to be also chemically distinct. Exclusion of NB1 from the isochron calculation does not significantly effect the results, which are 432 Ma and 0.7050 I.R. approximately.

From the work of Elias (1981) and Elias and Strong (1982), the medium-grained, equigranular to slightly feldspar porphyritic, weakly foliated, muscovite–biotite granite and granodiorite has an indicated age of 447 to approximately 427 Ma. Similarly, the initial Sr ratios range from 0.7050 to 0.7066.

New Rb–Sr Age Determinations

Attempts were made to date several units of the North Bay Granite Suite. Rb–Sr (whole-rock) age-dating of the East Bay Granite was attempted using samples from east of North Bay, and the Upper Salmon Road Granite in the northeastern corner of map area 11P/16. Bulk samples of gneissic granodiorite in the migmatite zone, north and east of North Bay (subunit 3d), and granite from the Dolland Brook Granite at Dolland Brook, were collected for U–Pb zircon analysis.

Two sets of samples were collected by the writer, and analyzed by Dr. B.J. Fryer at Memorial University of Newfoundland, under contract with the Geological Survey of Canada. This was done to determine the age of two major units of the North Bay Granite in map area 11P/16 (D'Espoir Brook). Samples A-1 to A-4 are from the Upper Salmon Road Granite (Unit 20) and samples B-1 to B-5 are from the East Bay Granite (Unit 11). The location of the samples is given in Figures 12 and 13. The results and a summary of the report of Fryer (1983) are presented below. Analytical methods are given in Fryer (1983).

Figure 12. *Location map of samples A1 to A4 used by Fryer (1983) for Rb–Sr isotopic dating of the Upper Salmon Road Granite.*

Figure 13. *Location map of samples B1 to B5 used by Fryer (1983) for Rb–Sr isotopic dating of the East Bay Granite.*

Rb and Sr abundances, Rb/Sr and $^{87}Sr/^{86}Sr$ ratios of the 9 samples analyzed are given in Table 4 along with the standard deviations of the mean for the Sr isotopic compositions. Weighted least squares regression analysis of the data for the samples is provided in Figures 11 to 14. The errors quoted for both the age and initial ratio are 1 standard deviation.

Table 4. Rb–Sr data for the North Bay Granite Suite, D'Espoir Brook map area. Samples A-1 to A-4 are from the Upper Salmon Road Granite (Unit 20); Samples B-1 to B-5 are from the East Bay Granite (Unit 11). The error quoted for the $^{87}Sr/^{86}Sr$ ratio is one standard deviation of the mean based on within-run statistics

Sample No.	Rb (g/t)	Sr (g/t)	$^{87}Rb/^{86}Sr$	$^{87}Sr/^{86}Sr$
Unit 20–Upper Salmon Road Granite				
A-1	147	180	2.377	0.722542 ± 39
A-2	143	158	2.621	0.724547 ± 26
A-3	137	205	1.940	0.720106 ± 31
A-4	155	161	2.794	0.724524 ± 14
Unit 11–southeastern part of East Bay Granite				
B-1	102	763	0.3860	0.706605 ± 20
B-2	103	353	0.8424	0.711302 ± 34
B-3	121	340	1.027	0.712892 ± 33
B-4	134	291	1.337	0.717684 ± 34
B-5	96	246	1.127	0.719010 ± 25

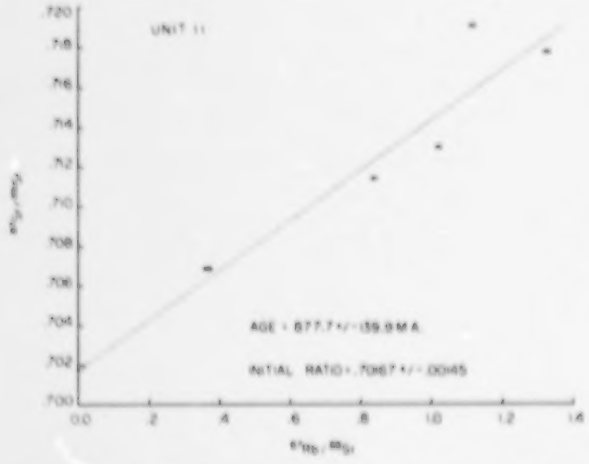

Figure 14. *$^{87}Sr/^{86}Sr$ vs. $^{87}Rb/^{86}Sr$ isochron for samples B1 to B5 of the East Bay Granite.*

The analytical data do not define isochrons and the interpretation of this data and previous work leave many unanswered questions. The five samples of the East Bay Granite are discussed first as they may shed considerable insight into the interpretation of Rb–Sr results on other granites of the area.

East Bay Granite

The five samples analyzed are medium-grained, muscovite–biotite granodiorites (e.g., Plate 19), which in hand specimen appear very homogeneous. They were specifically collected to be free of migmatite screens, schist and granitic gneiss, which are common in the sampled area, near the entrance to North Bay and East Bay but, due to the nature of the granite, they were unavoidably collected relatively (approximately 10 m) close to them. When regressed together, they scatter around a weighted least squares line, whose slope defines an age of 878 ± 140 Ma (Figure 14). Deleting successively, the most deviant points, namely B-5 (Figure 15) and B-4, B-5 (Figure 16), reduces both the ages and uncertainties significantly but even the most collinear 3 points (Figure 16) define an impossibly old age of 700 ± 20 Ma and anomalously low initial Sr ratio of 0.70276 ± 0.00017.

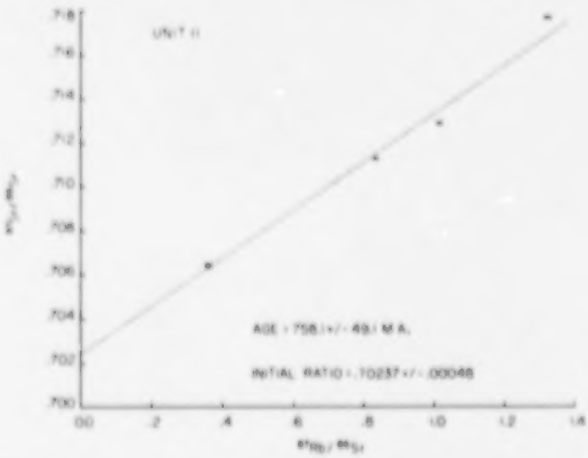

Figure 15. *$^{87}Sr/^{86}Sr$ vs. $^{87}Rb/^{86}Sr$ isochron for the East Bay Granite with sample B5 omitted.*

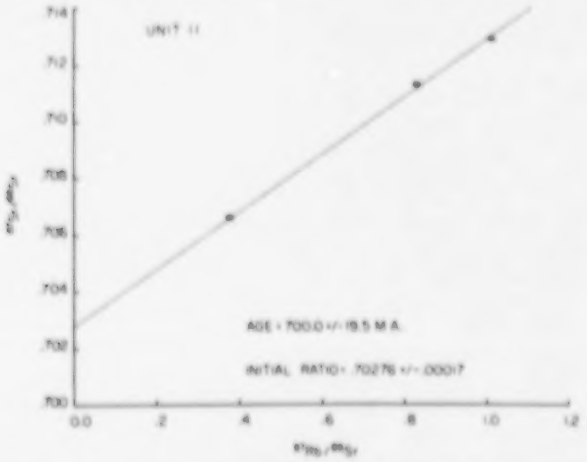

Figure 16. *$^{87}Sr/^{86}Sr$ vs. $^{87}Rb/^{86}Sr$ isochron for the East Bay Granite with samples B4 and B5 omitted.*

These results suggest one of two possibilities. Namely that the Rb–Sr systematics have been distorted by some later event causing a rotation of the points to give an increased

slope, hence old age, or that the assumption of constant initial Sr ratio for these samples is invalid and that at the time of crystallization of these rocks the initial Sr ratio was strongly positive but imperfectly correlated with their Rb/Sr ratios. The latter interpretation is preferred for several reasons. These samples were specifically chosen for study because of their lack of secondary alteration and minimal deformation. There are no megascopic signs of alteration of either the feldspars or the micas, which would be required to produce a secondary steepening of the isochron slope. An apparent increase in slope of the isochron could either be produced by a subsequent loss of Rb (but the micas are fresh!) or gain in Sr, preferably enriched in radiogenic Sr, for which there is equally no evidence. Variable contamination of the granitic magma by older more radiogenic Sr from the metamorphic screens, which would be correlated with an increase in Rb/Sr ratio of the liquid could easily account for the observed patterns in the data. The observation that the more deviant the data are from a reasonable geological age (430 to 370 Ma), the lower the Sr content of the sample suggests that synmagmatic contamination was the mechanism of isochron rotation (Figure 17).

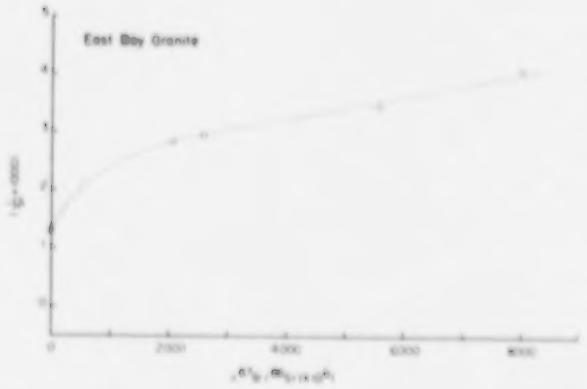

Figure 17. *Plot of (1/Sr x 1000) vs. ($\Delta^{87}Sr/^{86}Sr$ x 10^4) for samples B1 to B5 from the East Bay Granite.*

Despite the failure of Rb–Sr isotopic analyses to provide a meaningful age for this unit, they do provide evidence of an older sequence of rocks from which the granitic rocks have been either derived or have been contaminated. The extent of contamination suggests that the additional component must have been considerably older than the granite and hence probably of Precambrian age. This is supported by the preliminary interpretation of a 1500 Ma? zircon component determined by T.E. Krogh (Royal Ontario Museum) in similar screens within granite to the north and west of this locality (see below).

Upper Salmon Road Granite

The four samples of megacrystic granite (see Plate 29) were collected approximately 14 km east of D'Espoir Lake and to the west of those reported by Elias (1981), and do not define the same isochron as Elias' results (Figures 18 and 19). The four samples exhibit scatter beyond experimental error

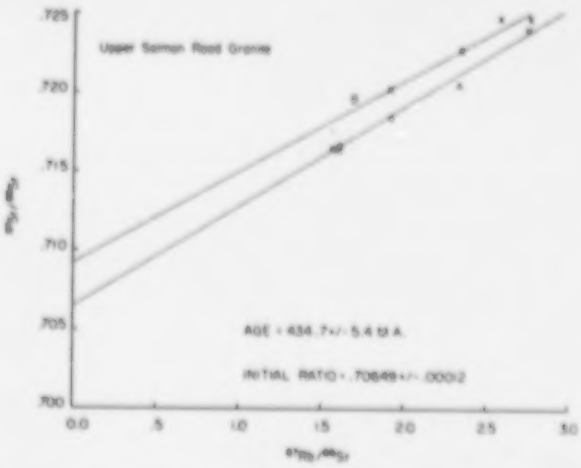

Figure 18. *$^{87}Sr/^{86}Sr$ vs. $^{87}Rb/^{86}Sr$ isochrons for the Upper Salmon Road Granite. Elias (1981) isochron (A) with data points shown by squares; Fryer (1983) isochron (B) from samples A1 to A4 (see Figure 19).*

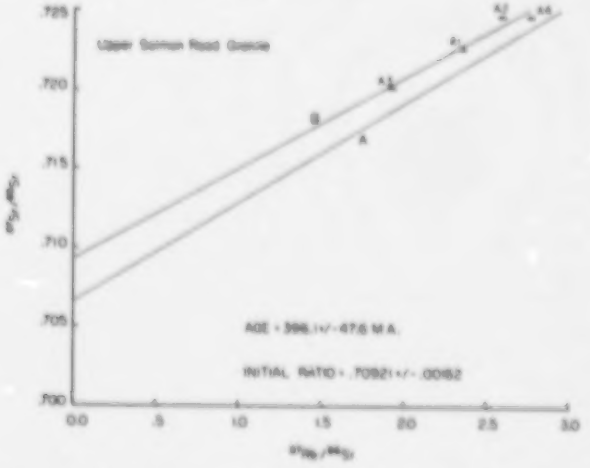

Figure 19. *$^{87}Sr/^{86}Sr$ vs. $^{87}Rb/^{86}Sr$ isochrons for the Upper Salmon Road Granite. Fryer (1983) isochron (B) from samples A1 to A4 indicated by crosses; Elias (1981) isochron (A) from Figure 18.*

and define a scatterchron of 396 ± 48 Ma having and initial Sr ratio of 0.7092 ± 0.0016. From the isochron or scatterchron lines included on each diagram, it is obvious that the data do not belong to the same populations with the possible exception of the highest Rb–Sr sample (NB80) of Elias (1981), which could conceivably belong to the A Series dataset.

The Rb–Sr results of this study do not provide age information on the granitoid rocks. They suggest that unrecognized problems of variable initial Sr ratios, at the time of crystallization, may plague these granitoid rocks at even the local scale. Instead, they may result from much older, probably Precambrian rocks, either being inhomogeneously

present in the source area of the granitic melts or they contaminated the granite melts subsequent to their formation.

New U-Pb Age Determinations

Zircon and monazite from the gneissic granodiorite (part of subunit 3d; see Plate 7b) within the migmatitic component (subunit 3d) and intruded by the East Bay Granite were analyzed for U–Pb age determination. The two samples are from widely separated areas. Sample 12-1 is from migmatite 6 km east of North Bay and sample 12-2 is from a migmatite screen 2.5 km south-southwest of D'Espoir Lake (Figure 20,a and b).

A bulk sample of the undeformed Dolland Brook Granite (Unit 17) was also collected for U–Pb age analysis. Analyses were carried out by Dr. T.E. Krogh of the Royal Ontario Museum.

Gneissic granodiorite–part of Subunit 3d

Monazites from samples 12-1 and 12-2 are slightly above concordia and have $^{207}Pb/^{235}U$ ages of 416 and 410 Ma, respectively. These monazites are in the process of being reset by the emplacement of the younger granite, and indicate that the inclusion was heated to temperatures approaching 600°C (T.E. Krogh, written communication, 1984).

The monazite ages on samples 12-1 and 12-2 lend support to the age of the North Bay Granite Suite given by Elias (1981). However, these ages also indicate that Elias' dates of 427 and 430 Ma are probably too old by perhaps 10 Ma. The monazite ages also indicate that the parental material of the migmatite is probably Ordovician or older.

Zircons were also extracted from samples 12-1 and 12-2. However, the results of U–Pb dating were less successful. Both, samples 12-1 and 12-2, have plenty of zircons but a mixed population consisting of clear, transparent, euhedral grains with either no or trace cores and cracked grains with abundant cores is obvious. The data on the diagram (see Figure 22) was obtained with clear, visible, core-free, crack-free grains which, in every case, were abraded to eliminate or reduce secondary lead loss that would pull them off of the 'anticipated' mixing line.

Sample 12-1 gives a mixing line with an indicated final magmatic crystallization age of approximately 450 Ma by conventional interpretation. Because the two lower samples have identical $^{207}Pb–^{206}Pb$ ages, it is possible that the mixing line has dropped and the magmatic crystallization stage occurred at 479 ± 2 Ma. This rock represents recycled crust with an age of contained zircons about 1500 Ma. No doubt there is absolute proof for an 'invisible' core component (T.E. Krogh, written communication, 1984).

Sample 12-2 gave three non-collinear points plotting below the mixing line. Here, a second recent Pb loss disturbance has appeared to destroy the initial two-stage line.

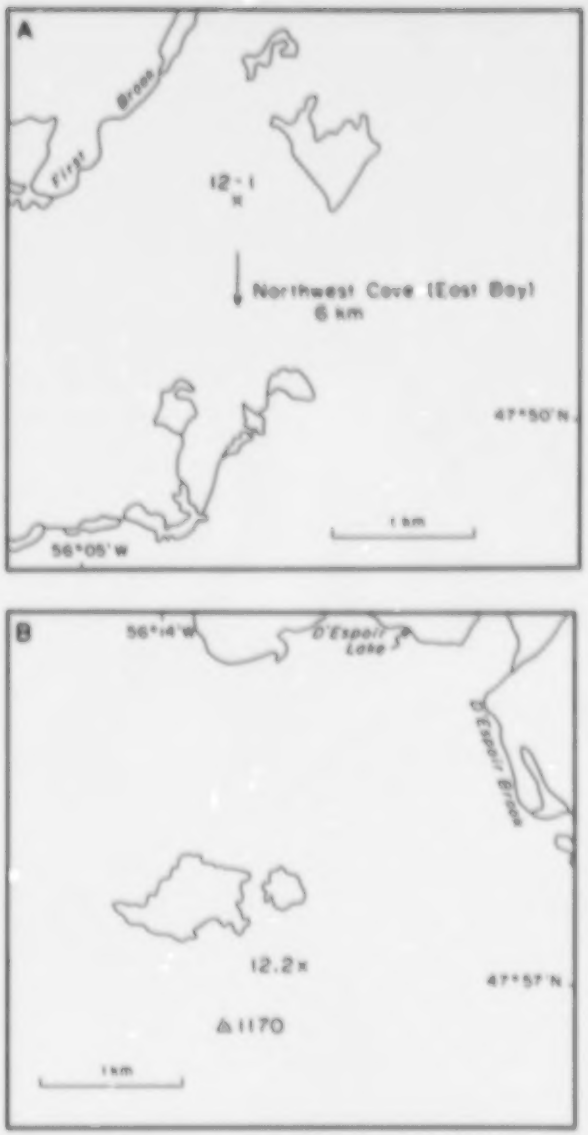

Figure 20. *(a) Location map of sample 12-1 used by T.E. Krogh (written communication, 1985) for U–Pb isotopic dating of zircons from subunit 3d migmatitic granodiorite screens within the East Bay Granite; (b) location map of sample 12-2 used by Krogh (written communication, 1985) for U–Pb isotopic dating of zircons from subunit 3d migmatitic granodiorite screens within the East Bay Granite.*

Note also, an attempt to go up the mixing line with sample 12-1 failed, as the new high point also lost Pb. (T.E. Krogh, written communication, 1984).

Dolland Brook Granite

A bulk sample of the Dolland Brook Granite (Unit 17; sample number LD33-1-83; see Plate 25a) was collected from Dolland Brook, approximately 15 km southwest of Dolland

Pond (Figure 21). This sample is a pink, massive, medium- to coarse-grained, K-feldspar porphyritic, biotite granite. Xenoliths are rare in this unit and, therefore, the effects of inheritance are minor compared to samples 12-1 and 12-2, and the samples analyzed by Fryer (1983), Elias (1981) and Cormier (1973, in Colman-Sadd, 1976). The following results are based on a report by Krogh (1985).

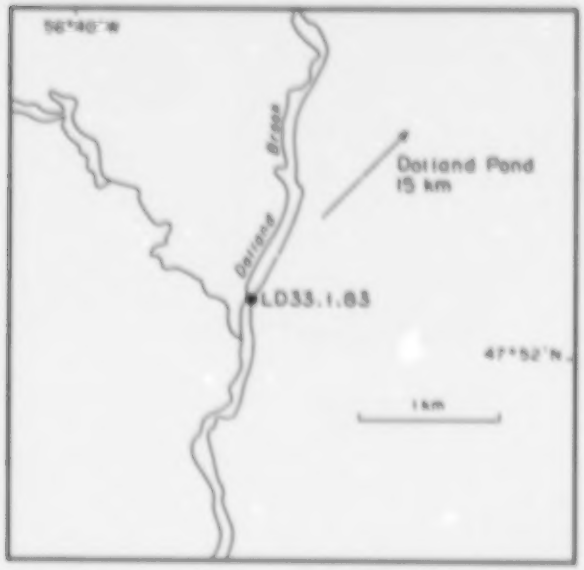

Figure 21. *Location map of sample LD33-1-83 used by T.E. Krogh (written communication, 1985) for U–Pb isotopic dating of zircons from the Dolland Brook Granite.*

The Dolland Brook Granite sample (LD33-1-83) contains zircons having a minor amount of inherited cores, especially apparent in the larger zircon grains. Two fractions of selected fine zircon needles were chosen to avoid cores, i.e., they contain a trace of longitudinal fractures, or are flat and are unlikely to contain cores. Both fractions of zircon have identical $^{207}Pb-Pb^{206}$ ages of 396 Ma, which very likely indicate the time of crystallization (Figure 22). Dunning *et al.* (1988) subsequently reported that the precise U–Pb (zircon) age for the Dolland Brook Granite based on these data is 396$^{+7}_{-5}$ Ma.

Monazite in the Dolland Brook Granite plots above concordia, outside of experimental error, by about 5 percent (Figure 22). Such data had not been obtained before, so, this sample was re-analyzed in duplicate and residues in the +200 and -200 mesh-size were chosen. All three analyses overlap within error, thus proving that the apparently impossible data are real. It is possible that monazite scavenges thorium from the U to Pb chain, which results in a large excess of Pb in the monazite. The effect has been seen before in very young magmatic rocks but its magnitude was such that it would not be detectable in a 400-Ma rock. It is thought that the large anomaly observed is probably produced when monazite forms in an already crystallized rock in which Th is not mobile, thus exaggerating the scavenging of Th from the U chain during the breakdown of other uranium-bearing phosphates.

The $^{207}Pb-^{235}U$ (monazite) ages of the 3 samples probably establish the age for the cooling of the granite below about 600°C at 390 ± 2 Ma.

Summary of New Age Determinations

The Rb–Sr determinations by Fryer (1983) do not give useful data on the age of the East Bay and Upper Salmon Road granites. The U–Pb data clearly indicate that the Dolland Brook Granite is 396-Ma old and cooled, through 600°C, at 390 Ma. Uranium–Lead (monazite) data on gneissic granodiorite screens within the East Bay Granite dates them 416 and 410 Ma; this may also indicate cooling below 600°C and possibly the approximate age of the East Bay Granite. U–Pb (zircon) ages of 450 Ma (by conventional interpretation) or 479 ± 2 Ma (assuming lead loss), on the same samples, date crystallization ages of the gneissic granodiorite screens. The gneissic granodiorite was in part derived from recycled crust that contained zircons dated at about 1500 Ma.

Description of the North Bay Granite Suite

Unit 8 and the D'Espoir Brook Granite (Unit 9)

Distribution

Some of the northern portion of the North Bay Granite Suite is composed of sheared, brecciated or mylonitic granite located along the Meelpaeg Lake Fault Zone. The main components of this elongate belt are coarse-grained, K-feldspar porphyritic, biotite granite (Unit 8), which has been intruded by leucocratic biotite–muscovite granite (the D'Espoir Brook Granite, Unit 9; Plate 17) and commonly occurs as inclusions in the D'Espoir Brook Granite. The biotite granite (Unit 8) is the main rock type southwest of D'Espoir Lake. However, the D'Espoir Brook Granite, which extends from Meelpaeg Lake (12A/2) to Salmon River (11P/16) is the dominant rock type. Within Unit 8 are numerous variably sized inclusions of migmatitic granodiorite 'gneiss' (see e.g., Plate 7b). Dykes of East Bay Granite have intruded the migmatitic gneiss.

Contact Relations

The contact between the D'Espoir Brook Granite and the Spruce Brook Formation is intrusive. Southwest of Meelpaeg Lake, several leucocratic granite dykes have intruded the Spruce Brook Formation and xenoliths of Spruce Brook Formation occur within the D'Espoir Brook Granite. Similarly, in map area 11P/16, parts of the Salmon River Dam Formation have been intruded by leucocratic granite dykes, and xenoliths of the Salmon River Dam Formation are found within the D'Espoir Brook Granite close to the intrusive contact, southeast of Dolland Pond.

The northeastern and northern contact of Unit 8 and the D'Espoir Brook Granite with the granitoid rocks and metasedimentary rocks of Component 2, to the northeast and

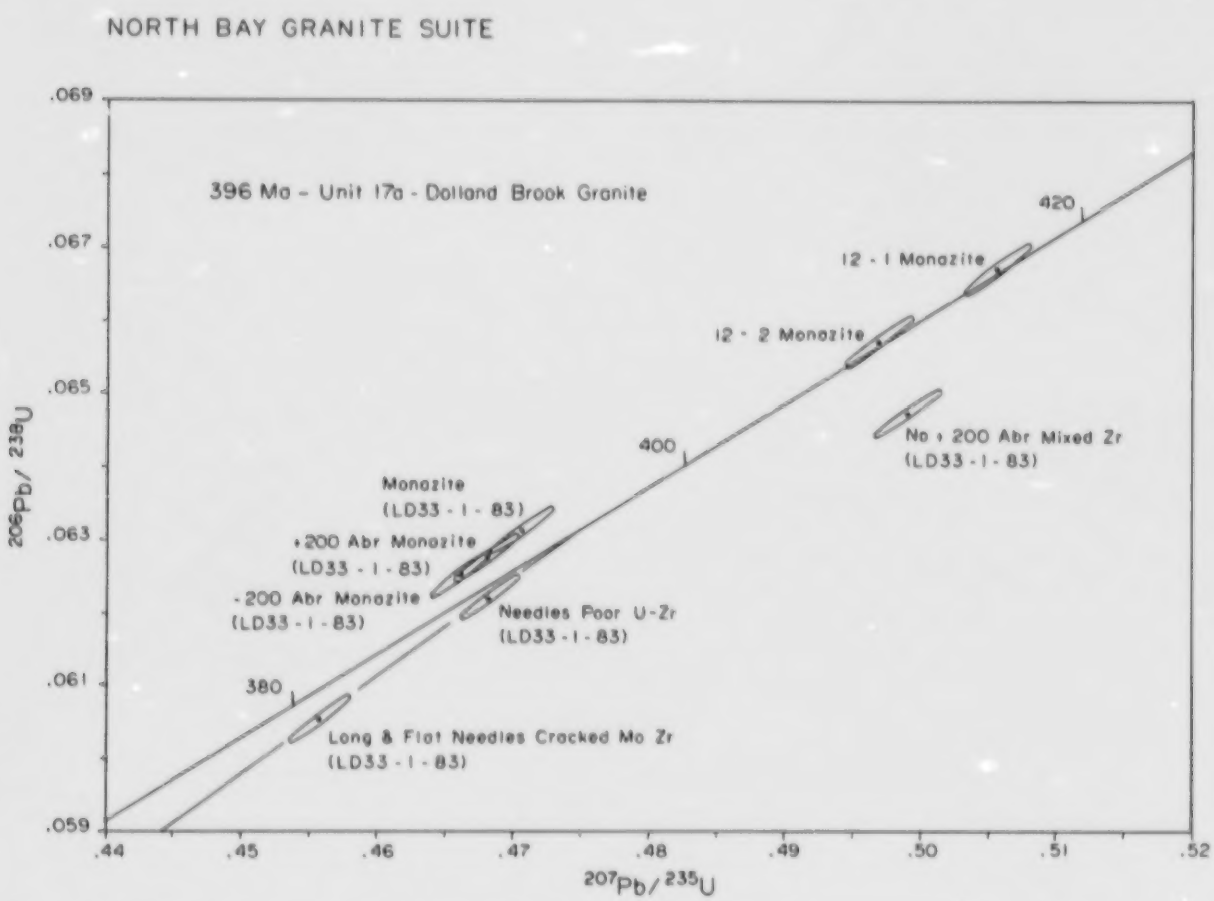

Figure 22. *$^{206}Pb/^{238}U$ vs. $^{207}Pb/^{235}U$ concordia for data obtained by T.E. Krogh (written communication, 1985) on samples 12-1, 12-2, and LD33-1-83. See text for details of plots.*

north, is the Meelpaeg Lake Fault Zone, which extends from Meelpaeg Lake to Salmon River and is the site of several large quartz veins (Plate 18) and magnesite (Unit 1). Similarly, the southwestern contact of Unit 8 and the D'Espoir Brook Granite with the Wolf Mountain and Dolland Pond granites (Unit 18 and subunit 19a) is also a fault. There is no evidence for an original intrusive contact. However, to the east of Dolland Pond, the nature of the southern contact of Unit 8 and the D'Espoir Brook Granite with the East Bay Granite is not exposed but there is probably an intrusive contact as dykes, similar to the East Bay Granite, have intruded Unit 8.

Exotic xenoliths within Unit 8 and the D'Espoir Brook Granite include foliated diorite and tonalite, migmatite and gneissic granodiorite. The gneissic granodiorite is similar to that described previously (subunit 3d). These xenoliths are most abundant between D'Espoir Lake and Dolland Pond and the gneissic xenoliths extend to the south into the East Bay and Bottom Brook granites. The xenoliths range in size from 1 to 20 m and are subangular to round. The diorite xenoliths in the D'Espoir Brook Granite are foliated to massive and biotite–hornblende-rich and form only a minor proportion of the xenolith population.

Petrography

The coarse-grained, porphyritic, biotite granite (Unit 8) is a strongly foliated, buff-coloured rock containing between 5 and 15 percent, 1- to 2-cm-long, augened feldspar phenocrysts, set in a foliated matrix of quartz, feldspar and biotite. Petrographic features of Unit 8 and all the other units of the North Bay Granite Suite are summarized in Table 5. Modal analyses are given in Table 6 and quartz:K-feldspar :plagioclase ratios are shown in Figure 23. In thin section, the elongate quartz is seen to occur as variably recrystallized to irregular sutured aggregates along with cataclastically deformed feldspar. Biotite is well aligned and variably altered to chlorite.

The D'Espoir Brook Granite (Unit 9) has a highly variable texture ranging from aplitic through hypidiomorphic-granular to pegmatitic (Plate 18a; see Table 5). Pegmatite and aplite are most abundant west of Wolf Lake. Modal analyses are given in Table 6 and quartz:K-feldspar:plagioclase ratios are shown in Figure 23.

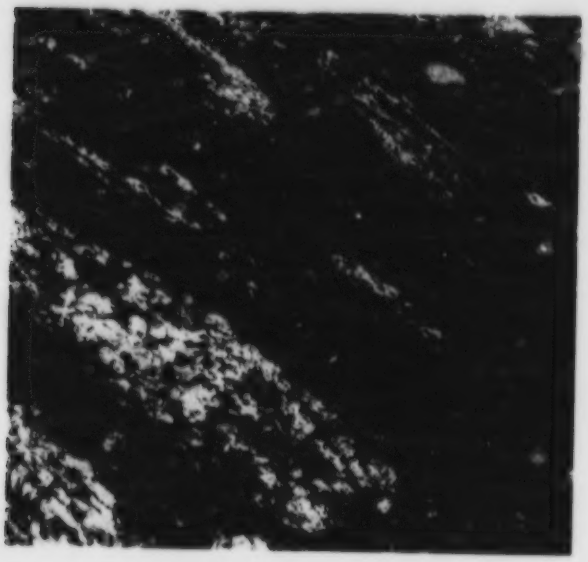

Plate 17. *Strongly foliated granite and pegmatite of the D'Espoir Brook Granite (Unit 9) having north-dipping foliation; on D'Espoir Brook, 1.5 km southeast of D'Espoir Lake; lens cap is 5 cm in diameter.*

Plate 18. *Ridge of vein quartz (Unit 24) injected along the Meelpaeg Lake Fault Zone; 1 km south of D'Espoir Lake.*

The degree of deformation of the D'Espoir Brook Granite varies from minor to intense having a strongly developed cataclastic foliation. The more intense cataclastic fabric occurs mainly in the vicinity of faults to which it is parallel. Locally, zones of strong deformation occur up to 3 km south of the northern contact, in the D'Espoir Lake–Salmon River area. West and southwest of Wolf Lake, the granite is strongly deformed throughout.

The generally strong foliation within Unit 8 and the D'Espoir Brook Granite is parallel to the faults bounding the units. The dip of the foliation is gentle to moderate (25 to 70°) and, in the Wolf Lake area, is consistently toward the east; between Dolland Brook and Salmon River the dip is toward the north or northeast (Plate 18a). These attitudes are plotted in Figure 24. The foliation in the granites is interpreted to be a regional S_2 fabric as previously foliated (S_1) metasedimentary rocks occur as inclusions in the granites.

The D'Espoir Brook Granite (Unit 9) is composed of anhedral to strongly flattened quartz, perthitic microcline plagioclase, aligned muscovite and biotite (where present) and euhedral garnet crystals (where present) 0.5 to 2 mm in diameter, and other accessory minerals. Modal proportions are given in Table 6 and quartz:K-feldspar:plagioclase ratios are shown in Figure 23. Narrow zones of granulated granite are found in some samples. Where well developed, the strong cataclastic foliations are defined by aligned mica, and flattened quartz, which displays new grain development or recrystallization textures. Feldspars are commonly distorted, broken or kinked. The aplites and pegmatites are generally more leucocratic than the granite and contain a higher proportion of muscovite, garnet and, locally, are tourmaline-bearing.

Wolf Lake North Granodiorite (Unit 10)

Distribution

The Wolf Lake North Granodiorite consists of variably deformed, feldspar-porphyritic, biotite granodiorite, and outcrops to the southeast of Meelpaeg Lake and to the southwest of Wolf Lake.

Contact Relations

Dykes of the Wolf Lake North Granodiorite cut the North Steady Pond and Spruce Brook formations, and xenoliths of the formations are found within the granodiorite close to the contact (Plate 19). Contact metamorphism has resulted in the development of andalusite porphyroblasts in subunit 3f of the North Steady Pond Formation, 15 km north of Dolland Pond. Andalusite porphyroblasts and fine sillimanite needles are present within psammites of the Spruce Brook Formation at the contact. Near the contact with the Wolf Lake North Granodiorite, at Meelpaeg Lake, garnet and coarse randomly orientated muscovite (probably related to contact metamorphism) form augen within the main tectonic fabric in the Spruce Brook Formation. The fabric within the Wolf Lake North Granodiorite is parallel to the main fabric in the Spruce Brook Formation; they may be contemporaneous and indicate that the granodiorite is pretectonic in relation to the development of the main fabric in the Spruce Brook Formation. Southwest of Wolf Lake, two small isolated areas of strongly sheared and altered diorite are exposed. The more

Table 5. Main features of the granitoid rocks in the North Bay Granite Suite

Unit	Rock type	Colour	Texture ;Grain-size	Pheno-crysts	Folia-tion	Alter-ation	Xeno-liths	Dyke, pegm* veins	Mica	Acces-sories
8	grnt, grdr	pink, buff	porph; coarse	K-feld	strong	seric, chlor, quartz veins	migm, psam, dior, tnlt	pegm, grdr	biot	zr, ap mt, sp
9	grnt	pink, white	equi, aplitic; coarse - medium	-	strong - weak - mylt	seric, quartz veins	unit 8, dior	pegm	biot musc	zr, ap gt, mt tour, al
10	grdr	grey, white	equi, porph; medium	plag, K-feld	strong	seric, chlor	migm, biot schist	-	biot	zr, ap mt
11	grdr grnt	grey, buff	equi; medium	-	moder-ate to weak	seric, chlor	migm, mica schist	pegm, grdr	biot musc	zr, ap mt, sp al
12	grdr grnt	grey, buff	porph; medium	plag, K-feld	moder-ate to weak	seric, chlor	migm, mica schist	pegm-grdr	biot musc	zr, ap mt, sp al
13	grnt	pink, orange	equi; medium	-	moder-ate	seric, chlor	-	-	biot musc	zr, ap mt
14	grnt grdr	buff	equi, porph; medium	plag, K-feld	weak - absent	seric, chlor, epid	psam schist	grnt, pegm	biot musc	zr, ap mt
15	grnt	buff	equi; medium	-	weak - absent	seric, chlor, quartz veins	biot-musc psam schist	pegm	biot musc	zr, ap mt, sp al
16	grnt	buff, white	equi; coarse	-	absent	quartz veins, chlor, seric	psam	pegm	musc biot	zr, ap mt, gt
17	grnt	pink, buff	porph, minor equi; coarse	K-feld	weak - absent	seric, chlor, quartz veins, hem	psam schist	apl, pegm	biot	zr, ap mt, al musc, tour
18	grnt	pink, buff	porph; coarse	K-feld	weak - absent	seric, chlor	psam schist	apl, pegm	biot musc	zr, ap mt
19	grnt	pink	porph; coarse	K-feld	weak - absent	seric, chlor, tour	psam schist	apl, pegm, qzfp	biot musc	zr, ap mt, gt
20	grnt	pink, grey	porph; coarse	K-feld	weak - absent	seric, chlor, epid	psam schist, dior, grnt	apl, pegm, qzfp	biot musc	zr, ap mt
21	grnt	pink, buff	porph; medium	K-feld	moder-ate to weak	seric, chlor	psam schist, amph	apl, pegm, qzfp	biot musc	zr, ap mt, gt

* abbreviations:

al	= allanite	epid	= epidote	migm	= migmatite	psam	= psammite
ap	= apatite	equi	= equigranular	mt	= magnetite	qzfp	= quartz–feldspar porphyry
apl	= aplite	grdr	= granodiorite	musc	= muscovite	seric	= sericite
amph	= amphibolite	grnt	= granite	mylt	= mylonitic	sp	= sphene
biot	= biotite	gt	= garnet	pegm	= pegmatite	tnlt	= tonalite
chlor	= chlorite	hem	= hematite	plag	= plagioclase	tour	= tourmaline
dior	= diorite	K-feld	= K-feldspar	porph	= porphyritic	zr	= zircon

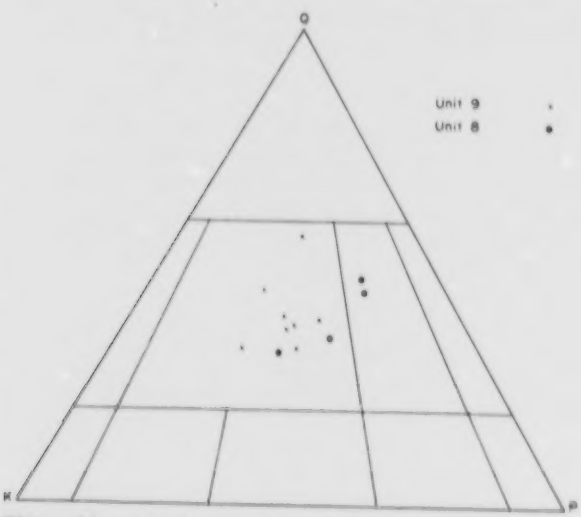

Figure 23. *Modal proportions of Q:K:P for Unit 8 and the D'Espoir Brook Granite (Unit 9); classification and abbreviations as in Figure 10.*

westerly outcrop is faulted against the D'Espoir Brook Granite; the relationship between the other area of diorite and the Meelpaeg Lake Granite is unknown.

Petrography

The Wolf Lake North Granodiorite is composed of mainly quartz, plagioclase, microcline and biotite (see also Table 5 for other features, Table 7 for modal analyses, and Figure 25 for quartz:K-feldspar:plagioclase ratios). The locally strong tectonic fabric, apparent in outcrop, is reflected by aligned mica, elongate, anhedral quartz aggregates and aligned feldspar phenocrysts. The psammite xenoliths are also elongate and aligned parallel to the foliation in the granodiorite (Plate 19).

In the southeastern part of the Wolf Lake North Granodiorite, muscovite–garnet granite dykes have intruded the foliated granodiorite. These dykes are locally abundant and much less deformed in comparison to the host granodiorite, and therefore, are probably unrelated to the granodiorite. A probable source is the nearby muscovite–biotite granite (Unit 15), which also contains garnet-bearing veins.

East Bay and Bottom Brook Granites (Units 11 and 12)

Distribution

The equigranular East Bay Granite (Plate 20) and the porphyritic Bottom Brook Granite (Plate 21) occur throughout the D'Espoir Brook (11P/16) map area. These granites generally appear to have a gradational contact.

The East Bay Granite has been intruded locally by biotite granodiorite and granite dykes, which are compositionally similar to the host rocks (Plate 20), suggesting [illegible] East Bay Granite may be composed of several similar granitoid phases.

A locally prominent feature of the East Bay Granite is biotite-rich layers or schlieren, which are commonly 2 to 5 mm thick, parallel, and form sets several metres thick. Along the eastern shore of Facheux Bay, in map area 11P/16, these poor- and rich-biotite layers are much thicker, ranging from 15 to 50 cm in thickness; some of the layer-sets may attain a thickness of 5 m (Plate 22). This layering is probably the result of crystal settling. Similar layering occurs in the McCallum Granite, to the south (Blackwood 1983, 1985), which is, in part, similar to the East Bay Granite. Blackwood (1985) describes feldspar phenocrysts that straddle the layer boundaries. The possibility of a correlation between parts of the East Bay and McCallum granites clearly exists.

The proportion of phenocrysts in the Bottom Brook Granite varies from less than 1 percent to 20 percent of the mode (Plate 21). Locally, the East Bay and Bottom Brook granites contain garnet–muscovite aplite veins and coarse-grained, garnet–muscovite granite pegmatite segregations and veins, with some gently dipping sheets covering 4 to 5 hectares, south of East Bay.

Contact Relations

The East Bay and Bottom Brook granites have intruded the Riches Island Formation south and east of East Bay (see also Colman-Sadd, 1976; Blackwood, 1985). Numerous dykes of granite (50 m by 1 km) have intruded the Riches Island Formation south of East Bay and large xenoliths of Riches Island Formation are abundant in the East Bay Granite on both sides of East Bay. Xenoliths of migmatized Baie d'Espoir Group (subunit 3d) are abundant over large areas.

Petrography

The granodiorites and granites of the East Bay and Bottom Brook granites are composed of quartz, perthitic K-feldspar, zoned plagioclase, biotite and muscovite and accessory minerals (Tables 5 and 8; Figure 26). Pyrite cubes (to 5 mm^3) and tourmaline rosettes (to 5 cm diameter) occur along joints in porphyritic granite (geochemistry sample location 1406), 2.5 km northwest of Brent Cove (Facheux Bay map area).

The granites have a hypidiomorphic-granular texture and a superimposed, variably developed, tectonic fabric deformed by aligned mica and feldspar phenocrysts. Locally, minor granophyric or myrmekitic intergrowths occur in the groundmass. Quartz commonly forms anhedral, variably elongate, sutured aggregates, even in apparently weakly deformed rocks. These aggregates are indicative of new-grain development and commonly show subgrain boundaries.

K-feldspar and plagioclase form the phenocryst phases in the Bottom Brook Granite and K-feldspar is generally more

Table 6. Modal analyses of Unit 8 and the D'Espoir Brook Granite

a. Unit 8

Sample No.	L16.2.83	L20.8.82	T21.4.82	T21.7A.82
Geochem No.	221624	-	221232	221233
Quartz (%)	25.8	29.6	36.0	37.0
K-feldspar	23.0	32.4	12.2	10.4
Plagioclase	38.2	30.6	32.6	29.4
Biotite	12.4	3.2	5.0	1.6
Muscovite	-	3.2	5.4	2.4
Garnet	-	-	-	-
Sericite	Tr*	0.8	1.6	1.4
Chlorite	Tr	0.2	6.0	14.6
Opaques	0.6	Tr	0.2	Tr
Others	Tr**	Tr**	Tr***	Tr**

* Tr–observed in thin section but not counted
** Apatite and zircon
*** Sphene (0.2%), epidote (0.8%), apatite and zircon

b. D'Espoir Brook Granite (Unit 9)

Sample No.	T30.3.82	L18.5.82	L18.6.82	L26.4.82
Geochem No.	-	221347	221348	-
Quartz (%)	39.4	43.4	29.0	34.8
K-feldspar	28.4	15.6	37.6	30.6
Plagioclase	18.2	17.2	20.4	27.8
Biotite	Tr	4.4	7.2	1.4
Muscovite	12.6	19.4	4.6	3.8
Garnet	1.2	-	-	-
Sericite	-	Tr	1.0	1.6
Chlorite	-	-	0.2	-
Opaques	0.2	Tr	-	-
Others	Tr*	Tr*	Tr**	Tr*

Sample No.	P3.3.83	P10.1.82	P17.7.83	L3.1.83
Geochem No.	-	-	21693	221601
Quartz (%)	24.8	36.8	34.2	36.4
K-feldspar	25.0	29.8	28.4	24.6
Plagioclase	24.8	26.2	27.8	33.4
Biotite	8.0	2.8	-	-
Muscovite	-	4.0	9.6	5.4
Garnet	-	-	-	0.2
Sericite	Tr	0.4	Tr	Tr
Chlorite	0.6	Tr		
Opaques	Tr	Tr	Tr	Tr
Others	Tr*	Tr*	Tr*	Tr*

* Zircon ** Zircon and apatite

abundant than plagioclase. The phenocrysts vary in size from 5 mm to rarely 2 cm in length. The K-feldspar phenocrysts are locally perthitic and show mainly simple twins but microcline twinning has developed locally. Zoned K-feldspar phenocrysts occur rarely. The K-feldspar phenocrysts commonly contain inclusions of quartz, plagioclase and biotite. Plagioclase phenocrysts commonly display oscillatory and normal zoning and locally contain inclusions of K-feldspar and plagioclase. Biotite and muscovite occur mainly as interstitial, 1- to 3-mm-long flakes.

Orientations of foliation and small-fold axes in veins generally trend northeasterly to easterly, subparallel to those in the Baie d'Espoir Group, to the south.

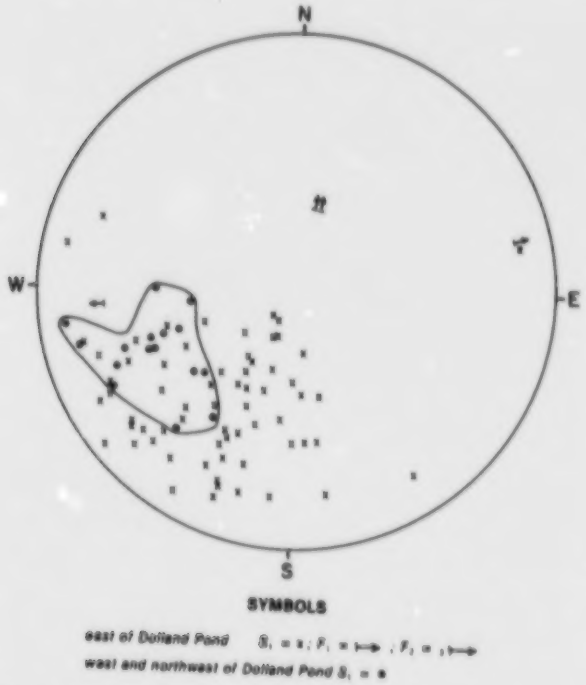

Figure 24. *Equal area stereographic projection of poles to main foliation, with plunge and direction of plunge of small folds, from Unit 8 granite and the D'Espoir Brook Granite.*

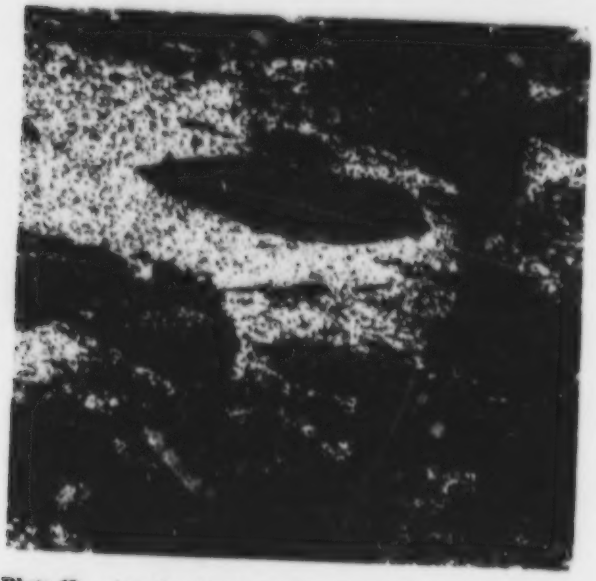

Plate 19. *Angular, biotite psammite xenoliths of the Spruce Brook Formation migmatite (subunit 2d) in the moderately foliated Wolf Lake North Granodiorite (Unit 10); northwest side of 7-km-long pond, northeast of Wolf Lake.*

Unit 13

Pink to orange, foliated, medium-grained, equigranular to slightly porphyritic, muscovite–biotite granite underlies a small area of the D'Espoir Brook map area, around the northern portion of Salmon River; this unit, which also occurs in the adjacent NTS map area 1M/13, has been tentatively assigned a Precambrian age (Colman-Sadd, 1976). The age-determination is based on 'a well-defined fabric that is discordant to the Salmon River Fault and to all structures in the Baie d'Espoir Group and North Bay Granite' (Colman-Sadd, 1976). This well-defined fabric has a southeasterly orientation and is parallel to the mylonitic fabrics in Units 8 and 9, exposed nearby, along the Meelpaeg Lake Fault Zone. Therefore, the southeasterly orientation is not considered to be evidence for a Precambrian age. This unit is similar, apart from colour, to the porphyritic Bottom Brook Granite and is probably the same age.

Meelpaeg Lake Granite (Unit 14)

Distribution

Buff, medium- to medium-coarse-grained, massive, equigranular, biotite granodiorite and granite underlie the area from the eastern shore of Wolf Lake northwestward to Meelpaeg Lake, where the unit is best exposed.

Contact Relations

The Meelpaeg Lake Granite has intruded and contact metamorphosed the semipelites of the Spruce Brook Formation (subunit 2a) at Wolf Lake and southwest of Meelpaeg Lake. Spruce Brook Formation xenoliths are common within the granite, close to the contacts, and dykes of the granite have also intruded the Spruce Brook Formation southwest of Meelpaeg Lake. An isolated outcrop of recrystallized quartz–plagioclase-crystal tuff, similar to subunit 3e of the North Steady Pond Formation, occurs west of Wolf Lake as a roof pendant or xenolith. The porphyroblasts are undeformed and overprint the tectonic fabric in the Spruce Brook Formation, indicating clearly the posttectonic nature of the granite. The contact of the Meelpaeg Lake Granite with the D'Espoir Brook Granite is the Meelpaeg Lake Fault Zone where the D'Espoir Brook Granite and the Meelpaeg Lake Granite are strongly sheared and brecciated. No indication of an originally intrusive contact was found. Contacts with the migmatites (subunit 2d) or the Wolf Lake Granite were not found. However, granitoid dykes, similar to the Meelpaeg Lake Granite, cut the migmatites on the islands in Meelpaeg Lake.

Petrography

The Meelpaeg Lake Granite is composed mainly of quartz, microcline-twinned and untwinned perthitic

Table 7. Modal analyses of the Wolf Lake North Granodiorite (Unit 10)

Sample No.	L4.2.83	L5.8.83	L12.6.83	L27.2.83	P31.20.83
Geochem No.	221602	221604	221620	-	221557
Quartz (%)	27.0	38.8	26.0	33.8	37.6
K-feldspar	-	13.2	11.6	19.4	-
Plagioclase	49.2	38.8	44.8	32.4	38.2
Biotite	19.2	7.2	17.6	13.8	20.0
Muscovite	1.0	-	-	-	-
Garnet	-	-	-	-	-
Sericite	3.2	1.0	Tr	Tr	Tr
Chlorite	0.4	0.8	Tr	0.4	0.6
Opaques	Tr	Tr	Tr	Tr	Tr
Others	Tr*	Tr**	Tr***	Tr+	Tr*

* Zircon and apatite; ** Apatite (0.2%) and zircon; *** also includes sphene; + also includes sphene (0.2%)

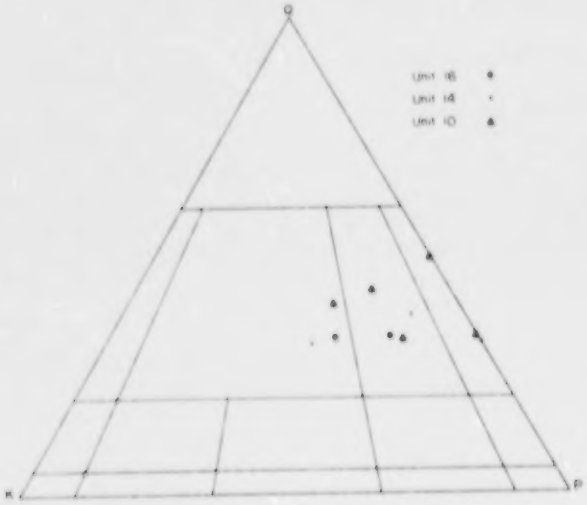

Figure 25. *Modal proportions of Q:K:P for the Wolf Lake North Granodiorite, Meelpaeg Lake and Wolf Lake granites; classification and abbreviations as in Figure 10.*

K-feldspar, strongly zoned plagioclase, biotite and accessory minerals (Table 5; Plate 23, a and b). Southwest of Meelpaeg Lake, the massive granite, which intruded the Spruce Brook Formation, also contains muscovite (Table 9 for modal analyses and Figure 25 for quartz:K-feldspar:plagioclase ratios).

Quartz occurs as interstitial, anhedral aggregates having undulose extinction. K-feldspar forms interstitial to ophitic crystals exhibiting inclusions of plagioclase and biotite. Subhedral plagioclase displays strong, normal to oscillatory zoning, and anorthite content ranges from An_{30} to An_{15}. Mantles of myrmekite have developed on some crystals. Biotite forms rectangular, 1- to 3-mm-long, brown–light-brown pleochroic flakes, which have numerous zircon inclusions.

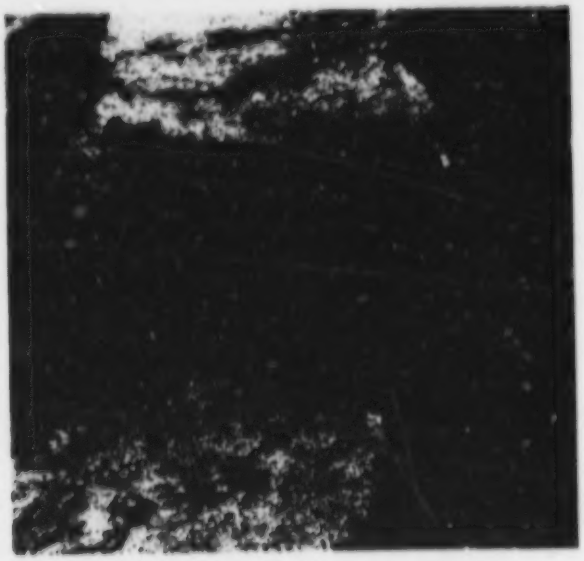

Plate 20. *Dyke of equigranular biotite granite cuts the East Bay Granite (Unit 11); 1.75 km northwest of Garland Cove, North Bay; hammer is 30 cm long.*

Unit 15

Distribution

A poorly exposed area of medium-grained, massive, equigranular, leucocratic, muscovite–biotite granite underlies the area between the two eastern zones of the Wolf Lake North Granodiorite (Unit 10), 5 to 10 km northeast of Wolf Lake. Small, partly fault-bound areas of altered granite, which have probably intruded the North Steady Pond Formation 6 km east of Wolf Lake, are correlated with Unit 15.

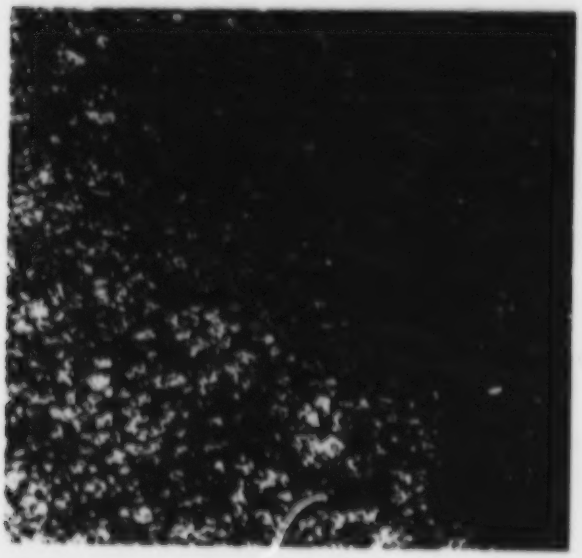

Plate 21. *Aligned feldspar phenocrysts in the Bottom Brook Granite (Unit 12); northeastern end of East Bay; lens cap is 5 cm in diameter.*

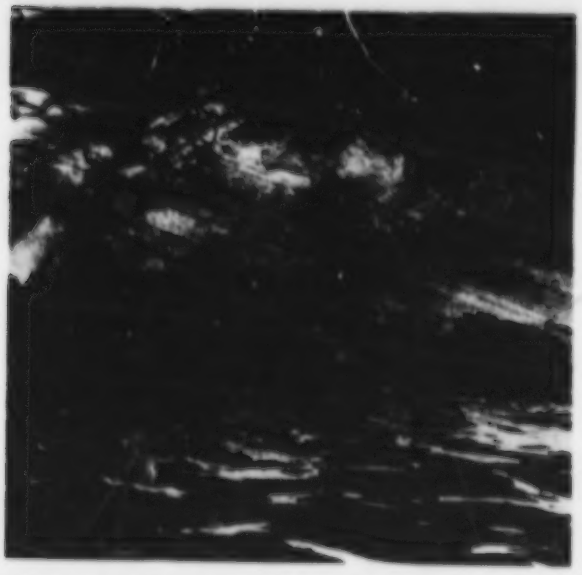

Plate 22. *Gently dipping, biotite-rich layers in the East Bay Granite (Unit 11); east side, northern end of Facheux Bay; layers are approximately 30 cm wide.*

Contact Relations

Contacts between the main mass of Unit 15 and the Wolf Lake North Granodiorite are not exposed. However, the high degree of deformation shown by the Wolf Lake North Granodiorite compared to Unit 15 indicates that the granodiorite is probably older and has been intruded by Unit 15. Numerous granite dykes have intruded the North Steady Pond Formation. Metasedimentary xenoliths are found in the granite along the southern contact, and the North Steady Pond Formation has been contact metamorphosed. The contact between the North Steady Pond Formation and the granite of Unit 5 was observed in one location and the granite contains a trace of molybdenite (geochemical sample location 1551[1]).

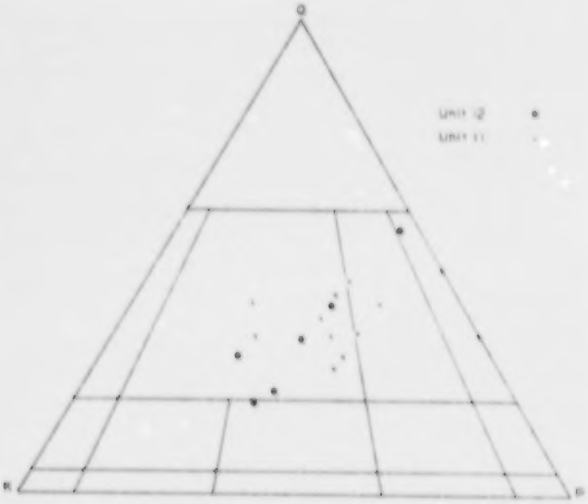

Figure 26. *Modal proportions of Q:K:P for the East Bay (Unit 11) and Bottom Brook (Unit 12) granites; classification and abbreviations as in Figure 10.*

Petrography of the Altered Granite

The two areas of altered granite, 6 km east of Wolf Lake, consist of quartz-rich and muscovite-rich, silicified green granite, respectively. The granites are separated by a northwest-trending fault that also separates the Spruce Brook and North Steady Pond formations. The granites are highly siliceous and sheared and are devoid of feldspar, which has been completely altered to sericite. Coarse muscovite flakes occur throughout the northern granite. This rock is similar to a greisen.

Wolf Lake Granite (Unit 16)

Distribution

A poorly exposed but quite distinctive unit of buff-coloured, medium–coarse grained (2 to 5 mm), generally massive, equigranular, biotite–muscovite granite (Plate 24) is located around the southern end of Wolf Lake (map area 12A/2) and the unit continues into the Dolland Brook map

[1] On Map 89-103, g.s.l. 1551 = 1557 located adjacent to 1678

Table 8. Modal analyses of the East Bay and Bottom Brook Granites

a. East Bay Granite

Sample No.	L1.5.82	L2.3.82	L3.11.82	L14.9.82	L18.12.82	L38.8.82
Geochem No.	-	221302	-	-	221354	-
Quartz (%)	33.6	38.4	37.4	32.2	27.2	32.2
K-feldspar	12.6	20.4	29.6	23.0	25.2	40.0
Plagioclase	37.6	32.8	26.2	30.8	40.4	24.4
Biotite	14.4	6.2	5.2	2.2	3.4	2.0
Muscovite	0.6	2.0	1.6	11.4	3.6	1.4
Garnet	-	-	-	0.4	-	-
Sericite	0.2	Tr	Tr	Tr	0.2	Tr
Chlorite	Tr	Tr	Tr	Tr	Tr	Tr
Opaques	Tr	0.2	Tr	Tr	Tr	Tr
Others	Tr*	Tr**	Tr**	Tr**	Tr**	Tr**

Sample No.	L40.1.82	T18.6.82	T24.10.82	T25.10.82	T27.8.82	L34.5.82
Geochem No.	221455	221218	221241	221243	221248	221275
Quartz (%)	38.0	28.8	28.0	32.2	39.2	24.6
K-feldspar	15.0	23.4	0.2	20.8	-	28.0
Plagioclase	31.6	33.8	57.8	41.0	44.6	40.2
Biotite	2.0	12.8	13.0	5.2	15.0	7.0
Muscovite	13.4	0.6	1.0	0.8	1.2	0.2
Garnet	-	-	-	-	-	-
Sericite	Tr	Tr	Tr	Tr	Tr	Tr
Chlorite	Tr	Tr	-	Tr	-	-
Opaques	Tr	0.6	Tr	Tr	Tr	Tr
Others	Tr**	Tr**	Tr**	Tr**	Tr**	Tr**

Tr* 1.0% epidote and trace zircon and apatite; Tr** zircon and apatite

b. Bottom Brook Granite

Sample No.	T6.5.82	T18.3.82	L15.5.82	L29.5.82	L29.10.82	L33.14.82
Geochem No.	-	-	221337	221378	221381	221399
Quartz (%)	21.0	49.4	17.4	36.2	30.0	26.2
K-feldspar	42.2	3.2+	44.0	21.6	29.8	41.6
Plagioclase	33.4	35.8	30.4	33.6	32.8	23.0
Biotite	2.6	10.4	6.8	6.2	6.8	8.2
Muscovite	0.8	0.6	0.8	1.6	0.4	-
Garnet	-	-	-	-	-	-
Sericite	Tr	Tr	0.2	Tr	Tr	Tr
Chlorite	Tr	Tr	Tr	Tr	Tr	Tr
Opaques	Tr	0.4	0.4	0.4	0.2	0.6
Others	Tr*	Tr**	Tr*	Tr***	Tr*	Tr*

* apatite and zircon; ** apatite (0.2%) and zircon; *** apatite (0.4%) and zircon; + hand specimen contains 1 cm K-feldspar phenocrysts

area (11P/15). This unit is generally homogeneous but locally contains a few small pegmatite and quartz veins.

Contact Relations

The Wolf Lake Granite has clearly intruded the orthoquartzite-cobble conglomerates and sandstones of subunit 2c of the Spruce Brook Formation, on the east side of Wolf Lake. A sharp contact is present and trends 150°. Several 30- to 60-cm-wide medium–coarse grained, granite dykes, identical to the main body of the granite, have intruded the conglomerate parallel to the 110°/50°N cleavage. The conglomerate has been contact metamorphosed, associated with the development of randomly orientated biotite and muscovite flakes.

The relationship of the Wolf Lake Granite to the other granitoid units is uncertain as contacts are not exposed. However, a fault contact with the D'Espoir Brook Granite along the Meelpaeg Lake Fault Zone is suspected, because

Plate 23. *(a) Meelpaeg Lake Granite (Unit 14) showing zoned plagioclase, biotite (grey, mottled) and plagioclase lath (white), set in poikilitic microcline; cross-polarized light; sample LI2-2-83; (b) oscillatory-zoned plagioclase set in poikilitic microcline; Meelpaeg Lake Granite (Unit 14); sample LI2-2-83; (as Plate 23a); scale for both plates: 25 mm = 1 mm; east side of Meelpaeg Lake.*

close to the assumed contact southwest of Wolf Lake, the Wolf Lake Granite is weakly deformed. Plagioclase laths are kinked and broken, mica flakes are warped and narrow fractures in the granite are filled with microcrystalline quartz. Generally, the Meelpaeg Lake and Wolf Lake granites are massive and have similar contact relationships with the Spruce Brook Formation and the D'Espoir Brook Granite. However, biotite in the Wolf Lake Granite is extensively altered to chlorite, whereas the Meelpaeg Lake Granite has relatively unaltered biotite. Quartz-filled fracture zones in the Wolf lake Granite may be related to hydrothermal alteration of the Wolf Lake Granite by the Meelpaeg Lake Granite but could also be related to late-stage hydrothermal fluids derived from the Wolf Lake Granite.

Petrography

The Wolf Lake Granite is composed of quartz, microcline, plagioclase, muscovite and biotite, and accessory minerals including garnet (see Tables 5 and 9 for modal analyses and Figure 25 for quartz:K-feldspar:plagioclase ratios). Quartz occurs mainly as anhedral crystals and displays extensive subgrain development and undulose extinction. Minor inclusions of biotite, muscovite and K-feldspar are present. K-feldspar occurs as 5- to 7-mm-long, microcline-twinned, subhedral perthite crystals having plagioclase inclusions. Plagioclase forms subhedral to euhedral crystals, 3 to 5 mm long, which contain sericitized cores. The plagioclase shows little variation in anorthite content that averages An_{16}. Inclusions of biotite are common in the plagioclase. Biotite and muscovite occur as 0.1- to 3-mm-long interstitial flakes. Garnet forms rare, euhedral inclusions in plagioclase.

Dolland Brook and Facheux Bay East Granites (Subunits 17a, 17b)

Distribution

Much of the area between Dolland Brook (11P/15) and Morgan Brook (11P/16) is underlain by the Dolland Brook Granite (subunit 17a). The Facheux Bay East Granite (subunit 17b) and a 1 km, unnamed plug of granite, similar to Unit 17 granite, are found in the D'Espoir Brook map area (11P/16). Unit 17 is mainly composed of pink, medium–coarse grained (2 to 5 mm diameter), K-feldspar porphyritic, massive to weakly foliated, biotite granite (Plate 25a). Minor isolated occurrences of equigranular muscovite–biotite granite and equigranular, biotite granite are also included in Unit 17.

Contact Relations

Intrusive contacts between the Dolland Brook and Facheux Bay East granites with the adjacent units are only rarely exposed but provide some critical information on the age of regional deformation and metamorphism. The Dolland Brook Granite is generally in fault contact with the migmatite of the Bay du Nord Group and the granite is highly brecciated along the fault. However, immediately south of 'Moon Pond', weakly foliated porphyritic granite (of subunit 17a) occurs to the southwest of this fault and is in intrusive contact with strongly foliated migmatite and foliated garnet–muscovite granite. This clearly indicates that the migmatization and deformation of the Bay du Nord Group occurred prior to

Table 9. Modal analyses of the Meelpaeg Lake Granite (Unit 14) and the Wolf Lake Granite (Unit 16)

	a. Meelpaeg Lake Granite			b. Wolf Lake Granite	
Sample No.	L12.2.83	L12.3.83	P30.18.83	14.2.83	P10.5.83
Geochem No.	221617	221618	221553	221623	-
Quartz (%)	23.4	33.6	29.0	29.9	30.4
K-feldspar	25.6	7.8	-	24.3	14.6
Plagioclase	40.8	47.2	62.8	37.8	48.6
Biotite	10.2	11.6	7.8	(chlorite)	(chlorite)
Muscovite	-	-	-	4.4	3.4
Garnet	-	-	-	Tr	0.4
Sericite	Tr	Tr	Tr	1.0	1.0
Chlorite	Tr	Tr	Tr	1.6	1.6
Opaques	Tr	Tr	0.2	Tr	Tr*
Others	Tr*	Tr**	Tr***	Tr*	Tr*

* Zircon; ** Allanite (0.4%), apatite (0.2%), sphene (0.2%) and zircon; *** Sphene (0.2%), apatite and zircon

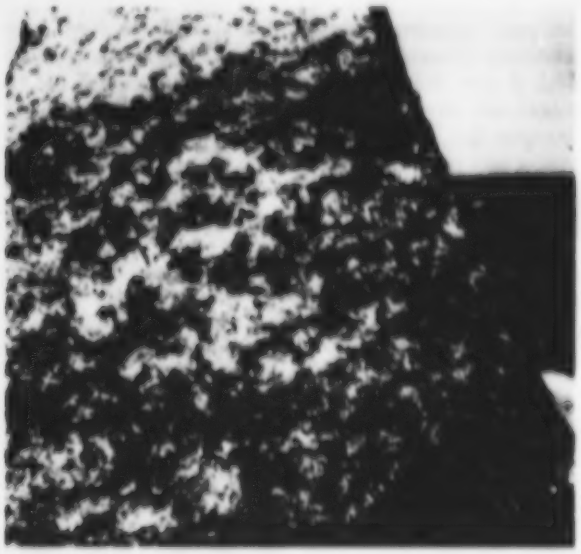

Plate 24. *Equigranular, massive, biotite–muscovite granite of the Wolf Lake Granite (Unit 16); southern end of Wolf Lake; lens cap is 5 cm in diameter.*

intrusion of the 396-Ma Dolland Brook Granite (see section on U–Pb ages).

Xenoliths of biotite–muscovite psammitic schist, migmatite, biotite–actinolite schist and foliated, leucocratic, muscovite–biotite granite occur only sparingly within the Dolland Brook and Facheux Bay East granites. The xenolith abundance increases with proximity to the Bay du Nord Group (Unit 4) and foliated granite southwest of Dolland Brook, and the zone of granite and migmatite to the west of North Bay (subunit 3d). This indicates that the source of the xenoliths is local, although some of the rock types of the xenoliths have not been observed in places within the map areas, e.g., hornblende–plagioclase (An_{40})–quartz–sphene schist.

Between Facheux Bay and North Bay, the Facheux Bay East Granite maps out as an oval-shaped body that disrupts an elongate west-trending zone of xenolith-rich granite (subunit 3d, and Units 11 and 12), which extends across the map area. This is interpreted to indicate that the Facheux Bay East Granite postdated the East Bay and Bottom Brook granites. Seven kilometres to the north, a small area of porphyritic biotite granite has intruded weakly foliated East Bay Granite.

Petrography

The essential mineralogy of the granites that comprise Unit 17 is quartz, K-feldspar, plagioclase and biotite plus accessory minerals (see Table 5). Modal analyses are given in Table 10 and quartz : K-feldspar : plagioclase ratios are shown in Figure 20.

The granites of Unit 17 have a groundmass that have a hypidiomorphic-granular texture and phenocrysts of twinned, perthitic microcline, averaging 2 cm in length, and contain inclusions of plagioclase, biotite and locally quartz. Groundmass K-feldspar is similar to the phenocrysts. Plagioclase forms interstitial subhedral and anhedral crystals. Zoning is weakly developed (An_{12-18}) and in some crystals is reflected by the varying extent of alteration to sericite. Patchy development of myrmekite occurs rarely. Quartz displays varying degrees of strain with commonly developed subgrains and ubiquitous undulose extinction. Serrated quartz–quartz grain boundaries are common. Muscovite occurs as a rare interstitial phase.

Sizable quartz veins (part of Unit 24) have been injected into the Dolland Brook Granite along faults adjacent to Dolland Brook (Plate 25b). These veins contain highly altered fragments of granite but no mineralization is evident.

Plate 25. *(a) Massive, K-feldspar-porphyritic, biotite granite of the Dolland Brook Granite (subunit 17a); site of geochronology sample LD33-1-83; on Dolland Brook, 13.5 km north of southern end of map area 11P/15E (see Figure 18); lens cap is 5 cm in diameter; (b) south-trending ridges of vein quartz (Unit 24) on the west side of Dolland Brook, 5 km northeast of Moon Pond.*

Wolf Mountain Granite (Unit 18)

Distribution

This unit is located mainly to the west of Dolland Brook and continues to the northwest into the Wolf Mountain (12A/2) map area. This unit is the host and probable source of significant tungsten and molybdenum showings in the Granite Lake area (Dickson, 1982, 1984; Tuach and Delaney, 1987). The Wolf Mountain Granite is a massive to very weakly foliated, pink to buff, medium–coarse to coarse-grained, K-feldspar porphyritic, muscovite–biotite granite (Plate 26). It is locally intruded by pegmatite and aplite veins. It is distinguished from the Dolland Brook Granite by the presence of muscovite and from the Dolland Pond (subunit 19a) and Morgan Brook granites (subunit 19b) by its coarser grain size.

Contact Relations

As exposure of the Wolf Mountain Granite is typically poor, contact relationships with the other units in the study area are poorly known. The contact between the Wolf Mountain Granite and the D'Espoir Brook Granite, although not exposed, is clearly a fault, which forms part of the Meelpaeg Lake Fault Zone. West of Wolf Lake, the Wolf Mountain Granite is strongly foliated and the fabric is parallel to that in the D'Espoir Brook Granite. To the north-northwest, in the Granite Lake area, the fault contact between the Wolf Mountain Granite and the Meelpaeg Lake Granite is exposed, and extensive mylonite and fault breccia zones are present (see Dickson, 1982). Static growth of sillimanite porphyroblasts in the Spruce Brook Formation, southwest of Meelpaeg Lake, was interpreted by Dickson (1982) to be related to intrusion of the Wolf Mountain Granite (Unit 7 of Dickson, 1982).

Petrography

The mineralogy of the Wolf Mountain Granite consists of quartz, perthitic microcline, plagioclase (An_{12}), biotite and muscovite, and accessory minerals (Table 5). Modal analyses are given in Table 11 and quartz:K-feldspar:plagioclase ratios are shown in Figure 27. The K-feldspar occurs as 1- to 3-cm-long phenocrysts (Plate 26) and also in the matrix of the granite. The phenocrysts contain inclusions of plagioclase, quartz and biotite. Quartz is mainly interstitial and displays undulose extinction. Slight compositional zoning is present in the euhedral plagioclase and is commonly indicated by highly sericitized cores and fresh rims, particularly in the inclusions in K-feldspar. Myrmekitic margins are common in [illegible] areas in both matrix and inclusion plagioclase. Biotite forms [illegible] to 5-mm flakes and books and is generally fresh. Inclusions of zircon are common. Muscovite occurs as small (1 mm diameter) interstitial, ragged flakes commonly associated with biotite. Zircon commonly occurs as zoned crystals.

Dolland Pond, Morgan Brook, Hughes Brook and D'Espoir Lake Granites (Subunits 19a to 19d)

Distribution

Unit 19 is composed of four areas of medium-grained, pink to buff, massive to weakly foliated, K-feldspar porphyritic, muscovite–biotite granite (Plate 27a). The Dolland Pond and Morgan Brook granites are located in the

Table 10. Modal analyses of Unit 17 of the North Bay Granite Suite

Sample No.	T5.4.82+	L4.5.82+	P12.1.83x	P13.2.83x	P21.1.83x
Geochem No.	-	-	-	-	221516
Quartz (%)	32.4	24.6	30.6	20.4	46.6
K-feldspar	21.0	35.8	28.4	42.4	13.0
Plagioclase	39.8	31.6	35.2	32.0	34.0
Biotite	6.4	6.2	2.0	4.0	6.4
Muscovite	-	-	0.8	0.8	-
Garnet	-	-	-	-	-
Sericite	0.2	Tr	Tr	Tr	Tr
Chlorite	Tr	Tr	2.6(biot)	Tr	Tr(biot)
Opaques	0.2	Tr	0.4	0.4	Tr
Others	Tr*	Tr**	Tr*	Tr*	Tr*

Sample No.	26.4.83x	L23.8.83x	L27.7.83x	L27.10.83x	L28.4.83x
Geochem No.	-	221635	221665	221668	-
Quartz (%)	26.0	16.2	28.6	29.2	29.8
K-feldspar	43.0	55.2	33 6	14.2y	24.4
Plagioclase	27.4	25.0	34.0	47.6	40.2
Biotite	2.8	3.0	3.4	8.2	5.4
Muscovite	0.4	-	-	-	0.2
Garnet	-	-	-	-	-
Sericite	Tr	Tr	0.2	0.6	Tr
Chlorite	Tr	Tr	Tr	0.2	Tr
Opaques	0.4	0.4	0.2	Tr	Tr
Others	Tr*	Tr***	Tr*	Tr*	Tr*

+ Facheux Bay East Granite; x Dolland Brook Granite; * Zircon and apatite; ** Tourmaline (1.8%) including trace apatite and zircon; *** Apatite (0.2%), allanite and zircon; y Contains K-feldspar phenocrysts in hand specimen

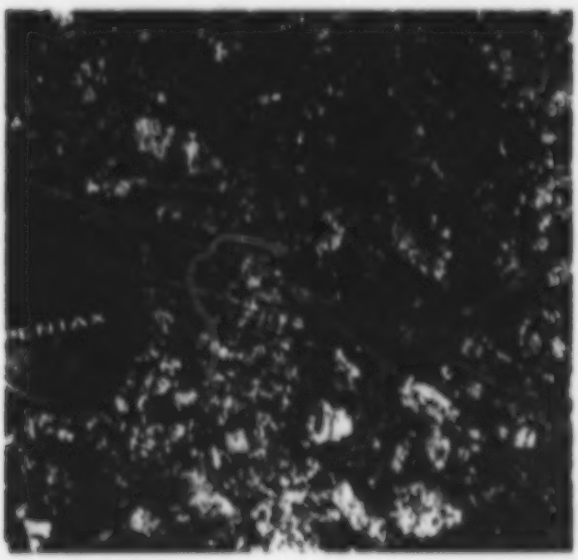

Plate 26. *Massive, K-feldspar-porphyritic, muscovite–biotite granite of the Wolf Mountain Granite (Unit 18); 12 km southwest of Dolland Pond (map area 11P/15); lens cap is 5 cm in diameter.*

northeastern and southeastern portions of the Dolland Brook map area respectively, and the Hughes Brook and the D'Espoir Lake granites are located in the northeastern part of the D'Espoir Brook map area.

The D'Espoir Lake Granite forms a small plug that has intruded the Spruce Brook Formation (subunit 2e). This area of granite, which lies outside the main mass of the North Bay Granite Suite and to the north of a fault separating the Spruce Brook and Salmon River Dam formations, is interpreted to be related to the other areas of K-feldspar porphyritic, muscovite–biotite granite.

A 15- by 100-m quartz vein (Unit 24) has been injected into the Morgan Brook Granite, along a fault in the southern Dolland Brook area (Plate 27b). Along a south-flowing tributary of Dolland Brook, 5 km north of the southern boundary of map area 11P/15, fine-grained scheelite occurs in 5-mm thick, widely spaced (1 to 2 m) tourmaline–quartz veins (McConnell, 1985). Tourmaline is uncommon in the Morgan Brook Granite and this scheelite occurrence appears to be unique. Thin rhyolite veins cut brecciated granite, 1.5 km northeast of the southern end of Dolland Brook. These veins may be related to the porphyry dykes (Unit 23) that have intruded Unit 21 west of Dolland Brook.

Contact Relations

The Meelpaeg Lake Fault Zone separates the Dolland Pond Granite from the D'Espoir Brook Granite. On Dolland

Table 11. Modal analyses of the Wolf Mountain Granite (Unit 18)

Sample No.	L8.2.83	L9.3.83	L9.7.83	L22.2.83	P11.3.83
Geochem No.	221609	221612	221614	221632	-
Quartz (%)	28.4	23.6	28.4	28.2	25.8
K-feldspar	29.2	45.8	37.8	29.2	34.4
Plagioclase	35.6	28.8	28.2	28.2	36.4
Biotite	4.2	0.6	3.4	5.4	7.6
Muscovite	1.6	0.4	1.2	0.8	0.4
Garnet	-	-	-	-	-
Sericite	0.2	Tr	Tr	Tr	Tr
Chlorite	Tr	0.4	-	Tr	Tr
Opaques	0.4	0.2	1.0	Tr	0.6
Others	*	**	Tr***	Tr***	Tr***

* Apatite (0.4%) and zircon; ** Apatite (0.2%) and zircon; *** Apatite and zircon

Figure 27. *Modal proportions of Q:K:P for Unit 17 and the Wolf Mountain Granite (Unit 18); classification and abbreviations as in Figure 10.*

Brook, leucocratic granite and beryl-bearing pegmatite of the D'Espoir Brook Granite are strongly mylonitized but a nearby exposure of the Dolland Pond Granite displays only a weak foliation. Northwest-trending faults are also interpreted to separate the Dolland Brook Granite and Unit 21 from the Morgan Brook Granite, southwest of Dolland Brook. In this area, the granitoid rocks are brecciated and locally, strongly foliated in the vicinity of several northwest-trending gullies. One of these gullies is the site of a 200- by 20-m quartz vein (Plate 27a). Metasedimentary xenoliths, probably from the Bay du Nord or Baie d'Espoir groups, are present in the Morgan Brook Granite. The contact between the Morgan Brook Granite and the East Bay Granite, near Morgan Brook (map area 11P/16), is assumed to be mainly an intrusive contact although the northern portion of the contact area is assumed to be a fault defined by topographic lineaments and coincident, linear, aeromagnetic anomalies.

Pelitic xenoliths of Spruce Brook Formation occur in the D'Espoir Lake Granite. Cordierite and andalusite porphyroblasts overprint the cleavage in the Salmon River Dam Formation on an island in D'Espoir Lake. The pelites at this locality contain isolated pods of granite, which are interpreted to be partial melts. These features indicate that the Spruce and Salmon River Dam formations were juxtaposed prior to intrusion of the D'Espoir Brook Granite.

The Spruce Brook Formation (subunit 2e) shows the effects of contact metamorphism close to the contact with the D'Espoir Lake Granite. Adjacent to the contact, the Spruce Brook Formation psammites contain well-aligned, fresh biotite, which may be mimetic on the pre-existing cleavage and the result of contact metamorphism.

Petrography

The various areas of Unit 19 contain the same essential mineralogy of quartz, perthitic microcline and plagioclase with minor biotite and muscovite, and accessory minerals (Table 12). Modal analyses are given in Table 11 and quartz: K-feldspar:plagioclase ratios are shown in Figure 28.

Phenocrysts of K-feldspar in Unit 19 are 5 to 20 mm in length and contain inclusions of quartz, plagioclase, biotite and rarely microcline. Plagioclase (An_{10} to An_{20}) occurs mainly in the matrix and rarely as small (5 mm diameter) phenocrysts. Oscillatory zoning in the phenocrysts is indicated by concentric zones of fresh and sericitized plagioclase and by varying anorthite contents in the fresh zones.

Quartz forms anhedral, variably deformed and recrystallized aggregates. Biotite occurs as 1- to 2-mm-long variably altered flakes having a poorly developed preferred orientation. Muscovite occurs as 1- to 2-mm-long ragged flakes commonly associated with biotite. In the Hughes Brook Granite, muscovite also forms coarse interstitial to ophitic flakes up to 3 mm in diameter. Near the northern contact of the Morgan Brook Granite with the Dolland Brook Granite, southeast of Dolland Brook, mica is apparently lacking in the sheared and altered granite (geochemistry sample location 221659).

Plate 27. *(a) Massive, equigranular, muscovite–biotite granite of the Morgan Brook Granite (subunit 19b); 1.5 km west of the southern end of Dolland Brook (map area 11P/15); coin is 18 mm in diameter; (b) ridge of vein quartz (Unit 24) injected along a fault into the Morgan Brook Granite (subunit 19b); 2 km north-northeast of the southern end of Dolland Brook.*

Garnet is particularly prominent in the Hughes Brook Granite, where the garnets vary in diamter from 0.1 mm to 15 mm and are generally fresh (Plate 28, a and b). The larger garnets are commonly fractured, veined by quartz, and partly altered to chlorite along the fractures. The euhedral shape of the larger garnets indicates that they crystallized early in the cooling. Small pinhead garnets also occur locally in pegmatites and in the D'Espoir Lake Granite.

Upper Salmon Road Granite (Unit 20)

Distribution

This unit forms a northeast-trending projection from the North Bay Granite Suite into the northeastern part of the D'Espoir Brook map area and continues into the St. Alban's (1M/13; Colman-Sadd, 1976), Cold Spring Pond (12A/1; Colman-Sadd, 1983) and Twillick Brook (2D/4; Colman-Sadd, 1980a) map areas. A poorly defined Rb–Sr isochron age of 396 ± 48 Ma was obtained from this unit (see section, Previous Rb–Sr Age Determinations). The dominant rock types in the Upper Salmon Road Granite are weakly foliated, coarse-grained, K-feldspar porphyritic, muscovite–biotite granite and biotite granodiorite (in map area 1M/13) retaining tabular K-feldspar phenocrysts ranging in length from 1 to 4 cm (Plate 29). Minor rock types include a very coarsely porphyritic variety associated with scattered 4- to 10-cm-long euhedral phenocrysts. This coarsely porphyritic variety forms entire outcrops but its relationship to the main rock types is uncertain. Small aplite and pegmatite veins and pods, and quartz veins occur within the Upper Salmon Road Granite.

Contact Relations

The Upper Salmon Road Granite has probably intruded the Salmon River Dam Formation psammite; rare limestone xenoliths occur in the granite. Small spots of sericite (possibly after cordierite) overprint the schistosity in the Salmon River Dam Formation pelites (subunit 3b). In a few places, 10- to 30-cm-long biotite psammite and, rarely, metadioritic xenoliths were found. The psammitic xenoliths are similar to the Salmon River Dam Formation psammites (subunit 3a). Similarly, Colman-Sadd (1983) has noted that the metamorphic grade of the Salmon River Dam Formation increases toward the granite contact.

The contact between the Upper Salmon Road Granite and an isolated exposure of medium-grained granodiorite (Unit 11?) in the northeastern corner of the D'Espoir Brook map area, is not exposed. To the north (map area 12A/1), a gradational contact between the granite and the granodiorite has been suggested by Colman-Sadd (1983) from a gradual increase in the abundance of muscovite and decrease in abundance of phenocrysts toward the granodiorite. However, a gradation is not apparent in the D'Espoir Brook map area. The granodiorite is distinctly different from the granite located 500 m to the south and there are no gradational changes within the Upper Salmon Road Granite toward the contact with the sedimentary rocks to the west. The granodiorite is similar to the East Bay and Bottom Brook granites and is interpreted to have been intruded by the Upper Salmon Road Granite.

The Meelpaeg Lake Fault Zone separates the Upper Salmon Road Granite and the D'Espoir Brook Granite. Intensity of deformation in the Upper Salmon Road Granite increases toward the fault but mylonitization is restricted to

Table 12. Modal analyses of Unit 19 of the North Bay Granite Suite

Sample No.	P28.7.83+	P30.21.83+	L26.1.83x	P25.13.83x	P26.1.83x	P30.23.83x
Geochem No.	-	221554	221641	-	221539	-
Quartz (%)	28.0	27.8	34.2	29.0	27.2	32.2
K-feldspar	31.8	36.4	36.6	30.8	22.6	28.4
Plagioclase	34.8	28.8	22.2	37.4	43.8	31.6
Biotite	3.4	3.2	5.2	2.0	6.2	3.2
Muscovite	1.4	3.6	0.8	0.6	0.2	2.8
Garnet	-	-	-	-	-	-
Sericite	0.2	Tr	0.2	0.2	Tr	0.8
Chlorite	Tr	Tr	Tr	Tr	Tr	Tr
Opaques	0.4	0.2	0.8	Tr	Tr	Tr
Others	Tr*	Tr*	Tr*	Tr*	Tr*	Tr*

Sample No.	T19.1.82x	T19.4.82x	L23.4.82y	L23.8.82y	L28.2.82z
Geochem No.	221219	221221	221261	221362	221373
Quartz (%)	42.4	26.4	28.6	35.6	30.6
K-feldspar	10.2	34.8	17.2	42.6	22.4
Plagioclase	44.2	32.2	42.6	17.0	38.2
Biotite	1.6	4.4	4.5	-	7.8
Muscovite	0.4	0.6	0.7	3.2	0.8
Garnet	-	-	6.3	1.0	0.2
Sericite	0.2	0.4	0.1	0.6	Tr
Chlorite	Tr	0.2	Tr	-	Tr
Opaques	1.0	1.0	Tr	Tr	Tr
Others	Tr**	Tr**	Tr*	Tr*	Tr**

+ Dolland Pond Granite; x Morgan Brook Granite; y Hughes Brook Granite; z D'Espoir Lake Granite; * Zircon; ** Zircon and apatite

Figure 28. *Modal proportions of Q:K:P for Unit 19 of the North Bay Granite Suite; classification and abbreviations as in Figure 10.*

the D'Espoir Brook Granite and slivers of Salmon River Dam Formation emplaced along the fault.

The Upper Salmon Road Granite may have postdated the main phase of deformation that affected the D'Espoir Brook Granite. The mylonitic granitoid rocks terminate just east of Salmon River (geochemical sample location 230I; Map 89-99). However, to the east, the granites are only moderately foliated and are similar to those of the Upper Salmon Road Granite and granite of Unit 13. A northeast-trending pond coincides with the projection of the Salmon River Dam Fault, which is interpreted to separate the Upper Salmon Road Granite and Unit 13 from the D'Espoir Brook Granite. Along Salmon River, coarsely porphyritic granite occurs in association with a variety of granitoid rocks ranging from hornblende diorite to garnet–muscovite granite and rarely xenoliths of mylonitic granite. It is possible that this area represents an intrusive breccia with the mylonitic granites representing remnants of the mylonite zone within the D'Espoir Brook Granite. Thus, these observations indicate that the Upper Salmon Road Granite postdated the D'Espoir Brook Granite.

Petrography

The main features of the Upper Salmon Road Granite are summarized in Table 5. Modal analyses are given in Table 13 and Quartz:K-feldspar:plagioclase ratios are shown in Figure 29. However, the coarsely K-feldspar porphyritic nature of the granites is not fully reflected in the modal analyses. K-feldspar occurs mainly as 1- to 4-cm-long tabulate microcline perthite phenocrysts having inclusions of plagioclase, quartz and biotite. The matrix K-feldspar is also perthitic microcline. Quartz occurs mainly as an interstitial

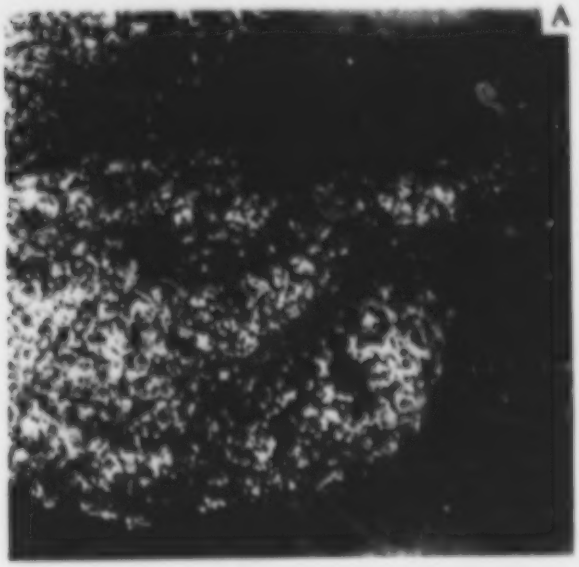

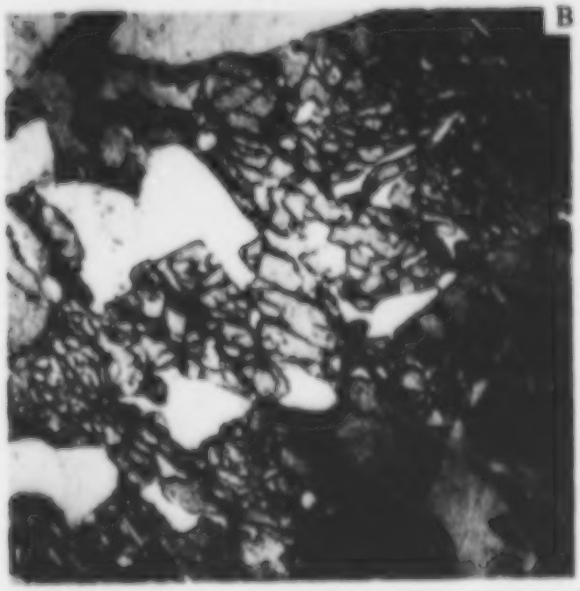

Plate 28. *(a) Massive, garnet–biotite–muscovite granite of the Hughes Brook Granite (subunit 19c) having prominent garnet phenocrysts (up to 1.5 cm in diameter); 7.5 km northeast of Thorney Cove, North Bay; (b) euhedral, fractured garnets (high relief) having quartz inclusions; fractures contain chlorite; Hughes Brook Granite (subunit 19c); plane-polarized light, sample L23-4-82; scale: 25 mm = 1 mm; location as Plate 28a.*

mineral, rarely forming crystals larger than 1 cm diameter, which may be phenocrysts. Locally, plagioclase displays numerous oscillatory zones and minor kinking. The plagioclase generally ranges in composition from An_{10} to An_{25}. Zones commonly show differences of about An_5. Biotite occurs as 1- to 3-mm-long flakes and rarely as 1- to 2-mm-thick books. Muscovite occurs mainly as 1-mm-long

Plate 29. *Euhedral microcline phenocrysts in the Upper Salmon Road Granite (Unit 20); north end of Salmon River (map area 11P/16); lens cap is 5 cm in diameter.*

interstitial flakes and is possibly an alteration product of feldspar.

Quartz veins are uncommon and barren. Pegmatite and aplite veins have a simple granite mineralogy. Alteration of the granite has occured along minor shear zones but these appear to be of limited extent.

Unit 21

Distribution

This unit, located to the southwest of Dolland Brook, consists of medium-grained, buff to grey, variably foliated to massive, feldspar porphyritic, muscovite–biotite granite and granodiorite.

Contact Relations

The relationship of Unit 21 to the other granitoid units has been described in previous sections. The relationship between Unit 21 and the Dolland Brook Granite, to the west, was indicated by Dickson and Delaney (1984c) to be probably intrusive, with Unit 21 older than the Dolland Brook Granite. This was based on the more conspicuous foliation in Unit 21 (Unit 5b of Dickson and Delaney, 1984a). However, granodiorite dykes, which intrude the Dolland Brook Granite, are now interpreted to be related to Unit 21. This indicates that the reverse intrusive relationship is probable.

Unit 21 probably intruded the Bay du Nord Group, although the contact is now a fault. Xenoliths of migmatite and metasedimentary rock, similar to the adjacent Bay du

Table 13. Modal analyses of the Upper Salmon Road Granite

Sample No.	L1.2.82	L10.1.82	L16.3.82	L17.2.82
Geochem No.	-	221314	221343	221344
Quartz (%)	34.6	28.0	31.0	36.4
K-feldspar	20.0	5.2	13.0	7.0
Plagioclase	36.0	52.4	44.0	45.8
Biotite	(chl)	13.6	9.4	8.2
Muscovite	1.0	-	5.4	2.4
Garnet	-	-	Tr	-
Sericite	1.6	0.4	1.0	2.0
Chlorite	6.6	Tr	0.6	0.2
Opaques	Tr	Tr	0.8	Tr
Others	Tr*	**	***	+

* Zircon, apatite, epidote; ** Allanite (0.4%) and zircon and apatite; *** Sphene (0.2%) with zircon, apatite; + Sphene (0.2%) with zircon, apatite and allanite.

Figure 29. *Modal proportions of Q:K:P for the Upper Salmon Road Granite (Unit 20) and Unit 21; classification and abbreviations as in Figure 10.*

Nord Group, are common within Unit 21 and provide evidence for an originally intrusive contact. Dykes of fine-grained and very fine-grained, sanidine-quartz–biotite porphyry (Unit 23) have intruded Unit 21. These dykes can be traced to the south toward the François granite from which they are probably derived (see Dickson *et al.*, 1985a).

Petrography

Unit 21 consists of essential quartz, microcline and plagioclase (An_{15-25}) with minor biotite and muscovite, and accessory minerals. Modal analyses are given in Table 14 and quartz:K-feldspar:plagioclase are given in Figure 29. Microcline phenocrysts are 1- to 2-cm-long and tabulate with inclusions of plagioclase, quartz and rarely biotite; microcline is also a groundmass mineral. Perthitic textures are variably developed. Plagioclase forms 5- to 10-mm-long, zoned phenocrysts in the matrix. Biotite and muscovite occur as 1- to 2-mm-long flakes having a variably developed tectonic alignment. Biotite is partly altered to chlorite and zircon inclusions are common.

Table 14. Modal analyses of Unit 21 of the North Bay Granite Suite

Sample No.	P23.4.83	P23.7.83	L26.6.83
Geochem No.	221526	-	-
Quartz (%)	38.4	35.2	29.4
K-feldspar	10.4	17.0	16.8
Plagioclase	39.6	38.4	49.4
Biotite	8.0	9.0	4.0
Muscovite	3.0	-	Tr
Garnet	-	-	-
Sericite	0.6	Tr	Tr
Chlorite	Tr	Tr	0.2
Opaques	Tr	0.4	0.4
Others	Tr*	Tr**	Tr**

* Pyrite, zircon, apatite ** Zircon and apatite

Unit 21 is similar to the late medium-grained, muscovite–biotite granites in the Burgeo granite (see Dickson *et al.*, 1985; O'Brien and Tomlin, 1985b; O'Brien *et al.*, 1986) and may provide a link between the Burgeo granite and North Bay Granite Suite.

OTHER INTRUSIVE ROCKS

INTRODUCTION

The North Bay Granite Suite has been intruded by a diverse assortment of rocks, most of which are interpreted to be unrelated to the North Bay Granite Suite. The age of these units is uncertain. Microgranite dykes (Unit 22) are of uncertain affinity but may represent a final phase of intrusion of the North Bay Granite Suite. Quartz–feldspar porphyry dykes (Unit 23) can be traced toward the posttectonic François granite to which they are certainly related. Major quartz veins (Unit 24) are all related to faults and are the products of a phase of hydrothermal activity of unknown age. Diabase dykes (Unit 25) are very rare and are clearly unrelated to the North Bay Granite Suite. Two distinct ages of diabase rocks are included in this unit and the ages are probably pre- and post-North Bay Granite Suite.

MICROGRANITE DYKES (UNIT 22)

Distribution and Contact Relations

Dykes of fine-grained, extremely tough, buff, finely porphyritic, massive, biotite microgranite occur to the northeast and northwest of Facheux Bay. The eastern dyke,

which has intruded the Facheux Bay Granite, has a southerly orientation, and is at least 300 m long and 10 m wide, and appears to be vertical. An easterly trending fault, which cuts one dyke, has a dextral component of displacement of about 5 m. This dyke is highly jointed with closely spaced parallel joints, 5 cm apart and orientated 080°/55°W.

Three kilometres northwest of Facheux Bay, along Bottom Brook, several narrow anastomosing microgranite dykes have intruded the Bottom Brook Granite. These dykes have a general easterly trend and vary in width from a few cm to about 1 m. The attitude of the dykes varies from horizontal to vertical.

Petrography

The dykes do not have a tectonic fabric and may represent the last phase of granitoid magmatism in the North Bay Granite Suite. In thin section, the eastern dyke contains 1- to 2-mm-long, generally highly altered plagioclase phenocrysts. Quartz forms as euhedral crystals, 1 mm in diameter and commonly having highly embayed margins, and as vermicular blebs, which commonly have an altered plagioclase nucleus. The alkali feldspar occurs as 1-mm-square, euhedral to corroded sanidine phenocrysts having finely disseminated K-feldspar in the matrix. Biotite flakes are 1 mm long, aligned, and altered to chlorite. The matrix consists of very fine-grained aggregates of quartz, K-feldspar, plagioclase and opaques, possibly formed by recrystallization of a glassy matrix, with secondary chlorite and epidote. The textures and mineralogy indicate that the dyke was probably emplaced as near-liquidus, relatively dry magma. The texture of the groundmass in the eastern dyke is similar to that found in the quartz–feldspar porphyry dykes (Unit 22), located to the west of Dolland Brook. However, as the microgranite dykes are some distance from the François granite and are restricted to the area around Facheux Bay, they are not considered to be related to the François granite.

QUARTZ–FELDSPAR PORPHYRY DYKES (UNIT 23)

Distribution and Contact Relations

This unit consists of at least four pink to grey, quartz–feldspar porphyry dykes that have intruded Unit 21, southwest of Dolland Brook. These vertical dykes are parallel and trend 010°. They locally have continuously exposed lengths of 300 m and are up to 25 m in width and can be traced discontinuously for at least 5 km into the La Hune map area to the south (Dickson *et al.*, 1985). There is a clear association of these dykes with the François granite as both the dykes and the François granite are posttectonic and highly siliceous rocks. Similar dykes are associated with the Chetwynd Granite, to the west of Burgeo, which is also a siliceous, posttectonic granite (O'Brien and Tomlin, 1985b).

Petrography

The porphyry dykes commonly contain 1- to 4-mm quartz and feldspar phenocrysts in an aphanitic to fine-grained matrix (Plate 30). A thin, grey dyke at the western margin of a thicker pink dyke (geochemical sample locations 1689 and 1690, respectively; Map 89-101) contains a much smaller proportion of phenocrysts, which are feldspar only. In hand specimen, the coarser dykes contain prominent grey, terminated quartz crystals, tabulate pink feldspar phenocrysts and biotite flakes up to 5 mm long. In thin section, quartz occurs as euhedral phenocrysts commonly with embayed margins. The feldspars are albite and sanidine. The albite has well-developed polysynthetic and simple albite twins. The sanidine has finely developed twinning. The feldspars are variably altered to fine-grained sericite. Biotite is completely altered to chlorite and opaque minerals (probably magnetite) and small rosettes of chlorite also occur in the dykes. Muscovite flakes 1 mm in diameter occur in the groundmass and appear to be primary as they commonly form isolated flakes as well as occurring in association with altered biotite.

Plate 30. *Euhedral quartz (white) and sanidine (grey) phenocrysts in quartz–feldspar porphyry dykes (Unit 23); cross-polarized light; sample L24-8-83; scale: 25 mm = 1 mm; 2.5 km southeast of Moon Pond.*

The groundmass consists of quartz, albite and K-feldspar with commonly developed intergrowths of quartz and feldspar. The groundmass in the aphanitic dyke consists of very fine-grained intergrowths of quartz and feldspar with randomly orientated flakes of biotite and muscovite.

QUARTZ VEINS (UNIT 24)

Distribution and Contact Relations

Numerous large quartz veins are associated with faults within or adjacent to the North Bay Granite Suite. The Meelpaeg Lake Fault Zone is the site of numerous quartz

veins. In the eastern part of the zone, between D'Espoir Brook and Dolland Brook, quartz veins occur along the faulted northern contact of the D'Espoir Brook Granite with the Salmon River Dam Formation. Between Dolland Brook and the Meelpaeg Lake area, the quartz veins have been injected along the faulted contact between the Wolf Mountain Granite and adjacent units. These veins are similar to those in the Dolland Brook–D'Espoir Brook area and consist of mainly extensive massive, composite quartz veins. Along the western margin of the D'Espoir Brook Granite 5 km west of Wolf Lake, thin (5 cm to 2 m) quartz veins cut sheared and altered D'Espoir Brook Granite, which has been brecciated in the fault zone.

In the central part of Dolland Brook, three large veins occur along a prominent north-trending lineament, which is interpreted to be a fault scarp (Plate 25b). These veins are exposed over a distance of 4 km, are 10 to 15 m thick and have exposed lengths of at least 100 m. Another large composite quartz vein is exposed 2 km east of Dolland Brook and forms a prominent northwest-trending ridge (Plate 27b) and has an exposed length of 100 m and is 10 to 15 m thick. This vein occurs along a northwest-trending fault and is sheared out at its northwestern end.

Petrography and Economic Potential

Along the Meelpaeg Lake Fault Zone, the longest vein is located 5 km east of Dolland Brook and is termed the 'Jocko Pond' quartz vein by Butler and Greene (1976). This vein is 600 by 100 m and is estimated to contain 1.2 million tonnes of 97.1 percent SiO_2. Three kilometres east of the 'Jocko Pond' vein, a series of thin veins have been injected into sheared, foliated granite (Unit 8), parallel to the foliation. These veins have little economic potential for SiO_2.

Farther to the east near D'Espoir Brook, two massive veins occur between the D'Espoir Brook Granite and the sedimentary rocks of the Salmon River Dam Formation. The smaller occurence is virtually free of inclusions and contains numerous veinlets within the one sheet. About 500 m to the west, the larger quartz vein is less pure with locally numerous inclusions of pelite (Plate 18). These veins are at least 30 m wide. The smaller vein on D'Espoir Brook is about 50 m long and that to the west is at least 300 m long.

Several quartz veins in the Meelpaeg Lake Fault Zone outcrop northwest of the study area (Dickson, 1982). Some of the veins contain tungsten mineralization and were included in a fluid-inclusion study by Delaney (1984). This study indicated minimum trapping temperatures varied between 180 and 250°C with the inclusions consisting of H_2O and less than 5 percent NaCl.

The Dolland Brook veins are composite with massive white quartz cut by numerous veinlets of grey quartz. Minor inclusions of epidotized and sericitized granite occur within the veins. No mineralization is apparent in these veins. Grab samples from the Dolland Brook and Meelpaeg Lake veins were assayed for gold but none was detected.

DIABASE DYKES (UNIT 25)

Distribution and Contact Relations

Only five diabase dykes were observed in the study area; they are included in Unit 25 although there are at least two ages of diabase dykes. The older set of dykes has intruded the Ordovician metasedimentary rocks of the Spruce Brook Formation to the southwest of Meelpaeg Lake, and the Salmon River Dam Formation 2 km to the west of D'Espoir Lake. The Spruce Brook Formation was subsequently intruded by granites of the North Bay Granite Suite. Two dykes have intruded the Bottom Brook Granite to the northeast of Facheux Bay.

Petrography

The dykes in the Spruce Brook Formation have been deformed and metamorphosed along with the host metasedimentary rocks to a schistose assemblage of blue-green hornblende, sphene, quartz, plagioclase and magnetite, indicative of upper-greenschist facies metamorphism. The main fabric is overprinted by randomly orientated biotite indicating a period of static metamorphism, possibly during intrusion of the North Bay Granite Suite. West of D'Espoir Lake, the dyke contains a weakly aligned assemblage of actinolite–biotite–sphene–quartz–albite–magnetite indicative of lower-greenschist facies metamorphism.

The two dykes in the Bottom Brook Granite are undeformed and have a northerly orientation. The more southwesterly dyke has irregular contacts with the granite and varies in width from 30 cm to 1 m and is at least 20 m long. The other dyke is parallel-sided with prominent 5-mm-wide chilled margins. It is 12 cm wide and has an exposed length of 15 m. Both dykes have similar textures and contain small phenocrysts of plagioclase and an alteration assemblage of chlorite and epidote, possibly after clinopyroxene. The groundmass is highly altered to assemblages of sericite and epidote and residual plagioclase and opaque minerals.

SUMMARY OF THE GEOLOGY OF THE NORTH BAY GRANITE SUITE

The North Bay Granite Suite is a composite pluton, which is divided into four major groups. These are, (a) the dominantly syn- to late tectonic granodioritic to granitic rocks in the Wolf Lake–Meelpaeg Lake area north and east of the Meelpaeg Lake Fault Zone (Units 10, 14, 15, 16 and 20), which commonly contain a moderate to strong regional fabric, although Unit 20 is massive within the D'Espoir Brook map area; (b) the elongate belt of mylonitic to massive, leucocratic granites and biotite granite (Units 8, 9 and 13), which extend from Meelpaeg Lake to Salmon River, along the Meelpaeg Lake Fault Zone; (c) the syn- to late tectonic, variably foliated, muscovite–biotite tonalite to granite suite located mainly to the east of Morgan Brook (Units 11 and 12); and (d) the mainly posttectonic, medium-coarse to coarse-grained, K-feldspar porphyritic, muscovite–biotite granites (Units 17, 18, 19 and

21) located mainly to the west of Morgan Brook and extending northwestward to Granite Lake (equivalent to Unit 7 of Dickson, 1982).

Group A forms a tectonically separate and generally petrographically distinct component of the North Bay Granite Suite and is termed Component 2. Groups B, C and D form a continuous belt of granitoid rocks and are referred to as Component 1.

The contacts between the main groups are generally poorly known. The leucocratic granites (Group B) are in fault contact with the granodiorites (Group A) and the porphyritic granites (Group D). The presence of a few granodiorite dykes in the leucogranite indicates that the tonalite to granite suite (Group C) has intruded the leucogranites. The porphyritic granites and the tonalite to granite suite have no exposed contacts but the presence of small plugs of porphyritic granite within the tonalite to granite suite permits the tentative conclusion that the porphyritic granites are younger than the tonalite to granite suite.

Within the tonalite to granite suite (Group C), abrupt contacts between the East Bay and Bottom Brook granites are generally absent. Small dykes of granodiorite, intrusive into very similar granodiorite, may indicate that multiple intrusions of similar granodiorite are present. However, sharp contacts between units have not been observed and gradual changes in texture and mineralogy are common. Within the coarse-grained granite terrane (Units 17 to 19), contacts between the phases are unexposed but the general similarity between the units indicates that gradational contacts may be present.

The tonalite to granite and granodiorite groups of the North Bay Granite Suite have been deformed with the Ordovician units and this deformation is interpreted as Acadian D_1. The porphyritic granites and leucogranites contain a cataclastic fabric which, in the Wolf Lake area, trends toward the north-northwest. The fabric in the nearby metasedimentary rocks trends northeast. The cataclastic deformation zone (Meelpaeg Lake Fault Zone) is apparently confined to a narrow brittle fault between the Spruce Brook Group and the Wolf Mountain Granite. To the northwest, the cataclastic zone widens and the granite (Unit 18) is juxtaposed against Meelpaeg Lake Granodiorite (Dickson, 1982) and the fabric maintains a north-northwesterly orientation. It is apparent that cataclasis postdated the fabrics in the metasedimentary rocks. The coarse-grained, porphyritic granites (Units 17, 18, and 19) are essentially undeformed and contain xenoliths of polydeformed metasedimentary rocks. Thus, these granites are tectonically the youngest component of the North Bay Granite Suite.

Radiometric dating of zircon and monazite from migmatitic inclusions in the tonalite–granite group (Units 11 and 12) indicate ages ranging from 478 Ma (zircon; or alternatively 450 Ma) to 410 or 416 Ma (monazite; T.E. Krogh, written communication, 1984, 1985). Unsatisfactory Rb–Sr dates of 430 and 427 Ma have been reported from the granodiorite component (Elias, 1981) and a new date of approximately 400 Ma has been obtained from the Upper Salmon Road Granite (Unit 20; Fryer, 1983). Thus, it is apparent that the tonalite–granite suite is Early Devonian to Early Silurian in age. The posttectonic Dolland Brook Granite was dated at 396 Ma (U–Pb zircon) with cooling below 600°C dated at 390 Ma (U–Pb monazite; T.E. Krogh, written communication, 1985). The radiometric ages for these two granites support the geological evidence, namely that the syntectonic East Bay and associated granites are older than the posttectonic Dolland Brook and associated granites.

GEOCHEMISTRY OF THE NORTH BAY GRANITE SUITE AND ASSOCIATED IGNEOUS ROCKS

INTRODUCTION

As part of a continuing regional geochemical study of granitoid rocks in Newfoundland, the granitoid rocks within the study area were systematically sampled. This study, which sampled the southeastern part of the North Bay Granite Suite, complements geochemical work carried out earlier in the Granite Lake area (12A/2W, 12A/3E, Dickson, 1982) and the St. Alban's (1M/13) and Twillick Brook (2D/4) areas (see Colman-Sadd *et al.*, 1981). In this study, samples were collected from map areas 12A/1, 12A/2, 12A/3, 11P/9, 11P/15E and 11P/16; samples from 11P/15W were collected by R.F. Blackwood of the Newfoundland Department of Mines and Energy.

SAMPLING AND FIELD METHODS

The sampling method used is based on a system devised by R.G. Garrett of the Geological Survey of Canada (GSC, written communication, 1979). The essential features are: 1) the proposed map area is divided into 2 by 2 km squares based on the U.T.M. grid system; 2) each square is subsequently divided into sixteen squares, one of which is chosen at random and this is the sample square; 3) the sample is taken as close as possible to the centre of the (0.5 km) square. If sampling at that location is not possible, it may be necessary to move to another square. However, the sample must be from the originally designated 2 by 2 km square; and 4) replication is carried out when units are defined and there is sufficient exposure to permit collection at the various levels of replication. This results in replication at outcrop (duplicate samples), 0.25 km, and 1 km levels for a total of 4 samples from each selected replicated square. A split of the powder, from one of the outcrop duplicates, gives an estimate of variability at the analytical level. Summary statistics of sample collections are given in Table 15.

Table 15. Sampling statistics for the North Bay Granite Suite in map areas 1M/13, 11P/9, 11P/15, 11P/16, 12A/1, 12A/2 and 12A/3E

Potential sampling sites at 1 per 4 km²	737
Actual number obtained	489
Replicate samples (from 5 squares)	15
Duplicates (analytical splits)	40
Total analyses from the North Bay Granite	544
Other samples (dykes, veins, shales, ultramafic rocks, etc.)	88

Samples were collected using an 8 pound (3.6 kg) sledge hammer, a chisel and a geology hammer. Where the outcrop was composed of one rock type, only one sample was taken. Where more than one rock type was present, then each was sampled, where possible, and the dominant rock type noted.

Samples were described briefly in the field and necessary measurements taken, e.g., schistosity, strike attitude, size of quartz veins and presence of xenoliths (Figure 30). Attributes such as grain size, mineralogy, colour, sample location, etc., were described at base camp using a coded description format (Appendix 4) based on a system devised by R.G. Garrett (GSC, written communication, 1979).

Gamma radiation was measured at most outcrops using either a Scintrex BGS-1 scintillometer or a Scintrex GIS-4 spectrometer. The scintillometer measures total radiation only, in counts per second (cps). The spectrometer can measure on four channels to give (i) total radiation, (ii) K+U+Th, (iii) U+Th, and (iv) Th. Measurements taken in the field showed that the two instruments gave similar total radiation readings for the same locality.

In the laboratory, samples were cleaned and broken into small fragments prior to crushing and pulverization. Samples were analyzed for major elements, Cu, Zn, Ni, Be, Li, Mo, Pb, F and loss-on-ignition at the Geological Survey Branch's Laboratory, and for Ba, Sr, Rb, Zr, Cr, V, Th, Y, Nb, Ga, La and Ce at the Department of Earth Sciences Laboratory, Memorial University, and for U at Neutron Activation Services Limited, Hamilton, Ontario. Selected quartz veins were analyzed for gold. A complete list of analyses with field data is given in Appendix 1. Estimates of precision are given in Appendix 2. Estimates of accuracy for each element analyzed are given in Appendix 3. The data for accuracy indicates that a high degree of accuracy was obtained for all but two elements. Lanthanum and Ce data obtained by XRF are inaccurate when compared to the accepted values for the standards used. Although the data for La and Ce have a high degree of precision (Appendix 2), the values obtained at Memorial University for the standards indicate that the data for the 'unknowns' i.e., the samples collected, must be considered meaningless.

GEOCHEMISTRY OF THE MAGNESITE (UNIT 1)

One sample of the magnesite occurrence near D'Espoir Lake was analyzed (Table 16). The quartz veins are the main source of SiO_2, and the high Mg/Ca ratio indicates that the dominant carbonate is magnesite. The relatively high Cr and Ni content confirms that the magnesite protolith was an ultramafic rock. The opaque phases may be the source of the high chromium content and are probably iron-rich chromite, as the analysis also indicates that significant proportions of iron oxides are present in the magnesite rock (see Plate 16b).

GEOCHEMISTRY OF THE BURGEO GRANITE (UNIT 6)

One sample of Burgeo granite has been analyzed from the 2 km of the granite within Dolland Brook (east half) map area. This sample is a fault brecciated, foliated, pink, medium-grained granite. The analysis is given in Table 17. This analysis is typical of the younger units of the Burgeo granite (Dickson *et al.*, 1989). Notable features include the low Rb and high Sr content, low Rb/Sr ratio and moderate K/Rb ratio. Thus, although the rock has a relatively high SiO_2 content of 71.1 percent, the low Rb/Sr ratio indicates that the granite is not strongly differentiated (e.g., Taylor, 1965). The association of this unit of the Burgeo granite with the migmatites of the Bay du Nord Group indicates a close genetic relationship. Blackwood (1984) has suggested a close temporal relationship between metamorphism and deformation of the Bay du Nord Group and the emplacement of the Burgeo granite. The analysis shows no anomalous values for any economic elements or indicator elements.

GEOCHEMISTRY OF THE NORTH BAY GRANITE SUITE

The North Bay Granite Suite is divided into two components by the Meelpaeg Lake Fault Zone, which extends from Meelpaeg Lake to Salmon River. The main mass of the North Bay Granite Suite, within map areas 1M/13, 11P/9, 15, 16, 12A/1 and 2 are called Component 1, and consists of Units 8, 9, 11, 12, 17, 18, 19 and 21. The part to the north of the fault zone, in the Salmon River and Wolf Lake areas, is called Component 2 and consists of Units 10, 14, 15, 16 and 20. These two components although composite, are generally distinctive in terms of rock type and deformation.

The mean geochemical composition of each unit in Components 1 and 2 is given in Table 18, a and b. A comparison of the mean values for each unit generally shows the expected trends of increasing or decreasing oxide or element concentrations with changes in SiO_2 content (Figure 31). Silicon dioxide content for each unit in each component shows a complete overlap and similarly, the values for most elements and oxides, at the same SiO_2 values, are essentially the same. Examples of this negative correlation with SiO_2 are given in Figure 31.

The East Bay and Bottom Brook granites (Units 11 and 12) of Component 1 are notable for their relatively high Sr contents. The incompatible elements K, Rb, Th, U and Li, show a generally positive correlation with SiO_2. However,

ABBREVIATED FIELD DATA SHEET

No	Fab	Tex	Xen	Gnt	Tourm	Brl	Fluor	Remarks

No . . . . . Number given sample in field.

Fab. . . . . Tectonic fabric, flow foliation etc., with measurements.

Tex. . . . . Porphyritic, equigranular etc., with proportion of phenocrysts.

Xen . . . . . Variety, proportion, shape etc., of any xenoliths in the granite.

Gnt., Tourm., Brl., and Fluor. . . . Garnet, Tourmaline, Beryl and Fluorine - Present or absent; proportion, mode of occurrence, etc.

Remarks . . . . any other notes or measurements taken in field *e.g.*, scintillometer readings.

Figure 30. *Data sheet used in field during sample collection by helicopter.*

Table 16. Analysis of magnesite (Unit I); Sample 2241372

SiO_2(wt.%)	25.00	Li (g/t)	28	Sr (g/t)	66
Al_2O_3	0.26	F	98	Y	ND*
Fe_2O_3#	1.23	V	16	Zr	ND
MgO	29.96	Cr	2265	Nb	ND
CaO	4.38	Ni	1286	Mo	ND
Na_2O	0.03	Cu	23	Ba	50
K_2O	0.05	Zn	20	Pb	ND
TiO_2	0.03	Ga	2	Th	ND
MnO	0.09	Rb	1	U	ND
P_2O_5	0.01	Ag	ND		
L.O.I.	35.82				

* ND = not detected # total iron as Fe_2O_3

Table 17. Chemical composition of the Burgeo granite in the Dolland Brook (east half) map area; sample 2241500

SiO_2(wt.%)	71.1	Li (g/t)	24	Y (g/t)	5
Al_2O_3	14.8	Be	3.8	Zr	96
Fe_2O_3	0.53	F	333	Nb	9
FeO	1.06	V	36	Mo	2
MgO	0.71	Cr	12	Ag	ND*
CaO	1.7	Ni	4	Ba	746
Na_2O	3.93	Cu	9	Pb	26
K_2O	4.04	Zn	52	Th	10
TiO_2	0.3	Ga	18	U	3.1
MnO	0.04	Rb	109	Rb/Sr	0.33
P_2O_5	0.10	Sr	327		
L.O.I.	0.93				

* = not detected

significant geochemical differences exist between the two components of the North Bay Granite Suite, such that even the most siliceous units of Component 2 have a lower K_2O content than most of the less siliceous units of Component 1; similar patterns are generally shown by Li, Rb, Th and U. These chemical differences support the tectonic division of the North Bay Granite Suite into two spatially separate components. Similar chemical differences also occur to the northwest of Meelpaeg Lake where Dickson (1982) has shown that the granitoid rocks juxtaposed along the Meelpaeg Lake Fault Zone are also chemically distinct (compare Units 4 and 7 in Dickson, 1982). The presence of a major shear zone along the contact between the two components shows that a significant tectonic boundary is present.

GEOCHEMISTRY OF THE UNITS OF COMPONENT 1 OF THE NORTH BAY GRANITE SUITE

Unit 8 and D'Espoir Brook Granite (Unit 9)

Unit 8 and D'Espoir Brook Granite (Unit 9) of the North Bay Granite Suite form the northern and northeastern edge of Component 1. These units, which have been deformed together, are petrographically distinct and this difference is clearly reflected in their geochemical composition. The biotite-rich, feldspar-porphyritic granite of Unit 8 has a distinctly higher FeO, MgO, CaO, TiO_2, V, Zn, Sr, Zr and Ba content compared to the D'Espoir Brook Granite, which is composed of garnet–biotite–muscovite granite and pegmatite. The D'Espoir Brook Granite contains significantly higher SiO_2, K_2O and Rb and consequently much higher Rb/Sr ratios (Table 17).

Variations diagrams of SiO_2 versus Al_2O_3, total iron as FeO, Na_2O, K_2O, Rb, Sr, Rb/Sr, Zr, Li, V and K/Rb for Unit 8 and the D'Espoir Brook Granite (Unit 9) are given in Figures 32 to 36. A prominent feature is the more extensive range shown by SiO_2 in Unit 8 compared to the D'Espoir Brook Granite. Aluminum shows a linear negative correlation with SiO_2 in Unit 8, whereas the D'Espoir Brook Granite shows little variation (Figure 32). Unit 8 shows well-developed linear variations of CaO and FeO having wider ranges when compared to the D'Espoir Brook Granite (Figure 33). Sodium oxide values are similar in Unit 8 and the D'Espoir Brook Granite. Potassium oxide in Unit 8 shows a poorly developed positive correlation with SiO_2 whereas the D'Espoir Brook Granite shows a poor correlation and has a wide range of values (Figure 33). The Rb variation in Unit 8 and the D'Espoir Brook Granite is similar to that shown by K_2O. Strontium shows a slight negative correlation with SiO_2 in Unit 8. In the D'Espoir Brook Granite, Sr shows a pronounced negative correlation with SiO_2 even though the change in SiO_2 values is less than 5 percent (Figure 34). Consequently, Rb/Sr ratios reflect the variation shown by Sr, particularly in the D'Espoir Brook Granite, which displays a pronounced increase in Rb/Sr ratios at the higher SiO_2 values. Zircon variations are similar to those shown by Sr with a pronounced depletion in the D'Espoir Brook Granite at the higher SiO_2 values (Figure 35). Lithium shows a weak negative correlation with SiO_2 in Unit 8, whereas Li shows a poor correlation with SiO_2 in the D'Espoir Brook Granite (Figure 35). Lithium values are generally distinctly lower in the D'Espoir Brook Granite compared to Unit 8. The positive correlation with SiO_2 shown by U in Unit 8 contrasts with the random variations shown by the D'Espoir Brook Granite. Potassium/rubidium ratios for the D'Espoir Brook Granite (Unit 9) show a trend toward lower values, whereas K/Rb ratios are relatively constant in Unit 8 (Figure 36).

A plot of Na_2O+K_2O (Alk_{tot}):total iron as FeO (FeO_{tot}):MgO (Figure 37) shows more variation in Unit 8 than in the D'Espoir Brook Granite, which forms a relatively tight cluster. Unit 8 also shows a trend similar to that of calc-alkaline granitoid rocks.

The variation diagrams for Unit 8 and the D'Espoir Brook Granite indicate that there is probably no direct relationship between the two units although they commonly occur together. The linear variations shown by Unit 8 generally do not coalesce with the values for the D'Espoir Brook Granite. This corresponds with the distinctly different rock types of Unit 8 and the D'Espoir Brook Granite with

Table IB(a). Mean composition of each unit of Component 1 of the North Bay Granite Suite

i: Major elements (in weight percent).

Unit	8	9	11	12	17	18	19	21
n (#)	7	34	198	63	123	60	36	2
SiO_2	67.73	72.93	71.04	71.02	70.28	72.75	71.71	70.85
Al_2O_3	15.63	14.64	15.17	14.96	14.95	14.45	14.64	14.80
Fe_2O_3	0.68	0.28	0.37	0.43	0.65	0.58	0.47	0.64
FeO	2.67	0.91	1.34	1.44	1.36	0.73	1.21	1.31
MgO	1.15	0.36	0.65	0.67	0.72	0.40	0.54	0.61
CaO	2.20	1.00	1.71	1.74	1.63	1.01	1.29	1.51
Na_2O	3.39	3.63	3.89	3.70	3.73	3.70	3.60	3.65
K_2O	3.89	4.87	4.15	4.58	4.93	5.14	4.99	5.14
TiO_2	0.56	0.21	0.31	0.34	0.39	0.24	0.32	0.37
MnO	0.07	0.06	0.05	0.05	0.05	0.04	0.05	0.06
P_2O_5	0.22	0.14	0.11	0.10	0.13	0.09	0.10	0.09
LOI	1.06	0.75	0.76	0.68	0.73	0.79	0.73	0.70

ii: Trace elements (in g/t).

Unit	8	9	11	12	17	18	19	21
Li	77	59	48	47	92	77	48	37
Be	6.9	6.9(8)*	4.6(26)	4.2(18)	3.8(95)	4.1(57)	4.9(19)	3.6
P	668	469	445	561	635	623	444	465
V	63	14	30	31	40	21	27	37
Cr	13	7	6	5	8	5	6	10
Ni	9	2	4	3	3	1	3	3
Cu	13	5	13	15	9	7	9	22
Zn	64	37	49	49	51	44	51	44
Ga	19	18	19	19	19	20	19	17
Rb	178	222	166	182	201	274	227	190
Sr	163	92	268	294	253	135	196	224
Y	36	21	17	18	16	17	23	14
Zr	195	85	130	164	165	132	93	172
Nb	17	16	10	11	14	20	16	14
Mo	3	2	3	3	2	3	2	2
Ag	0.1	0.1	0.1	0.1	0.1	0.1	0.1	0.1
Sn	-	9 (1)	2 (46)	2 (4)	2 (22)	5 (27)	1 (1)	-
Ba	561	351	633	735	766	499	592	824
W	-	0.1(1)	0.3(47)	0.9(4)	0.8(22)	2.4(27)	0.1(1)	-
Pb	22	27	30	25	28	29	31	32
Th	14	9	13	17	25	27	25	44
U	4.1	4.2	3.9	3.9	5.0	6.8	7.5	4.7

Note: La and Ce are not considered to be accurate; see data on accuracy.

La	21	11	17	19	44	36	28	67
Ce	44	21	30	37	100	86	68	206

number of analyses
* number in brackets is number of analyses if not equal to 'n'.

Table 8(b). Mean composition of each unit of Component 2 of the North Bay Granite Suite.

i: Major elements (in weight percent).

UNIT	10	13	14	15	16	20
n (#)	19	1	7	9	5	18
SiO_2	65.67	72.35	67.00	73.74	74.20	68.71
Al_2O_3	15.71	14.56	15.84	13.89	13.77	15.47
Fe_2O_3	0.86	0.52	0.75	0.27	0.07	0.71
FeO	3.58	0.97	2.90	0.82	0.86	2.15
MgO	1.92	0.49	1.29	0.26	0.28	1.19
CaO	2.93	1.26	2.68	0.66	0.55	2.81
Na_2O	3.52	3.65	3.94	3.75	3.82	3.58
K_2O	3.52	4.58	3.41	4.64	4.41	3.48
TiO_2	0.73	0.27	0.63	0.16	0.13	0.49
MnO	0.09	0.04	0.07	0.06	0.05	0.07
P_2O_5	0.22	0.11	0.19	0.06	0.09	0.15
LOI	1.11	0.85	1.00	0.81	0.93	0.82

ii: Trace elements (in g/t).

UNIT	10	13	14	15	16	20
Li	49	69	51	30	37	46
Be	2.8	-	3.5	3.9	4.8	4.0(1)
F	733	441	780	277	218	490
V	85	30	68	13	11	53
Cr	24	5	20	12	5	7
Ni	8	3	6	2	1	9
Cu	12	10	12	3	3	10
Zn	76	44	72	27	28	51
Ga	20	18	20	17	16	17
Rb	121	259	112	208	154	144
Sr	240	271	303	52	81	170
Y	38	13	17	33	16	23(17)
Zr	248	120	191	68	43	154
Nb	18	14	17	13	13	12
Mo	3	2	3	6	2	3
Ag	0.1	0.1	0.1	0.1	0.1	0.1
Sn	-	0.1	-	-	-	0.7
Ba	640	660	617	217	280	409
W	-	0.1	-	-	-	0.1(3)
Pb	15	27	13	24	24	20
Th	14	21	9	14	9	11(17)
U	2.9	3.9	2.1	5.6	2.5	2.8

Note: La and Ce are not considered to be accurate; see data on accuracy.

La	34	30	36	14	9	21(17)
Ce	98	67	88	42	36	35(17)

number of analyses

* number in brackets is number of analyses if not equal to 'n'.

little evidence of intermediate compositions. Unit 8 does not contain muscovite or garnet and pegmatite and aplite veins are absent. Hence, it is concluded that the D'Espoir Brook Granite, which is dominated by muscovite–garnet pegmatite and granite, is unrelated to Unit 8.

The East Bay and Bottom Brook Granites (Units 11 and 12)

Variation diagrams for East Bay and Bottom Brook granites are given in Figures 38 to 43. The diagrams indicate that the two units are virtually identical in terms of the elements presented. Strong negative correlations of Al_2O_3, CaO and total iron as FeO, with SiO_2 are apparent (Figures 38 and 39). Sodium oxide shows little variation with SiO_2, although the East Bay Granite contains some values well below 3 percent and one value above 6 percent. Sodium oxide values for the Bottom Brook Granite are much less varied when compared to the East Bay Granite. Similar patterns are exhibited by K_2O (Figure 40). The Bottom Brook Granite shows a general positive correlation of K_2O with SiO_2. The East Bay Granite shows a generally similar trend but several values are depleted in K_2O and others are strongly enriched in K_2O.

Rubidium values for the East Bay Granite are relatively constant up to SiO_2 values of 70 percent (Figure 41). At higher SiO_2 values, numerous samples are depleted in Rb but a general trend of increasing Rb values is apparent. In the Bottom Brook Granite, Rb shows a positive correlation with SiO_2 but no strong enrichment trend is apparent.

The wide range of Sr and Rb values present in the East Bay and Bottom Brook granites is reflected particularly by the Rb/Sr ratios, which show a wide scatter at the same SiO_2 value (Figures 41 and 42). This indicates that differentiation of the magma started with highly variable initial compositions, a feature that has been noted in the section on Rb–Sr systematics for the East Bay Granite (see Radiometric Dating Section), where even close-spaced samples have highly variable values for Rb and Sr.

In the East Bay and Bottom Bay granites, Li has a negative correlation with SiO_2 (Figure 42), and Zr shows a differentiation trend very similar to that shown by Sr (Figure 43). Uranium shows a weak, positive correlation with SiO_2 (Figure 43). Some samples with over 70 percent SiO_2 values are particularly enriched compared to the general trend.

Potassium/rubidium ratios for the East Bay Granite show a constant range of values with no decrease in K/Rb values apparent at the higher Rb levels (Figure 44). The K/Rb ratios for the Bottom Brook Granite show a general increase toward the higher Rb values but are generally similar to those of the East Bay Granite. The break in slope shown by Sr may reflect the replacement of plagioclase by K-feldspar as the main crystallizing feldspar phase.

A plot of total alkalis (A) total iron as FeO (F) MgO (M) for the East Bay and North Bay granites (Figure 43) shows

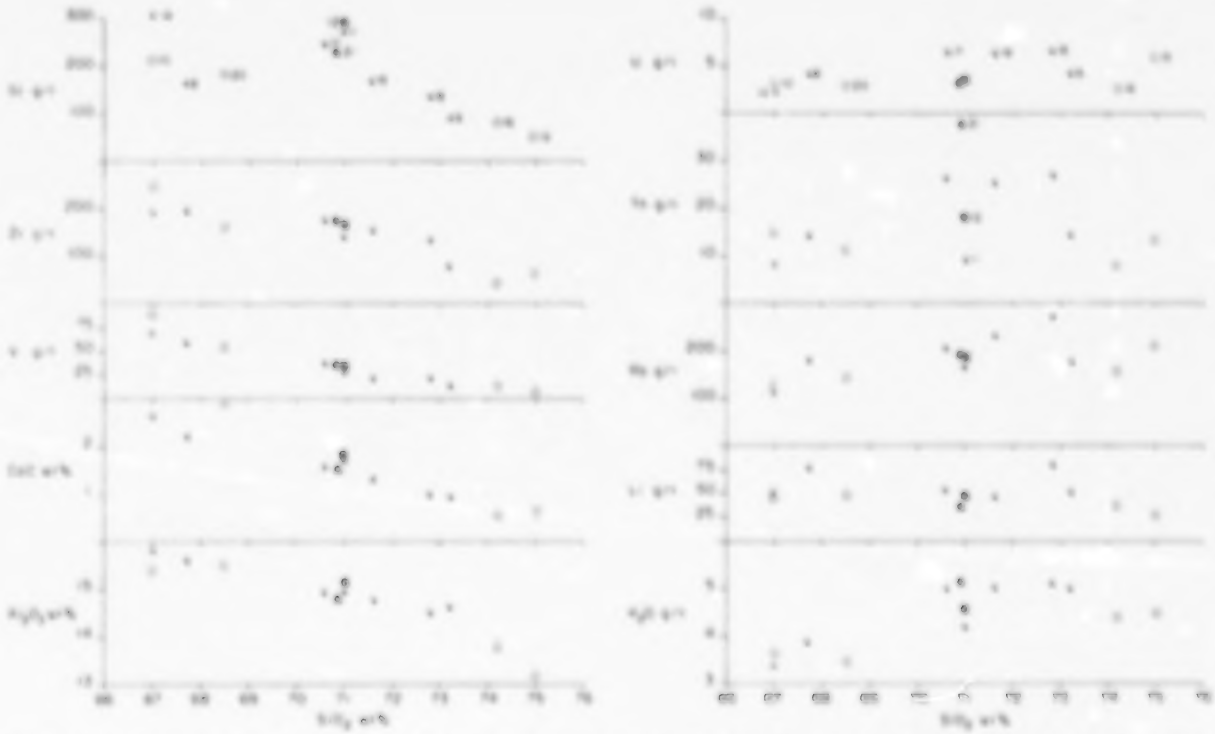

Figure 31. *Variation diagrams for means of selected oxides and elements for the units in each component of the North Bay Granite Suite; solid symbols for Component 1 and open symbols (circles and crosses) for Component 2.*

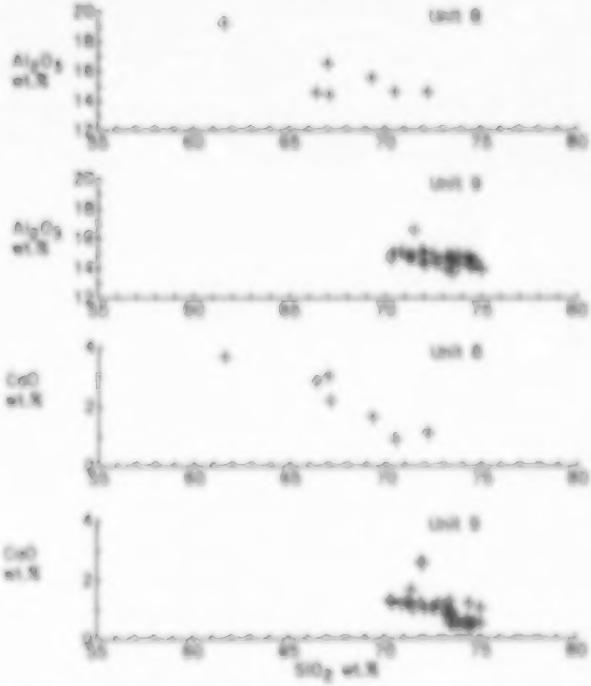

Figure 32. *Variation diagrams for Al_2O_3 and CaO vs. SiO_2 (all weight percent) for Unit 8 and the D'Espoir Brook Granite (Unit 9).*

a pronounced linear variation from compositions relatively enriched in FeO_{tot} and MgO. These trends are similar to the calc-alkaline trends shown by the batholiths of the Coastal Batholith of Peru and other calc-alkaline batholiths such as the Sierra Nevada and the Coastal Batholith of British Columbia (Figure 45).

Dolland Brook and Facheux Bay East Granites (subunits 17a, 17b), Wolf Mountain Granite (Unit 18), the Dolland Pond, Morgan Brook, Hughes Brook and D'Espoir Lake Granites (subunits 19a to 19d) and Unit 21

These granites have been grouped together as they are petrographically similar and dominate the western part of the study area from Granite Lake to Morgan Brook. Variation diagrams of selected elements versus SiO_2 are given in Figures 46 to 56. A feature of this unit is the restricted SiO_2 range of the units with the most variable (the Dolland Brook and Facheux Bay East granites (subunits 17a,b) ranging from 65 to 75 percent SiO_2 and the others (the Wolf Mountain Granite (Unit 18) and the Dolland Pond, Morgan Brook, Hughes Brook and D'Espoir Lake Granites (subunits 19a to d) ranging from 68 to 75 percent. Alumina and FeO_{tot} display linear negative correlations with SiO_2 within a narrow range at similar SiO_2 values (Figures 46 and 47).

Calcium oxide is more variable but still shows a strong negative correlation with SiO_2 (Figure 48) and is distinctly

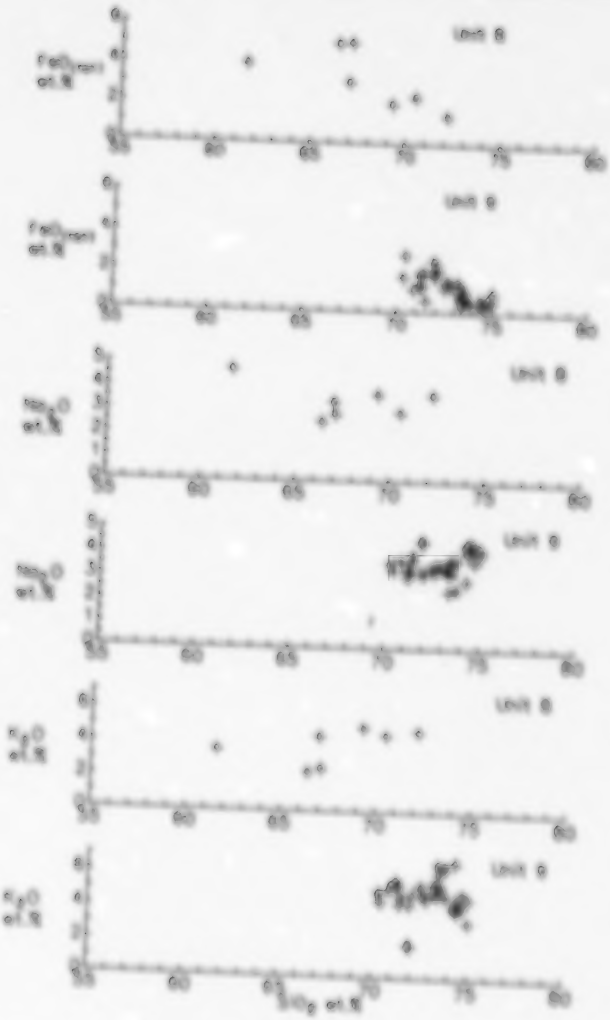

Figure 53. *Variation diagrams of FeO, Na_2O and K_2O vs. SiO_2 (all weight percent) for Unit 8 and the D'Espoir Brook Granite (Unit 9).*

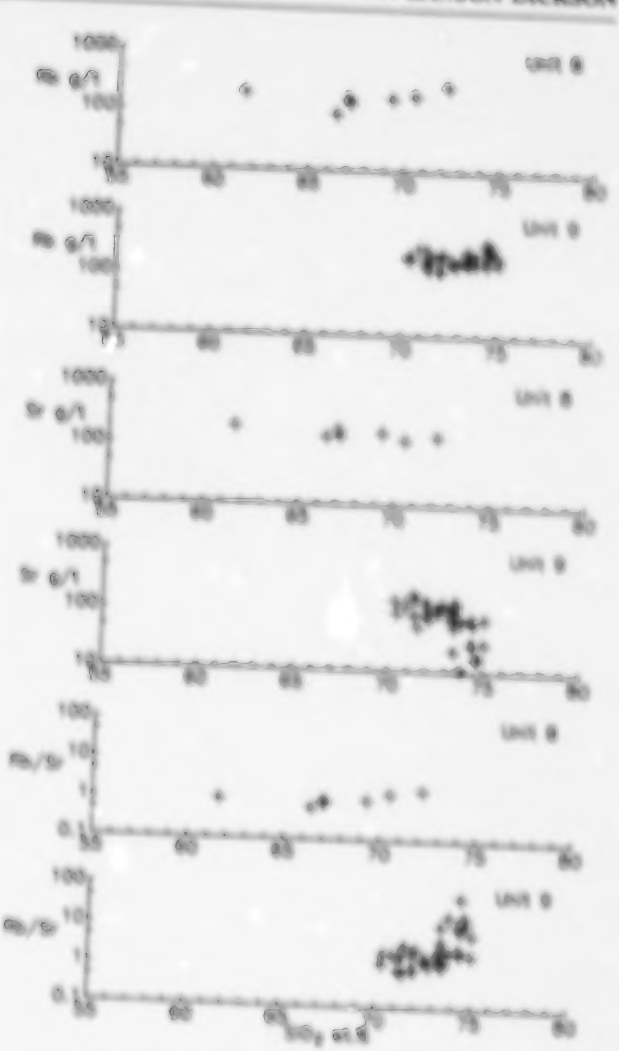

Figure 54. *Variation diagrams of $\log_{10}$ Rb, $\log_{10}$ Sr (in g/t) and $\log_{10}$ Rb/Sr vs. SiO_2 (in weight percent) for Unit 8 and the D'Espoir Brook Granite (Unit 9).*

depleted at SiO_2 values over 70 percent. Sodium oxide shows little variation with SiO_2 and has virtually identical ranges in all four units (Figure 49). Potassium oxide varies mainly between 4 and 6 percent and shows little correlation with SiO_2 (Figure 50). The Dolland Brook and Pacheux Bay East granites show a wide spread in K_2O values at the lower SiO_2 values. This may reflect minor alteration of feldspar and biotite resulting in leaching of K_2O. The higher K_2O values may reflect a higher modal percentage of K-feldspar, which would increase K_2O values and decrease SiO_2 toward feldspar compositions. Rubidium values, like K_2O, show little variation with SiO_2 with no indication of Rb enrichment at the higher SiO_2 values (Figure 51).

Strontium shows a strong negative correlation with SiO_2 in the three main units (Units 17 to 19, Figure 52). The Wolf Mountain Granite and the various components of Unit 19 are more strongly depleted in Sr, when compared to the Dolland Brook and Pacheux Bay East granites (Unit 17). The Wolf Mountain Granite is the most strongly depleted in Sr at the highest SiO_2 values. These variations are reflected in Rb/Sr ratios. A feature of the Rb/Sr ratios (Figure 53) is that in Unit 17, the majority of values are less than 1, whereas in the Wolf Mountain Granite (Unit 18) and subunits 19a,b,c and d, the majority are greater than 1, indicating that Units 18 and 19 are the most differentiated.

Lithium values are widely scattered in Unit 17 and the Wolf Mountain Granite and show little systematic variation with SiO_2 (Figure 54). However, numerous samples from the Wolf Mountain Granite are relatively enriched in Li with values in excess of 800 g/t. Unit 19 shows a weak negative correlation of Li with SiO_2.

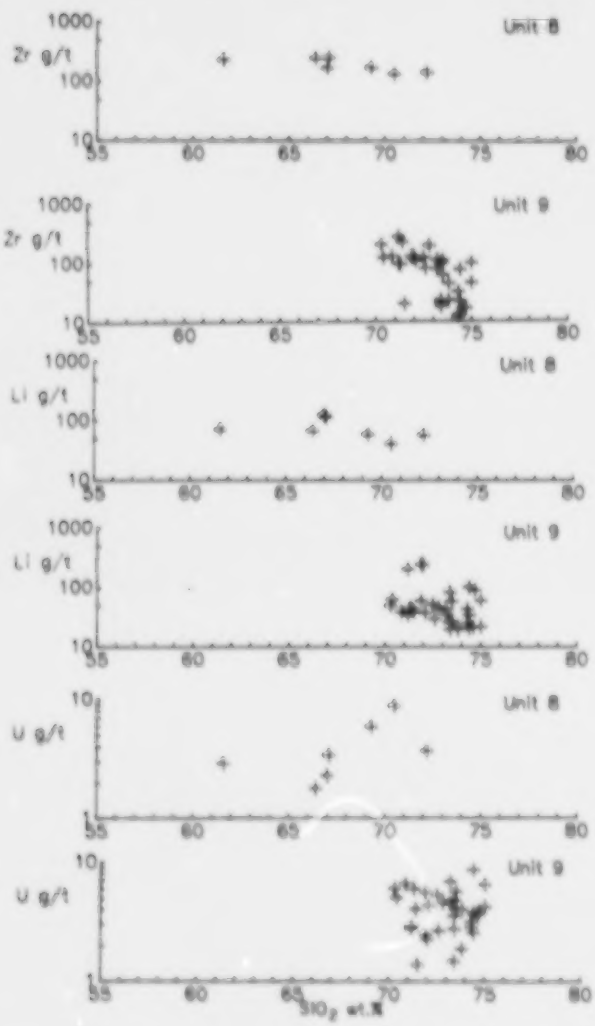

Figure 35: *Variation diagrams of $\log_{10}$ Zr, $\log_{10}$ Li and $\log_{10}$ U (in g/t) vs. SiO_2 (all weight percent) for Unit 8 and the D'Espoir Brook Granite (Unit 9).*

Uranium values for Units 17, 18, 19 and 21 are generally around background for granitoid rocks with isolated values above the normal range for granites of 2 to 8 g/t (see Wedepohl, 1978; Figure 55). Zirconium in Units 17, 18 and 19 display a strong negative correlation with SiO_2 (Figure 56). However, in Unit 17 this depletion trend is less pronounced than in Units 18 and 19, which show strong depletion trends at the higher SiO_2 values.

Potassium/rubidium ratios for Units 17, 18, 19 and 21 are given in Figure 57. Units 17 and 19 show similar patterns with a strong increase in Rb and K/Rb ratios. Ratios range from about 400 to 150 for Units 17 and 19. The Wolf Mountain Granite shows no trend for K versus Rb and the ratios cluster around 150. This ratio is much lower than the average K/Rb ratio of 230 for granitoid rocks (Taylor, 1965) and indicates again that the Wolf Mountain Granite is strongly

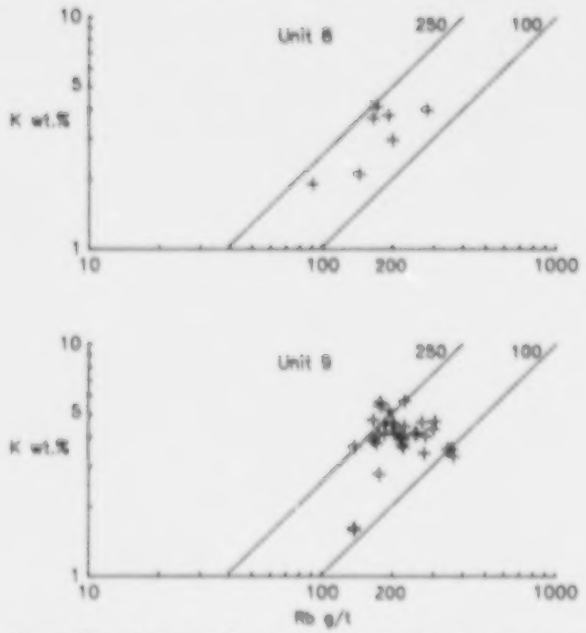

Figure 36: *Variation diagrams of $\log_{10}$ K (in weight percent) vs. $\log_{10}$ Rb (in g/t) for Unit 8 and the D'Espoir Brook Granite (Unit 9).*

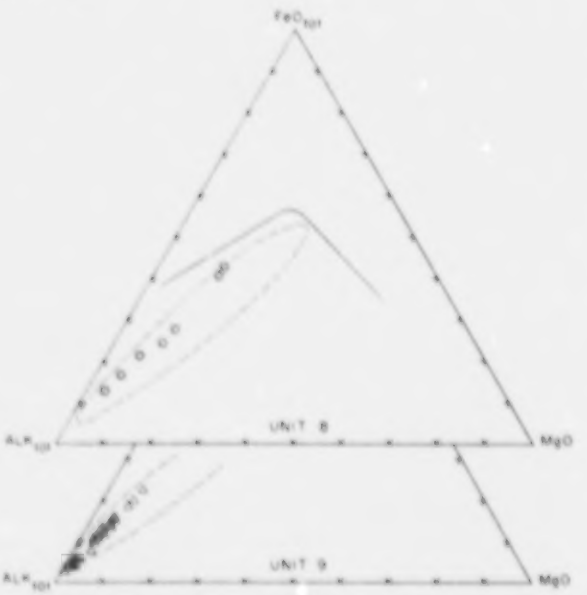

Figure 37. *Plot of $K_2O + Na_2O$ (Alk_{tot}):Total iron as FeO (FeO_{tot}):MgO (all weight percent) for Unit 8 and the D'Espoir Brook Granite (Unit 9). Curved line separates tholeiitic compositions (above) from calc-alkaline (below); from Irvine and Baragar (1971). Dashed line indicates field of calc-alkaline granitoid rocks from part of the Coastal Batholith of Peru; from Atherton et al. (1979).*

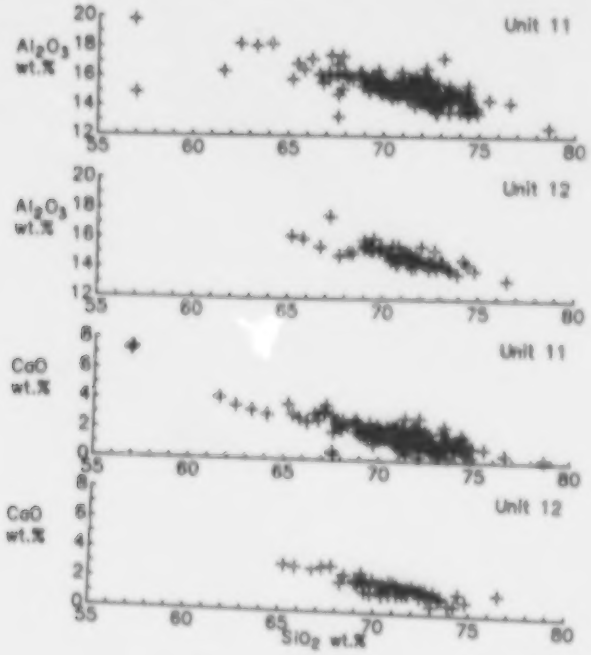

Figure 38. *Variation diagrams of Al_2O_3 and CaO vs. SiO_2 (all weight percent) for the East Bay Granite (Unit 11) and the Bottom Brook Granite (Unit 12).*

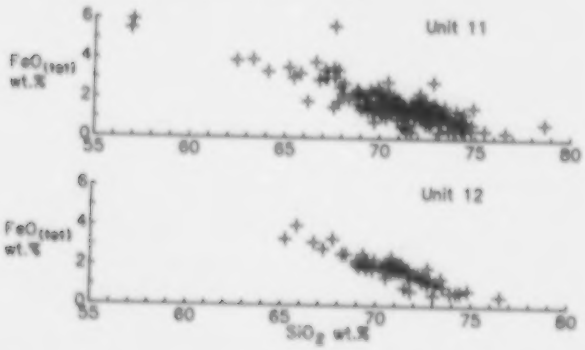

Figure 39. *Variation diagram of total iron as FeO (FeO_{tot}) vs. SiO_2 (all weight percent) for the East Bay Granite (Unit 11) and the Bottom Brook Granite (Unit 12).*

differentiated, when compared to the granites of Units 17 and 19. Unit 19 has K/Rb ratios of around 300 and is the least evolved of these four units.

A plot of Na_2O+K_2O:total iron as FeO:MgO (Figure 58) indicates that Units 17, 18, 19 and 21 lie within the field of calc-alkaline granitoid rocks of Atherton *et al.* (1979) but occupy only the Na_2O+K_2O-enriched part. This suggests that these relatively evolved granitoid rocks do not form part of a continuous trend typical of calc-alkaline granitoid rocks, and are probably not calc-alkaline.

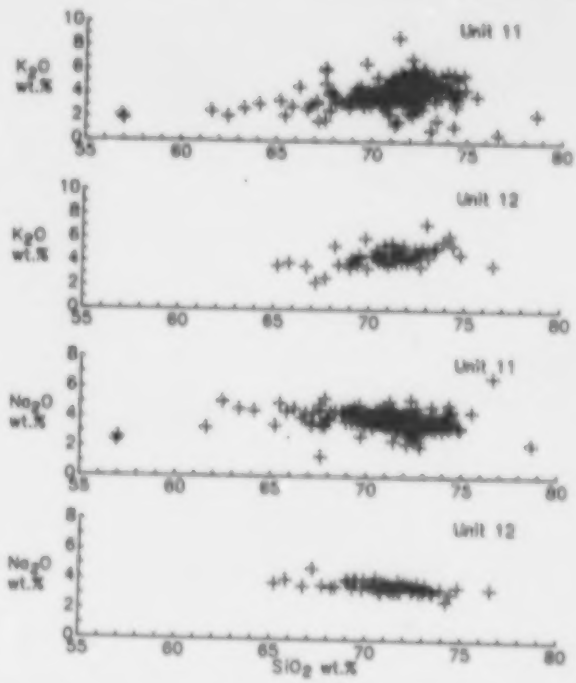

Figure 40. *Variation diagrams of K_2O and Na_2O vs. SiO_2 (all weight percent) for the East Bay Granite (Unit 11) and the Bottom Brook Granite (Unit 12).*

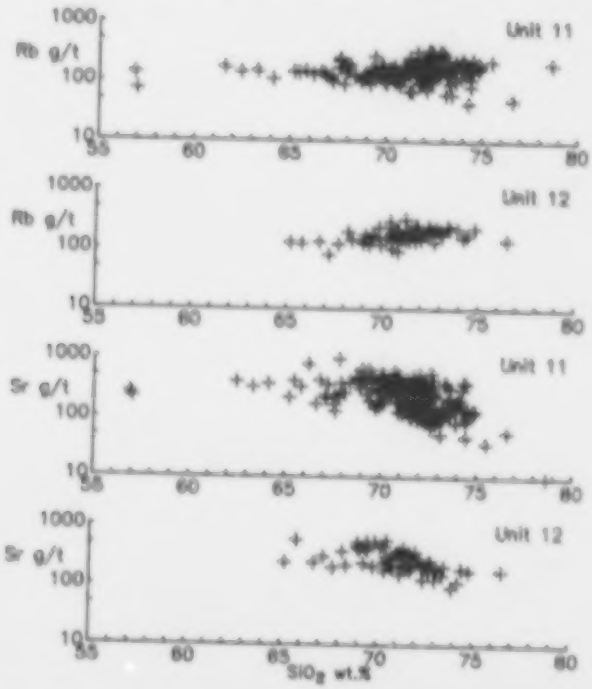

Figure 41. *Variation diagrams of $\log_{10}$ Rb and $\log_{10}$ Sr (in g/t) vs. SiO_2 (in weight percent) for the East Bay Granite (Unit 11) and the Bottom Brook Granite (Unit 12).*

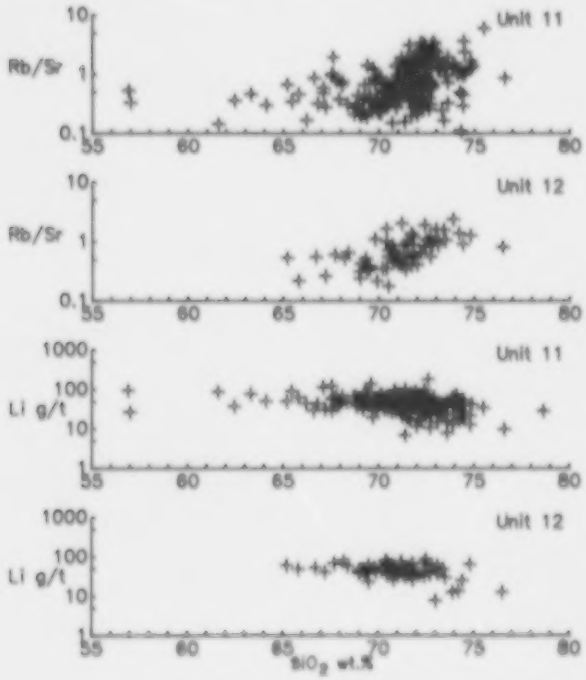

Figure 42. *Variation diagrams of $\log_{10}$ Rb/Sr ratios and $\log_{10}$ Li (in g/t) vs. SiO_2 (in weight percent) for the East Bay Granite (Unit 11) and the Bottom Brook Granite (Unit 12).*

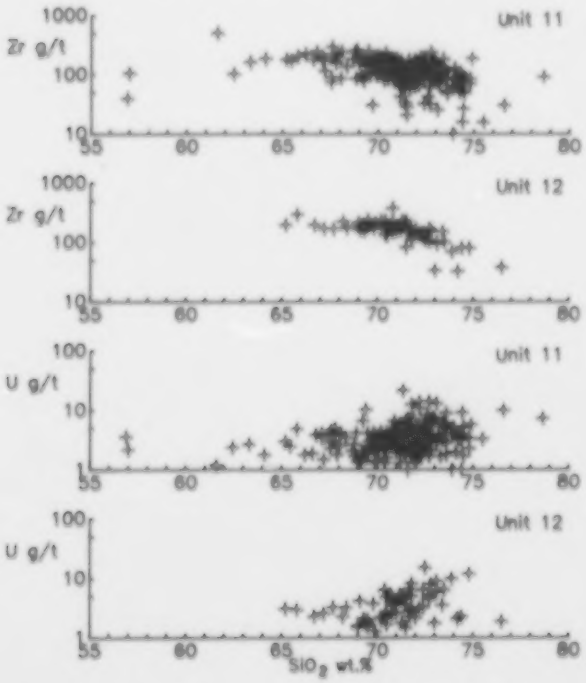

Figure 43. *Variation diagrams of $\log_{10}$ Zr and $\log_{10}$ U (in g/t) vs. SiO_2 (in weight percent) for the East Bay Granite (Unit 11) and Bottom Brook Granite (Unit 12).*

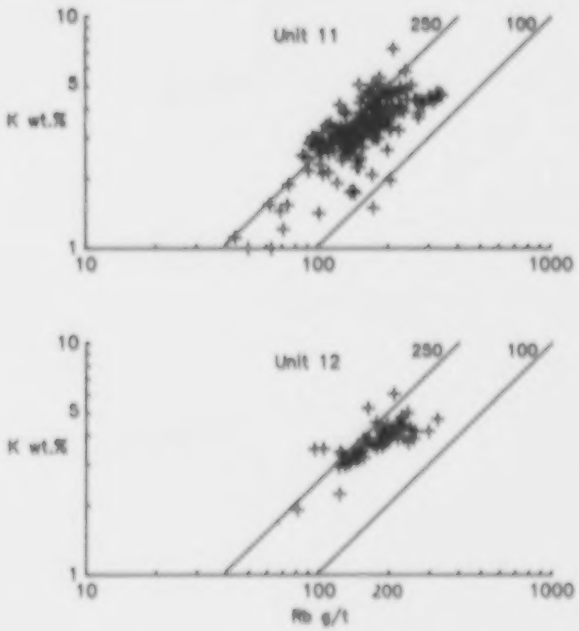

Figure 44. *Variation diagrams of $\log_{10}$ K (in weight percent) vs. $\log_{10}$ Rb (in g/t) for the East Bay Granite (Unit 11) and Bottom Brook Granite (Unit 12).*

GEOCHEMISTRY OF COMPONENT 2 OF THE NORTH BAY GRANITE SUITE

Component 2 of the North Bay Granite Suite comprises the Wolf Lake North Granodiorite (Unit 10), the Meelpaeg Lake Granite (Unit 14), Unit 15, the Wolf Lake Granite (Unit 16) and the Upper Salmon Road Granite (Unit 20). Units 10 and 14 are distinctly biotite-rich granodiorite and granite when compared to Units 15 and 16, which are garnet–biotite–muscovite granites. Unit 20 is a K-feldspar–plagioclase-porphyritic, biotite granite.

Variation diagrams of selected elements plotted against SiO_2 for Units 10, 14, 15, 16 and 20 are given in Figures 59 to 70. Silicon dioxide values for each of these units indicate that they can be divided into three groups. The Wolf Lake North Granodiorite and the Meelpaeg Lake Granite have a wide range of SiO_2 values from 60 to 72 percent SiO_2. Unit 15 and the Wolf Lake Granite have much more restricted ranges and vary from 72 to 75 percent SiO_2. The Upper Salmon Road Granite is intermediate between these two groupings and ranges from 64 to 72 percent SiO_2. The Wolf Lake North Granodiorite, the Meelpaeg Lake Granite and the Upper Salmon Road Granite show strong differentiation trends with a negative correlation of Al_2O_3, total iron (as FeO) and CaO with SiO_2 (Figures 59 to 61). Unit 15 and the Wolf Lake Granite also have negative correlations of Al_2O_3, FeO and CaO with SiO_2 but are much more depleted in these elements compared to the Wolf Lake North, Meelpaeg Lake

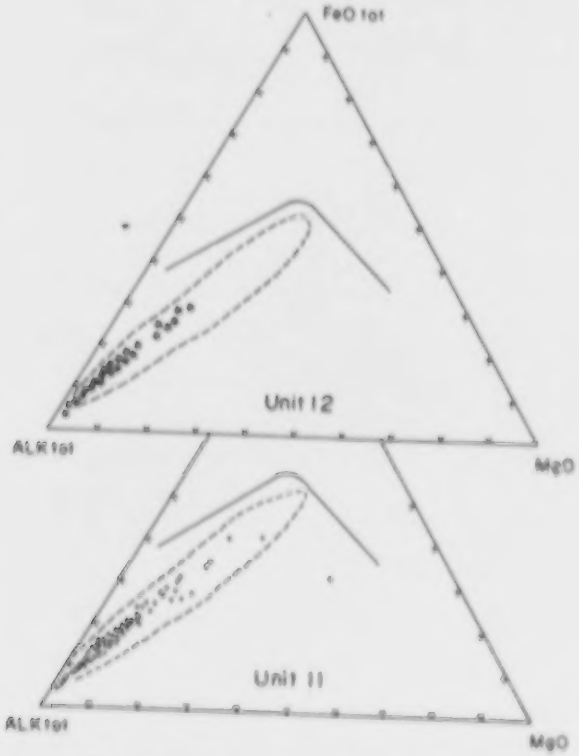

Figure 45. *Plot of $K_2O + Na_2O$ (Alk_{tot}):Total iron as FeO (FeO_{tot}):MgO (all weight percent) for the East Bay Granite (Unit 11) and Bottom Brook Granite (Unit 12). Curved line separates tholeiitic compositions (above) from calc-alkaline (below); from Irvine and Baragar (1971). Dashed line indicates field of calc-alkaline granitoid rocks from part of the Coastal Batholith of Peru; from Atherton et al. (1979).*

and Upper Salmon Road granites. Sodium oxide values are similar in all five units and show no correlation with SiO_2 (Figure 62). Potassium oxide values show a strong positive correlation with SiO_2 in the Wolf Lake North Granodiorite and the Meelpaeg Lake Granite (Figure 63). This differs from Unit 15, the Wolf Lake Granite and the Upper Salmon Road Granite, which show no correlation with SiO_2.

Rubidium values mirror the changes shown by K_2O with a positive correlation with SiO_2 shown by the Wolf Lake North Granodiorite and the Meelpaeg Granite and no correlation shown by Unit 15, the Wolf Lake and Upper Salmon Road Granite (Figure 64). Strontium values have strong negative correlations with SiO_2 and Unit 15 shows a strong depletion of Sr at the higher SiO_2 values (Figure 65). These changes are reflected in plots of Rb/Sr ratios against SiO_2 with high Rb/Sr ratios present in Unit 15 (Figure 66). The Wolf Lake North Granodiorite, Meelpaeg Lake and Upper Salmon Road granites have Rb/Sr ratios, which are generally less than 1, whereas Unit 15 and the Wolf Lake Granite have ratios greater than 1, indicating that they are more differentiated.

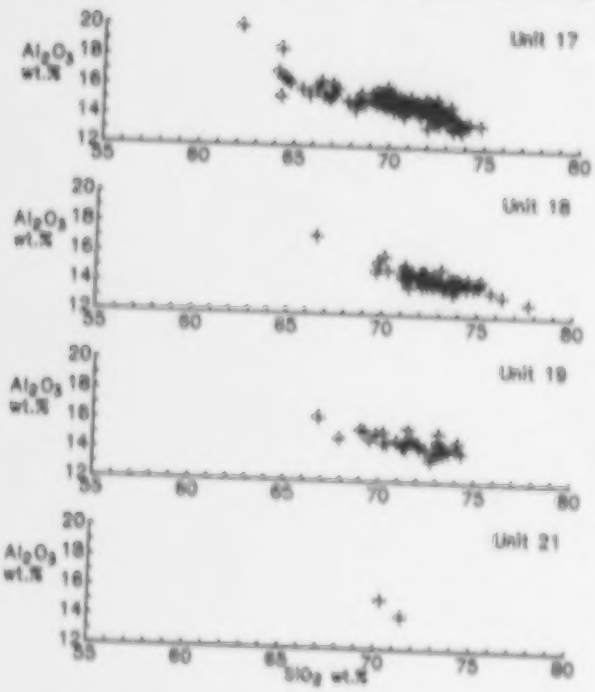

Figure 46. *Variation diagrams of Al_2O_3 vs. SiO_2 (both weight percent) for Unit 17, the Wolf Mountain Granite (Unit 18), and Units 19 and 21 of the North Bay Granite Suite.*

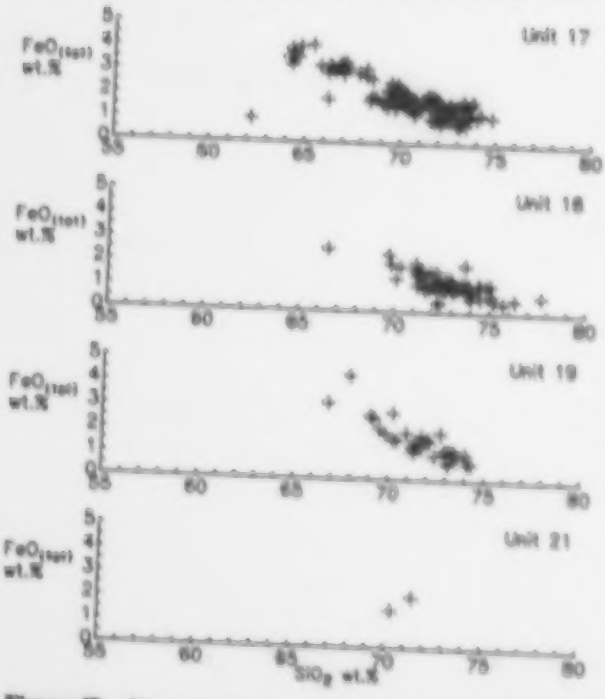

Figure 47. *Variation diagrams of total iron as FeO (FeO_{tot}) vs. SiO_2 (both weight percent) for Unit 17, the Wolf Mountain Granite (Unit 18), and Units 19 and 21 of the North Bay Granite Suite.*

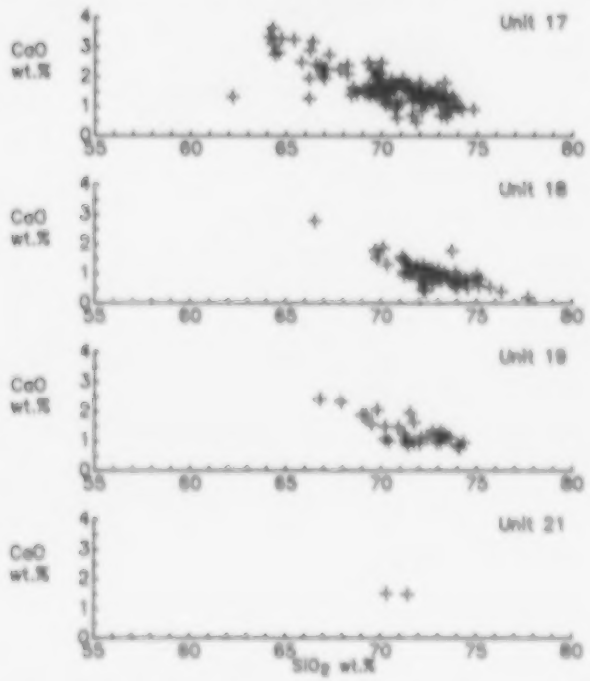

Figure 48. *Variation diagrams of CaO vs. SiO_2 (both weight percent) for Unit 17, the Wolf Mountain Granite (Unit 18), and Units 19 and 21 of the North Bay Granite Suite.*

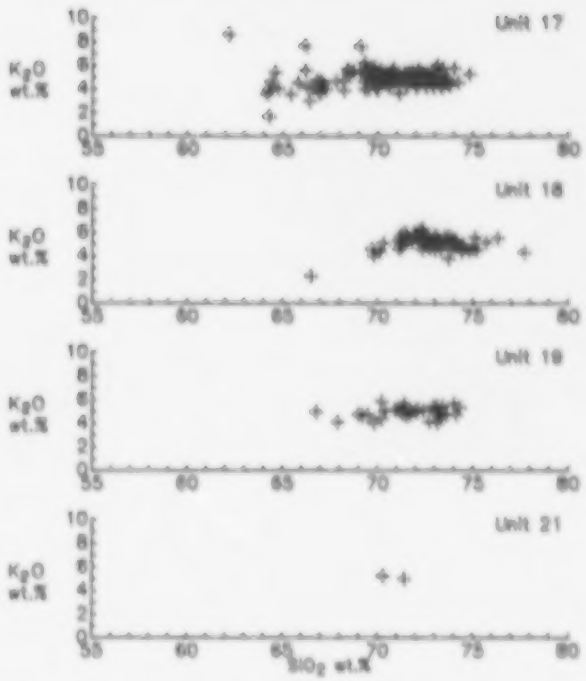

Figure 50. *Variation diagrams of K_2O vs. SiO_2 (both weight percent) for Unit 17, the Wolf Mountain Granite (Unit 18), and Units 19 and 21 of the North Bay Granite Suite.*

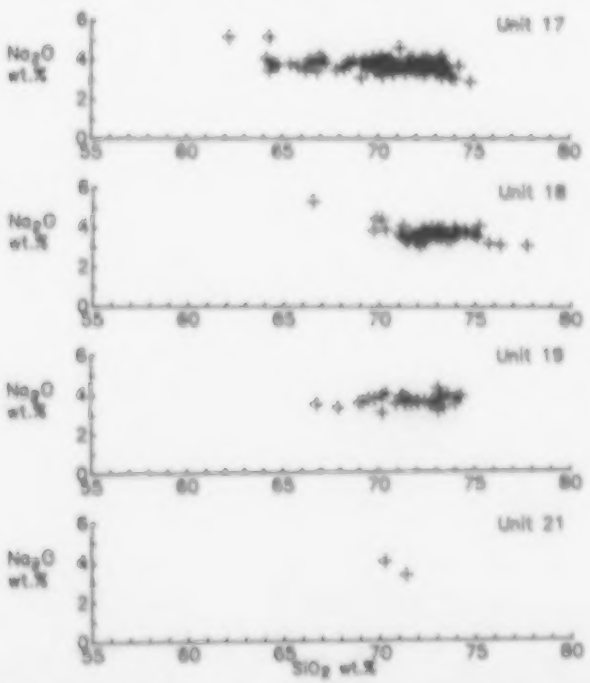

Figure 49. *Variation diagrams of Na_2O vs. SiO_2 (both weight percent) for Unit 17, the Wolf Mountain Granite (Unit 18), and Units 19 and 21 of the North Bay Granite Suite.*

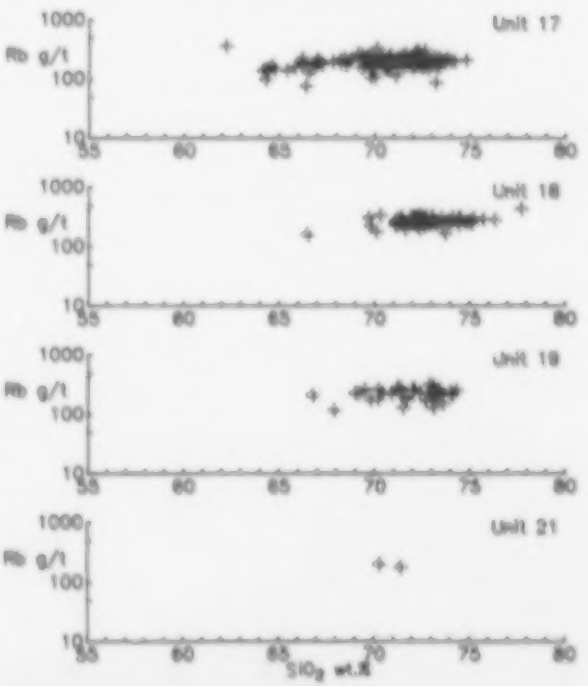

Figure 51. *Variation diagrams of $\log_{10}$ Rb (in g/t) vs. SiO_2 (in weight percent) for Unit 17, the Wolf Mountain Granite (Unit 18), and Units 19 and 21 of the North Bay Granite Suite.*

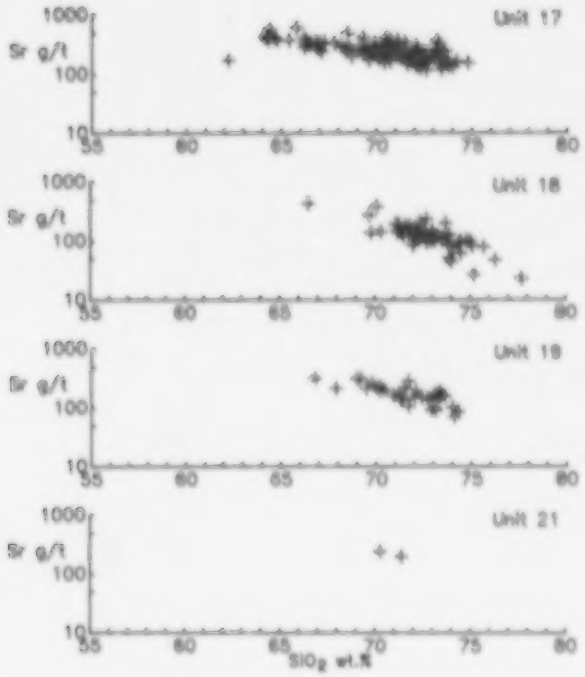

Figure 52. *Variation diagrams of $\log_{10}$ Sr (in g/t) vs. SiO_2 (in weight percent) for Unit 17, the Wolf Mountain Granite (Unit 18), and Units 19 and 21 of the North Bay Granite Suite.*

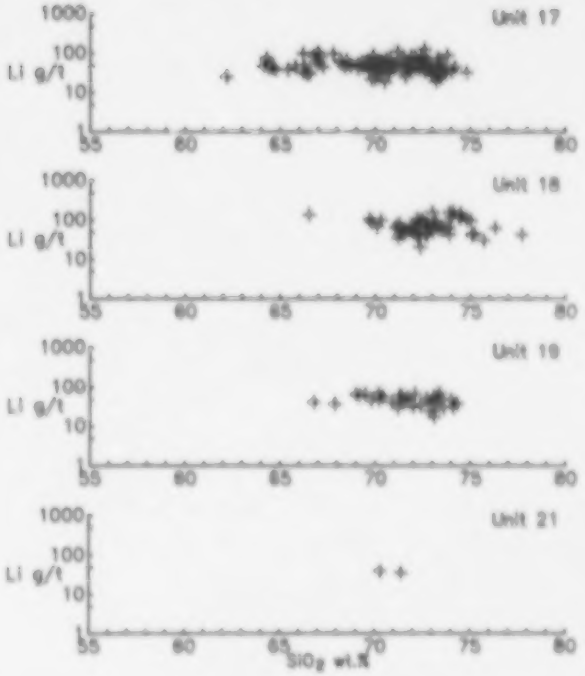

Figure 54. *Variation diagrams of $\log_{10}$ Li (in g/t) vs. SiO_2 (in weight percent) for Unit 17, the Wolf Mountain Granite (Unit 18), and Units 19 and 21 of the North Bay Granite Suite.*

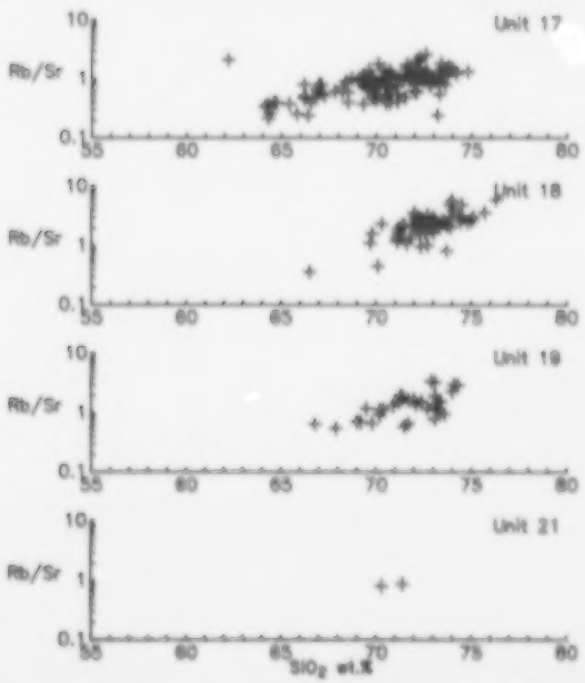

Figure 53. *Variation diagrams of $\log_{10}$ Rb/Sr (in g/t) vs. SiO_2 (in weight percent) for Unit 17, the Wolf Mountain Granite (Unit 18), and Units 19 and 21 of the North Bay Granite Suite.*

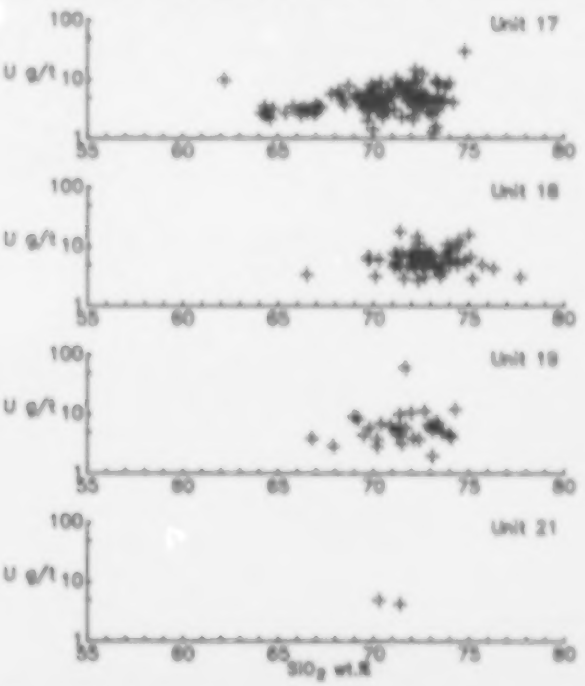

Figure 55. *Variation diagrams of $\log_{10}$ U (in g/t) vs. SiO_2 (in weight percent) for Unit 17, the Wolf Mountain Granite (Unit 18), and Units 19 and 21 of the North Bay Granite Suite.*

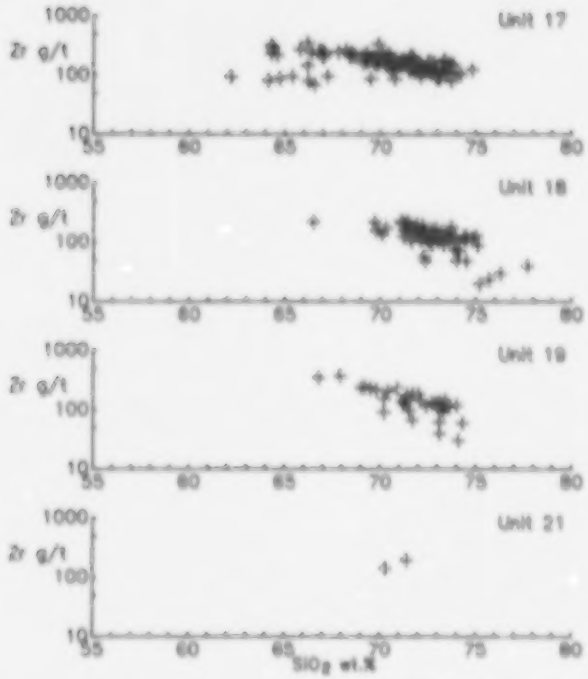

Figure 56. *Variation diagrams of $\log_{10}$ Zr (in g/t) vs. SiO_2 (in weight percent) for Unit 17, the Wolf Mountain Granite (Unit 18), and Units 19 and 21 of the North Bay Granite Suite.*

Zirconium values for Unit 15 and the Wolf Lake Granite also indicate their strongly differentiated chemistry with Zr content dropping to 20 g/t (Figure 67). The Wolf Lake North Granodiorite, Meelpaeg Lake and Upper Salmon Road granites have weak depletion trends of Zr with SiO_2 and Zr values remain at a relatively high 150 g/t, even at the higher SiO_2 values.

Lithium values exhibit strong negative correlations with SiO_2 in the Meelpaeg Lake Granite, Unit 15 and the Wolf Lake Granite, little correlation with the Wolf Lake North Granodiorite, and a weak positive correlation with SiO_2 in the Upper Salmon Road Granite (Figure 68). The depletion trends probably reflect the low biotite content in Unit 15 and the Wolf Lake Granite, with the reverse observed in the Wolf Lake North Granodiorite and the Upper Salmon Road Granite.

Uranium values for the Wolf Lake North Granodiorite, Meelpaeg Lake and Upper Salmon Road granites show a positive correlation with SiO_2, reflecting the incompatible nature of U (Figure 69). Unit 15 and the Wolf Lake Granite, which exhibit little variation in the major elements, similarly, do not show any linear variation in U values. Unit 15 displays strong trends in Rb/Sr ratios and would have been expected to show some U enrichment trend. However, even though the U values in Unit 15 are twice that of the Wolf Lake Granite, they are not considered as enriched. Potassium versus Rb (Figure 70) indicates that K/Rb ratios are similar in Units

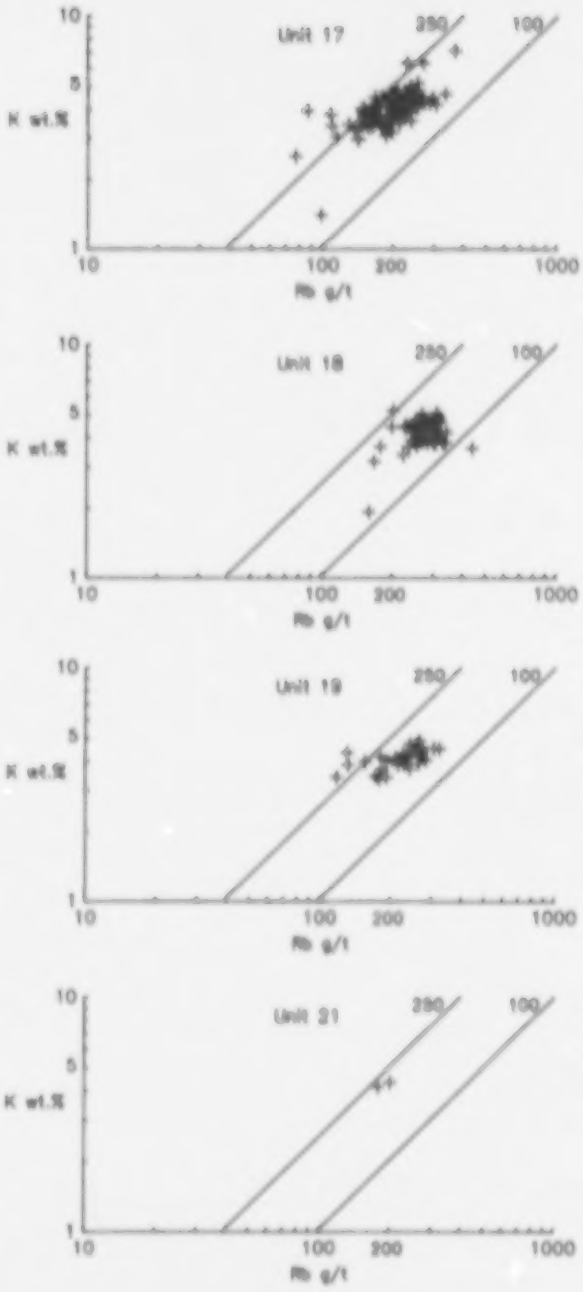

Figure 57. *Variation diagrams of $\log_{10}$ K (in weight percent) vs. $\log_{10}$ Rb (in g/t) for Unit 17, the Wolf Mountain Granite (Unit 18), and Units 19 and 21 of the North Bay Granite Suite.*

10, 14, 16 and 20 having a linear positive correlation of K with Rb. Unit 15 shows a negative correlation of K with Rb and K/Rb ratios decreasing to almost 100.

The plot of Na_2O+K_2O:total iron as FeO:MgO (Figure 71) shows that the Wolf Lake North Granodiorite and the

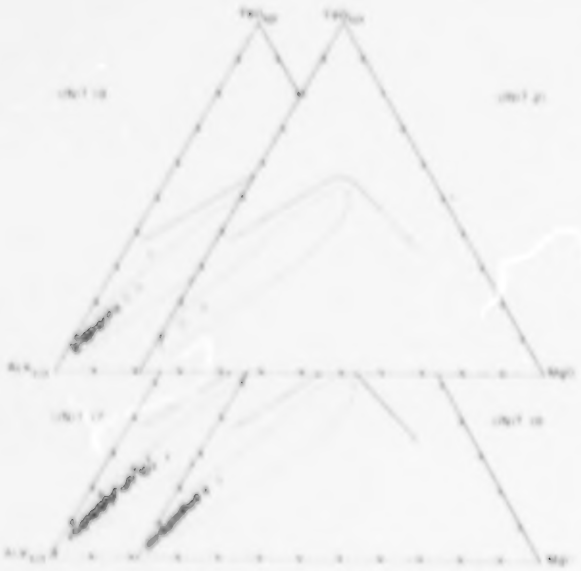

Figure 58. *Plot of $K_2O + Na_2O$ ($Alk_{wt.\%}$) Total iron as FeO ($FeO_{wt.\%}$):MgO (all weight percent) for Unit 17, and the Wolf Mountain Granite (Unit 18), and Units 19 and 21 of the North Bay Granite Suite. Curved line separates tholeiitic compositions (above) from calc-alkaline (below); from Irvine and Baragar (1971). Dashed line indicates field of calc-alkaline granitoids from part of the Coastal Batholith of Peru; from Atherton et al. (1979).*

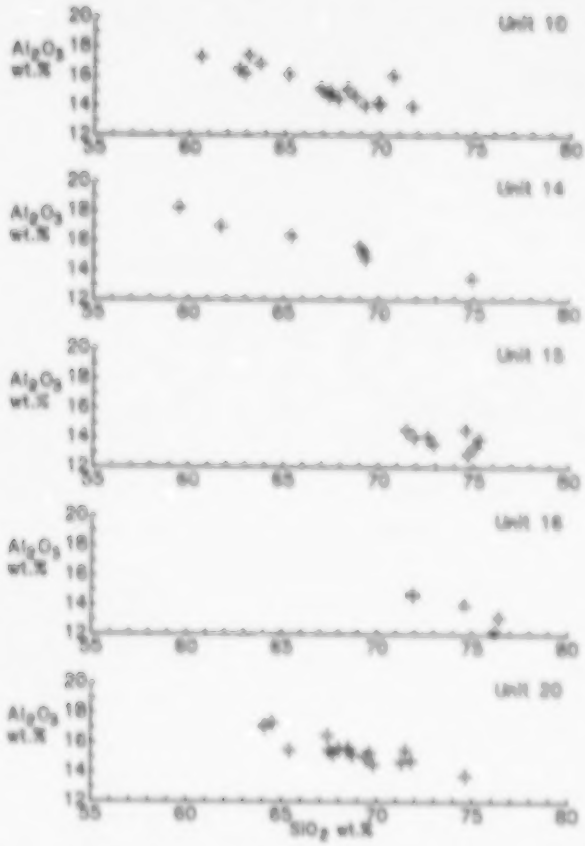

Figure 59. *Variation diagrams of Al_2O_3 vs. SiO_2 (both weight percent) for the Wolf Lake North Granodiorite (Unit 10), the Meelpaeg Lake Granite (Unit 14), Unit 15, the Wolf Lake Granite (Unit 16) and the Upper Salmon Road Granite (Unit 20) of the North Bay Granite Suite.*

Meelpaeg Lake Granite define calc-alkaline trends and occupy much of the calc-alkaline granitoid field. Unit 15, the Wolf Lake Granite and the Upper Salmon Road Granite occupy a small part of the field and do not define calc-alkaline trends.

From the various geochemical plots, the Wolf Lake North Granodiorite and the Meelpaeg Lake Granite are similar in many respects and are clearly unrelated to the adjacent Unit 15 and the Wolf Lake Granite. The Upper Salmon Road Granite, which is spatially separated from the other Units, shows some similarity to the Wolf Lake North Granodiorite and the Meelpaeg Lake Granite, but is distinctive in several aspects of chemistry and certainly in most petrographic features.

PETROGENESIS OF THE NORTH BAY GRANITE SUITE

Factors that must be considered in interpreting the source rocks and evolution of the various units of the North Bay Granite include the following:

1. Units 11 and 12 of Component 1 have been deformed with the Riches Island Formation. Units 10, 14, 15, 16 and 20 of Component 2 have been deformed with the Spruce Brook and Salmon River Dam formations. These syntectonic granitoid rocks and associated metasedimentary rocks were deformed during a regional D_3 orogenic event, clearly a period of higher heat flow, pressure and fluid mobility.

2. Units 8 and 9 (also Unit 13) are strongly deformed and occur along a major fault. Deformation may be related to late shearing and/or overthrusting of the Salmon River Dam Formation probably during the later stages of regional orogenesis. Thus, Units 8 and 9 are also syntectonic granitoid rocks.

3. Units 17 (the Wolf Mountain Granite) and 19 of Component 1 contain either a weak fabric or are massive. Xenoliths of schistose metasedimentary rock are common along the contact of these units with the Bay du Nord Group. These essentially posttectonic granitoid rocks have been dated at 396 Ma.

4. Units 11 and 12 contain ubiquitous xenoliths of migmatitic metasedimentary rock probably derived from the Baie d'Espoir Group. The intrusive relationship of Units 11 and 12 with the metasedimentary rocks indicates that either the granite has formed an extremely wide intrusive breccia zone (as indicated by Blackwood, 1985) or there was incomplete separation of the magma from the parent partially melted

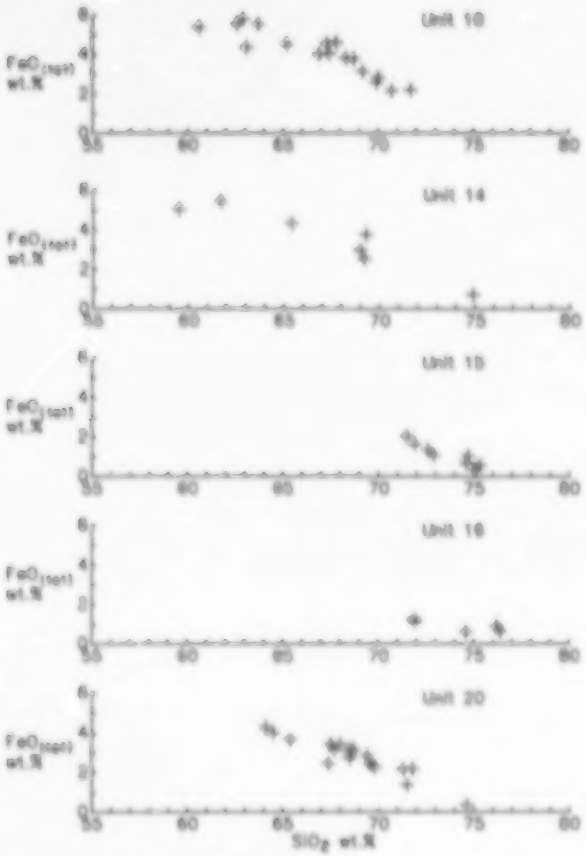

Figure 60. *Variation diagrams of total iron as FeO (FeO_{tot}) vs. SiO_2 (both weight percent) for the Wolf Lake North Granodiorite (Unit 10), the Meelpaeg Lake Granite (Unit 14), Unit 15, the Wolf Lake Granite (Unit 16), and the Upper Salmon Road Granite (Unit 20) of the North Bay Granite Suite.*

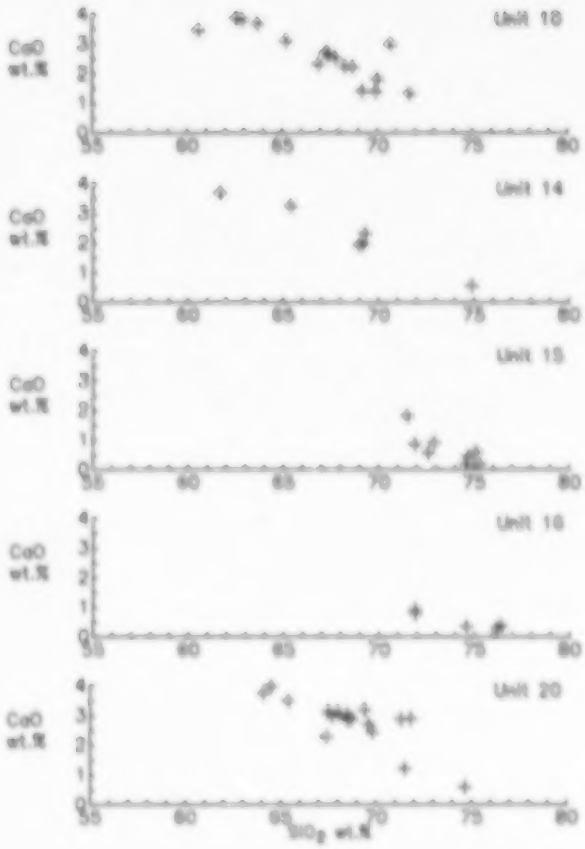

Figure 61. *Variation diagrams of CaO vs. SiO_2 (both weight percent) for the Wolf Lake North Granodiorite (Unit 10), the Meelpaeg Lake Granite (Unit 14), Unit 15, the Wolf Lake Granite (Unit 16) and the Upper Salmon Road Granite (Unit 20) of the North Bay Granite Suite.*

metasedimentary and metavolcanic rocks. The chaotic Sr isotopic compositions obtained by Fryer (1983; see Radiometric Dating Section) and the scatter shown in plots of Sr vs. SiO_2 (Figure 41) may reflect this incomplete magma separation with resultant inhomogeneous magma.

5. The common occurrence of coarse muscovite in Units 10 and 15, and the presence of muscovite–garnet assemblages in Units 9, 16 and parts of Unit 19 suggest that these granites are peraluminous (e.g., Clarke, 1981). The ratio of $Al_2O_3/(CaO+Na_2O+K_2O)$, in molecular weight percent, (A/CNK) is also used to determine if a rock is peraluminous. Similarly, corundum normative granites are peraluminous (although care must be taken when there is the possibility of alkali loss and therefore a relatively high proportion of alumina). Mean values of A/CNK are listed in Table 19 and the distribution of ratios for the sample population are shown on Figure 72, a and b. The A/CNK and normative corundum values indicate that all the units are peraluminous although some have distinctly higher values.

6. The A/CNK ratios are used to divide the various units into two groups, namely the I-type (igneous source) and S-type (sedimentary source) granitoid rocks of Chappell and White (1974). Units 8, 9, 15 and 16, which have the highest A/CNK ratios (over 1.10) and normative corundum values over 1 percent, can be equated with the S-type granites and the remaining units with I-type granites as originally defined by Chappell and White (1974). A-type (alkaline affinity) granites (Loiselle and Wones, 1979; White, 1979), which appear to be related to I-type granites (Tuach *et al.*, 1986), are characterized by a positive correlation of 'high-field-strength' elements, such as Zr, Y, and Nb, with SiO_2. However, these geochemical features are taken from peralkaline intrusives. From Figure 31, it can be seen that mean Zr shows a general negative correlation with SiO_2. Sodium oxide vs. K_2O distributions have been used by White and Chappell (1983) to indicate the fields of I-, S- and A-type granitoid rocks. Figure 73 shows how the distribution of Na_2O vs. K_2O compares to those of the White and Chappell (1983) for southeastern Australian granitoid rocks.

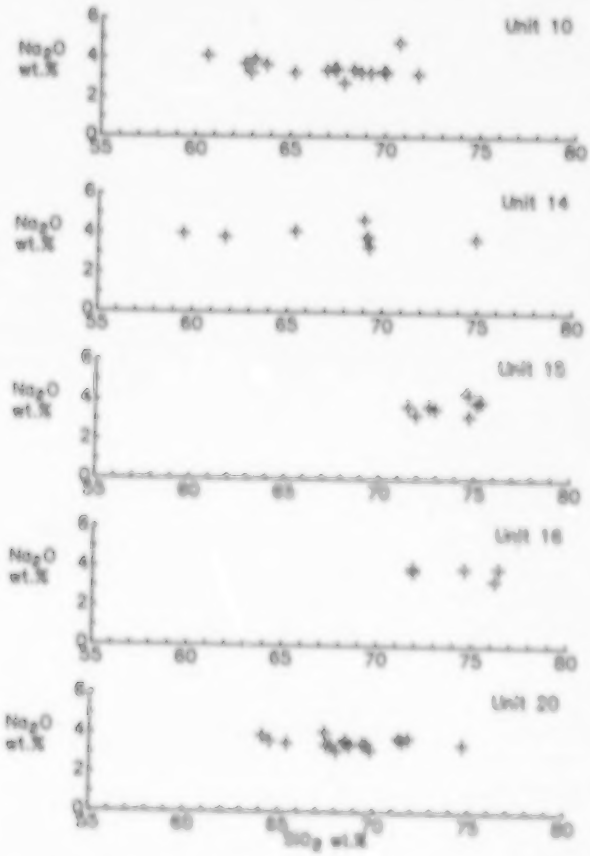

Figure 62. *Variation diagrams of Na_2O vs. SiO_2 (both weight percent) for the Wolf Lake North Granodiorite (Unit 10), the Meelpaeg Lake Granite (Unit 14), Unit 15, the Wolf Lake Granite (Unit 16) and the Upper Salmon Road Granite (Unit 20) of the North Bay Granite Suite.*

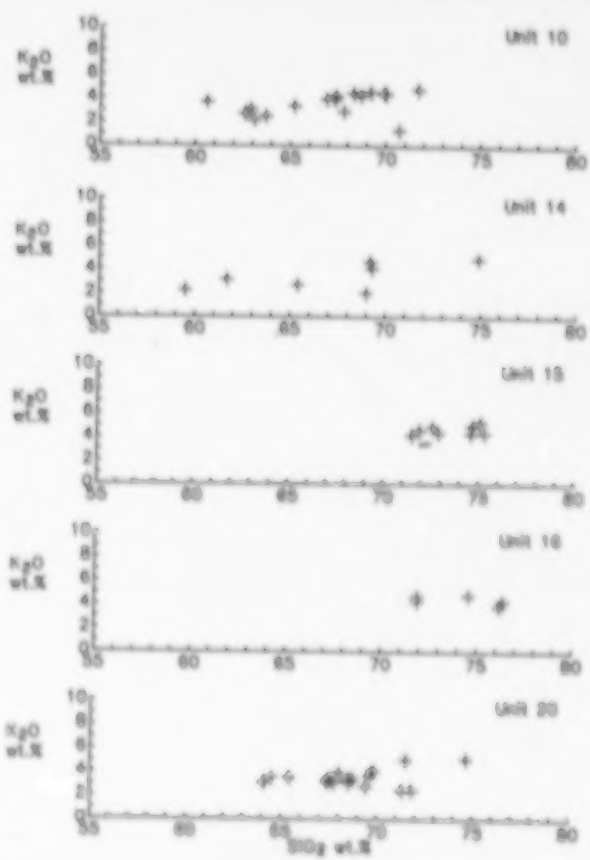

Figure 63. *Variation diagrams of K_2O vs. SiO_2 (both weight percent) for the Wolf Lake North Granodiorite (Unit 10), the Meelpaeg Lake Granite (Unit 14), Unit 15, the Wolf Lake Granite (Unit 16) and the Upper Salmon Road Granite (Unit 20) of the North Bay Granite Suite.*

An obvious feature of these plots is that only two analyses (from Unit 11) fall in the field of S-type granites (although with the overlap of I- and S-type granites one of these analyses may be I-type). The majority of the analyses from Component 1 fall in the A-type field with numerous analyses lying above the I- and A-type fields. Units 8, 9, 11, 12, 15, 16 and 19, which are the muscovite–garnet granites, lie in the A-type field with the generally more mafic granitoid rocks of Units 10, 14 and 20 lying mainly within the I-type granite field.

A possible problem with using chemical characteristics of rock types in one area is that the rock chemistry may be different from similar rocks in other regions. Thus, the low sodium content of S-type granites of Chappell and White (1974) appears to be atypical of partial melts of metasedimentary rocks. Currie and Pajari (1981), Strong and Hanmer (1981) and Anderson and Rowley (1981) listed analyses of peraluminous (S-type) granites from different tectonic regimes. These granites are significantly enriched in Na_2O (> 3.5 percent) compared to the typical values of < 3.2 percent Na_2O of Chappell and White (1974).

7. Units 10, 14 and 20, which lie within the I-type field, also display linear variations on AFM diagrams (Figure 71) indicative of calc-alkaline magmatism. Unit 11 also shows calc-alkaline affinities on an AFM diagram (Figure 45) although it lies outside the field of I-type granites of White and Chappell (1983; Figure 73). This apparent deviation can be explained, as above, by the restricted database of White and Chappell (1983). Calc-alkaline suites typically display linear chemical variations that extend from basic to acidic compositions. Only Units 10, 14 and 20 have low silica values that can be termed intermediate.

The only mafic rocks are isolated dioritic xenoliths associated with Unit 11, which may be unrelated, but may also be an early differentiate or part of an early intrusion that induced partial melting of the Baie d'Espoir Group. Colman-Sadd (1984) has shown that a sizable body of gabbro has intruded several foliated granitoid rocks and the Ordovician sedimentary and volcanic units in the Cold Spring Pond map area, to the north of D'Espoir Lake. The granitoid units would form part of Component 2 of the North Bay Granite suite.

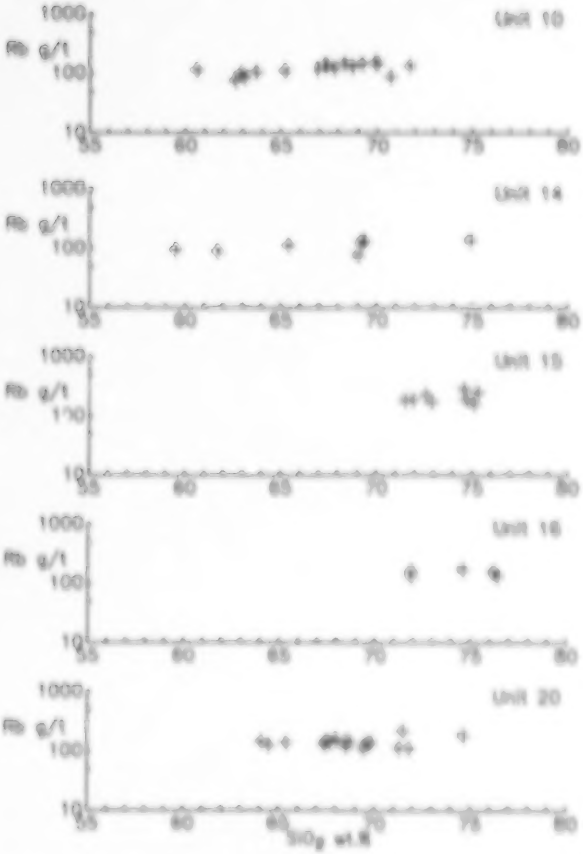

Figure 64. *Variation diagrams of $\log_{10}$ Rb (in g/t) vs. SiO_2 (in weight percent) for the Wolf Lake North Granodiorite (Unit 10), the Meelpaeg Lake Granite (Unit 14), Unit 15, the Wolf Lake Granite (Unit 16), and the Upper Salmon Road Granite (Unit 20) of the North Bay Granite Suite.*

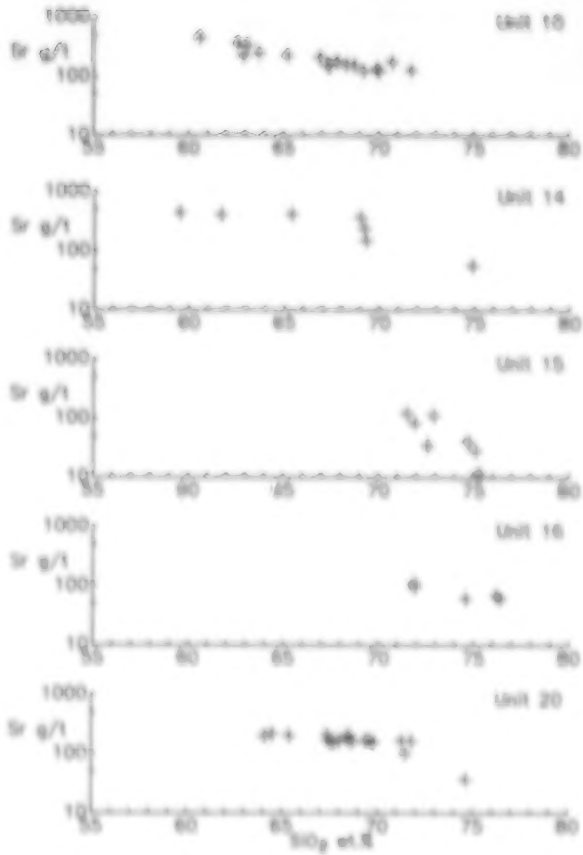

Figure 65. *Variation diagrams of $\log_{10}$ Sr (in g/t) vs. SiO_2 (in weight percent) for the Wolf Lake North Granodiorite (Unit 10), the Meelpaeg Lake Granite (Unit 14), Unit 15, the Wolf Lake Granite (Unit 16), and the Upper Salmon Road Granite (Unit 20) of the North Bay Granite Suite.*

The gabbro may be a late phase of the syn- to late tectonic calc-alkaline suite defined by Units 10 and 14. The North Bay Granite Suite is acidic with average SiO_2 contents in excess of 70 percent although some units vary toward 65 percent SiO_2. Such restricted compositions indicate that fractionation of these magmas from basic or intermediate parent magmas is an unlikely source.

8. Most units contain granitic pegmatites that commonly contain muscovite. In particular, Units 9 and 16 contain abundant pegmatite and quartz veins. These indicate that the magmas contained a significant proportion of water during late-stage crystallization. Similarly, it may be argued that the primary magma was formed from sedimentary rocks and the magmas are close to minimum melts that have undergone little differentiation and are close to their source rocks. A plot of normative quartz (Q):albite (ab):orthoclase (or) for Units 9 and 16 indicates a trend from the cotectic at 5 kb toward the ternary minimum at 3 kb (Figure 74). This trend is virtually identical to that obtained from similar rocks, located in a similar structural position in northeastern Newfoundland, and described by Currie and Pajari (1981). They proposed that the peraluminous granites studied were formed by partial melting of the deeper parts of the host Middle Ordovician Davidsville Group pelites. The highest grade metamorphism of the Davidsville Group occurs around the plutons indicated by the development of andalusite–K-feldspar–quartz–muscovite assemblages and locally developed pods of granite.

9. Units 9, 15 and 16 of the North Bay Granite Suite intruded parts of the high-grade metamorphic rocks of the Spruce Brook Formation, north of Wolf Lake. Here the metasedimentary rocks contain andalusite and sillimanite (subunit 2a) and, to the east, the formation has been extensively migmatized. In the D'Espoir Lake area, Unit 9 has intruded the Salmon River Dam Formation but the grade of metamorphism is low. However, migmatitic xenoliths that have been correlated with other parts of the Baie d'Espoir Group occur in parts of Unit 9 and may be a restite phase following partial melting.

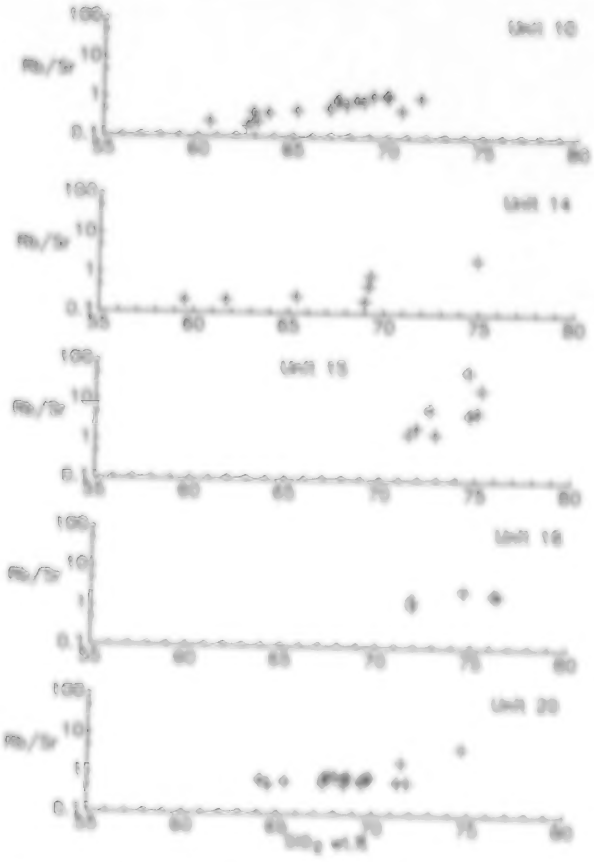

Figure 66. *Variation diagrams of $\log_{10}$ Rb/Sr (in g/t) vs. SiO_2 (in weight percent) for the Wolf Lake North Granodiorite (Unit 10), the Meelpaeg Lake Granite (Unit 14), Unit 15, the Wolf Lake Granite (Unit 16), and the Upper Salmon Road Granite (Unit 20) of the North Bay Granite Suite.*

10. Garnet is a prominent accessory mineral in the biotite granite of Unit 19 northeast of North Bay. The garnet crystals, which occur as two-size populations, are generally fresh with minor alteration of the larger garnets (over 5 mm) restricted to fractures. This indicates that all the garnets are igneous. The presence of two-size populations indicates two periods of garnet crystallization. Microprobe analyses of these garnets has not been carried out to determine their composition. Abbott (1981) indicated a possible system for crystallizing two garnet phases. If garnet and biotite are crystallizing together, an increase of the MnO/(FeO+MgO+MnO) ratio will lead to the crystallizing of garnet alone.

11. Units 17, 18 and 19 have geochemical compositions that show little variation, indicating limited fractional crystallization. When the large area of these units is considered, a process of widespread partial melting must have taken place. The narrow, contact metamorphic aureoles, generally low-grade metamorphism of the country rocks, and the sharp intrusive contacts, indicate that the exposed country rocks were not the source rocks for the granitic magmas. The very limited occurrence of pegmatites indicates limited water

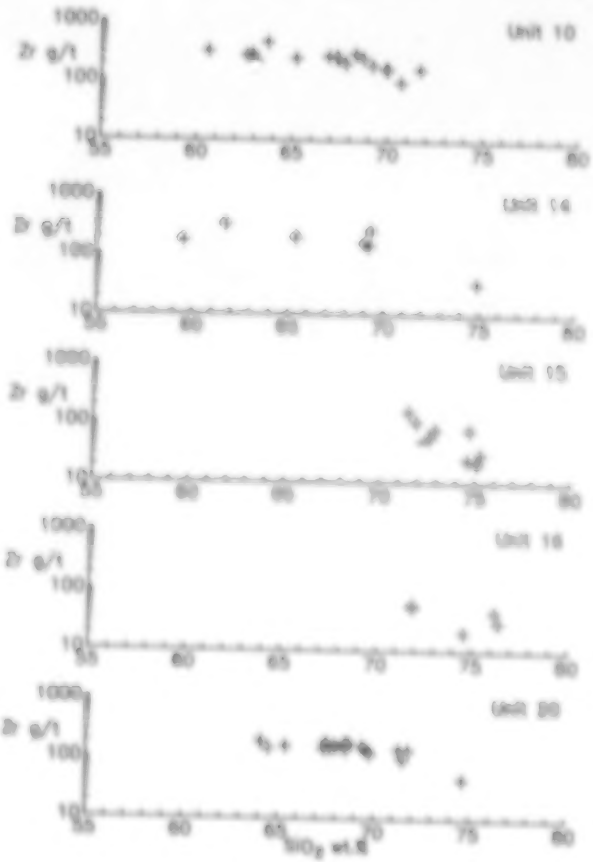

Figure 67. *Variation diagrams of $\log_{10}$ XZr (in g/t) vs. SiO_2 (in weight percent) for the Wolf Lake North Granodiorite (Unit 10), the Meelpaeg Lake Granite (Unit 14), Unit 15, the Wolf Lake Granite (Unit 16), and the Upper Salmon Road Granite (Unit 20) of the North Bay Granite Suite.*

in the residual liquids and therefore, much drier conditions during melting of the source rocks. The source was probably the mid-crust as either more mafic compositions or possibly peralkaline magmas would be expected from the lower crust (e.g., Wyllie *et al.*, 1976). Melting was probably induced by crustal thickening during the Acadian Orogeny with crystallization at 396 Ma.

12. Units 10 and 14, which are the most mafic granodiorites in the North Bay Granite Suite, must have been derived from a source at least as mafic as the granodiorites in these units. Such relatively mafic intrusives may have been derived from partially melted lower crust and fractionally crystallized. Such an origin has been suggested for the more mafic granitoid rocks of the Sierra Nevada Batholith (Presnall and Bateman, 1973). This process requires a heat source to induce melting, and underplating of the lower crust by melts derived from a subducting lithospheric plate has been proposed (e.g., Presnall and Bateman, 1973). Atherton and Sanderson (1985) proposed that the upper mantle and subducting oceanic crust could also be the initial source of granodiorite.

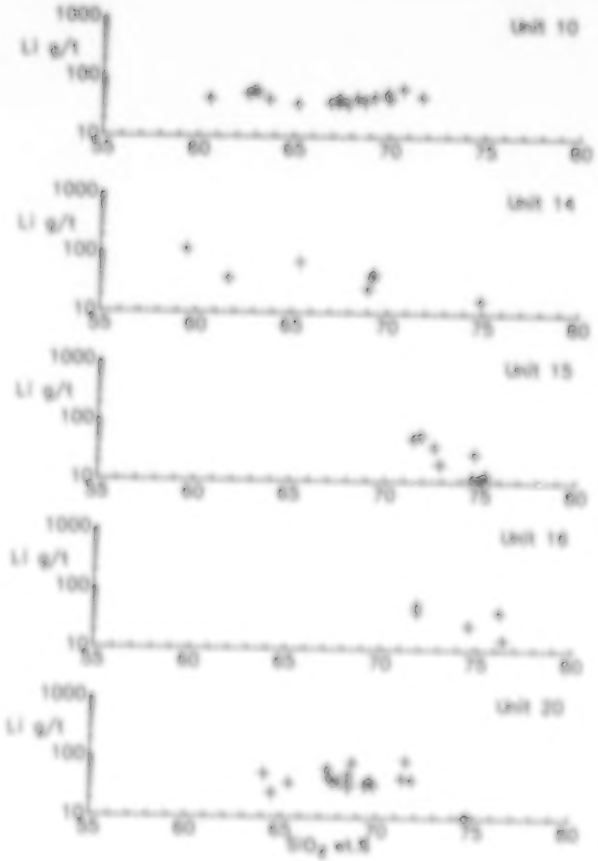

Figure 68. *Variation diagrams of $\log_{10}$ Li (in g/t) vs. SiO_2 (in weight percent) for the Wolf Lake North Granodiorite (Unit 8), the Mewipsey Lake Granite (Unit 14), Unit 15, the Wolf Lake Granite (Unit 16), and the Upper Salmon Road Granite (Unit 20) of the North Bay Granite Suite.*

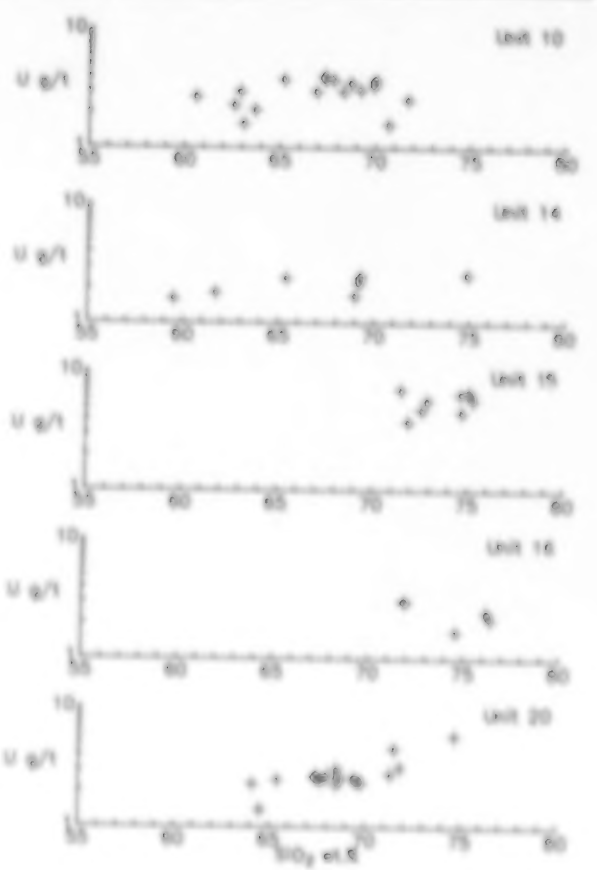

Figure 69. *Variation diagrams of $\log_{10}$ U (in g/t) vs. SiO_2 (in weight percent) for the Wolf Lake North Granodiorite (Unit 8), the Mewipsey Lake Granite (Unit 14), Unit 15, the Wolf Lake Granite (Unit 16), and the Upper Salmon Road Granite (Unit 20) of the North Bay Granite Suite.*

13. Pearce *et al.* (1984) proposed that certain trace elements and SiO_2 can be used to discriminate granites (i.e., quartz diorites to granite of Streckeisen, 1976) formed in different tectonic settings. These are defined as ocean-ridge granites (ORG), volcanic-arc granites (VAG), collisional granites (COLG), and within-plate granites (WPG). Boundaries between the various tectonic settings are defined using various plots of Rb, Y, Nb, Ta, Yb and SiO_2 from analyses of granites from well-defined tectonic settings. Figure 75 shows the empirical boundaries between the tectonic settings using Rb vs. Y+Nb values for the type examples (from Pearce *et al.*, 1984). Plots of the other trace elements noted above support the main conclusion of Pearce *et al.* (1984) that certain trace elements can be used to define the tectonic setting of granites. Silicon dioxide variation in COLG granites is mainly confined to a range of 73 to 76 percent, whereas in the other groups there is a spectrum from 56 to 77 percent SiO_2.

Collisional granites can be divided into syn- and postectonic varieties. The synectonic, collisional granites (syn-COLG) are typically peraluminous, containing muscovite. The post-collisional (post-COLG) typically are biotite granites, which may contain hornblende and show calc-alkaline trends and lie below the syn-COLG boundary in the VAG field (Pearce *et al.*, 1984).

The granites of the North Bay Granite Suite form a significant component of a Siluro-Devonian orogen, commonly termed the Acadian but recently interpreted to be part of the Salinic Orogeny (possibly equivalent to the Caledonian Orogeny; Dunning *et al.*, 1988, 1990), the result of the collision of continental blocks during closure of the Iapetus Ocean (Colman-Sadd, 1982; Williams, 1984). Colman-Sadd (1982) has also postulated that following collision during the Ordovician, subduction-related magmatism may have been renewed during the Siluro-Devonian with the resulting magma production and intrusion of granitic magmas. The North Bay Granite Suite should fall in the COLG field but if there is some mantle input from subduction-related magmatism, then a portion of the suite may fall in the VAG field. Harker diagrams for each unit of the North Bay Granite Suite indicate that the majority of the

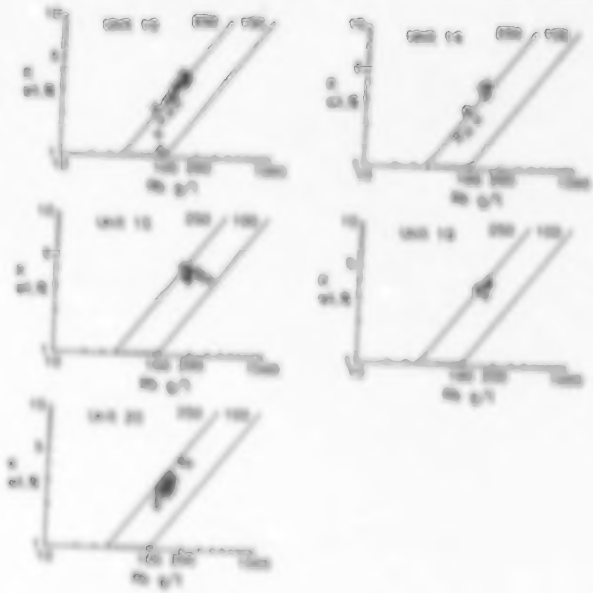

Figure 70. *Variation diagrams of $\log_{10}$ K (in weight percent) vs. $\log_{10}$ Rb (in ppm) for the Wolf Lake North Granodiorite (Unit 8), the Mewipsaig Lake Granite (Unit 14), Unit 15, the Wolf Lake Granite (Unit 16), and the Upper Salmon Road Granite (Unit 20) of the North Bay Granite Suite.*

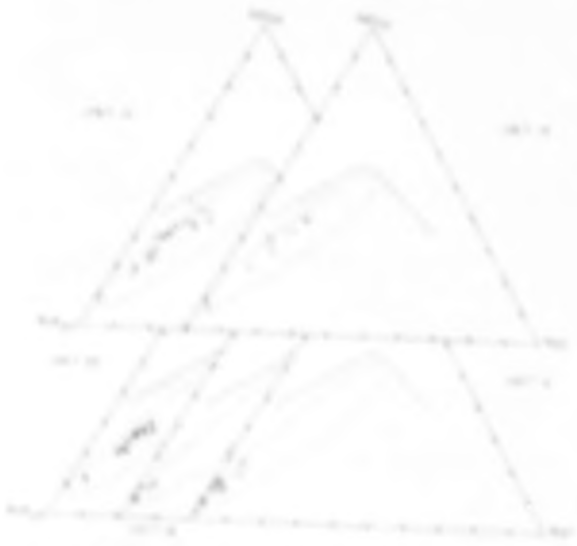

Figure 71. *Plot of $K_2O + Na_2O$ (Alk$_{wt}$) Total iron as FeO (FeO$_{wt}$) MgO (all weight percent) for the Wolf Lake North Granodiorite (Unit 8), the Mewipsaig Lake Granite (Unit 14), Unit 15, the Wolf Lake Granite (Unit 16), and the Upper Salmon Road Granite (Unit 20) of the North Bay Granite Suite. Curved line separates tholeiitic compositions (above) from calc-alkaline (below); from Irvine and Baragar (1971). Dashed line indicates field of calc-alkaline granitoids from part of the Coastal Batholith of Peru; from Atherton et al. (1979).*

Table 19. *Mean of A/CNK [molecular weight $Al_2O_3/(CaO+Na_2O+K_2O)$] and COR (normative corundum in weight percent) for each unit of Components 1 and 2 of the North Bay Granite Suite*

a. Component 1

Unit	A/CNK	min.	max.	COR	min.	max
8	1.15	1.04	1.58	2.48	1.17	3.63
9	1.12	1.00	1.22	2.00	0.16	3.53
11	1.08	0.95	1.50	1.42	0.00	5.05
12	1.05	0.98	1.18	1.02	0.22	2.33
17	1.04	0.96	1.14	0.90	0.00	2.24
18	1.07	1.00	1.26	1.34	0.00	3.03
19	1.06	0.99	1.16	1.19	0.01	2.28
21	1.04	1.02	1.05	0.72	0.40	1.03

b. Component 2

Unit	A/CNK	min.	max.	COR	min.	max
10	1.06	0.98	1.18	1.41	0.35	2.49
14	1.06	1.01	1.16	1.35	0.71	2.45
15	1.23	1.01	2.12	1.93	0.27	4.31
16	1.14	1.11	1.19	1.96	1.40	2.27
20	1.05	0.97	1.13	1.11	0.10	2.64

units show silica ranges similar to that for the syn-COLG granites of Pearce *et al.* (1984).

Plots of Rb vs. Y+Nb for each unit of the North Bay Granite Suite are shown in Figure 75. The clearly peraluminous, possibly crust-derived and syntectonic D'Espoir Brook Granite (Unit 9) should lie within the syn-COLG granite field but only a few of the samples plot in this field. Similarly, the other syntectonic granites (*i.e.*) such as the East Bay and Bottom Brook granites (Units 11 and 12), which commonly contain muscovite and garnetiferous pegmatites, also lie along and below this boundary. This may indicate that the boundary between the VAG and syn-COLG granites is too high in terms of Rb.

The syntectonic Wolf Lake North Granodiorite (Unit 8) and Upper Salmon Road Granite (Unit 20), which are generally lower in SiO_2 than the other units, lie entirely within the VAG field and show a calc-alkaline trend. This may indicate that these units contain a mantle component and provide some support for the Colman-Sadd (1982) model. The posttectonic granitoid rocks (mainly Units 17 to 19) also lie mainly in the VAG field. This feature, according to Pearce *et al.* (1984), can be explained only by mixing crustal and mantle components. There is insufficient evidence from the North Bay Granite Suite for a mantle component. Mafic xenoliths occur only rarely. Initial Sr ratios of 0.7053 and 0.7066 (Elias, 1981) may indicate that these relatively low values are the result of mixing crustal and mantle components.

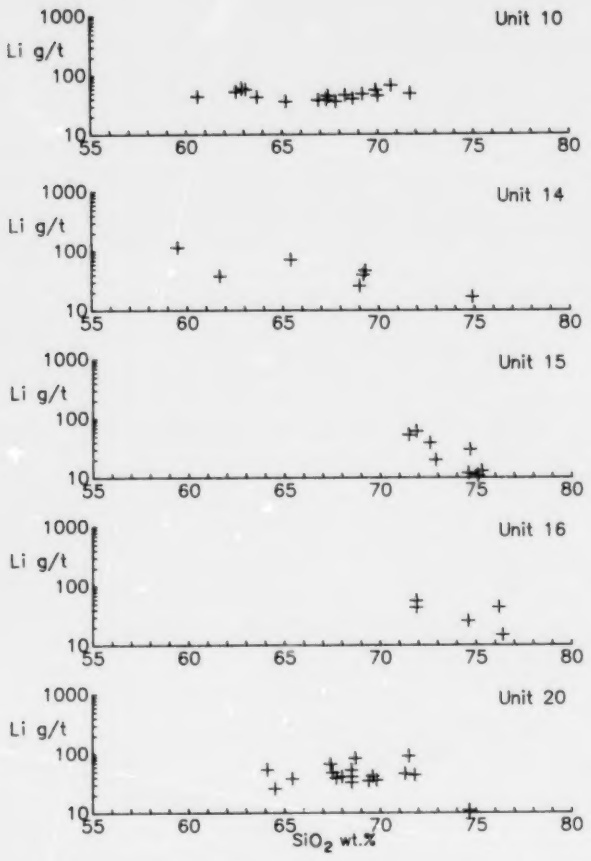

Figure 68. *Variation diagrams of log_{10} Li (in g/t) vs. SiO_2 (in weight percent) for the Wolf Lake North Granodiorite (Unit 10), the Meelpaeg Lake Granite (Unit 14), Unit 15, the Wolf Lake Granite (Unit 16), and the Upper Salmon Road Granite (Unit 20) of the North Bay Granite Suite.*

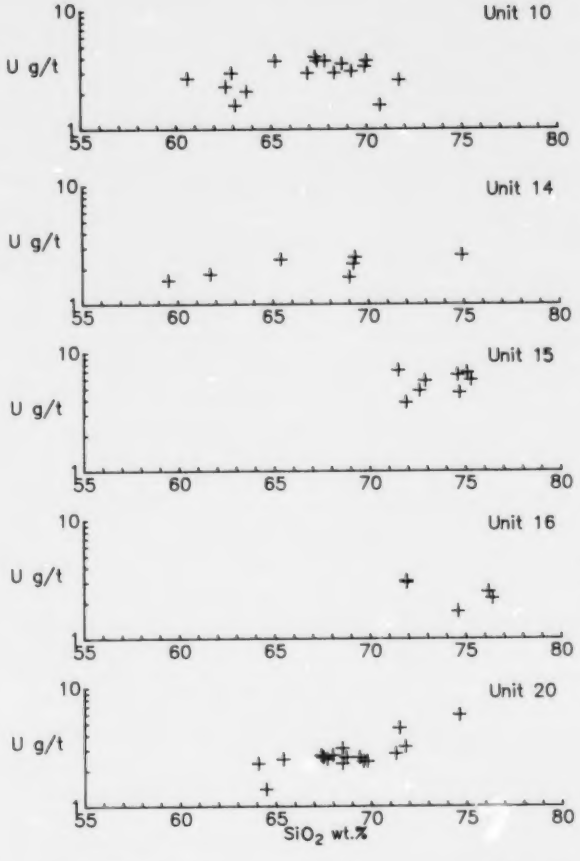

Figure 69. *Variation diagrams of log_{10} U (in g/t) vs. SiO_2 (in weight percent) for the Wolf Lake North Granodiorite (Unit 10), the Meelpaeg Lake Granite (Unit 14), Unit 15, the Wolf Lake Granite (Unit 16), and the Upper Salmon Road Granite (Unit 20) of the North Bay Granite Suite.*

13. Pearce *et al.* (1984) proposed that certain trace elements and SiO_2 can be used to discriminate granites (i.e., quartz diorites to granite of Streckeisen, 1976) formed in different tectonic settings. These are defined as ocean-ridge granites (ORG), volcanic-arc granites (VAG), collisional granites (COLG), and within-plate granites (WPG). Boundaries between the various tectonic settings are defined using various plots of Rb, Y, Nb, Ta, Yb and SiO_2 from analyses of granites from well-defined tectonic settings. Figure 75 shows the empirical boundaries between the tectonic settings using Rb vs. Y+Nb values for the type examples (from Pearce *et al.*, 1984). Plots of the other trace elements noted above support the main conclusion of Pearce *et al.* (1984) that certain trace elements can be used to define the tectonic setting of granites. Silicon dioxide variation in COLG granites is mainly confined to a range of 70 to 76 percent, whereas in the other groups there is a spectrum from 56 to 77 percent SiO_2.

Collisional granites can be divided into syn- and posttectonic varieties. The syntectonic, collisional granites (syn-COLG) are typically peraluminous, containing muscovite. The post-collisional (post-COLG) typically are biotite granites, which may contain hornblende and show calc-alkaline trends and lie below the syn-COLG boundary in the VAG field (Pearce *et al.*, 1984).

The granites of the North Bay Granite Suite form a significant component of a Siluro-Devonian orogen, commonly termed the Acadian but recently interpreted to be part of the Salinic Orogeny (possibly equivalent to the Caledonian Orogeny; Dunning *et al.*, 1988, 1990), the result of the collision of continental blocks during closure of the Iapetus Ocean (Colman-Sadd, 1982; Williams, 1984). Colman-Sadd (1982) has also postulated that following collision during the Ordovician, subduction-related magmatism may have been renewed during the Siluro-Devonian with the resulting magma production and intrusion of granitic magmas. The North Bay Granite Suite should fall in the COLG field but if there is some mantle input from subduction-related magmatism, then a portion of the suite may fall in the VAG field. Harker diagrams for each unit of the North Bay Granite Suite indicate that the majority of the

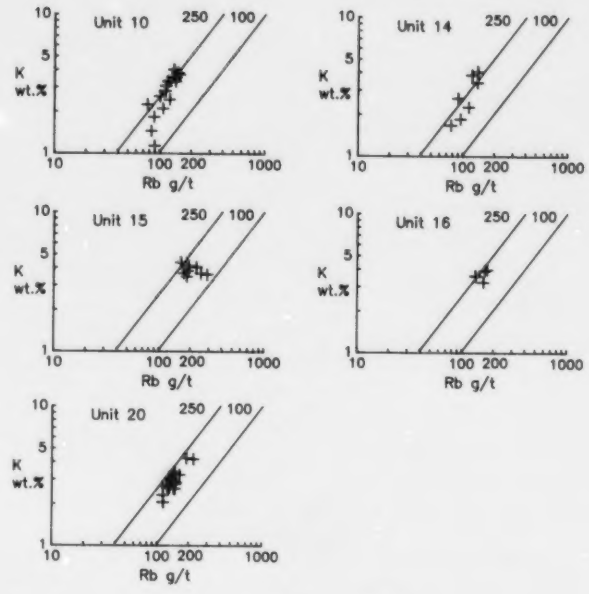

Figure 70. *Variation diagrams of $\log_{10}$ K (in weight percent) vs. $\log_{10}$ (in g/t) for the Wolf Lake North Granodiorite (Unit 10), the Meelpaeg Lake Granite (Unit 14), Unit 15, the Wolf Lake Granite (Unit 16), and the Upper Salmon Road Granite (Unit 20) of the North Bay Granite Suite.*

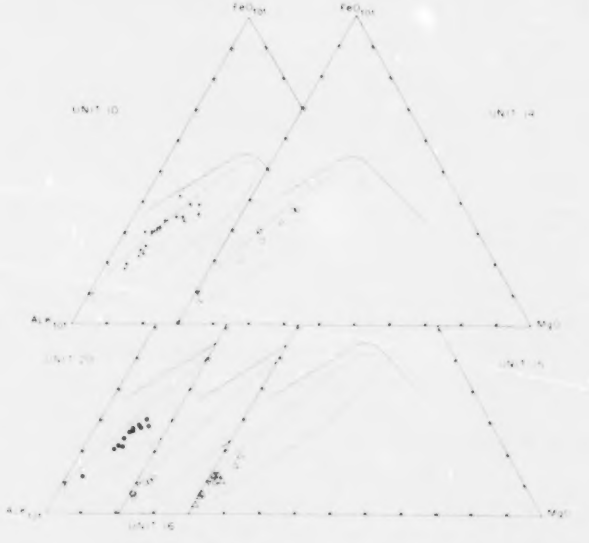

Figure 71. *Plot of K_2O + Na_2O (Alk_{tot}):Total iron as FeO (FeO_{tot}):MgO (all weight percent) for the Wolf Lake North Granodiorite (Unit 10), the Meelpaeg Lake Granite (Unit 14), Unit 15, the Wolf Lake Granite (Unit 16), and the Upper Salmon Road Granite (Unit 20) of the North Bay Granite Suite. Curved line separates tholeiitic compositions (above) from calc-alkaline (below); from Irvine and Barager (1971). Dashed line indicates field of calc-alkaline granitoids from part of the Coastal Batholith of Peru; from Atherton et al. (1979).*

Table 19. Mean of A/CNK [molecular weight $Al_2O_3/(CaO+Na_2O+K_2O)$] and COR (normative corundum in weight percent) for each unit of Components 1 and 2 of the North Bay Granite Suite

a. Component 1

Unit	A/CNK	min.	max.	COR	min.	max
8	1.15	1.04	1.28	2.48	1.17	3.63
9	1.12	1.00	1.22	2.00	0.16	3.53
11	1.08	0.95	1.50	1.42	0.00	5.05
12	1.05	0.98	1.18	1.02	0.22	2.33
17	1.04	0.96	1.14	0.90	0.00	2.24
18	1.07	1.00	1.26	1.34	0.00	3.03
19	1.06	0.99	1.16	1.19	0.01	2.28
21	1.04	1.02	1.05	0.72	0.40	1.03

b. Component 2

Unit	A/CNK	min.	max.	COR	min.	max
10	1.06	0.98	1.18	1.41	0.35	2.49
14	1.06	1.01	1.16	1.35	0.71	2.45
15	1.23	1.01	2.12	1.93	0.27	4.31
16	1.14	1.11	1.19	1.96	1.40	2.27
20	1.05	0.97	1.15	1.11	0.10	2.64

units show silica ranges similar to that for the syn-COLG granites of Pearce *et al.* (1984).

Plots of Rb vs. Y+Nb for each unit of the North Bay Granite Suite are shown in Figure 75. The clearly peraluminous, possibly crust-derived and syntectonic D'Espoir Brook Granite (Unit 9) should lie within the syn-COLG granite field but only a few of the samples plot in this field. Similarly, the other syntectonic granites *(s.s.)* such as the East Bay and Bottom Brook granites (Units 11 and 12), which commonly contain muscovite and garnetiferous pegmatites, also lie along and below this boundary. This may indicate that the boundary between the VAG and syn-COLG granites is too high in terms of Rb.

The syntectonic Wolf Lake North Granodiorite (Unit 10) and Upper Salmon Road Granite (Unit 20), which are generally lower in SiO_2 than the other units, lie entirely within the VAG field and show a calc-alkaline trend. This may indicate that these units contain a mantle component and provide some support for the Colman-Sadd (1982) model. The posttectonic granitoid rocks (mainly Units 17 to 19) also lie mainly in the VAG field. This feature, according to Pearce *et al.* (1984), can be explained only by mixing crustal and mantle components. There is insufficient evidence from the North Bay Granite Suite for a mantle component. Mafic xenoliths occur only rarely. Initial Sr ratios of 0.7053 and 0.7066 (Elias, 1981) may indicate that these relatively low values are the result of mixing crustal and mantle components.

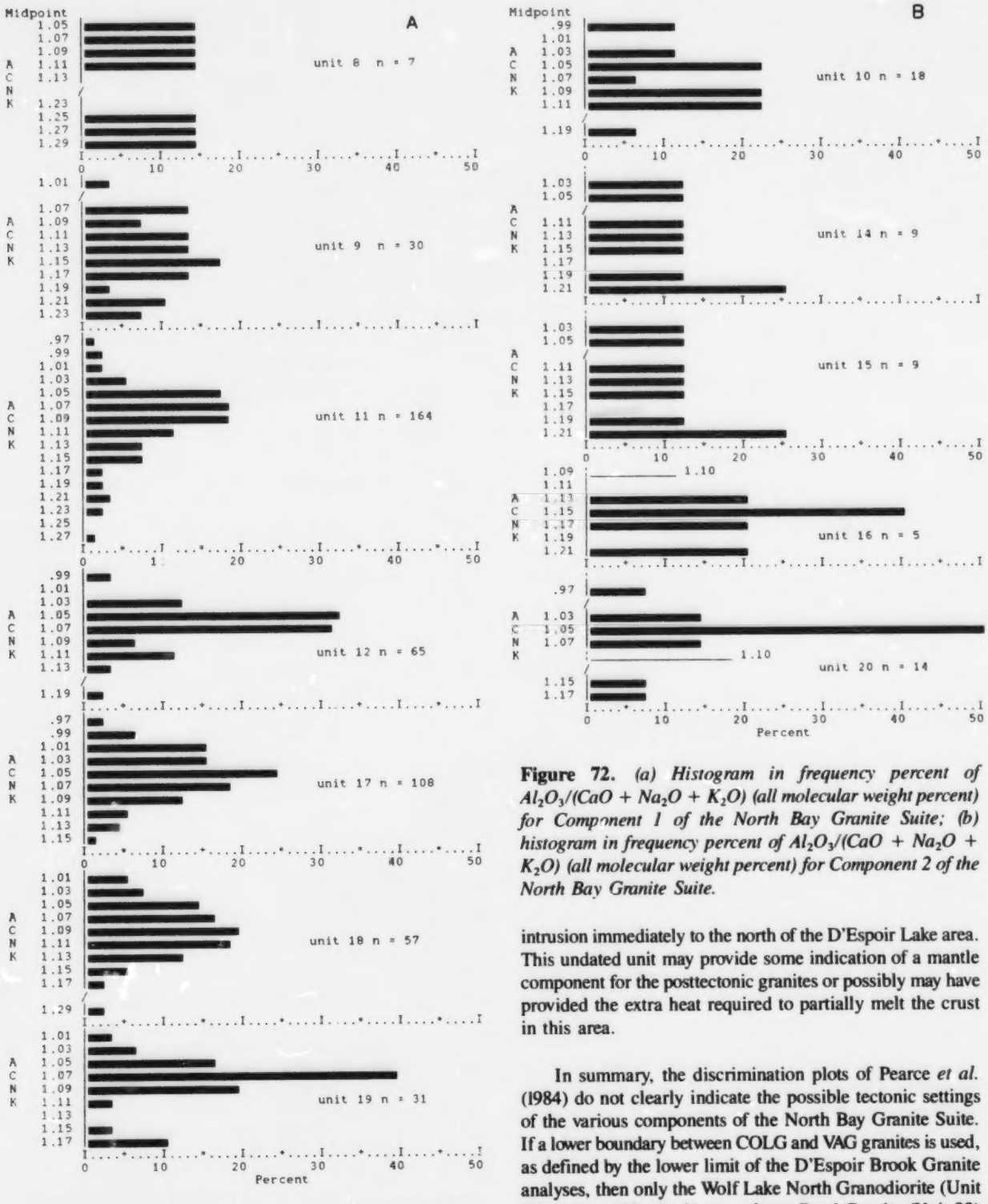
A
B
Midpoint
unit 8 n = 7
unit 9 n = 30
unit 11 n = 164
unit 12 n = 65
unit 17 n = 108
unit 18 n = 57
unit 19 n = 31
unit 10 n = 18
unit 14 n = 9
unit 15 n = 9
unit 16 n = 5
unit 20 n = 14
Percent

Figure 72. *(a) Histogram in frequency percent of $Al_2O_3/(CaO + Na_2O + K_2O)$ (all molecular weight percent) for Component 1 of the North Bay Granite Suite; (b) histogram in frequency percent of $Al_2O_3/(CaO + Na_2O + K_2O)$ (all molecular weight percent) for Component 2 of the North Bay Granite Suite.*

However, the values obtained by Fryer (1983; see New Rb–Sr Age Determinations Section) cast some doubt on the usefulness of Sr isotopes in this part of the North Bay Granite Suite. Colman-Sadd (1984) has described a massive gabbro intrusion immediately to the north of the D'Espoir Lake area. This undated unit may provide some indication of a mantle component for the posttectonic granites or possibly may have provided the extra heat required to partially melt the crust in this area.

In summary, the discrimination plots of Pearce *et al.* (1984) do not clearly indicate the possible tectonic settings of the various components of the North Bay Granite Suite. If a lower boundary between COLG and VAG granites is used, as defined by the lower limit of the D'Espoir Brook Granite analyses, then only the Wolf Lake North Granodiorite (Unit 10) and possibly the Upper salmon Road Granite (Unit 20) would not be classified as collisional granites. This would then require a volcanic arc origin for these units with little involvement of continental crust.

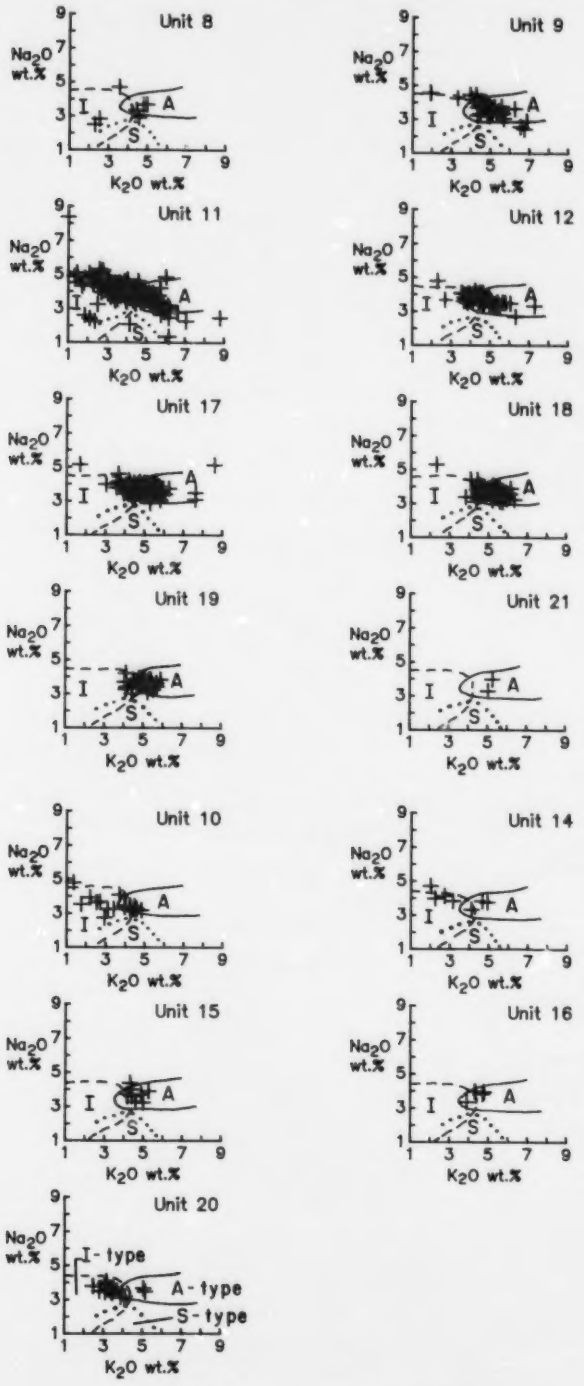

Figure 73. *Variation diagrams of Na_2O vs. K_2O (both weight percent) for east unit of the North Bay Granite Suite. Fields of I-, S- and A-type granites based on data graphically represented in White and Chappell (1983).*

The Wolf Lake North Granodiorite has intruded the continental-derived metasedimentary rocks of the Spruce Brook Formation that are extensively migmatized. However, the neosome of the migmatite is less deformed than the Wolf Lake North Granodiorite indicating that migmatization postdated intrusion and deformation of the granodiorite. The earliest foliation in the paleosome of the migmatite predates that in the granodiorite as schistose xenoliths are found in the granodiorite. Furthermore, the neosome is distinctly more leucocratic than the granodiorite. Thus, the migmatite is not the source of the granodiorite, which must have been derived from a different source with a more mafic composition.

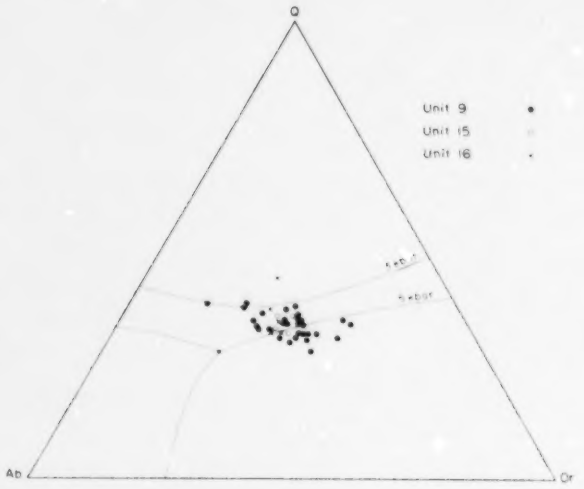

Figure 74. *Plot of normative quartz (Q):albite (A): orthoclase (Or) for Units 9, 15 and 16 of the North Bay Granite Suite. After Currie and Pajari (1981); cotectics from Tuttle and Bowen (1958).*

The average K_2O content of the Wolf Lake North Granodiorite is 3.52 percent and the K_2O:Na_2O ratio is 1. This is similar to that found in granodiorites of the subduction-related calc-alkaline suites of California which have a continental basement (e.g., Carmichael *et al.*, 1974, p. 580, analysis 3). The Wolf Lake North Granodiorite is distinctly more potassic than the 65 percent SiO_2 granitoids of the subduction-related Coastal Batholith of Peru (e.g., Atherton, 1984, p. 170), which are not underlain by continental crust. Similar features are shown by the Upper Salmon Road Granite but as it is more peraluminous, contains abundant K-feldspar and has an initial Sr ratio of 0.7092 (albeit poorly defined), indicating that it contains a greater component of continental crust material.

SUMMARY OF PETROGENETIC PROCESSES

Units 8, 9, 15, 16 of the North Bay Granite Suite are strongly peraluminous granites with abundant pegmatites that have been emplaced into the high-grade metasedimentary rocks. It is concluded that partial melting of the lower parts of the metasedimentary sequence is the source of magmas. Locally, Units 11 and 12 contain abundant migmatitic

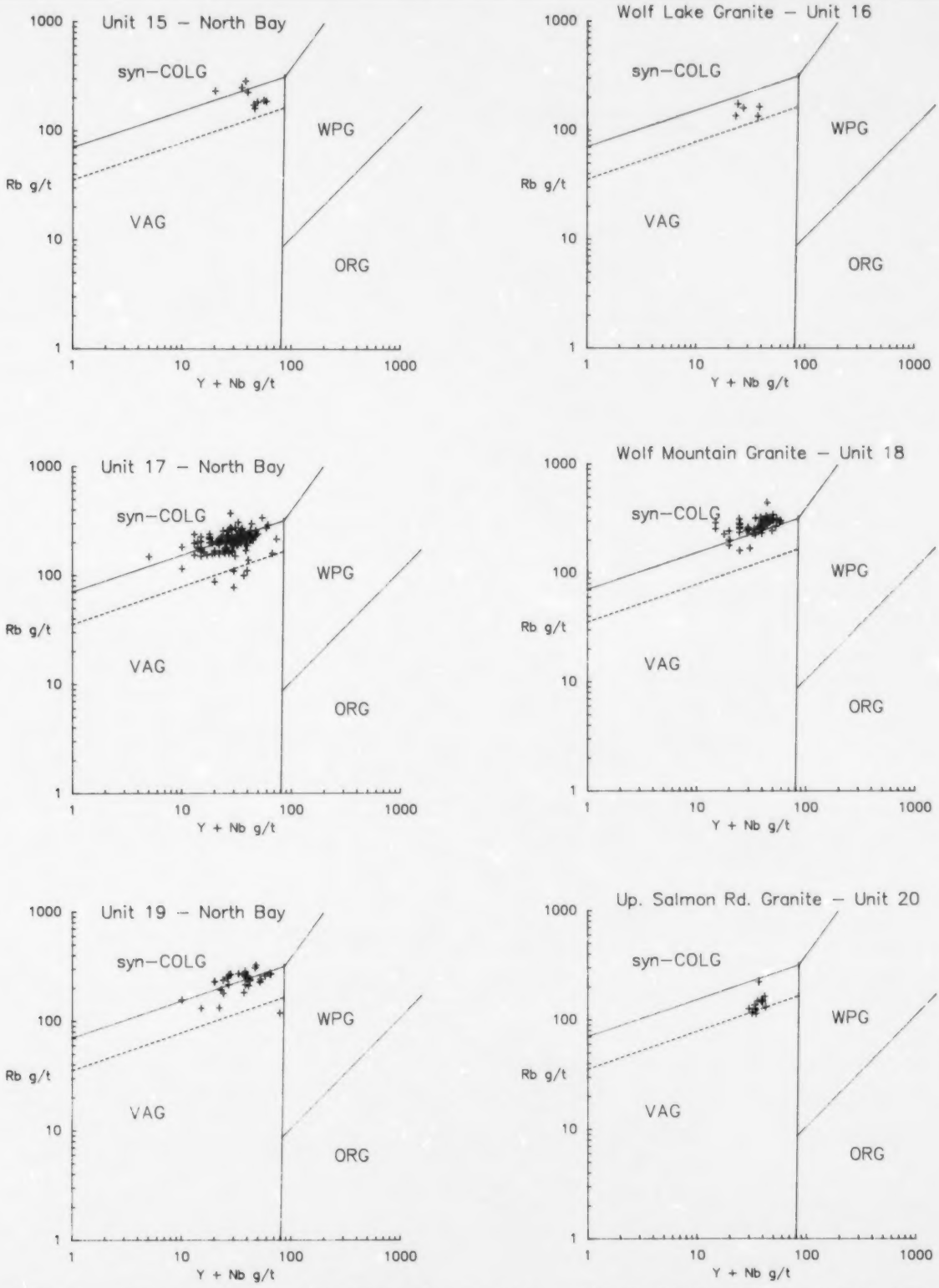

Figure 75. *Logarithmic plot of Rb (g/t) vs. Y + Nb (g/t) for each unit (except Unit 21) of the North Bay Granite Suite. Boundaries shown (solid lines) are from Pearce et al. (1984). Dashed line is lower limit of D'Espoir Brook Granite analyses. Abbreviations: VAG = volcanic-arc granites; ORG = ocean-ridge granites; syn-COLG = syn-collisional granites; WPG = within-plate granite.*

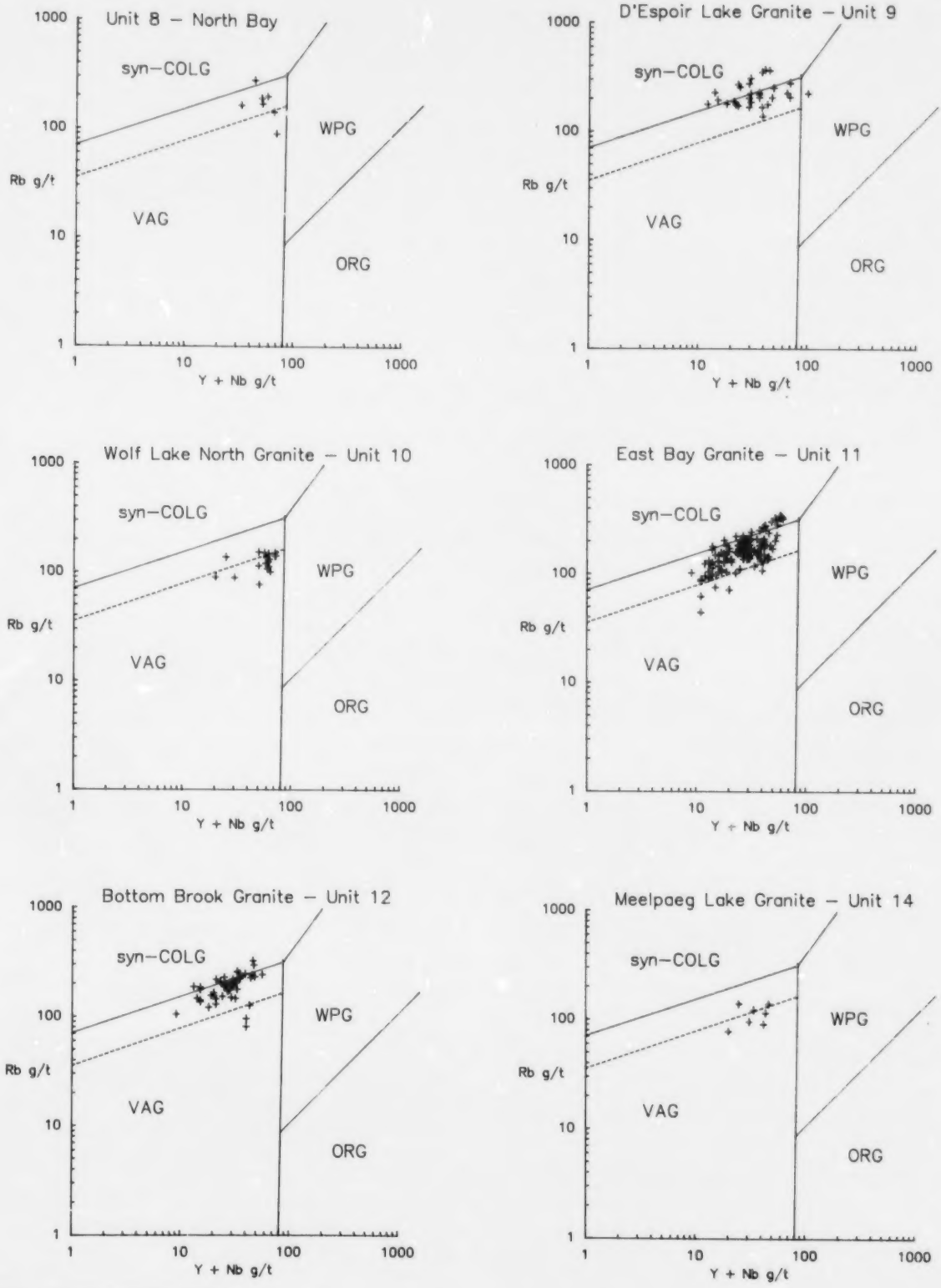

Figure 75. *(Continued).*

Table 20. (a) Chemistry of the quartz–sanidine–porphyry dykes (Unit 23). Major elements in weight percent; trace elements in g/t

Samp	SiO_2	Al_2O_3	Fe_2O_3	FeO	MgO	CaO	Na_2O	K_2O	TiO_2	MnO	P_2O_5	LOI
1689	76.4	12.70	0.19	0.78	0.03	0.28	3.82	5.00	0.07	0.03	0.01	0.55
1690	76.0	13.05	0.22	0.69	0.01	0.28	4.15	4.76	0.10	0.02	0.01	0.55

Samp	U	F	Th	Rb	Sr	Y	Zr	Nb	Ga	Ba	Cu	Zn	Pb	Li	Be
1689	14	98	67	509	4	63	114	56	19	10	3	34	35	42	4
1690	16	144	58	582	3	77	113	82	24	10	5	40	48	38	4

(b) Chemistry of the diabase dyke (Unit 25). Major elements in weight percent; trace elements in g/t.

Samp	SiO_2	Al_2O_3	Fe_2O_3	FeO	MgO	CaO	Na_2O	K_2O	TiO_2	MnO	P_2O_5	LOI
1304	55.9	15.65	2.76	4.94	3.69	6.04	3.81	1.83	1.43	0.14	0.74	3.30

Samp	U	F	Th	Rb	Sr	Y	Zr	Nb	Ga	Ba	Cu	Zn	Pb	Li	Cr	Ni
1304	1	925	1	85	642	39	361	20	16	740	37	117	9	62	49	31

xenoliths, which are probably the high-grade equivalents of the Baie d'Espoir Group; partial melting of the lower parts of the group is probably the source of the magma. Incomplete separation of the magma from its source rocks is indicated by poorly defined trends on Harker diagrams (e.g., Figure 41) and strontium isotopes, which do not define isochrons (e.g., Figures 11 to 16) and also have a high degree of variability over small distances. Units 17, 18 and 19 are compositionally restricted granites, which probably formed by partial melting at mid-crustal levels. They subsequently intruded into the Bay du Nord Group and the older granitoid rocks near the end of the Acadian Orogeny (ca. 396 Ma).

Units 10, 14 and 15 have features typical of calc-alkaline granitoid rocks but with the lack of gabbroic compositions, the source of the magma is probably the lower crust with melting induced by underplating of the crust during subduction.

GEOCHEMISTRY OF THE OTHER IGNEOUS UNITS

Two samples from posttectonic quartz–sanidine–porphyry dykes, which have intruded the North Bay Granite Suite, were analyzed (Table 20a). These dykes are characterized by high SiO_2, total Na_2O+K_2O, U, Y, extremely enriched Rb, severely depleted Sr, and consequently very high Rb/Sr ratios and low K/Rb ratios. These features are also characteristic of the nearby François granite (McConnell, 1984b; Dickson, unpublished data) to which these dykes must be related. This chemistry is similar to several other posttectonic granitoid rocks in southern Newfoundland such as the Chetwynd Granite (Chorlton, 1978; S.J. O'Brien, Newfoundland Department of Mines and Energy, unpublished data), the Ackley Granite (Dickson, 1983; Tuach *et al.*, 1986), and the Harbour Breton Granite (Strong *et al.*, 1974; D. Furey, personal communication, 1986) which are considered to be A-type granites (Tuach *et al.*, 1986).

One sample from one of the two posttectonic diabase dykes (Unit 25) was analyzed (Table 20b). This dyke is probably continental tholeiite based on the low TiO_2, moderately high Zr, and moderately low Rb values (see Floyd and Winchester, 1975).

ECONOMIC POTENTIAL OF THE NORTH BAY GRANITE SUITE

Within the area of the North Bay Granite described in this report, the known mineral occurrences are of limited significance. These occurrences, along with others in the Ordovician units, have been compiled by Brewer (1986) based on reports by Dickson and Tomlin (1983), Dickson and Delaney (1984a), and McConnell (1985). Regional lake sediment surveys by Butler and Davenport (1978) and Davenport and Butler (1982) show that, of the elements analyzed, only tungsten displayed high anomalous values.

Detailed prospecting and geochemical surveys by McConnell (1984b, 1985) resulted in the discovery of scheelite mineralization east of Dolland Brook (= Dolland Brook south anomaly of McConnell, 1985). He described the occurrence thus: 'Several thin tourmaline–quartz–scheelite veins were found (0.5 to 1 cm wide) and traced with ultraviolet light. It is estimated that the veins carry about 1–3 percent scheelite in a tourmaline–quartz matrix with accessory pyrite. Exposure is limited to the bottom and sides of the brook.' The showing occurs in medium–coarse grained, K-feldspar porphyritic, muscovite–biotite granite (Unit 19) and is the only known metallic mineralization in the unit. Pegmatites are rare in this unit and are apparently barren. McConnell (1985) reported pyrite–quartz veins within the 'Dolland Brook north (tungsten) anomaly'. Geochemical analyses of the mineralized rock and stream sediment show values of over 400 g/t W (J. McConnell, personal communication, 1986). The host granite is a medium- to coarse-grained, biotite granite (Unit 18) having a trace of muscovite that may be secondary. In this poorly exposed area, there is little indication of other mineral occurrences.

Pyrite–tourmaline vein mineralization, of extremely limited extent, occurs 3 km northwest of Brent Cove, Facheux Bay (map area 11P/9; Plate 31). The mineralization consists of 5-mm pyrite cubes and 5-cm diameter, bladed tourmaline rosettes. An examination of the outcrop area failed to discover any further mineralization. The pyrite and tourmaline occur along a joint in feldspar-porphyritic granite (Unit 11) indicating postmagmatic mineralization.

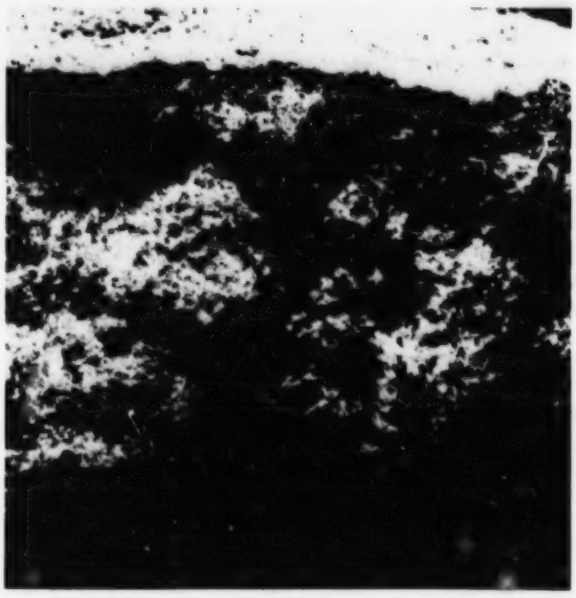

Plate 31. *Tourmaline rosettes (black, top left of photograph) and pyrite cubes (black, centre) in the East Bay Granite (Unit 11); 3 km northwest of Brent Cove, Facheux Bay (map area 11P/9); lens cap is 5 cm in diameter.*

A trace of molybdenite was located in medium-grained, muscovite–biotite granite (Unit 15) approximately 5 km west of Wolf Lake. The molybdenite occurs as rare, 1- to 2- mm flakes in the granite. No significance is placed on this occurrence. However, to the south of this occurrence, two small areas of granite (Unit 15) were located in the vicinity of the faulted contact of the Spruce Brook and North Steady Pond formations (subunits 2a,b and 3g). The granite is locally cut by greisen veins composed of quartz and green muscovite. The veins cut medium-grained, muscovite granite and trend 140 to 180°. The largest veins are 10 to 15 m long and up to 30 cm wide. A geochemical analysis of a grab sample (number 2241503 in Appendix 1) indicated high Rb, very low Sr and severe depletion of Na_2O. There is no fluorine enrichment. Tin analyses are not available but an examination of a thin section indicated no unusual minerals such as cassiterite. Winek (1954), among many others, described the extensive quartz vein and pegmatite-hosted molybdenite occurrences within the Riches Island Formation immediately east of the East Bay Granite and north of Lamipidoes Passage. These pegmatites can be traced into the East Bay Granite but molybdenite mineralization has not been discovered in map area 11P/16.

Grid sampling carried out over the North Bay Granite Suite resulted in few geochemical anomalies of economic minerals. A high uranium value (60.6 g/t) was obtained from granite southeast of Morgan Brook. This sample (2241293), from part of Unit 17, is a pink, K-feldspar porphyritic, biotite granite. There is, however, nothing unusual about the other analyzed elements and, therefore, the significance of this uranium value is uncertain.

Molybdenum values are commonly less than 10 g/t with five isolated values ranging from 15 to 46 g/t Mo. Copper values over 30 g/t are rare in most units of the North Bay Granite Suite. However, Units 11 and 12 have numerous Cu values over 30 g/t with the highest value being 101 g/t. These above-average values are generally single-element anomalies with Mo, Pb, Zn, having background values. Sample 2241201 (west side of North Bay) also contains anomalous Zn (718 g/t) and Pb (364 g/t). Sample 2241244, which contains 101 g/t Cu, also contains 115 g/t Zn. The host rocks show no obvious signs of mineralization and are one-point anomalies. The lake-sediment anomalies for these elements do not correspond with the rock geochemical anomalies. No obvious anomalies were obtained from the regional rock geochemistry survey and only sample 2241201 is possibly worthy of follow-up work. The area contains several large quartz veins. These have been described in detail earlier in the report where the economic potential of the veins is also described.

B.P.-Selco Limited have staked ground to the North of D'Espoir Lake. The area staked is underlain by mainly felsic volcanic rocks that have been assigned to the Spruce Brook Formation (subunit 2e). The only exposure of volcanic rock in the D'Espoir Lake map area is strongly schistose sericitic rhyolite. To the north, in the Cold Spring Pond map area (12A/1), Colman-Sadd (1984) described the unit as felsic crystal tuff and granite which, in one area, contains disseminations of pyrite and other undetermined sulphide minerals. This mineral occurrence is located only a few hundred metres north of the D'Espoir Lake map area.

In the Pomley Cove area, strongly cleaved, graphitic pyritic slate, which forms part of the Riches Island Formation, was analyzed. This sample is enriched in Ba (3122 g/t), Ni (54 g/t), and V (319 g/t). Gold was not analyzed. Barite is well known, in the Bay d'Espoir area, and is commonly associated with vein Pb–Zn mineralization (Swinden, 1982). Much of the Bay d'Espoir area has been staked and is actively being explored for gold with recent discoveries to the east of the St. Alban's area.

A recent development in Newfoundland is bedrock-aggregate quarrying. In the Stephenville area of western Newfoundland, limestone is currently quarried and crushed for export to the eastern United States. A similar operation using granite has been proposed for Red Island in Placentia Bay in eastern Newfoundland and another using quartzite has also been proposed for the Long Harbour area of northern Placentia Bay. A recent report by Bragg *et al.* (1990) included a preliminary survey of the East Bay Granite between East Bay and Lampidoes Passage. The granite here forms high cliffs (> 100 m) and on Lampidoes Passage the lower slopes are mantled by an extensive talus slope, composed of 1- to 3-m granite blocks. The granite is fresh, hard, medium grained and contains about 8 percent total mica (see Table 8, sample L2.3.82). The mica occurs as 1 to 3 mm flakes and there is very minor alteration of the biotite to chlorite; feldspars are fresh having only a dusting of sericite mica. Jointing is common with well-spaced vertical and horizontal joints (approximately 1 to 2 m spacing). Similar rock types are exposed along East Bay and North Bay. The supply of raw material is virtually unlimited.

Lampidoes Passage is very deep with a narrow shoreline, which make access to the area by ship feasible. Along East Bay and North Bay, rock platforms and shallow coves adjacent to the cliffs could provide sites for harbours or crushing plants.

SUMMARY

The North Bay Granite Suite is a 4000 km² composite batholith, which underlies the southeastern portion of the Hermitage Flexure. The granite suite has intruded the Baie d'Espoir and Bay du Nord groups of the Dunnage Zone, and the Spruce Brook Formation of the Gander Zone (Williams *et al.*, 1988). These Ordovician units are composed mainly of clastic sedimentary rocks and minor felsic volcanic rocks.

The North Bay Granite Suite consists of 14 rock types, some of which form widely separated intrusions. The North Bay Granite Suite is divided by the Meelpaeg Lake Fault Zone, which extends from Granite Lake to Salmon River. The main part of the suite lies to the south of the fault zone and consists of leucocratic, muscovite–biotite–garnet granite, muscovite–biotite granite and granodiorite, and K-feldspar porphyritic, biotite granite. To the north of the fault zone, the main rock types are biotite granodiorite and granite, and leucocratic garnet–biotite–muscovite granite.

The Spruce Brook Formation consists of quartz-rich psammite and semipelite overlain by a sequence of pelite and pelite breccia capped by extensive, coarse-grained, quartz-rich sandstones, granule, and cobble conglomerates dominated by quartzite clasts. This formation is probably a shallow-marine deposit that was reworked in a beach environment to produce the coarse-grained, clastic units. Thus, a possibly significant time-break is apparent within the Spruce Brook Formation as it is defined in this report.

The Baie d'Espoir Group is dominated by clastic sediments deposited in a submarine fan environment. The Salmon River Dam Formation is the oldest unit of the Baie d'Espoir Group and consists mainly of turbiditic greywacke and slate. The Riches Island Formation is highly metamorphosed and consists of micaceous semipelite and psammite. Within the North Bay Granite Suite, sizable areas of migmatite are considered to be part of the Riches Island Formation. The North Steady Pond Formation is dominated by sandstone, crystal tuff and epiclastic sandstone with minor black and grey pelite units. This formation is interpreted to have been deposited in a proximal environment, close to a volcanic centre.

The Bay du Nord Group lies to the southwest of the North Bay Granite Suite and is continuous with the Baie d'Espoir Group. The group is dominated by high-grade psammitic schists, which have been extensively migmatized and intruded by leucogranites. The contact zone of the group with the Burgeo granite has been mylonitized along the Dragon Bay fault zone. The metasedimentary rocks have been polydeformed and metamorphosed during the Silurian–Devonian Acadian Orogeny. The Spruce Brook Formation has a simple classical deformation with open folds and a vertical axial-planar schistosity; the northern portion of the Spruce Brook Formation is extensively migmatized. In the East Bay area, the Riches Island Formation is recumbently folded and verges to the south. Later deformation has produced open, upright folds that plunge gently to the northeast. The Salmon River Dam Formation, in the D'Espoir Lake area, is similarly deformed although the recumbent folds may verge to the north. However, to the east, the Salmon River Dam Formation forms upright, isoclinal folds. The grade of metamorphism of the Baie d'Espoir Group ranges from lower-greenschist facies to amphibolite facies at the North Bay Granite Suite. Cordierite, andalusite and garnet porphyroblasts are extensively developed in the contact metamorphic aureole of the granite suite.

The older units of the North Bay Granite Suite have been deformed with the Baie d'Espoir Group and contain the second fabric. The younger units are weakly deformed and

are essentially posttectonic. The granitoid rocks along the Meelpaeg Lake Fault Zone have been extensively mylonitized and between Dolland Brook and Salmon River, the foliation dips gently to the north. A major thrust contact may be present between the North Bay Granite Suite and the Salmon River Dam Formation. The posttectonic Dolland Brook Granite has been dated at 396 Ma (U–Pb zircon date). Attempts at dating some of the other units using the Rb–Sr whole-rock method were less successful but indicate that the older units have ages in the range of 430 to 400 Ma.

The North Bay Granite Suite was sampled using a 2 by 2 km grid. Geochemical analyses indicate that the older granodiorites, to the north of the Meelpaeg Lake Fault Zone, are calc-alkaline and therefore, may have been derived from the mantle or lower crust. The garnet–biotite–muscovite granites are geochemically similar. A plot of normative Q:Ab:Or indicates that their compositions plot near the ternary minimum at 5 kb water pressure. These granites are similar to the Aspen Cove, Middle Ridge and Ragged Harbour granites and occupy a similar structural position in the Gander Zone. These granites probably formed by partial melting of the Ordovician metasedimentary rocks. The syn-Acadian muscovite–biotite granites are intimately associated with migmatites and show poorly developed, differentiation trends. This, together with their heterogeneous Sr isotopic compositions, may indicate that the granite magmas have not separated fully from their parent metasedimentary rocks and have not homogenized or differentiated in a magma chamber.

The posttectonic K-feldspar porphyritic, muscovite–biotite (rarely + garnet) granites have geochemical characteristics similar to the posttectonic granites of southern Newfoundland, being generally moderate to high-silica granites and limited chemical variation. These granites are probably formed by partial melting of lower crust under relatively dry conditions. Mineral occurrences within the study area are of limited extent.

There is apparently some potential for gold in the Spruce Brook Formation volcanic rocks and the ground at D'Espoir Lake is currently held. There is also some gold potential in the Riches Island Formation pyritic units. Tungsten mineralization occurs in the posttectonic Dolland Brook Granite near Dolland Brook. Extensive quartz veins occur along the major faults. These veins have no sulphide mineralization and a few grab samples were assayed but gold was not detected. The East Bay Granite has good potential as a source of bedrock aggregate.

ACKNOWLEDGMENTS

This project was carried out with senior assistants Stephen L. Tomlin and Paul W. Delaney. Their efforts in the field were essential to the project. Barry N. Wheaton of Frederickton, Newfoundland, continued to excel as a boatman and geological assistant. Glen Case of St. John's provided capable assistance during his initiation into field work. The logistical support of Wayne Ryder, Sydney Parsons and James Barrett of the Newfoundland Department of Mines and Energy, and Gordon Arnold, Geological Survey of Canada, permitted the smooth execution of field work. Reviews by Dr. S.P. Colman-Sadd and Dr. J. Tuach are appreciated.

REFERENCES

Abbey, S.
1980: Studies in 'standard samples' for use in the general analysis of silicate rocks and minerals. Part 6: 1979 edition of 'usable' values. Geological Survey of Canada, Paper 80-14, 30 pages.

Abbott, R.N., Jr.
1981: AFM liquidus projections for granitic magmas with special reference to hornblende, biotite and garnet. Canadian Mineralogist, Volume 19, pages 103-110.

Anderson, F.D.
1967: Structural studies in the Baie d'Espoir Group, Newfoundland. *In* Collected Papers on Geology of the Atlantic Region–Hugh Lilly Memorial Volume. *Edited by* E.R.W. Neale and H. Williams. Geological Association of Canada, Special Paper 4, pages 193-200.

Anderson, J.L. and Rowley, M.C.
1981: Synkinematic intrusion of peraluminous and associated metaluminous granitic magmas, Whipple Mountains, California. Canadian Mineralogist, Volume 19, pages 83-103.

Atherton, M.P.
1983: The Coastal Batholith of Peru. *In* Andean Magmatism. Chemical and Isotopic Constraints. *Edited by* R.S. Harmon and B.A. Barreiro. Shiva Publishing Limited, Nantwich, England, pages 168-179.

Atherton, M.P., McCourt, W.J., Sanderson, L.M. and Taylor, W.P.
1979: The geochemical character of the segmented Peruvian Coastal Batholith and associated volcanics. *In* Origin of Granite Batholiths: Geochemical Evidence. *Edited by* M.P. Atherton and J. Tarney. Shiva Publishing, Nantwich, England, pages 45-64.

Atherton, M.P. and Sanderson, L.M.
1985: The chemical variation and evolution of the superunits of the segmented Coastal Batholith. *In*

Magmatism at a Plate Edge—the Peruvian Andes. *Edited by* W.S. Pitcher, M.P. Atherton, E.J. Cobbing and R.D. Beckinsale. Blackie and Sons, Glasgow, pages 208-227.

Baird, D.M., Scott, H.S., Moore, J.C.B. and Walker, W.
1951: Reconnaissance geology of east-central Newfoundland between Sir Charles Hamilton Sound and Bay d'Espoir. Photographic Survey Corporation, unpublished report, 155 pages. [NFLD 446]

Blackwood, R.F.
1983: Geology of the Facheux Bay (11P/9) map area, Newfoundland. *In* Current Research. Newfoundland Department of Mines and Energy, Mineral Development Division, Report 83-1, pages 26-40.

1984: Geology of the Dolland Brook (11P/15W) map area, south-central Newfoundland. *In* Current Research. Newfoundland Department of Mines and Energy, Mineral Development Division, Report 84-1, pages 198-210.

1985: Geology of the Facheux Bay (11P/9) map area, southern Newfoundland. Newfoundland Department of Mines and Energy, Mineral Development, Report 85-4, 56 pages.

Boyce, W.D.
1987: Cambrian–Ordovician trilobite biostratigraphy in central Newfoundland. *In* Current Research. Newfoundland Department of Mines and Energy, Mineral Development Division, Report 87-1, pages 335-341.

Bragg, D., Dickson, L. and St. Croix, L.
1990: A preliminary assessment of the south coast of Newfoundland as an area having potential for bedrock aggregate exports. *In* Current Research, Newfoundland Department of Mines and Energy, Geological Survey Branch, Report 90-1, pages 13-18.

Brewer, K.
1986: Mineral Occurrence Map, Burgeo (11P), Newfoundland. Newfoundland Department of Mines and Energy, Mineral Development Division, Map 86-33.

Bucknell, W.R.
1984: North Bay Project. Report on soil geochemistry. License 2277, 2295-2300. NTS 1M/13, 11P/15/16, 12A/2, Newfoundland. Rio Algom Exploration Inc., unpublished report. [NFLD 1357]

Butler, A.J. and Davenport, P.H.
1978: A lake sediment geochemical survey of the Meelpaeg Lake area, central Newfoundland. Department of Mines and Energy, Mineral Development Division, Open File NFLD. (986), 36 pages.

Butler, A.J. and Greene, B.A.
1976: Silica resources of Newfoundland. Newfoundland Department of Mines and Energy, Mineral Development Division, Report 76-2, 68 pages.

Carmichael, I.S.E., Turner, F.J. and Verhoogen, J.
1974: Igneous Petrology. McGraw-Hill, New York, 739 pages.

Chappell, B.W. and White, A.J.R.
1974: Two contrasting granite types. Pacific Geology, Volume 8, pages 173-174.

Chorlton, L.B.
1978: The geology of the La Poile map area (11O/9), Newfoundland. Newfoundland Department of Mines and Energy, Mineral Development Division, Report 78-5, 14 pages.

Chorlton, L. and Knight, I.
1983: Geology of the Grandys Lake area (11O/15), Newfoundland. Newfoundland Department of Mines and Energy, Mineral Development Division, Report 83-7, 125 pages.

Clarke, D.B.
1981: The mineralogy of peraluminous granites: a review. Canadian Mineralogist, Volume 19, pages 3-18.

Colman-Sadd, S.P.
1974: The geologic development of the Bay d'Espoir area, southeastern Newfoundland. Ph.D. thesis, Memorial University of Newfoundland, St. John's, Newfoundland, 271 pages.

1976: Geology of the St. Alban's map area, Newfoundland (1M/13). Newfoundland Department of Mines and Energy, Mineral Development Division, Report 76-4, 19 pages.

1980a: Geology of parts of Burnt Hill area (2D/5), Newfoundland. *In* Current Research. Newfoundland Department of Mines and Energy, Mineral Development Division, Report 80-1, pages 44-49.

1980b: Geology of the Twillick Brook map area, Newfoundland (2D/4). Newfoundland Department of Mines and Energy, Mineral Development Division, Report 79-2, 23 pages.

1980c: Geology of south-central Newfoundland and evolution of the eastern margin of Iapetus. American Journal of Science, Volume 280, pages 991-1017.

1982: Two stage continental collision and plate driving forces. Tectonophysics, Volume 90, pages 263-282.

1983: Geology of the east half of the Cold Spring Pond map area (12A/1), Newfoundland. *In* Current Research. Newfoundland Department of Mines and Energy, Mineral Development Division, Report 83-1, pages 16-25.

1984: Geology of the Cold Spring Pond map area (west part) 12A/1, Newfoundland. *In* Current Research. Newfoundland Department of Mines and Energy, Mineral Development Division, Report 84-1, pages 211-219.

1985: Geology of the west part of the Great Burnt Lake (12A/8) area. *In* Current Research. Newfoundland Department of Mines and Energy, Mineral Development Division, Report 85-1, pages 105-113.

1986: Geology of the east part of the Snowshoe Pond (12A/7) area, Newfoundland. *In* Current Research. Newfoundland Department of Mines and Energy, Mineral Development Division, Report 86-1, pages 179-188.

1987: Geology of part of the Snowshoe Pond (12A/7) map area, Newfoundland. *In* Current Research. Newfoundland Department of Mines and Energy, Mineral Development Division, Report 87-1, pages 297-310.

Colman-Sadd, S.P., Dickson, W.L., Elias, P. and Davenport, P.H.
1981: Rock geochemical data from plutonic intrusions of south-central Newfoundland. Newfoundland Department of Mines and Energy, Mineral Development Division, Open File Newfoundland 1157.

Colman-Sadd, S.P., Greene, B.A. and O'Driscoll, C.F.
1979: Gaultois map area. Newfoundland Department of Mines and Energy, Mineral Development Division, Open File Map 79-104.

Colman-Sadd, S.P. and Russell, H.A.J.
1982: Geology of the Miguels Lake map area (2D/12), Newfoundland. *In* Current Research. Newfoundland Department of Mines and Energy, Mineral Development Division, Report 82-1, pages 30-50.

Colman-Sadd, S.P. and Swinden, H.S.
1982: Geology and mineral potential of south-central Newfoundland. Newfoundland Department of Mines and Energy, Mineral Development Division, Report 82-8, 102 pages.

1984: A tectonic window in central Newfoundland? Geological evidence that the Dunnage Zone may be allochthonous. Canadian Journal of Earth Sciences, Volume 21, pages 1349-1367.

Cooper, J.R.
1954: The La Poile–Cinq Cerf map area, Newfoundland. Geological Survey of Canada, Memoir 276, 62 pages.

Currie, K.L. and Pajari, G.E., Jr.
1981: Anatectic peraluminous granites from the Carmanville area, northeastern Newfoundland. Canadian Mineralogist, Volume 19, pages 147-162.

Dallmeyer, R.D.
1980: Geochronology report. *In* Current Research. Newfoundland Department of Mines and Energy, Mineral Development Division, Report 80-1, pages 143-146.

Davenport, P.H. and Butler, A.J.
1981: Fluorine in lake sediment in the Meelpaeg Lake area, central Newfoundland. Newfoundland Department of Mines and Energy, Mineral Development Division, Open File Nfld. (1222).

1982: Tungsten in lake sediment over granitoids in south-central Newfoundland. Newfoundland Department of Mines and Energy, Mineral Development Division, Open File Nfld. (1302).

Dec, T. and Colman-Sadd, S.P.
1990: Timing of ophiolite emplacement onto the Gander Zone: Evidence from provenance studies in the Mount Cormack subzone. *In* Current Research. Newfoundland Department of Mines and Energy, Geological Survey Branch, Report 90-1, pages 289-303.

Delaney, P.W.
1984: Molybdenum–tungsten mineralization at Granite Lake, Newfoundland. Unpublished B.Sc. (Honours) thesis, Memorial University of Newfoundland, St. John's, Newfoundland, 39 pages.

Dickson, W.L.
1982: Geology of the Wolf Mountain (12A/2W) and Burnt Pond (12A/3E) map area, Newfoundland. Newfoundland Department of Mines and Energy, Mineral Development Division, Report 82-5, 43 pages.

1983: Geology, geochemistry and mineral potential of the Ackley Granite and parts of the North West Brook and Eastern Meelpaeg Complexes, southeast Newfoundland (parts of map areas 1M/10,11, 14,15,16; 2D/1,2,3 and 7). Newfoundland Department of Mines and Energy, Mineral Development Division, Report 83-6, 129 pages.

1984: Mineralized granites in southern Newfoundland. *In* Mineral Deposits of Newfoundland–A 1984 Perspective. *Compiled by* H.S. Swinden. Newfoundland Department of Mines and Energy, Mineral Development Division, Report 84-3, pages 149-163.

Dickson, W.L., Blackwood, R.F., Delaney, P.W. and Poole, J.
1985a: La Hune (11P/10), Newfoundland. Newfoundland Department of Mines and Energy, Mineral Development Division, Map 8463.

1985b: Ramea (11P/11), Newfoundland. Newfoundland Department of Mines and Energy, Mineral Development Division, Map 8464.

Dickson, W.L. and Delaney, P.W.
1984a: Geology of the Wolf Mountain (east half) and Dolland Brook (east half) map areas, south-central Newfoundland. *In* Current Research, Part A. Geological Survey of Canada, Paper 84-1A, pages 537-544. *Also in* Current Research. Newfoundland Department of Mines and Energy, Mineral Development Division, Report 84-1, pages 232-241.

1984b: Wolf Mountain (12A/2E), Newfoundland. Newfoundland Department of Mines and Energy, Mineral Development Division, Map 8426.

1984c: Dolland Brook (11P/15E), Newfoundland. Newfoundland Department of Mines and Energy, Mineral Development Division, Map 8427.

Dickson, W.L., Delaney, P.W. and Poole, J.
1985: Geology of the Burgeo Granite and associated rocks in the Ramea (11P/11) and La Hune (11P/10) map areas, southern Newfoundland. *In* Current Research. Newfoundland Department of Mines and Energy, Mineral Development Division, Report 85-1, pages 145-153.

Dickson, W.L., O'Brien, S.J. and Hayes, J.P.
1989: Aspects of the mid-Paleozoic magmatic history of the south-central Hermitage Flexure area, Newfoundland. *In* Current Research. Newfoundland Department of Mines, Geological Survey of Newfoundland, Report 89-1, pages 81-95.

Dickson, W.L. and Tomlin, S.L.
1983: Geology of the Bay D'Espoir Brook map area (11P/16) and part of the Facheux Bay map area (11P/9), south-central Newfoundland. *In* Current Research, Part A, Geological Survey of Canada, Paper 83-1A, pages 285-290. *Also in* Current Research. Newfoundland Department of Mines and Energy, Mineral Development Division, Report 83-1, pages 51-56.

1984: D'Espoir Brook (11P/16), Newfoundland. Newfoundland Department of Mines and Energy, Mineral Development Division, Map 8428.

Dunlop, W.B.
1954: Exploration in the Bay d'Espoir area. NALCO, unpublished report, 13 pages. [1M (41)]

Dunning, G.R. and Krogh, T.E.
1985: Geochronology of ophiolites of the Newfoundland Appalachians. Canadian Journal of Earth Sciences, Volume 22, pages 1659-1670.

Dunning, G.R., Krogh, T.E., O'Brien, S.J., Colman-Sadd, S.P. and O'Neill, P.
1988: Geochronologic framework for the Central Mobile Belt in southern Newfoundland and the importance of Silurian orogeny. Geological Association of Canada–Mineralogical Association of Canada–Canadian Society of Petroleum Geologists Joint Annual Meeting. Program with Abstracts, Volume 13, page A34.

Dunning, G.R., O'Brien, S.J., Colman-Sadd, S.P., Blackwood, R.F., O'Neill, P., Dickson, W.L., and Krogh, T.E.
1990: Silurian orogeny in the Newfoundland Appalachians. Journal of Geology, Volume 98, pages 895-913.

Elias, P.
1981: Geochemistry and petrology of granitoid rocks of the Gander Zone, Bay d'Espoir area, Newfoundland. Unpublished M.Sc. thesis, Memorial University of Newfoundland, St. John's, Newfoundland, 271 pages.

Elias, P. and Strong, D.F.
1982: Paleozoic granitoid plutonism of southern Newfoundland: contrasts in timing, tectonic setting and level of emplacement. Transactions of the Royal Society of Edinburgh: Earth Sciences, Volume 73, pages 43-57.

Floyd, P.A. and Winchester, J.A.
1975: Magma type and tectonic setting discrimination using immobile elements. Earth and Planetary Sciences, Volume 27, pages 211-218.

Fryer, B.J.
1983: Results of whole rock Rb–Sr isotopic analysis of granitic rocks of the D'Espoir Brook map-area, southern Newfoundland. Unpublished report for the Geological Survey of Canada, 8 pages. [11P/16 (127)]

Geological Survey of Canada
1983a: Gamma ray spectrometry survey, south coast Newfoundland, 1983. Geophysical series map 36611(15)G, Dolland Brook (11P/15). Newfoundland Department of Mines and Energy, Mineral Development Division, Open File NFLD(1318).

1983b: Gamma ray spectrometry survey, south coast Newfoundland, 1983. Geophysical series map 36611(16)G, D'Espoir Brook (11P/16). Newfoundland Department of Mines and Energy, Mineral Development Division, Open File NFLD(1318).

1983c: Gamma ray spectrometry survey, south coast Newfoundland, 1983. Geophysical series map 35112(2)G, Dolland Brook (12A/2). Newfoundland Department of Mines and Energy, Mineral Development Division, Open File NFLD(1318).

Harland, W.B., Cox, A.V., Lewellyn, P.G., Picton, C.A.G., Smith, A.G. and Walters, R.
1982: A geological time scale. Cambridge University Press, Cambridge, 128 pages.

Irvine, L.N. and Baragar, W.R.A.
1971: A guide to the chemical classification of the common volcanic rocks. Canadian Journal of Earth Sciences, Volume 8, pages 523-548.

Jewell, W.B.
1939: Geology and mineral deposits of the Baie d'Espoir area. Geological Survey of Newfoundland, Bulletin 17, 29 pages. [Nfld 3]

Kerr, P.F.
1959: Optical Mineralogy. McGraw-Hill Book Co. Ltd., New York, 442 pages.

Kean, B.F.
1983: Geology of the King George IV Lake map area 12A/4. Newfoundland Department of Mines and Energy, Mineral Development Division, Report 83-4, 67 pages.

Krogh, T.E.
1985: Determination of U-Pb zircon geochronological ages. Unpublished report, Newfoundland Department of Mines and Energy, Mineral Development Division. [NFLD 1504; also LAB 706]

Klein, G.D.
1985: The control of depositional depth, tectonic uplift, and volcanism or sedimentation processes in the back-arc basins of the western Pacific Ocean. Journal of Geology, Volume 93, pages 1-25.

Loiselle, M.C. and Wones, D.R.
1979: Characteristics and origin of anorogenic granites. Geological Society of America. Abstracts with Programs, Volume 11, Number 7, page 468.

McConnell, J.M.
1983: Soil, stream and rock geochemical surveys of three Newfoundland granitoids. *In* Current Research. Newfoundland Department of Mines and Energy, Mineral Development Division, Report 83-1, pages 126-131.

1984a: Geochemical surveys over three tungsten anomalies in the North Bay Batholith. *In* Current Research. Newfoundland Department of Mines and Energy, Mineral Development Division, Report 84-1, pages 242-244.

1984b: Follow-up geochemistry over three mineralized granites in south-central Newfoundland. Newfoundland Department of Mines and Energy, Mineral Development Division, Open File NFLD(1429), 44 pages.

1985: Follow-up geochemistry: a discussion of field work over metalliferous and mineralized granitoid terrain in Newfoundland. *In* Current Research. Newfoundland Department of Mines and Energy, Mineral Development Division, Report 85-1, pages 165-167.

North American Commission on Stratigraphic Nomenclature
1983: North American stratigraphic code. American Association of Petroleum Geologists, Bulletin, Volume 67, Number 5, pages 841-875.

O'Brien, S.J. and Dickson, W.L.
1986: Burgeo (11P), Newfoundland. Newfoundland Department of Mines and Energy, Mineral Development Division, Map 86-32.

O'Brien, S.J., and Tomlin, S.L.
1984: Geology of the White Bear River map area(11P/14), southern Newfoundland. *In* Current Research. Newfoundland Department of Mines and Energy, Mineral Development Division, Report 84-1, pages 220-231.

1985a: Geology of the west half of the Burnt Pond map area (12A/3), south central Newfoundland. *In* Current Research. Newfoundland Department of Mines and Energy, Mineral Development Division, Report 85-1, pages 124-131.

1985b: Geology of the Burgeo map area (11P/12), southwest Newfoundland. *In* Current Research. Newfoundland Department of Mines and Energy, Mineral Development Division, Report 85-1, pages 114-123.

O'Brien, S.J., Dickson, W.L. and Blackwood, R.F.
1986: Geology of the central portion of the Hermitage Flexure area, Newfoundland. *In* Current Research. Newfoundland Department of Mines and Energy, Mineral Development Division, Report 86-1, pages 114-123.

Palster, U.
1984: North Bay Project, Newfoundland. NTS areas 1M/13, 11P/15,16, 12A/2. Geological mapping and stream sediment sampling program. Rio Algom Exploration Inc. [NFLD 1357]

Pearce, J.A., Harris, N.B.W. and Tindle, A.G.
1984: Trace element discrimination diagrams for the tectonic interpretation of granitic rocks. Journal of Petrology, Volume 25, pages 956-983.

Phendler, R.W.
1950: Geology of the Lake Ebbegunbaeg area. Buchans Mining Company, unpublished report, 5 pages. [12A(65)]

Presnall, D.C. and Bateman, P.C.
1973: Fusion relations in the system $NaAlSi_3O_8$–$CaAl_2Si_2O_8$–$KAlSi_3O_8$–SiO_2–H_2O and the origin of granite magmas in the Sierra Nevada Batholith. Geological Society of America Bulletin, Volume 84, pages 3181-3202.

Riley, G.C.
1957: Red Indian Lake (west half). Geological Survey of Canada, map 8-1957.

Scott, H.S. and Conn, H.K.
1950: Preliminary report on the geology of the Buchans Mining Company concession in central and south-central Newfoundland. Photographic Survey Corporation Limited, Geological Division, unpublished report, 12 pages. [12A(7)]

Smyth, W.R.
1979: Dolland Brook (11P/15). Newfoundland Department of Mines and Energy, Mineral Development Division, Map 79-54.

Streckeisen, A.L.
1976: To each plutonic rock its proper name. Earth Science Reviews, Volume 2, pages 1-33.

Strong, D.F., Dickson, W.L., O'Driscoll, C.F. and Kean, B.F.
1974: Geochemistry of eastern Newfoundland granitoid rocks. Newfoundland Department of Mines and Energy, Mineral Development Division, Report 74-3, 140 pages.

Strong, D.F. and Hanmer, S.K.
1981: The leucogranites of southern Brittany: origin by faulting, frictional heating, fluid flux and fractional melting. Canadian Mineralogist, Volume 19, pages 163-176.

Swinden, H.S.
1982: Metallogenesis in the Bay D'Espoir area, southern Newfoundland: summary and implications for regional metallogeny in the Newfoundland Central Mobile Belt. Canadian Institute of Mining and Metallurgy Bulletin, Volume 75, pages 172-183.

1988: Geology and economic potential of the Pipestone Pond area (12A/1NE, 12A/8E), central Newfoundland. Newfoundland Department of Mines, Mineral Development Division, Report 88-2, 88 pages.

Taylor, S.R.
1965: The application of trace element data to problems in petrology. Physics and Chemistry of the Earth, Volume 6, pages 133-213.

Tuach, J. and Delaney, P.W.
1987: Tungsten–molybdenum in the Granite Lake–Meelpaeg Lake area, Newfoundland. *In* Current Research. Newfoundland Department of Mines and Energy, Mineral Development Division, Report 87-1, pages 113-127.

Tuach, J., Davenport, P.H., Dickson, W.L. and Strong, D.F.
1986: Geochemical trends in the Ackley Granite, southeast Newfoundland: their relevance to magmatic–metallogenic processes in high silica granitoid systems. Canadian Journal of Earth Sciences, Volume 23, pages 747-765.

Tuttle, O.F. and Bowen, N.L.
1958: Origin of granite in the light of experimental studies in the system $NaAlSi_3O_8$–$KAlSi_3O_8$–SiO_2–H_2O. Geological Society of America, Memoir 74, 153 pages.

Twenhofel, W.H. and McClintock, P.
1940: Surface of Newfoundland. Geological Society of America, Bulletin, Volume 51, pages 1665-1726.

Wedepohl, K.H. (Editor)
1978: Handbook of Geochemistry. Volume II-5. Springer-Verlag, Berlin–Heidelberg.

White, A.J.R.
1979: Sources of granite magmas. Geological Society of America, Abstract Program, Volume 11, page 539.

White, A.J.R. and Chappell, B.W.
1983: Granitoid types and their distribution in the Lachlan Fold Belt, southeastern Australia. *In* Circum-Pacific plutonic terranes. *Edited by* J.A. Roddick. Geological Society of America, Memoir 159, pages 21-34.

Widmer, K.
1950: The geology of the Hermitage Bay area, Newfoundland. Ph.D. thesis, Princeton University, Princeton, New Jersey, 459 pages.

Williams, H.
1970: Red Indian Lake (east half), Newfoundland. Geological Survey of Canada, Map 1196A.

1971: Burgeo (east half), Newfoundland. Geological Survey of Canada, Map 1280A.

1978: Tectonic-lithofacies map of the Appalachian Orogen. Memorial University of Newfoundland, Map Number 1.

1984: Miogeoclines and suspect terranes of the Caledonian–Appalachian Orogen: tectonic patterns in the North Atlantic region. Canadian Journal of Earth Sciences, Volume 21, pages 887-901.

Williams, H., Colman-Sadd, S.P. and Swinden, H.S.
1988: Tectonostratigraphic subdivisions of central Newfoundland. *In* Current Research. Geological Survey of Canada, Paper 88-1B, pages 91-98.

Williams, H., Kennedy, M.J. and Neale, E.R.W.
1970: The Hermitage Flexure, the Cabot Fault and the disappearance of the Newfoundland Central Mobile Belt. Geological Society of America Bulletin, Volume 81, pages 1563-1568.

Winek, T.A.
1954: Molybdenite deposits of Baie d'Espoir. NALCO, St. John's, Newfoundland. Unpublished report, 23 pages. [1M/40]

Winkler, H.G.F.
1976: Petrogenesis of Metamorphic Rocks, 4th Edition. Springer-Verlag, New York, 334 pages.

Wyllie, P.J., Huang, W.-L., Stern, C.R. and Maaloe, S.
1976: Granitic magmas: possible and impossible sources, water contents, and crystallization sequences. Canadian Journal of Earth Sciences, Volume 13, pages 1007-1019.

Note: Geological Survey Branch file numbers are shown in square brackets at the end of each unpublished report.

LIST OF APPENDIXES

APPENDIX 1

Explanatory Notes
Explanation of Abbreviations
- Field Data–Part 1
- Field Data–Part 2
- Major-Element-Oxide Data
- Trace-Element Data
- Normative-Mineral Data

a–Field Data
b–Field Data
c–Major-Element–Oxide Data
d–Trace-Element Data
e–Normative-mineral Data

APPENDIX 2 PRECISION OF MAJOR- AND TRACE-ELEMENT DETERMINATIONS

a–Precision of major-element determinations based on 40 analytical splits
b–Precision of trace element determinations based on analytical splits

APPENDIX 3 ACCURACY

a–Accuracy of major-element determinations at the Newfoundland Department of Mines and Energy, Geological Survey Branch Laboratory. Usable values from Abbey (1980)
b–Accuracy of trace elements, determined by the Newfoundland Department of Mines and Energy, Geological Survey Branch Laboratory. Usable values from Abbey (1980)
c–Accuracy of trace elements determined by XRF at the Department of Earth Sciences, Memorial University of Newfoundland. Usable values from Abbey (1980)

APPENDIX 4

a–Detailed sample location and description card used to format data
b–Explanation of Coding Scheme for Granite Sample Card

Appendix 1

EXPLANATORY NOTES TO ACCOMPANY DATA LISTINGS FOR THE REPORT ON THE NORTH BAY GRANITE SUITE

The listings to accompany the printed report are available on microfiche and as 5 ASCII reports. Each report has an identical sequence so that each page contains data for the same samples.

NOTE THAT THE REPORTS HAVE A 132 COLUMN FORMAT.

PAGE BREAK SHOWN BY ASCII SYMBOL (ALT 12).

Each report contains a listing of the sample number and corresponding laboratory file number.

The data are listed as two sets of field data, one set each of major and trace element geochemical data, and a set of CIPW normative data.

EXPLANATION OF ABBREVIATIONS

FIELD DATA – PART 1

NTS SHEET – National Topographic System map sheet number; all sheets lie within NTS Zone 21.
UTM EAST – UTM easting in metres.
UTM NORTH – UTM northing in metres.
SAMPLE TYPE – 'Grab' single sample from an outcrop. 'split' analytical split obtained from powder of sample listed in Part 2 of field data listing; field data are identical.
COLOUR – '20-50% black' rock with 20–50% mafic minerals '50-80% black' rock with 50–80% mafic minerals.
GRAIN SIZE – (details given in report).

FIELD DATA – PART 2

ALTERATION – 'gossanous' sulphide minerals altered to iron hydroxides.
– 'chlorite' ferromagnesian minerals (usually biotite) altered to chlorite.
MEGACRYSTS – Phenocrysts, larger-than-average crystals or metamorphic porphyroblasts.
HBL – Hornblende: 0 = absent; 1 = present.
BIOT – Biotite: 0 = absent; 1 = present.
FABRIC – 'regional' = regional tectonic fabric.
'massive' = undeformed.
'cataclastic'–brecciated or mylonitic fabric.
'composite'–regional fabric with later cataclastic fabric.
GT – Garnet: 0 = absent; 1 = present.
MU – Muscovite: 0 = absent; 1 = present.
SULF – Sulfide: 0 = absent; 1 = present.
SCIN CPS – Gamma ray scintillometer or spectrometer reading in 'counts per second'.
U+TH CPS – Gamma ray spectrometer reading of uranium + thorium 'counts per second'.
TH CPS – Gamma ray spectrometer reading of thorium 'counts per second'.
SPLIT OF – If number is given then the sample is either the original sample or the split. Where field data are listed the split was obtained from this sample; where stars (*) are listed rather than field data, this sample is the split.

MAJOR ELEMENT OXIDE DATA

– All values given in weight per cent (wt. percent).
LOI – Loss on ignition; volatile loss at 1100° C.

TRACE ELEMENT DATA

– All values in grams per tonne (g/t).

NORMATIVE MINERAL DATA

– CIPW normative values in weight per cent.

QZ = quartz
OR = orthoclase
AB = albite
AN = anorthite
CO = corundum
DI = diopside
HY = hypersthene (EN + FS; see below)
OL = olivine
MT = magnetite
HM = hematite
IL = ilmenite
RU = rutile
AP = apatite
CR = chromite
ZR = zircon
FL = fluorite
EN = enstatite
FS = ferrosilite

Appendix 2

Precision of major- and trace-element determinations.

Appendix 2a: Precision of major-element determinations based on 40 analytical splits.

	Difference Max.	Min.	Mean	S.D.*	Precision #
SiO_2 wt.%	1.70	0.10	0.59	0.50	0.84
Al_2O_3	1.35	0.00	0.20	0.23	1.35
TiO_2	0.08	0.00	0.02	0.02	6.54
Fe_2O_3	0.40	0.00	0.00	0.10	29.78
FeO	0.50	0.00	0.07	0.09	5.92
MnO	0.02	0.00	0.00	0.00	8.03
MgO	0.08	0.00	0.02	0.02	2.57
CaO	0.20	0.00	0.04	0.04	2.46
Na_2O	0.31	0.00	0.06	0.07	1.60
K_2O	0.23	0.00	0.05	0.05	1.12
P_2O_5	0.06	0.00	0.01	0.01	11.26
L.O.I.	0.32	0.00	0.05	0.05	6.33

* 1 standard deviation
# precision from formula: P = mean of 100x(abs(V-Vl)/(V+Vl)/2)
Note: V = first value, Vl = second value, abs = absolute value (i.e., difference expressed as a positive number)

Appendix 2b: Precision of trace-element determinations based on analytical splits.

	Difference Max.	Min.	Mean	St. Dev.*	Precision#	Number
Li	5	0	1.67	1.23	3.06	40
F	425	8	82.07	84.01	16.75	40
V	28	0	4.65	5.15	13.87	40
Cr	2	0	0.83	0.75	20.64	6
Ni	7	0	0.68	1.25	20.28	40
Cu	4	0	0.55	0.85	3.41	40
Zn	6	0	1.60	1.52	3.20	40
Ga	4	0	1.46	1.28	7.22	37
Rb	47	0	4.77	7.73	2.75	40
Sr	36	0	5.50	7.68	2.14	40
Y	10	0	2.31	2.10	15.68	35
Zr	20	0	5.50	4.62	3.89	40
Nb	10	0	1.45	1.78	13.15	40
Mo	13	0	0.85	2.18	20.25	40
Ag	0.1	0.0	0.01	0.03	5.71	35
Sn	5	0	0.88	1.82	28.20	9
Ba	476	0	31.90	74.10	5.29	40
La	34	0	5.25	6.79	23.46	32
Ce	37	0	7.91	8.69	15.66	32
W	2.9	0	1.00	1.36	52.04	9
Pb	8	0	2.14	2.14	8.59	40
Th	9	0	3.41	2.66	31.32	32
U	1.4	0.0	0.29	0.31	9.65	40

* 1 standard deviation
# precision from formula: P = mean of 100x(abs(V-Vl)/(V+Vl)/2)
Note: V = first value, Vl = second value, abs = absolute value (i.e., difference expressed as a positive number)

Appendix 3

Accuracy of the major- and trace-element determinations

Appendix 3a: Accuracy of major-element determinations at the Newfoundland Department of Mines and Energy, Mineral Development Division Laboratory. Usable values from Abbey (1980).

a. Standard: AGV-1

OXIDE	Usable Value	X	S	n	max	min
SiO_2	59.61	58.83	0.39	2	59.1	58.55
Al_2O_3	17.19	17.29	0.13	2	17.38	17.20
Fe_2O_3(total)	6.78	6.91	0.21	2	7.06	6.76
MgO	1.52	1.50	0.04	2	1.52	1.47
CaO	4.94	4.96	0.02	2	4.97	4.94
Na_2O	4.32	4.32	0.06	2	4.36	4.27
K_2O	2.92	3.00	0.01	2	3.01	2.99
TiO_2	1.06	1.09	0.01	2	1.10	1.08
MnO	0.10	0.10	0.00	2	0.10	0.10
P_2O_5	0.51	0.47	0.03	2	0.49	0.45

b. Standard: BCR-1

OXIDE	Usable Value	X	S	n	max	min
SiO_2	54.53	53.83	0.96	4	54.90	52.60
Al_2O_3	13.72	13.49	0.30	4	13.75	13.10
Fe_2O_3(total)	13.41	13.48	0.24	4	13.81	13.28
MgO	3.48	3.51	0.06	4	3.58	3.44
CaO	6.97	7.02	0.16	4	7.23	6.84
Na_2O	3.30	3.26	0.06	4	3.31	3.18
K_2O	1.70	1.74	0.04	4	1.80	1.71
TiO_2	2.26	2.28	0.08	4	2.35	2.17
MnO	0.18	0.19	0.01	4	0.20	0.17
P_2O_5	0.36	0.37	0.00	4	0.37	0.36

c. Standard: BHVD-1

OXIDE	Usable Value	X	S	n	max	min
SiO_2	49.93	49.38	0.32	2	49.6	49.15
Al_2O_3	13.85	13.86	0.20	2	14.0	13.72
Fe_2O_3(total)	12.24	12.45	0.23	2	12.61	12.29
MgO	7.31	7.28	0.11	2	7.35	7.20
CaO	11.33	11.26	0.35	2	11.51	11.01
Na_2O	2.29	2.23	0.03	2	2.25	2.21
K_2O	0.54	0.51	0.01	2	0.51	0.50
TiO_2	2.69	2.78	0.03	2	2.80	2.76
MnO	0.17	0.18	0.01	2	0.18	0.17
P_2O_5	0.28	0.27	0.01	2	0.27	0.26

Appendix 3a. (continued)

d. Standard: BX-N

OXIDE	Usable Value	X	S	n	max	min
SiO_2	7.40	7.48	0.13	3	7.60	7.35
Al_2O_3	54.21	54.52	0.47	3	55.05	54.15
Fe_2O_3(total)	23.17	22.54	0.28	3	22.29	22.85
MgO	0.11	0.07	0.01	3	0.08	0.07
CaO	0.17	0.13	0.01	3	0.13	0.12
Na_2O	0.04	0.02	0.01	3	0.02	0.01
K_2O	0.05	0.04	0.00	3	0.04	0.04
TiO_2	2.37	2.33	0.02	3	2.34	2.31
MnO	0.05	0.05	0.01	3	0.05	0.04
P_2O_5	0.13	0.15	0.04	3	0.19	0.12

e. Standard: DR-N

OXIDE	Usable Value	X	S	n	max	min
SiO_2	52.85	52.68	0.39	3	53.0	52.25
Al_2O_3	17.52	17.67	0.10	3	17.75	17.56
Fe_2O_3(total)	9.70	9.56	0.18	3	9.77	9.42
MgO	4.40	4.31	0.12	3	4.42	4.18
CaO	7.05	7.05	0.16	3	7.16	6.86
Na_2O	2.99	2.93	0.04	3	2.96	2.88
K_2O	1.70	1.72	0.08	3	1.77	1.63
TiO_2	1.09	1.06	0.02	3	1.08	1.05
MnO	0.22	0.22	0.01	3	0.22	0.21
P_2O_5	0.25	0.22	0.01	3	0.23	0.21

f. Standard: DT-N

OXIDE	Usable Value	X	S	n	max	min
SiO_2	36.45	36.64	0.11	4	36.80	36.55
Al_2O_3	59.20	58.39	0.39	4	58.95	58.12
Fe_2O_3(total)	0.66	0.54	0.01	4	0.55	0.53
MgO	0.04	0.04	0.01	4	0.05	0.04
CaO	0.04	0.02	0.01	4	0.03	0.01
Na_2O	0.04	0.03	0.00	4	0.03	0.03
K_2O	0.12	0.12	0.02	4	0.14	0.10
TiO_2	1.40	1.23	0.09	4	1.36	1.18
MnO	0.008	0.00	0.00	4	0.00	0.00
P_2O_5	0.09	0.06	0.01	4	0.06	0.04

Appendix 3a. (continued)

g. Standard: FK-N

OXIDE	Usable Value	X	S	n	max	min
SiO_2	65.80	64.38	1.00	4	65.10	62.95
Al_2O_3	18.64	18.71	0.17	4	18.85	18.55
Fe_2O_3(total)	?	0.08	0.01	4	0.09	0.08
MgO	0.01	0.01	0.01	4	0.02	0.01
CaO	0.11	0.09	0.01	4	0.10	0.08
Na_2O	2.58	2.52	0.03	4	2.57	2.50
K_2O	12.83	13.42	0.27	4	13.70	13.10
TiO_2	0.02	0.03	0.03	4	0.07	0.00
MnO	0.01	0.01	0.01	4	0.01	0.00
P_2O_5	0.02	0.01	0.01	4	0.02	0.01

h. Standard: G-2

OXIDE	Usable Value	X	S	n	max	min
SiO_2	69.82	68.60	0.00	2	68.60	68.60
Al_2O_3	15.35	15.44	0.12	2	15.52	15.35
Fe_2O_3(total)	2.69	2.59	0.06	2	2.63	2.54
MgO	0.75	0.75	0.01	2	0.75	0.74
CaO	1.96	1.94	0.03	2	1.96	1.91
Na_2O	4.06	4.11	0.06	2	4.15	4.07
K_2O	4.46	4.52	0.06	2	4.56	4.47
TiO_2	0.48	0.50	0.03	2	0.52	0.48
MnO	0.03	0.04	0.01	2	0.04	0.03
P_2O_5	0.13	0.12	0.00	2	0.12	0.12

i. Standard: GS-N

OXIDE	Usable Value	X	S	n	max	min
SiO_2	65.98	65.40	0.03	3	65.70	65.10
Al_2O_3	14.71	14.65	0.09	3	14.70	14.55
Fe_2O_3(total)	3.71	3.76	0.04	3	3.80	3.73
MgO	2.31	2.24	0.03	3	2.27	2.21
CaO	2.51	2.47	0.06	3	2.54	2.42
Na_2O	3.79	3.80	0.05	3	3.85	3.75
K_2O	4.64	4.74	0.16	3	4.90	4.58
TiO_2	0.68	0.68	0.02	3	0.06	0.05
MnO	0.06	0.05	0.01	3	0.06	0.05
P_2O_5	0.28	0.28	0.02	3	0.29	0.26

Appendix 3a. (continued)

j. Standard: GSP-1

OXIDE	Usable Value	X	S	n	max	min
SiO_2	67.32	66.55	1.91	2	67.90	65.20
Al_2O_3	15.28	15.09	0.01	2	15.10	15.08
Fe_2O_3(total)	4.30	4.33	0.05	2	4.36	4.29
MgO	0.97	0.96	0.01	2	0.96	0.95
CaO	2.03	2.02	0.01	2	2.02	2.01
Na_2O	2.81	2.80	0.04	2	2.83	2.77
K_2O	5.51	5.55	0.11	2	5.62	5.47
TiO_2	0.66	0.69	0.01	2	0.70	0.68
MnO	0.04	0.05	0.01	2	0.04	0.05
P_2O_5	0.28	0.27	0.02	2	0.28	0.25

k. Standard: MAG-1

OXIDE	Usable Value	X	S	n	max	min
SiO_2	51.19	51.62	0.39	2	51.90	51.35
Al_2O_3	16.46	16.82	0.02	2	16.83	16.80
Fe_2O_3(total)	6.98	7.28	0.05	2	7.31	7.24
MgO	3.13	3.12	0.01	2	3.12	3.11
CaO	1.38	1.45	0.01	2	1.45	1.44
Na_2O	3.91	3.98	0.03	2	4.00	3.96
K_2O	3.72	3.57	0.03	2	3.59	3.55
TiO_2	0.75	0.75	0.01	2	0.76	0.74
MnO	0.10	0.10	0.00	2	0.10	0.10
P_2O_5	0.18	0.16	0.01	2	0.16	0.15

l. Standard: MRG-1

OXIDE	Usable Value	X	S	n	max	min
SiO_2	39.32	39.03	0.32	2	39.25	38.80
Al_2O_3	8.50	8.66	0.21	2	8.80	8.51
Fe_2O_3(total)	17.82	17.81	0.18	2	17.94	17.68
MgO	13.49	13.65	0.23	2	13.81	13.49
CaO	14.77	14.78	0.42	2	15.07	14.48
Na_2O	0.71	0.72	0.01	2	0.73	0.71
K_2O	0.18	0.18	0.01	2	0.18	0.17
TiO_2	3.69	3.89	0.19	2	4.02	3.75
MnO	0.17	0.19	0.01	2	0.20	0.18
P_2O_5	0.06	0.07	0.01	2	0.07	0.06

Appendix 3a. (continued)

m. Standard: QLO-1

OXIDE	Usable Value	X	S	n	max	min
SiO_2	65.93	65.27	0.51	3	65.70	64.70
Al_2O_3	16.37	16.45	0.18	3	16.65	16.30
Fe_2O_3(total)	4.29	4.36	0.10	3	4.44	4.25
MgO	1.04	1.00	0.01	3	1.01	0.99
CaO	3.24	3.20	0.04	3	3.24	3.16
Na_2O	4.23	4.28	0.04	3	4.32	4.25
K_2O	3.63	3.73	0.10	3	3.81	3.61
TiO_2	0.62	0.62	0.03	3	0.65	0.60
MnO	0.09	0.10	0.01	3	0.10	0.09
P_2O_5	0.26	0.27	0.01	3	0.27	0.26

n. Standard: RGM-1

OXIDE	Usable Value	X	S	n	max	min
SiO_2	73.47	73.00	1.39	3	73.90	71.40
Al_2O_3	13.80	13.65	0.38	3	14.05	13.30
Fe_2O_3(total)	1.89	1.81	0.06	3	1.88	1.76
MgO	0.28	0.28	0.02	3	0.03	0.27
CaO	1.15	1.20	0.03	3	1.24	1.18
Na_2O	4.12	4.13	0.09	3	4.19	4.03
K_2O	4.35	4.47	0.12	3	4.55	4.34
TiO_2	0.27	0.31	0.02	3	0.32	0.28
MnO	0.04	0.04	0.01	3	0.05	0.04
P_2O_5	0.05	0.02	0.01	2	0.03	0.01

o. Standard: SCO-1

OXIDE	Usable Value	X	S	n	max	min
SiO_2	63.40	62.40	0.95	3	63.00	61.30
Al_2O_3	13.70	13.78	0.30	3	14.09	13.50
Fe_2O_3(total)	5.22	5.28	0.34	3	5.65	4.97
MgO	2.76	2.68	0.04	3	2.71	2.63
CaO	2.64	2.60	0.09	3	2.69	2.51
Na_2O	0.95	0.93	0.02	3	0.95	0.92
K_2O	2.82	2.79	0.03	3	2.82	2.77
TiO_2	0.62	0.58	0.06	3	0.61	0.51
MnO	0.05	0.05	0.01	3	0.06	0.04
P_2O_5	0.22	0.22	0.04	3	0.26	0.18

Appendix 3a. (continued)

p. Standard: SDC-1

OXIDE	Usable Value	X	S	n	max	min
SiO_2	66.15	65.28	0.60	2	65.70	64.85
Al_2O_3	15.75	15.72	0.05	2	15.75	15.68
Fe_2O_3(total)	6.85	6.98	0.04	2	7.00	6.95
MgO	1.70	1.71	0.01	2	1.71	1.70
CaO	1.39	1.47	0.04	2	2.07	2.04
Na_2O	2.10	2.06	0.02	2	2.07	2.04
K_2O	3.24	3.29	0.08	2	3.34	3.23
TiO_2	1.00	1.00	0.00	2	1.00	1.00
MnO	0.12	0.12	0.00	2	0.12	0.12
P_2O_5	0.18	0.15	0.01	2	0.16	0.14

q. Standard: STM-1

OXIDE	Usable Value	X	S	n	max	min
SiO_2	59.66	58.15	0.78	2	58.70	57.60
Al_2O_3	18.44	18.40	0.78	2	18.95	17.85
Fe_2O_3(total)	5.20	5.14	0.09	2	5.20	5.07
MgO	0.10	0.11	0.01	2	0.11	0.10
CaO	1.09	1.13	0.02	2	1.14	1.11
Na_2O	8.95	8.93	0.01	2	8.94	8.92
K_2O	4.29	4.47	0.02	2	4.48	4.45
TiO_2	0.13	0.14	0.00	2	0.14	0.14
MnO	0.22	0.21	0.03	2	0.23	0.19
P_2O_5	0.16	0.07	0.04	2	0.10	0.04

r. Standard: SY-2

OXIDE	Usable Value	X	S	n	max	min
SiO_2	60.10	59.65	0.03	4	60.10	59.50
Al_2O_3	12.12	12.11	0.15	4	12.15	11.90
Fe_2O_3(total)	6.28	6.29	0.18	4	6.43	6.07
MgO	2.70	2.67	0.03	4	2.71	2.64
CaO	7.98	8.14	0.12	4	8.30	8.02
Na_2O	4.34	4.31	0.08	4	4.39	4.21
K_2O	4.48	4.61	0.03	4	4.63	4.57
TiO_2	0.14	0.17	0.02	4	0.19	0.16
MnO	0.32	0.32	0.02	4	0.34	0.31
P_2O_5	0.43	0.43	0.01	4	0.44	0.42

Appendix 3a. (continued)

s. Standard: UB-N

OXIDE	Usable Value	X	S	n	max	min
SiO_2	39.43	40.00	0.46	3	40.40	39.50
Al_2O_3	2.92	2.92	0.02	3	2.93	2.90
Fe_2O_3(total)	8.34	8.55	0.13	3	8.67	8.42
MgO	35.21	37.81	1.08	3	38.70	36.61
CaO	1.20	1.19	0.02	3	1.21	1.18
Na_2O	0.10	0.13	0.00	3	0.13	0.13
K_2O	0.02	0.02	0.01	3	0.03	0.01
TiO_2	0.11	0.12	0.01	3	0.12	0.11
MnO	0.12	0.14	0.01	3	0.14	0.13
P_2O_5	0.04	0.01	0.01	3	0.02	0.01

Appendix 3b: Accuracy of trace elements, determined by the I.C.P. method at the Newfoundland Department of Mines and Energy, Mineral Development Division Laboratory. Usable values from Abbey (1980).

Standard: SY-2

ELEMENT	Usable Value	X	S	n	max	min
Zr g/t	280	323.5	16.3	2	335	312
Th	380?	402.0	14.1	2	412	392
Y	130	142.0	9.9	2	149	135
Nb	23?	26.5	0.7	2	27	26
Ga	28	26.5	0.7	2	27	26
La	88	74.5	2.1	2	76	73
Ce	210?	169.0	11.3	2	177	161

Standard: MRG-1

ELEMENT	Usable Value	X	S	n	max	min
Zr g/t	105	113.5	12.0	2	122	105
Th	1?	N.D.*	–	2	N.D.	N.D.
Y	16?	9.5	0.7	2	10	9
Nb	20?	12.5	0.7	2	12	13
Ga	18?	25.5	0.7	2	26	25
La	10?	27.5	2.12	2	29	26
Ce	25?	42.5	4.9	2	46	39

*N.D. = not detected

Appendix 3c: Accuracy of trace elements determined by X.R.F. at the Department of Earth Sciences, Memorial University of Newfoundland. Usable values from Abbey (1980).

Standard : SY-2

ELEMENT	Usable Value	X	S	n	max	min
Ba g/t	480	434.4	9.3	7	444	421
Sr	275	262.0	4.1	7	269	256
Rb	220	224.0	4.4	7	231	220
Zr	280	286.0	5.3	7	292	282
Cr	12	5.0	0.0	7	5	5
V	52	44.1	2.3	7	48	41
Th	380	405.3	6.0	7	413	397
Y	130	166.9	2.6	7	170	162
Nb	23?	35.9	1.7	7	39	34
Ga	28	26.0	1.9	7	30	25
La	88	29.3	5.5	7	37	22
Ce	210	57.7	1.6	7	60	55

Standard : MRG-1

ELEMENT	Usable Value	X	S	n	max	min
Ba g/t	50?	162	–	1		
Sr	260	257	–	1		
Rb	8	12	–	1		
Zr	105	110	–	1		
Cr	450	379	–	1		
V	520	563	–	1		
Th	1?	8	–	1		
Y	16?	10	–	1		
Nb	20?	25	–	1		
Ga	18?	21	–	1		
La	10?	<2	–	1		
Ce	25?	70	–	1		

Appendix 4

Appendix 4a: Detailed sample location and description card used to format data.

GRANITE SAMPLE CARD

PROJECT NO AREA PHOTO COLLECTOR DATE

NTS Sheet	Sample No	Zone	UTM East	UTM North	Rock Type	Age	Mo	Cpx	Opx	Hbl	Bio	Mag	Hb Bi	S	Scint TC	Scint U+Th	Scint Th	Tab	gar	Tourm	Bot	Mo		Rel No	Rep No	Orig Sample No of Split

10 20 30 40 50 60 70 80

Appendix 4b. Explanation of Coding Scheme for Granite Sample Card.

COL. 28–31

DLMT	Dolomite
LMSN	Limestone
BKSH	Black Shale
SHLE	Shale
SLSN	Siltstone
SNDS	Sandstone
ARKS	Arkose
CGLM	Conglomerate
QRTZ	Quartzite
CHRT	Chert
GRCK	Greywacke
SLTE	Slate
SCHS	Schist
SPDS	Spotted Slate
HRFL	Hornfels
SKRN	Skarn
GRSN	Greisen
QRZD	Qtz. Diorite
GRDR	Granodiorite
QZMZ	Qtz. Monzonite
ALSK	Alaskite
GRNT	Granite
SDCG	Sodic Granite
DORT	Diorite
MNZN	Monzonite
SENT	Syenite
ALKS	Alkali Syenite
QZPP	Qtz. Porphyry
FPPP	Feld. Porphyry
QZFP	Qtz.–Feld. Porphyry
DCIT	Dacite
RDCT	Rhyodacite
RYLT	Rhyolite
ANDS	Andesite
TRCD	Trachyandesite
TRCT	Trachyte
TUFF	Tuff
BSLT	Basalt
DIBS	Diabase
GBBR	Gabbro
SRPN	Serpentinite
VEIN	Vein Material
GNSS	Gneiss
APLT	Aplite

COL. 32–33

04	Proterozoic
10	Paleozoic
12	Cambrian
14	Ordovician
16	Silurian
17	Silurian–Devonian
18	Devonian
20	Carboniferous
24	Permian
30	Mesozoic
32	Triassic
34	Jurassic
36	Cretaceous
42	Tertiary

COL. 34

1	Single grab sample
2	Channel sample
3	Composite sample
4	Drill Core
5	Other

COL. 35–Color

0	white	<20%
1	White & Black	20–50%
2	Black & White	50–80%
3	Black	>80%
4	Gray	
5	Green	
6	Buff	
7	Orange or Yellow	
8	Red or Purple	
9	Pink	

COL. 36–Grain size in mm

0	<0.004 glassy
1	0.004–0.025 aphanitic
2	0.025–0.062 aphanitic
3	0.062–0.250 v.f. grained
4	0.25 – 0.50 v.f. grained
5	0.50 – 1.00 fine grained
6	1.00 – 2.00 med. grained
7	2.00 – 5.00 med.–coarse grained
8	5.00 –10.0 coarse grained
9	>10.0 v.c. grained

COL. 37–Texture

0	Uniform
1	Variable
2	Aplitic
3	Porphyritic
4	Miarolitic
5	Myrmekitic
6	Megacrystic
7	Pegmatitic
8	Other

COL. 38–Primary features

0	Massive
1	Bedded
2	Crossbedded
3	Slump structured
4	Oriented megacrysts
5	Trachytic

COL. 39

0	Fresh
1	Weathered
2	Gossanous
3	Hydrothermal, white
4	Hydrothermal, rusty
5	Chloritized mafics

COL. 40

0	Feldspars clear
1	Feldspars clouded

COL. 41

0	No megacrysts
1	Feld. megacrysts
2	Qtz. megacrysts
3	Qtz. & Feld. megacrysts
4	Metamorphic porphyroblasts
5	Other

COL. 42–43

Hb. & Biot. content of total dark minerals, on scales of 0–9. 09–no hornblende, 90–no biotite

COL. 44

0	Sulfides absent
1	Sulfides present

COL. 45–49

Scintillometer reading of Total counts per second

COL. 50–53

Scintillometer reading of U + Th counts per second

COL. 54–55

Scintillometer reading of Th counts per second

COL. 55

0	No fabric
1	Cataclastic fabric
2	General tectonic fabric
3	Igneous flow fabric
4	Composite 1 + 2
5	Composite 1 + 3
6	Composite 2 + 3
7	Composite 2 + 2

COL. 56

0	Garnet absent
1	Garnet present

COL. 57

0	Tourmaline absent
1	Tourmaline present

COL. 58

0	Beryl absent
1	Beryl present

COL. 59

0	Fluorite absent
1	Fluorite present

COL. 60

0	Primary muscovite absent
1	Primary muscovite present

COL. 70–71

Pluton number

COL. 72–73

Replicate number 00 or 01. Used in analysis of variance calculation

COL. 74–79

Original sample number of analytical splits

MAPS
NOT
FILMED

CARTES
OMISES